

ВОЈНОСАНИТЕТСКИ ПРЕГЛЕД

Часопис лекара и фармацеута Војске Србије

Military Medical and Pharmaceutical Journal of Serbia



Vojnosanitetski pregled

Vojnosanit Pregl 2022; February Vol. 79 (No. 2): pp. 103–210.



VOJNOSANITETSKI PREGLED

The first issue of *Vojnosanitetski pregled* was published in September 1944
The Journal continues the tradition of *Vojno-sanitetski glasnik* which was published between 1930 and 1941

PUBLISHER

University of Defence, Ministry of Defence of the Republic of Serbia, Belgrade, Serbia

EDITOR-in-CHIEF

Col. Prof. Tihomir Ilić, MD, PhD

EXECUTIVE EDITOR

Aleksandra Gogić, PhD

PUBLISHER'S ADVISORY BOARD

Lieutenant-General Assoc. Prof. **Goran Radovanović**, PhD,
(President)
Major General Assoc. Prof. **Bojan Zrnić**, PhD,
(Deputy President)
Lieutenant Col. **Sladon Đorđević**
Col. Prof. **Tihomir Ilić**, MD, PhD
Col. **Miće Suvajac**
Assoc. Prof. **Jovanka Šaranović**, PhD
Col. Assist. Prof. **Ivan Vulić**, PhD

INTERNATIONAL EDITORIAL BOARD

Prof. **Jovan Antonović** (Sweden)
Prof. **Rocco Bellantone** (Italy)
Prof. **Thorsten Gehrke** (Germany)
Prof. **Hanoch Hod** (Israel)
Prof. **Abu-Elmagd Kareem** (USA)
Prof. **Thomas John** (USA)
Prof. **Hiroshi Kinoshita** (Japan)
Prof. **Celestino Pio Lombardi** (Italy)
Prof. **Philippe Morel** (Switzerland)
Prof. **Kiyotaka Okuno** (Japan)
Prof. **Mirjana Pavlović** (USA)
Prof. **Hitoshi Shiozaki** (Japan)
Prof. **H. Ralph Schumacher** (USA)
Prof. **Sadber Lale Tokgozogl** (Turkey)
Assist. Prof. **Tibor Tot** (Sweden)

EDITORIAL BOARD (from Serbia)

Col. Prof. **Miroslav Vukosavljević**, MD, PhD (president)
Prof. **Bela Balint**, MD, PhD, FSASA
Brigadier General (ret.) Prof. **Miodrag Čolić**, MD, PhD,
FSASA
Assoc. Prof. **Dragana Daković**, DDM, PhD
Prof. **Silva Dobrić**, BPharm, PhD
Col. Prof. **Boban Đorđević**, MD, PhD
Assoc. Prof. **Branislava Glišić**, MD, PhD
Prof. **Vladimir Jakovljević**, MD, PhD
Prof. **Zoran Krivokapić**, MD, PhD, FSASA
Prof. **Nebojša Lalić**, MD, PhD, FSASA
Col. Assoc. **Srdan Lazić**, MD, PhD
Prof. **Sonja Marjanović**, MD, PhD
Prof. **Željko Mijušković**, MD, PhD
Col. Prof. **Dragan Mikić**, MD, PhD
Prof. **Željko Miković**, MD, PhD
Prof. **Branka Nikolić**, MD, PhD
Prof. **Milica Ninković**, MD, PhD
Col. Prof. **Slobodan Obradović**, MD, PhD
Prof. **Miodrag Ostojić**, MD, PhD, FSASA
Lieut. Col. Assoc. Prof. **Aleksandar Perić**, MD, PhD
Prof. **Đorđe Radak**, MD, PhD, FSASA
Prof. **Dejan Radenković**, MD, PhD
Assoc. Prof. **Duška Stamenković**, MD, PhD
Assist. Prof. **Zvezdana Stojanović**, MD, PhD
Prof. **Ljubomir Todorović**, DDM, PhD
Prof. **Danilo Vojvodić**, MD, PhD
Assoc. Prof. **Biserka Vukomanović Đurđević**, MD, PhD

Technical Secretary and Main Journal Manager

Aleksandra Gogić, PhD

EDITORIAL OFFICE

Editorial staff: Snežana R. Janković, primarius, MD

Language editors: Ivana Biga, Branka Dimitrov, Irena Jonović,
Mila Karavidić, Sanja Korićanac,
Valentina Rapajić, Mirjana Vučić

Technical editor: Dragana Milanović

Proofreading: Ljiljana Milenović, Brana Savić

Technical editing: Vesna Totić, Jelena Vasilj



ISSN 0042-8450
eISSN 2406-0720
Open Access
(CC BY-SA)

Editorial Office: University of Defence, Faculty of Medicine of the Military Medical Academy, Center for Medical Scientific Information, Crnotravska 17, 11 040 Belgrade, Serbia. E-mail: vsp@vma.mod.gov.rs

Papers published in the *Vojnosanitetski pregled* are indexed in: Science Citation Index Expanded (SCIE), Journal Citation Reports/Science Edition, SCOPUS, Excerpta Medica (EMBASE), Google Scholar, EBSCO, Biomedicina Serbica, Serbian Citation Index (SCIndex), DOAJ. Contents are published in *Giornale di Medicina Militare* and *Revista de Medicina Militara*. Reviews of original papers and abstracts of contents are published in *International Review of the Armed Forces Medical Services*.

The Journal is published monthly. Subscription: Giro Account No. 840-19540845-28, refer to number 122742313338117. To subscribe from abroad phone to +381 11 3608 997. Subscription prices per year: individuals 5,000.00 RSD, institutions 10,000.00 RSD, and foreign subscribers 150 €

VOJNOSANITETSKI PREGLED

Prvi broj *Vojnosanitetskog pregleda* izašao je septembra meseca 1944. godine
Časopis nastavlja tradiciju *Vojno-sanitetskog glasnika*, koji je izlazio od 1930. do 1941. godine

IZDAVAČ

Ministarstvo odbrane Republike Srbije, Univerzitet odbrane, Beograd, Srbija

GLAVNI UREDNIK

Prof. dr sc. med. **Tihomir Ilić**, pukovnik

ODGOVORNI UREDNIK

Dr sc. **Aleksandra Gogić**

IZDAVAČKI SAVET

Prof. dr **Goran Radovanović**, general-potpukovnik
(predsednik)
Prof. dr **Bojan Zrnić**, general-major
(zamenik predsednika)
Sladan Đorđević, ppuk.
Prof. dr sc. med. **Tihomir Ilić**, puk.
Mičo Suvajac, puk.
Prof. dr **Jovanka Šaranović**
Doc. dr **Ivan Vulić**, puk.

MEĐUNARODNI UREĐIVAČKI ODBOR

Prof. **Jovan Antonović** (Sweden)
Prof. **Rocco Bellantone** (Italy)
Prof. **Thorsten Gehrke** (Germany)
Prof. **Hanoch Hod** (Israel)
Prof. **Abu-Elmagd Kareem** (USA)
Prof. **Thomas John** (USA)
Prof. **Hiroshi Kinoshita** (Japan)
Prof. **Celestino Pio Lombardi** (Italy)
Prof. **Philippe Morel** (Switzerland)
Prof. **Kiyotaka Okuno** (Japan)
Prof. **Mirjana Pavlović** (USA)
Prof. **Hitoshi Shiozaki** (Japan)
Prof. **H. Ralph Schumacher** (USA)
Prof. **Sadber Lale Tokgozoglul** (Turkey)
Assist. Prof. **Tibor Tot** (Sweden)

UREĐIVAČKI ODBOR (iz Srbije)

Prof. dr sc. med. **Miroslav Vukosavljević**, pukovnik
(predsednik)
Akademik **Bela Balint**
Akademik **Miodrag Čolić**, brigadni general u penziji
Prof. dr sc. stom. **Dragana Daković**
Prof. dr sc. pharm. **Silva Dobrić**
Prof. dr sc. med. **Boban Đorđević**, pukovnik
Prof. dr sc. med. **Branislava Glišić**
Prof. dr sc. med. **Vladimir Jakovljević**
Akademik **Zoran Krivokapić**
Akademik **Nebojša Lalić**
Prof. dr sc. med. **Srdan Lazić**, pukovnik
Prof. dr sc. med. **Sonja Marjanović**
Prof. dr sc. med. **Željko Mijušković**
Prof. dr sc. med. **Dragan Mikić**, pukovnik
Prof. dr sc. med. **Željko Miković**
Prof. dr sc. med. **Branka Nikolić**
Prof. dr sc. med. **Milica Ninković**
Prof. dr sc. med. **Slobodan Obradović**, pukovnik
Akademik **Miodrag Ostojić**
Prof. dr sc. med. **Aleksandar Perić**, potpukovnik
Akademik **Đorđe Radak**
Prof. dr sc. med. **Dejan Radenković**
Prof. dr sc. med. **Duška Stamenković**
Doc. dr sc. med. **Zvezdana Stojanović**
Prof. dr sc. stom. **Ljubomir Todorović**
Prof. dr sc. med. **Danilo Vojvodić**
Prof. dr sc. med. **Biserka Vukomanović Đurđević**

Tehnički sekretar i glavni menadžer časopisa

Dr sc. **Aleksandra Gogić**

REDAKCIJA

Stručna redakcija: Prim. dr Snežana R. Janković

Urednici za engleski i srpski jezik: Ivana Biga, Branka Dimitrov,
Irena Jonović, Mila Karavidić, Sanja Korićanac,
Valentina Rapajić, Mirjana Vučić

Tehnički urednik: Dragana Milanović

Korektori: Ljiljana Milenović, Brana Savić

Kompjutersko-grafička obrada: Vesna Totić, Jelena Vasilj



ISSN 0042-8450
eISSN 2406-0720
Open Access
(CC BY-SA)

Adresa redakcije: Univerzitet odbrane, Medicinski fakultet Vojnomedicinske akademije, Centar za medicinske naučne informacije, Crnotravska 17, 11 040 Beograd, Srbija. Informacije o pretplati (tel.): +381 11 3608 997. E-mail (redakcija): vsp@vma.mod.gov.rs

Radove objavljene u „Vojnosanitetskom pregledu“ indeksiraju: Science Citation Index Expanded (SCIE), Journal Citation Reports/Science Edition, SCOPUS, Excerpta Medica (EMBASE), Google Scholar, EBSCO, Biomedicina Serbica, Srpski citatni indeks (SCIIndeks), DOAJ. Sadržaje objavljuju *Giornale di Medicina Militare* i *Revista de Medicina Militara*. Prikaze originalnih radova i izvoda iz sadržaja objavljuje *International Review of the Armed Forces Medical Services*.

Časopis izlazi dvanaest puta godišnje. Pretplate: Žiro račun br. 840-19540845-28, poziv na broj 122742313338117. Za pretplatu iz inostranstva obratiti se službi pretplate na tel. +381 11 3608 997. Godišnja pretplata: 5 000 dinara za građane Srbije, 10 000 dinara za ustanove iz Srbije i 150 € za pretplatnike iz inostranstva. Kopiju uplatnice dostaviti na gornju adresu.



CONTENTS / SADRŽAJ

ORIGINAL ARTICLES / ORIGINALNI RADOVI

Slavica Vujović, Andjelka Šćepanović, Milan Terzić, Milena Djurović

Diagnostic validity of a marker model of first trimester in pregnancy in prediction of birth weight

Dijagnostička valjanost modela zasnovanog na markerima prvog trimestra trudnoće u predviđanju mase ploda na rođenju.....

107

Goran Kolarević, Dražan Jaroš, Goran Marošević, Dejan Ignjatić, Dragoljub Mirjanić

Dosimetric verification of clinical radiotherapy treatment planning system

Dozimetrijska verifikacija kliničkog sistema za planiranje radioterapije

115

Kristina Stanojević, Goran Radovanović, Dragana Makajić-Nikolić, Gordana Savić, Barbara Simeunović, Nataša Petrović

Selection of the optimal medical waste incineration facility location: A challenge of medical waste risk management

Izbor optimalne lokacije postrojenja za spaljivanje medicinskog otpada: izazov u upravljanju rizikom od medicinskog otpada

125

Nebojša Manojlović, Ivana Tufegdžić, Elizabeta Ristanović, Dubravko Bokonić

Simultaneous and alternative IgG seroreactivity against *Helicobacter pylori* antigens VacA, 30 kDa and 50 kDa is a better biomarker approach for the outcome of infection than VacA and 50 kDa alone

Istovremena i alternativna IgG seroreaktivnost protiv *Helicobacter pylori* antigena VacA, 50 kDa i 30 kDa je bolji biomarkerski model ishoda infekcije nego VacA i 50 kDa pojedinačno

133

Maja Petrović, Mirko Resan, Gordana Stanković Babić, Tatjana Šarenac Vulović, Marija Radenković, Aleksandar Veselinović, Marija Trenkić, Marija Cvetanović

Analysis of structural and vascular changes of the optic disc and macula in different stages of primary open angle glaucoma

Analiza strukturnih i vaskularnih promena optičkog diska i makule u različitim stadijumima primarnog glaukoma otvorenog ugla

142

Elena Joveva, Gordana Djordjević, Vuk Milošević, Anita Arsovska, Miroslava Živković

Degree of cognitive impairment in patients with carotid stenosis in relation to cerebral ischemic lesions

Stepen kognitivnog oštećenja kod bolesnika sa karotidnom stenozom u odnosu na cerebralne ishemijske lezije

150

Shahabe Saquib Abullais, Nabeeh Abdullah Al-Qahtani, Talib Amin Naqash, Abdul Ahad Khan, Suraj Arora, Shaeesta Bhavikatti

Evaluation of mechanical properties of three commonly used suture materials for clinical oral applications: an *in vitro* study

Procena mehaničkih svojstava tri najčešće korišćena šavna materijala za oralnu primenu u kliničkoj stomatologiji – *in vitro* studija

155

Biserka Vukomanović Djurdjević, Bojana Andrejić Višnjić, Aleksandar Perić, Dane Nenadić, Nenad Baletić

Application of P16, P63, cyclin D1 immunostaining and nuclear morphometric analysis for assessment of cervical dysplasia

Primena imunohistohemijskih markera P16, P63, ciklin D1 i morfometrijske analize u proceni težine displazije grlića materice

162

Xueyang Zhang, Yongbo Wang, Simengge Yang, Junwei Zong, Xuejiao Wang, Ran Bai

Beneficial effects of liraglutide on peripheral blood vessels

Korisni efekti liraglutida na periferne krvne sudove.....

168

Milan M. Mitković, Saša Milenković, Ivan Micić, Predrag Stojilković, Igor Kostić, Milorad B. Mitković

Comparative analysis of operation time and intraoperative fluoroscopy time in intramedullary and extramedullary fixation of trochanteric fractures

Uporedna analiza trajanja operacije i intraoperativne fluoroskopije kod intramedularne i ekstramedularne fiksacije trohanternih preloma..... 177

SHORT COMMUNICATION /KRATKO SAOPŠTENJE

Danijela Randjelović, Sunčica Srećković, Tatjana Šarenac Vulović, Nenad Petrović

Distance visual acuity in air force pilots and student pilots when exposed to + Gz acceleration in human centrifuge

Oštrina vida na daljinu kod pilota borbene avijacije i studenata pilota izloženih + Gz ubrzanju u humanoj centrifugi 183

CASE REPORT / KAZUISTIKA

Aleksandar Dimić, Vladimir Stojilković, Tamara Vujačić

The use of piezoelectric instrumentation and platelet rich fibrin matrix in septorhinoplasty: report of two cases

Primena piezoelektričnih instrumenata i fibrina bogatog trombocitima u septorinoplastici 188

Srdjan Stošić, Slavica Sotirović-Seničar

Imaging findings of familial adenomatous polyposis-associated aggressive mesenteric fibromatosis:

A rare case report

Agresivna mezenterijalna fibromatoza udružena sa familijarnom adenomatoznom polipozom – karakteristike dobijene primenom *imaging* tehnika snimanja..... 192

Milan Borković, Goran Čuturilo, Nataša Cerovac

Ring chromosome 20: a further contribution to the delineation of epileptic phenotype

Ring hromozom 20: doprinos boljem sagledavanju karakteristika epileptičnog fenotipa..... 196

LETTER TO THE EDITOR (RESEARCH LETTER) / PISMO UREDNIKU

Katarina Janičijević, Maja Sazdanović, Mirjana A. Janičijević Petrović, Zoran Kovačević

In Memory of Dr Elizabeth Ross

Sećanje na dr Elizabetu Ros..... 201

Dragomir Marisavljević, Andrija Bogdanović

Clinical alert: “non-clonal” myelodysplastic syndrome

Kliničko upozorenje: „neklonski” mijelodisplastični sindrom 204

Nebojša Jovanović

Clinical characteristics of gynecological patients treated in MINUSCA level II military hospital, Bangui, Central African Republic

Kliničke karakteristike ginekoloških pacijentkinja lečenih u MINUSCA vojnoj bolnici nivoa 2, Bangui, Centralnoafrička Republika 206

INSTRUCTIONS TO THE AUTHORS / UPUTSTVO AUTORIMA..... 208



Elisabeth Ross (February 14, 1878 – February 14, 1915) was a Scottish medical doctor who arrived in Serbia in January 1915, during the First World War, and volunteered in Kragujevac, one of the Serbian cities hardest affected by the typhus epidemic. Dr. Ross died from typhus on her 37th birthday, on February 14, 1915, three weeks after arriving in Kragujevac.

On February 14, her birth and death date, memorial ceremonies are held each year in Kragujevac and at other locations in Serbia to commemorate her work for the people of Serbia (see pp. 201-203).

Elizabet Ros (14. februar 1878 – 14. februar 1915) bila je škotska lekarka koja je stigla u Srbiju u januaru 1915, tokom Prvog svetskog rata, i prijavila se kao dobrovoljac u Kragujevcu, jednom od srpskih gradova najteže pogođenim epidemijom tifusa. Dr Ros je umrla od tifusa na svoj 37. rođendan, 14. februara 1915. godine, tri nedelje po dolasku u Kragujevac.

Na datum njenog rođenja i smrti, 14. februara, svake godine se u Kragujevcu i na drugim mestima u Srbiji održavaju komemoracije u znak sećanja na njen rad za narod Srbije (videti str. 201-203).



Diagnostic validity of a marker model of first trimester in pregnancy in prediction of birth weight

Dijagnostička valjanost modela zasnovanog na markerima prvog trimestra trudnoće u predviđanju mase ploda na rođenju

Slavica Vujović^{*†}, Andjelka Šćepanović^{*†}, Milan Terzić^{‡§¶}, Milena Djurović[¶]

^{*}University of Montenegro, Faculty of Medicine, [†]Department of Pharmacy, Podgorica, Montenegro; [‡]Nazarbayev University, School of Medicine, Department of Medicine, Astana, Kazakhstan; [§]University Medical Center, National Research Center of Mother and Child Health, Clinical Academic Department of Women's Health, Astana, Kazakhstan; [¶]University of Pittsburgh, School of Medicine, Department of Obstetrics, Gynecology and Reproductive Sciences, Pittsburgh, USA; [¶]Human Reproduction, Budva, Montenegro

Abstract

Background/Aim. Nowadays, low birth weight is considered to be one of the main causes of cardiovascular diseases or metabolic syndrome occurring later in life. Many studies have shown a strong impact of abnormal birth weight onto the future development, however, due to its stronger influence onto the development, a special emphasis is placed on low birth weight as compared to higher one. There is still no high-percentage accuracy test that will clearly classify expectant women under the risk of giving birth to a child too low or too big for gestational age. The aim of this paper was to set up a model that may indicate future low or high birth weight. **Methods.** This study included 191 expectant women who were divided into three groups, based on the birth weight (group 1: < 3,000 g; group 2: 3,000–4,000 g; group 3: > 4,000 g). The values of biochemical (pregnancy associated plasma protein A – PAPP-A, free β human chorionic gonadotropin) and ultrasonographic markers (nuchal translucency) as well as their

multiple of the median (MoM) were determined and compared among groups. **Results.** It was shown that the values of PAPP-A MoM were considerably lower in groups of expectant women that had a fetus with low body weight ($p = 0.003$, $p = 0.001$). Statistically significant correlation between PAPP-A MoM and the newborn's weight ($r_s = 0.221$, $p = 0.001$) was proven among the groups examined within this study. **Conclusion.** The usage of a combination of biochemical parameters, sonographic and demographic data in screening program increases the chances for early identification of fetuses that are under higher risk for growth restriction or increased growth. Also, the increase in the value of PAPP-A MoM causes the increase of fetus' body weight.

Key words:

chorionic gonadotropin, beta subunit, human; diagnosis; fetal growth retardation; forecasting; pregnancy; pregnancy-associated plasma protein-a; pregnancy trimester, first; ultrasonography.

Apstrakt

Uvod/Cilj. Danas se smanjena porođajna masa ploda smatra jednim od glavnih uzročnika nastanka kardiovaskularnih oboljenja ili metaboličkog sindroma koji nastupaju kasnije tokom života. Mnoge studije su pokazale jak uticaj abnormalne porođajne mase ploda na kasniji razvoj, međutim, zbog jačeg uticaja na razvoj jedinke, poseban akcenat se stavlja na smanjenu porođajnu masu u odnosu da povišenu. Još uvek ne postoji test koji bi sa visokoprocenatnom tačnošću jasno klasifikovao trudnice sa visokim rizikom od rađanja deteta s manjom ili većom porođajnom masom s obzirom na gestacijsko doba. Cilj

ovog rada je bio postavljanje modela koji bi mogao upućivati na buduću smanjenu ili prekomernu masu novorođenčeta. **Metode.** Studijom je bila obuhvaćena 191 trudnica, koje su na osnovu telesne mase novorođenčeta, bile podeljene u tri grupe: grupa 1 (> 3 000 g), grupa 2 (3 000–4 000 g), grupa 3 (> 4000 g). Za svaku grupu su određene i međusobno upoređene vrednosti biohemijskih markera (plazma proteina A povezanog sa trudnoćom – PAPP-A i slobodne β jedinice humanog horionskog gonadotropina) i ultrasonografskih markera (nuhalna translucencija), kao i njihovih multiplih medijana (MoM). **Rezultati.** Nađeno je da su vrednosti PAPP-A MoM bile znatno niže u grupama trudnica koje su imale plod sa

malom telesnom masom ($p = 0,003$, $p = 0,011$). Među ispitivanim grupama je dokazana pozitivna, statistički značajna korelacija između PAPP-A MoM i mase novorođenčeta ($r_s = 0,221$, $p = 0,001$). **Zaključak.** Korišćenjem kombinacije biohemijskih parametara, sonografskih i demografskih podataka u *screening* programu uvećava se šansa za ranu identifikaciju fetusa koji su pod povišenim rizikom od restrikcije u rastu ili povećanog

rasta. Takođe, sa porastom vrednosti PAPP-A MoM raste i telesna masa fetusa.

Ključne reči:

horionski gonadotropin, beta subjedunica; dijagnoza; fetus, zaostajanje u rastu; predviđanje; trudnoća; plazma, protein a, udružen sa trudnoćom; trudnoća, prvi trimestar; ultrasonografija.

Introduction

There are just few chapters in humane medicine that largely exceed the ambitions of a discipline that studies them. One of such examples is the entity of children born small or big for the gestational age. Although at first glance it may be regarded as a typical pediatric topic, these issues deserve greater interest of endocrinologists, biochemists, gynecologists.

Even though the impact of adverse factors from the external environment is undisputable, there are disorders that have the roots in the period of fetal growth. Hence, many pathological conditions or diseases during the phase of growing up or during middle age are actually the consequence of a disturbed fetal growth. We may say, fetal growth is a result of many factors, including genetics, nutrition, mother's metabolism, endocrinological factors, the goodness of placental function and perfusion, but also the ability of the fetus itself to respond to all the factors that influence it ¹. Nowadays, low birth weight is considered one of the main causes of cardiovascular diseases or metabolic syndrome that occur later in life. Low birth weight is an important determinant of child's health and a major risk factor for several noncommunicable diseases later in life including coronary heart disease, stroke, hypertension and type 2 diabetes ².

Low levels of plasmatic pregnancy-associated plasma protein-A (PAPP-A) and high levels of free-beta human chorionic gonadotropin (fβ-hCG) could influence the outcome of pregnancy ³. Abdel Moety et al. ⁴ study suggests that first-trimester uterine artery impedance, as measured by Doppler ultrasound as well as low serum biomarkers (β-hCG and PAPP-A) can be used for prediction of preeclampsia and birth weight. Until today, many researchers have tried to find an ideal combination of parameters which would be good indicators of birth weight, however, there is still no test that has high percentage of accuracy to clearly classify expectant women under high risk of giving birth to a child who is too small or too big for the gestational age. Law et al. ⁵ explain that the limitation of these studies is the usage of exclusively one marker in prediction, wrong combination of markers, or usage of a wrong parameter in wrong time. This paper examines the predictive ability of two biochemical markers (PAPP-A, fβ-hCG) in combination with ultrasonographic marker "nuchal translucency" (NT) measured at first trimester. Biochemical parameters may be good indicators of placental, fetal, but also motherly condition, hence biochemical screening may be

used as an additional tool in diagnosing many complications in pregnancy such as: gestational diabetes, pregnancy-induced hypertension, intrauterine fetal suffering, etc. ⁶.

Low birth weight is a much serious issue compared to high birth weight. Existing scientific literature shows a strong correlation between low birth weight and neonatal mortality, which is why this issue is given a lot of significance within public health ⁷.

It was believed for many years that the fetus is a passive user of "uteroplacental capacities". Nowadays, fetal growth is explained as much more complex phenomenon, being a consequence of an active interaction among a mother, placenta and fetus in the process of providing nutrients. Termination or damage caused to any of these components damages the growth potentials. A mechanism of cell proliferation, hypertrophy and differentiation is coordinated by peptide growth factors, but also by other intercellular intermediaries that act in paracrine and autocrine manner.

Many studies have shown that children born small for gestation age (SGA) face higher risk to later develop insulin resistance, obesity, arterial hypertension, dyslipidemia, metabolic disorders of carbohydrates i.e. all components of metabolic syndrome ⁸. Epidemiological studies have proven the connection between adverse intrauterine effects and later risks of facing chronic diseases.

The aim of this study was to establish a model, based on first trimester marker, that could indicate future low or high birth weight.

Methods

Examinees, Ethics statement and clinical information

This study comprises 191 expectant women who had their regular checks in the Center for Women's Reproductive Health of the Primary Health Care Center in Podgorica, Montenegro. The study protocol was reviewed and approved by the Ethics Commission. All expectant women agreed to using the data for the purpose of scientific work. Combined screening for trisomy 21, 18 and 13 has been performed in the laboratory of the Clinical Center of Montenegro in Podgorica, between 10 and 13 weeks gestation.

Based on the birth weight, the examinees were divided into three groups (group 1: < 3,000 g; group 2: 3,000–4,000 g; group 3: > 4,000 g), so the parameters were analyzed and compared by the groups.

Study protocol and measurements

The screening implied the determination of the value of β -hCG and PAPP-A by using a commercial immunofluorescent test (AutoDELFIA), while the results have been expressed in mmol. An ultrasound for a routine ultrasound check of the examinees has been used to determine the dimension of NT (SIMENS, SC2000 ultrasound system).

All measurements of examined biochemical parameters were performed on a device Beckman Coulter Access2, Florida, USA.

Within the risk assessment performed by Double test, the results are expressed as multiple of median (MoM) for a given gestation week. MoM is a statistical measure showing to which extent the result differs from its median in population, and is calculated through a formula given below ⁹.

$$\text{MoM (patient)} = \frac{\text{Result (patient)}}{\text{Median (population)}}$$

A low PAPP-A is defined as a maternal serum PAPP-A value < 0.4 MoM, with increased frequency of adverse obstetrical outcomes noted below this level ¹⁰.

Pearson correlation coefficient was used to determine the correlation between biochemical parameters and future fetal weight.

In cases where a statistically significant difference was found between the methods, receiving operating characteristic (ROC) curves were made to determine the predictor potential of the parameters, while the values are plotted as curve with the corresponding p value.

Results

Table 1 shows mean values and SD, as well as minimum and maximum values in terms of examined variables for three examined groups.

Mean value of biochemical parameter PAPP-A in the group having the birth weight lower than 3,000 g was 1.00 (± 0.71), in the group having the birth weight from 3,000 g to 4,000 g was 1.25 (± 0.71), while in the group having the birth weight above 4,000 g was 1.36 (± 0.99) and that difference was statistically significant ($p = 0.003$) (Figure 1).

Table 1

Descriptive statistical indicators of multiple of median biochemical and ultrasonographic parameters of the examinees in the groups

Parameters	Group 1 (n = 77) < 3,000 g		Group 2 (n = 90) 3,000 g–4,000 g		Group 3 (n = 24) > 4,000 g	
	mean \pm SD	median	mean \pm SD	median	mean \pm SD	median
Biochemical						
PAPP-A MoM	1.00 \pm 0.71	0.86 (0.13–4.86)	1.25 \pm 0.71	1.11 (0.31–4.56)	1.36 \pm 0.99	1.08 (0.31–4.56)
f β -hCG MoM	1.52 \pm 9.02	1.17 (0.16–79.60)	1.24 \pm 0.62	1.14 (0.22–3.69)	1.23 \pm 0.55	1.11 (0.38–2.27)
Ultrasonographic						
NT MoM	0.99 \pm 0.30	0.93 (0.45–1.69)	1.03 \pm 0.28	1.03 (0.43–1.79)	1.11 \pm 0.27	1.10 (0.61–1.69)

PAPP-A – pregnancy-associated plasma protein-A; MOM – multiple of median; f β -hCG – free-beta human chorionic gonadotropin; NT – nuchal translucency; SD – standard deviation.

Description of the groups is given in the paragraph Methods.

The hCG was considered raised if levels were more than 2MoM ¹¹.

Statistical data processing

SPSS statistical program Windows 10 version was used for data processing, working under Microsoft Windows environment. A diagram in the form of curves and dendrograms has been done within Origin statistical program.

A hypothesis on the normality of results distribution has been firstly checked, and depending on that, parameter and nonparameter technics applied. Mann-Whitney U test and Kruskal Wallis H test (non-parameter test) were applied for parameters for which the hypothesis on the normality of results distribution does not apply. For those parameters to which the hypothesis on the normality of results distribution applies, t -test was applied to independent samples of one-factor analysis of the variance (parameter techniques).

Descriptive statistic measures were used for the description of significant parameters: frequency (n), percentage (%), mean value, standard deviation (SD), median and scope.

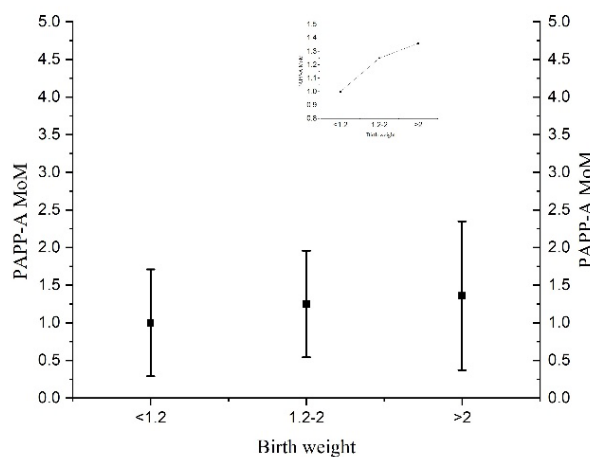


Fig. 1 – An overview of arithmetic mean and a standard deviation, as well as growth trend in terms of parameters PAPP-A MoM for three examined groups of expectant women.

For abbreviations see under Table 1.

In the group of examinees with newborn's birth weight lower than 3,000 g average value of PAPP-A MoM was 1.00, which is statistically considerably lower as compared to the values reached in the group where newborn's weight ranged between 3,000 g to 4,000 g ($p = 0.001$) and in the group higher than 4,000 g ($p = 0.025$), while PAPP-A MoM value did not statistically differ between the groups having the weight 3,000 g–4,000 g and $> 4,000$ g (Table 2).

Mean value of the biochemical parameter $\text{f}\beta\text{-hCG}$ MoM, in the group where the birth weight was lower than 3,000 g was $1.52 (\pm 9.02)$, in the group where birth weight ranged from 3,000 g to 4,000 g was $1.24 (\pm 0.62)$, while in the group where the birth weight was over 4,000 g was $1.23 (\pm 0.55)$. Statistically significant difference in terms of examined parameter among the three groups was not proven ($p = 0.830$) (Figure 2).

Mean value of the ultrasonographic parameter NT MoM in the group where the birth weight was lower than 3,000 g was $0.99 (\pm 0.30)$, in the group where the birth weight ranged from 3,000 g to 4,000 g was $1.03 (\pm 0.28)$, while in the group where the birth weight was over 4,000 g was $1.11 (\pm 0.27)$. Statistically significant difference in terms of examined parameter among the three examined groups was not proven ($p = 0.173$) (Figure 3).

Values of multiple of median PAPP-A lower than 1.2 in the group 1 were found with 61 examinees, interval MoM 1.2–2 was found with 9 examinees, while the values of MoM

higher than 2 were found with 7 expectant women from the group 1.

Values of multiple of median PAPP -A lower than 1.2 in the group 2 were found with 62 examinees, interval MoM 1.2–2 was found with 40 examinees, while the values of MoM higher than 2 were found with 12 expectant women altogether from the group 2.

Values of MoM PAPP -A lower than 1.2 in the group 3 were found with 13 examinees, interval MoM 1.2–2 was found with 8 examinees, while the values of multiple of median higher than 2 were found with 3 expectant women altogether from the group 3.

Statistically significant difference was found in the percentage of the examinees of the group 1 for the interval of MoM lower than 1.2 as compared to the group 2 and the group 3. Intervals of MoM 1.2–2 and > 2 were statistically significantly less present in the group 1 as compared to the groups 2 or 3 ($\chi^2 = 15.03$, $p = 0.005$) (Figure 4).

In the group 1, 39 examinees had the values of $\text{f}\beta\text{-hCG}$ MoM lower than 1.2, 22 examinees had the value of this parameter in the interval from 1.2 to 2, while 16 examinees had the values of $\text{f}\beta\text{-hCG}$ MoM higher than 2.

In the group 2, 63 examinees had the values of $\text{f}\beta\text{-hCG}$ MoM lower than 1.2, 40 examinees had the value of this parameter in interval from 1.2 to 2, while 11 examinees had the values of $\text{f}\beta\text{-hCG}$ MoM higher than 2.

In the group 3, 14 examinees had the values of $\text{f}\beta\text{-hCG}$

Table 2

Results of testing the difference in values of PAPP-A MoM among three examined groups

Comparison	Mann Whitney <i>U</i> test	<i>p</i> -value
Group 1/Group 2	3,159.00	0.001
Group 1/Group 3	643.50	0.025
Group 2/Group 3	1,358	0.957

Group 1: $< 3,000$ g; Group 2: 3,000 g–4,000 g; Group 3: $> 4,000$ g.

For abbreviations see under Table 1.

Description of the groups is given in the paragraph Methods.

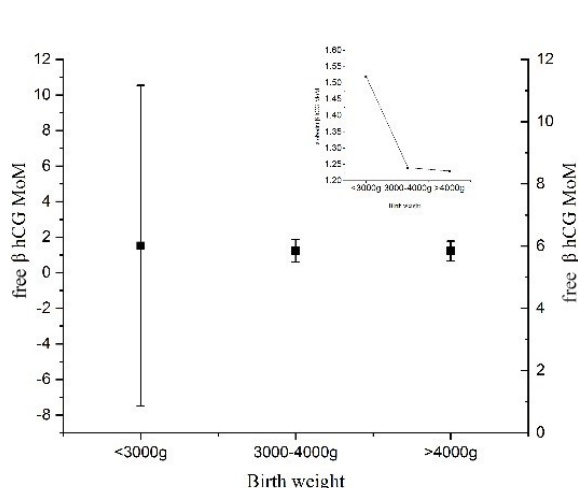


Fig. 2 – An overview of arithmetic mean and a standard deviation as well as a downward trend in terms of parameters $\text{f}\beta\text{-hCG}$ MoM for three examined groups of expectant women.

For abbreviations see under Table 1.

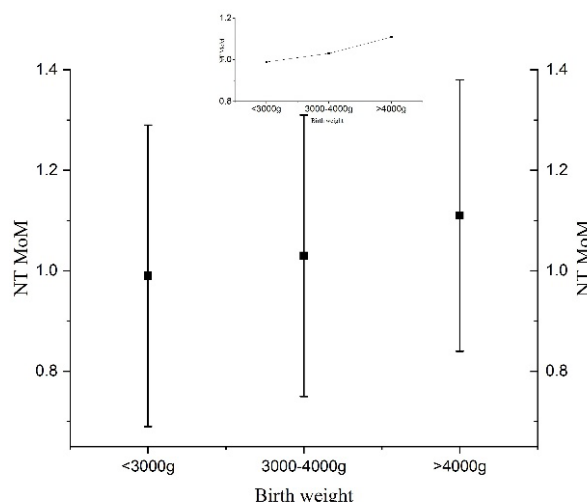
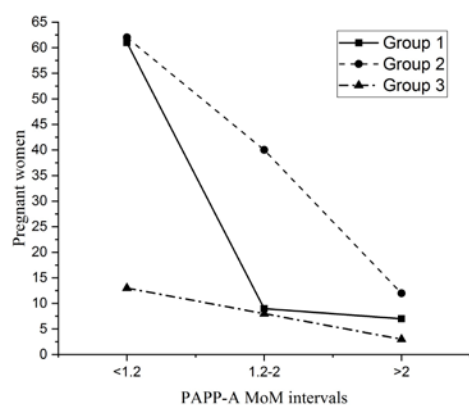


Fig. 3 – An overview of arithmetic mean and a standard deviation as well as the growth trend in terms of NT MoM parameters for three examined groups of expectant women.

For abbreviations see under Table 1.

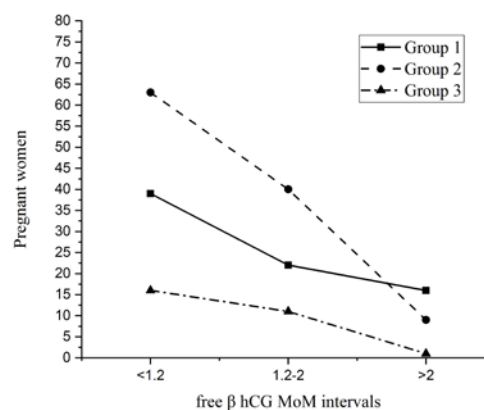


Group1: < 3,000 g; Group 2: 3,000 g–4,000 g; Group 3: > 4,000 g.

Fig. 4 – An overview of the number of examinees with different intervals of MoM PAPP-A in examined groups.

For abbreviations see under Table 1.

Description of the groups is given in the paragraph Methods.

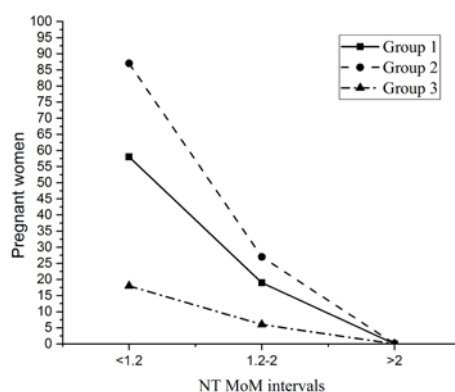


Group1: < 3,000 g; Group 2: 3,000 g–4,000 g; Group 3: > 4,000 g.

Fig. 5 – An overview of the number of examinees with different intervals MoM of fβ-hCG in examined groups.

For abbreviations see under Table 1.

Description of the groups is given in the paragraph Methods.



Group 1: < 3,000 g; Group 2: 3,000 g–4,000 g; Group 3: > 4,000 g.

Fig. 6 – An overview of the number of examinees with different intervals of MoM NT in examined groups.

For abbreviations see under Table 1.

Description of the groups is given in the paragraph Methods.

MoM lower than 1.2, 9 examinees had the value of this parameter in interval from 1.2 to 2, while only 1 examinee had the values of fβ-hCG MoM higher than 2 (Figure 5).

The frequency of the value of fβ-hCG MoM according to different intervals of MoM (< 1.2, 1.2–2, > 2) did not statistically significantly differ as compared to three examined groups of examinees ($\chi^2 = 7.03$, $p = 0.134$).

In the group 1, the values of MoM NT lower than 1.2 were found with 58 examinees, values of MoM in the interval 1.2–2 were found with 19 examinees. None of the examinees in the group 1 had the value of MoM NT higher than 2.

In the group 2, the values of MoM NT lower than 1.2 were found with 87 examinees, values of MoM in the interval 1.2–2 were found with 27 examinees. None of the examinees in the group 2 had the value of MoM NT higher than 2.

In the group 3, the values of MoM NT lower than 1.2 were found with 18 examinees, values of MoM in the interval 1.2–2 were found with 6 examinees. None of the examinees in the group 3 had the value of MoM NT higher than 2.

The frequency of the value of NT MoM according to different intervals of MoM (< 1.2, 1.2–2, > 2) did not statistically significantly differ as compared to three examined groups of patients ($\chi^2 = 0.034$, $p = 0.983$) (Figure 6).

Correlation of NT MoM with PAPP-A MoM or fβ-hCG MoM ($p = > 0.05$) was not proven. What was proven is a weak, positive, statistically significant correlation between PAPP-A MoM and fβ-hCG MoM ($r_s = 0.207$, $p = 0.002$). Therefore, the increase of value in PAPP-A MoM triggers the increase of the value of fβ-hCG MoM.

A correlation of ultrasonographic parameter NT MoM and a biochemical parameter fβ-hCG MoM with birth weight

was not proven, however what was proven is a positive, statistically significant correlation between PAPP-A MoM and newborn's weight ($r_s = 0.221$, $p = 0.001$). The increase in the value of PAPP-A MoM triggers the increase of the fetal body weight (Table 3).

We used the ROC to examine diagnostic validity of the models NT MoM, PAPP-A MoM, fβ-hCG MoM in prediction of birth weight. Only one variable (PAPP-A MoM) gave a unique statistical contribution to the model (Figure 7).

Intervals of MoM showed that the first group of examinees had considerably higher percentage of examinees whose values of PAPP-A MoM were lower than 1.2. ($p = 0.005$). Our results comply with the findings by previous studies^{12–14}.

Some authors also describe a significant positive correlation between concentration of PAPP-A in the first trimester and relative newborn's body weight, and between the concentration of PAPP-A in later pregnancy and newborn's body weight^{14, 15}. Our results confirm these assertions

Table 3

Proven correlations between examined parameters, their correlation with birth weight and demographic characteristics

	NT MoM	PAPP-A MoM	fβ-hCG MoM	Birth weight
NT MoM	1.000			
correlation coefficient				
<i>p</i> -value				
PAPP-A MoM		1.000		
correlation coefficient	-0.008			
<i>p</i> -value	0.905			
fβ-hCG MoM			1.000	
correlation coefficient	-0.046	0.207		
<i>p</i> -value	0.499	0.002		
Birth weight				1.000
correlation coefficient	0.123	0.221	-0.033	
<i>p</i> -value	0.071	0.001	0.632	

For abbreviations see under Table 1.

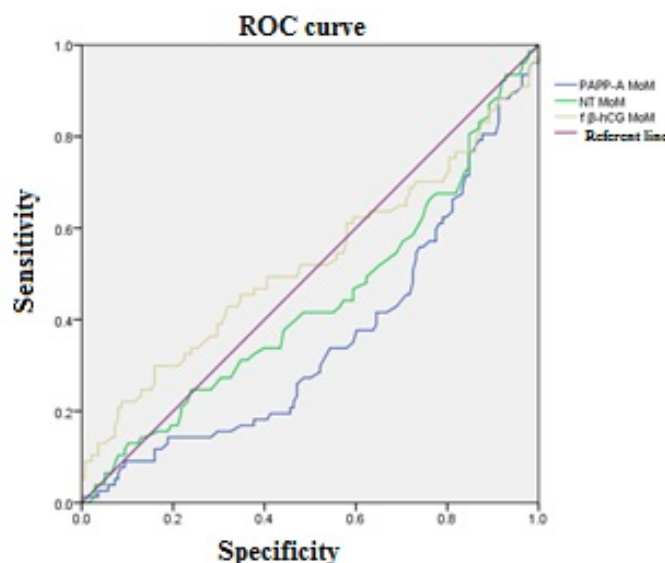


Fig. 7 – Receiver operating characteristic (ROC) curve for inflection points of PAPP-A MoM, fβ-hCG MoM and NT MoM in determining birth weight with 95% confidence interval [Area under ROC curve for PAPP-A MoM: 0.358 ($p = 0.001$); Area under ROC curve for fβ-hCG MoM: 0.044 ($p = 0.557$); Area under ROC curve for NT MoM: 0.042 ($p = 0.138$)].

For abbreviations see under Table 1.

Discussion

By analyzing the values of biochemical parameters among examined groups, this study was found that the values of PAPP-A MoM had been considerably lower in groups of expectant women whose fetus had small body weight ($p = 0.003$, $p = 0.011$). Additionally, comparison of the in-

tervals of MoM showed that the first group of examinees had considerably higher percentage of examinees whose values of PAPP-A MoM were lower than 1.2. ($p = 0.005$). Low concentrations of PAPP-A in the first trimester envisage weak growth of the fetus, however this may indicate the birth of smaller, but completely healthy baby. On the other hand, we may say that smaller placenta is responsible for low fetal growth, therefore, there can exist a subgroup of normal pregnancies where the size and capacity of the placenta cause the fetal growth restriction⁵.

There are opposing opinions related to predictive value of PAPP-A for the occurrence of macrosomia. While some cannot find statistically significant differences in the values of PAPP-A between the expectant women having physiological pregnancy and those with macrosomic fetus, others talk about correlation between PAPP-A and macrosomia^{10, 16}. They explain the correlation with large amount of insulin-like growth factor due to increased values of PAPP-A which stimulates intrauterine growth. We did not proven statistically significant difference in the values of PAPP-A among the examinees, however the analysis of the data clearly indicates the difference among the groups ($G1 = 2.36$, $G4 = 2.65$) which adheres to the results found in 2011 by Tarim et al.¹⁷.

Another study's findings demonstrated that in pregnancies resulting in the birth of small for gestational age (SGA) infants, the maternal serum PAPP-A levels at 11+0 to 13+6 weeks of gestation decrease, and in normal pregnancies, there was a significant association between the serum levels of this metabolite and birth weight, which may be predetermined¹⁸. Our study's results are consistent with the hypothesis that impaired placentation plays a role in the pathogenesis of SGA.

The connection between low PAPP-A values in the first trimester of pregnancy and slow fetal growth, followed by low birth weight later on lies in specific function of pregnancy associated plasma protein A as IGFBP-4 protease. IGFBP-4 is a powerful inhibitor of insulin like growth factor (IGF). IGF plays a significant role in the invasion of trophoblast, influencing early development and vascularization of placenta. Under the influence of PAPP-A, IGF binding protein (IGFBP) cleaves, thus releasing IGF into circulation. In this way, high concentrations of PAPP-A lead to better development of the fetus¹⁹.

Many studies have shown a strong correlation of $\text{f}\beta\text{-hCG}$ and birth weight. A study carried out by Barjaktarović et al.² indicates the existence of the connection between low values of free $\beta\text{-hCG}$ in later stages of the first trimester of pregnancy and higher risk of SGA. A huge study carried out in the Netherlands on a sample of 8,195 expectant women showed a correlation between a $\text{f}\beta\text{-hCG}$ and uterine and fetal functions such as umbilical cord development, suppression of myometrial contractions, the promotion of growth and differentiation of fetal organs but also angiogenesis and regulation of immune tolerance. These findings underline the importance of hCG throughout gestational physiology and suggest that variations in hCG levels may be associated with adverse clinical outcomes such as fetal loss, preeclampsia, preterm delivery and fetal growth restriction and newborn's birth weight²⁰. However, there are studies that prove not such a strong connection between the said parameter and birth weight. The correlation does exist, however, it is considerably lower from those between the PAPP-A and the birth weight²¹. Our research did not prove this con-

nection ($p \geq 0.05$) and the results gained comply with Güdücü et al.²².

Information that low values of $\text{f}\beta\text{-hCG}$ may trigger low birth weight indicate that the birth weight is dependant on the development of placenta during the first and second trimester pregnancy. Free $\beta\text{-hCG}$ is a hormone produced in placenta immediately after implantation, hence low values may indicate a slow or pathological placentation²³.

The results of this study are comparable with the results of the studies that show that the values of $\text{f}\beta\text{-hCG}$ in the serum of an expectant woman measured in the first trimester are almost equal between experimental and control group^{24, 25}. By analyzing the data given in our research, we may notice an upward trend of this parameter with the increase of the body weight of the fetus, which may indicate that actually higher values of $\text{f}\beta\text{-hCG}$ may be predictors of low body weight at birth (body weight $< 2,500 \text{ g} = 78.84$; body weight $> 4,000 \text{ g} = 69.41$). Early vascular damage of the placenta also show decreased oxygenation, which leads to hyperplasia syncytiotrophoblast, and as a consequence of all of this there may occur an increased production of $\text{f}\beta\text{-hCG}$ ²⁶. Further research is needed to identify hCG receptor(s) and associated intracellular signaling cascades and to increase understanding of its role in achieving conception and in pregnancy-related disorders²⁷.

In their research, Poon et al.²⁸ found a considerable increase of fetal nuchal translucence with the increase of fetal weight, as well as that low NT is connected to low fetal body weight. However, our study did not render the same assumption, but we do notice an upward trend of growth of NT with the increase of fetal body weight. The examined groups in this research had little number of expectant women, hence it leaves the room to possibly believe that the conclusions drawn from our research is the result of a low number of samples, hence it requires further and deeper research on bigger study.

Conclusion

By analyzing the values of biochemical parameters among examined groups in this study, a positive, statistically significant correlation between PAPP-A MoM and the newborn's weight ($r_s = 0.221$, $p = 0.001$) has been established. Increase in value of the PAPP-A MoM causes the rise of fetus' body weight. It may be established that using the combination of biochemical parameters, sonographic and demographic data in screening programs increases the opportunity for early identification of fetuses that are exposed to higher risk of future low or high birth weight.

Conflict of interest

None of the authors of this manuscript have a conflict of interest.

R E F E R E N C E S

1. *Cetin I, Alvino G, Radaelli T, Pardi G.* Fetal nutrition: a review. *Acta Paediatr Suppl* 2005; 94(449): 7–13.
2. *Barjaklarovic M, Korevaar TI, Jaddoe VW, de Rijke YB, Visser TJ, Peeters RP, et al.* Human chorionic gonadotropin (hCG) concentrations during the late first trimester are associated with fetal growth in a fetal sex-specific manner. *Eur J Epidemiol* 2017; 32(2): 135–44.
3. *Cignini P, Maggio Savasta L, Gulino FA, Vitale SG, Mangiafico L, Mesoraca A, et al.* Predictive value of pregnancy-associated plasma protein-A (PAPP-A) and free beta-hCG on fetal growth restriction: results of a prospective study. *Arch Gynecol Obstet* 2016; 293(6): 1227–33.
4. *Abdel Moety GA, Almohamady M, Sherif NA, Raslana AN, Mohamed TF, El Moneam HM, et al.* Could first-trimester assessment of placental functions predict preeclampsia and intrauterine growth restriction? A prospective cohort study. *J Matern Fetal Neonatal Med* 2016; 29(3): 413–7.
5. *Law LW, Leung TY, Sabota DS, Chan LW, Fung TY, Lau TK.* Which ultrasound or biochemical markers are independent predictors of small-for-gestational age? *Ultrasound Obstet Gynecol* 2009; 34(3): 283–7.
6. *Tran HA.* Biochemical tests for abnormalities in pregnancy. *Aust Prescr* 2006; 29: 48–52.
7. *Joseph KS, Kramer MS.* Recent trends in infant mortality rates and proportions of low birth weight live births in Canada. *CMAJ* 1997; 157(6): 535–41.
8. *Barker DJ.* The developmental origins of adult disease. *J Am Coll Nutr* 2004; 23(6 Suppl): 588S–95S.
9. *Bishop JC, Dunstan FD, Nix BJ, Reynolds TM, Swift A.* All MoMs are not equal: some statistical properties associated with reporting results in the form of multiples of median". *Am J Hum Genet* 1993; 52(2): 425–30.
10. *Patil M, Panchanadikar TM, Wagh G.* Variation of Papp-A Level in the First Trimester of Pregnancy and Its Clinical Outcome. *J Obstet Gynaecol India* 2014; 64(2): 116–9.
11. *Goto E.* Maternal Blood Biomarkers of Placentation to Predict Low-Birth-Weight Newborns: A Meta-Analysis. *J Obstet Gynecol Canada* 2017; 39(8): 635–44.
12. *Gentile M, Schifano M, Lunardi S, Naninin C, Moscuzza F, Sergiampietri C, et al.* Maternal PAPP-A levels at 11–13 weeks of gestation predict fetal and neonatal growth. *Open J Obstetric Gynecol* 2015; 5(6): 365–72.
13. *Huynh L, Kingdom J, Akhtar S.* Low pregnancy-associated plasma protein A level in the first trimester. *Can Fam Physician* 2014; 60(10): 899–903. (English, French)
14. *Baer RJ, Lyell DJ, Norton ME, Currier RJ, Jelliffe-Pawlowski LL.* First trimester pregnancy-associated plasma protein-A and birth weight. *Eur J Obstet Gynecol Reprod Biol* 2016; 198: 1–6.
15. *Pedersen JF, Sorensen S, Ruge S.* Human placental lactogen and pregnancy-associated plasma protein A in first trimester and subsequent fetal growth. *Acta Obstet Gynecol Scand* 1995; 74(7): 505–8.
16. *Langhoff-Roos J, Wibell L, Gebre-Medhin M, Lindmark G.* Placental hormones and maternal glucose metabolism. A study of fetal growth in normal pregnancy. *Br J Obstet Gynaecol* 1989; 96(3): 320–6.
17. *Tarim E, Hacivelioglu SO, Çok T, Bagis HT.* First trimester maternal serum PAPP-A levels and macrosomia in nondiabetic mothers. *Turk J Med Sci* 2011; 41(4): 581–6.
18. *Sung KU, Rob JA, Eoh KJ, Kim EH.* Maternal serum placental growth factor and pregnancy-associated plasma protein A measured in the first trimester as parameters of subsequent pre-eclampsia and small-for-gestational-age infants: A prospective observational study. *Obstet Gynecol Sci* 2017; 60(2): 154–62.
19. *Tul N, Pusejak S, Osredkar J, Spencer K, Novak-Antolic Z.* Predicting complications of pregnancy with first-trimester maternal serum free-beta-hCG, PAPP-A and inhibin-A. *Prenat Diagn* 2003; 23(12): 990–6. doi:10.1002/pd.735
20. *Korevaar TI, Steegers EA, de Rijke YB, Schalekamp-Timmermans S, Visser WE, Hofman A, et al.* Reference ranges and determinants of total hCG levels during pregnancy: the Generation R Study. *Eur J Epidemiol* 2015; 30(9): 1057–66.
21. *Chang YS, Chen CN, Jeng SF, Su YN, Chen CY, Chou HC, et al.* The sFlt-1/PIGF ratio as a predictor for poor pregnancy and neonatal outcomes. *Pediatr Neonatol* 2017; 58(6): 529–33.
22. *Güdücü N, Gönenç G, İşi H, Yiğiter AB, Dünder İ.* First and second trimester hCG levels have no value in predicting small for gestational age infants. *Cumhuriyet Med J* 2013; 35: 215–20.
23. *Kirkegaard I, Henriksen TB, Uldbjerg N.* Early fetal growth, PAPP-A and free beta-hCG in relation to risk of delivering a small-for-gestational age infant. *Ultrasound Obstet Gynecol* 2011; 37(3): 341–7.
24. *Ong KK, Dunger DB.* Birth weight, infant growth and insulin resistance. *Eur J Endocrinol* 2004; 151 Suppl 3: U131–9.
25. *Smith GC, Stenhouse EJ, Crossley JA, Aitken DA, Cameron AD, Connor JM.* Early pregnancy levels of papp-a and the risk of intrauterine growth restriction premature birth, preeclampsia and stillbirth. *J Clin Endocrinol Metab* 2002; 87(4): 1762–7.
26. *Lin CC, Lindheimer MD, River P, Moawad AH.* Fetal outcome in hypertensive disorders of pregnancy. *Am J Obstet Gynecol* 1982; 142(3): 255–60.
27. *Nwabunobi Ch, Arlier S, Schatz F, Guzeloglu-Kayisli O, Lockwood CJ, and Kayisli U.* hCG: Biological Functions and Clinical Applications. *Int J Mol Sci* 2017; 18(10): 2037.
28. *Poon LC, Maiz N, Valencia C, Pasencia W, Nicolaides KH.* First trimester maternal serum papp-a and preeclampsia. *Ultrasound Obstet Gynecol* 2009; 33(1): 23–33.

Received on March 28, 2020

Revised on May 3, 2020

Accepted on July 6, 2020

Online First July, 2020



Dosimetric verification of clinical radiotherapy treatment planning system

Dozimetrijska verifikacija kliničkog sistema za planiranje radioterapije

Goran Kolarević^{*†}, Dražan Jaroš^{*†}, Goran Marošević^{*†}, Dejan Ignjatić^{*},
Dragoljub Mirjanić[†]

^{*}International Medical Centers Affidea, Center for Radiation Therapy, Banja Luka,
Bosnia and Herzegovina; [†]University of Banja Luka, Faculty of Medicine, Bosnia and
Herzegovina

Abstract

Background/Aim. In the past two decades, we have witnessed the emergence of new radiation therapy techniques, radiotherapy treatment planning system (TPS) with calculating algorithms for the dosage calculation in a patient, units for multislice computed tomography (CT) and image-guided treatment delivery. The aim of the study was investigating the significant difference in dosimetric calculation of radiotherapy TPS in relation to the values obtained by measuring on the linear accelerator (LINAC), and the accuracy of dosimetric calculation between calculating algorithms Analytical Anisotropic Algorithm (AAA) and Acuros XB in various tissues and photon beam energies. **Methods.** For End-to-End test we used the heterogeneous phantom CIRS Thorax002LFC, which anatomically represents human torso with a set of inserts known as relative electron densities (RED) for obtaining a CT calibration curve, comparable to the “reference” CIRS 062M phantom. For the AAA and Acuros XB algorithms and for 6 MV and 16 MV photon beams in the TPS Varian Eclipse 13.6, four 3D conformal (3DCRT), and one intensity modulated (IMRT) and volumetric modulated arc

(VMAT) radiotherapy plans were made. Measurements of the absolute dose in Thorax phantom, by PTW-Semiflex ionization chamber, were carried out on three Varian-DHX LINACs. **Results.** The difference between “reference” and measured CT conversion curves in the bone area was 3%. For 476 phantom measurements, the difference between measured and TPS calculated dose of 3–6%, was found in 30 (6.3%) cases. According to regression analysis, the standardized Beta coefficient for relative errors, 6 MV vs. 16 MV, was 0.337 (33.7%, $p < 0.001$). Mean relative errors for AAA and Acuros XB, using Mann-Whitney test, for bones were 1.56% and 2.64%, respectively ($p = 0.004$). **Conclusion.** End-to-End test on Thorax002LFC phantom proved the accuracy of TPS dose calculation in relation to the one delivered to a patient by LINAC. There was a significant difference for photon energies relative errors (higher values are obtained for 16 MV vs. 6 MV). A statistically significant minor relative error in AAA vs. Acuros XB was found for the bone.

Key words:
algorithms; models, theoretical; radiotherapy;
radiotherapy planning, computer-assisted; thorax.

Apstrakt

Uvod/Cilj. Poslednje dve decenije svedoci smo pojave novih tehnika radijacione terapije, sistema za planiranje tretmana (SPT) radioterapijom sa algoritima za izračunavanje doze kod bolesnika, jedinica za višerednu (*multislice*) kompjuterizovanu tomografiju (KT) i slikom-vođeno praćenje. Cilj rada je bio da se utvrdi da li postoji značajna razlika u izračunavanju doze primenom SPT u odnosu na vrednosti dobijene merenjem na linearnom akceleratoru (LINAC), kao i razlika u tačnosti dozimetrijskog proračuna kalkulacionih algoritama *Analytical Anisotropic Algorithm (AAA)* i *Acuros XB* u zavisnosti od tipa tkiva i energije fotonskih snopova. **Metode.** Za *End-to-End* test koristili smo heterogeni fantom CIRS Thor-

ax002LFC, koji anatomski odgovara ljudskom torzu sa setom umetaka poznate relativne elektronske gustine za dobijanje KT kalibracione krive, koja se poredi sa referentnim vrednostima, dobijenim CIRS 062M fantomom. Za *AAA* i *Acuros XB* algoritme kao i za 6 MV i 16 MV fotonske snopove u *SPT Varian Eclipse 13.6*, napravljena su četiri 3D konformalna (3DCRT), jedan intenzitetom modulisan (IMRT) i jedan zapreminski modulisan lučni (VMAT) plan radioterapije. Merenja apsolutne doze u mernim pozicijama *Thorax* fantoma, jonizacionom komorom *PTW-Semiflex*, sprovedena su na tri *Varian-DHX* LINAC-a. **Rezultati.** Razlika „referentne” i merene KT konverzije krive u oblasti kostiju bila je 3%. Od ukupno 476 mernih tačaka, razlika između izmerene i SPT izračunate doze od 3–6%, je nađena u 30 tačaka (6.3%).

Regresionom analizom je utvrđen standardizovani koeficijent Beta za relativne greške, 6 MV vs. 16 MV, koji je iznosio 0,337 (33,7%, $p < 0,001$). Srednje vrednosti relativnih grešaka za AAA i Acuros XB za kosti, koristeći Mann-Whitney test, su bile 1,56% i 2,64% ($p = 0,004$). **Zaključak.** End-to-End test na Thorax002LFC fantomu je dao potvrdu ispravnog računanja doze primenom SPT u odnosu na dozu isporučenu pacijentu pomoću LINAC-a.

Introduction

It is beyond any doubt that modern radiotherapy (RT) technologically represents the most complex branch of medicine today. In the treatment of malignant diseases, as a cure, we use ionizing radiation directed towards the volume in which the tumor cells are located in order to permanently destroy them with the maximum possible protection of the surrounding healthy tissue.

In the past two decades, with the development of information technology, we have witnessed the emergence of the new ones: radiation therapy techniques, radiotherapy treatment planning systems (TPS) with calculating algorithms for the dosage calculation in a patient, units for multislice computed tomography (CT) and image-guided treatment delivery, which enables better and more precise treatments for patients.

Based on the data set previously measured on the Linear accelerator (LINAC) and CT simulator, TPS calculates three-dimensional (3D) dose distribution in a patient. Unfortunately, many cases of incorrect data imports and usage of TPS were published, which also led to accidents with lethal outcomes^{1,2}.

Namely, 28% of accidents in RT are due to the wrong TPS dose calculations caused by: poor knowledge of TPS, incorrect data entered in TPS and lack of TPS calculation quality assurance (QA) – QA TPS³. International recommendations are that the delivered dose of radiation in the patient is no more than 5% different than prescribed, and the incidence of TPS calculation errors is less than 3–4% depending on the complexity of the RT treatment and anatomy. On the other hand, sub-dosage of the tumor of 5% affects the reduction of the treatment curability by around 20%, which points to the importance of the accuracy and precision of each procedure performed during the implementation of RT treatment⁴.

Therefore, the implementation of the QA-TPS procedure (such as the End-to-End test) for TPS in RT is crucial for reducing the number of accidents. There are several studies that have helped develop guidelines and protocols for LINAC-based QA TPS for 3D Conformal Radiotherapy (3DCRT)⁵⁻⁸ and Intensity Modulated Radiotherapy (IMRT)^{9,10} depending on the calculation algorithm used in TPS^{11,12}. Nowadays, in addition to 3DCRT and IMRT radiation techniques, volumetric modulated arc therapy (VMAT) is also used in routine practice.

It is clear that preparation and implementation of an End-to-End test is of great importance, which is used to con-

Postojala je značajna razlika između fotonskih energija relativnih grešaka (dobijene su veće vrednosti za 16 MV u odnosu na 6 MV). Utvrđena je statistički značajno manja relativna greška za kost kod AAA u odnosu na AcurosXB.

Ključne reči:

algoritmi; modeli, teorijski; radioterapija; radioterapija, kompjutersko planiranje; toraks.

trol the overall precision of the entire RT chain. It is made up of a set of practical tests conducted on a heterogeneous phantom. In general, the End-to-End test consists of recording a calibration curve on a CT simulator and comparing it with a reference (entered into TPS), as well as creating characteristic RT plans of all RT techniques, energies of photon beams and calculating algorithms, irradiation-prepared plans on LINAC and measuring doses in defined phantom positions (tissue types).

Based on the End-to-End test, we have launched a dosimetric study to investigate: a) whether there is a significant difference in the dosimetric calculation of TPS (for: 3DCRT, IMRT and VMAT radiation techniques) in relation to the value obtained by LINAC measuring in the phantom, b) whether there is a significant difference in the accuracy of the dosimetric calculation between the calculation algorithms Analytical Anisotropic Algorithm (AAA) and Acuros XB, depending on the type of tissue in which the dose is applied and on photon beam energies.

Methods

Under the same, standardized, methodological principles, this study investigated the influence of various RT factors: radiation techniques, photon beam energy, calculation algorithm and tissue types, in regards to the TPS calculated dose.

Dosimetric tests cover all techniques of external beam radiotherapy (EBRT) and anatomical structures are similar to those encountered while working with patients.

All-round testing was carried out at the same facility in a relatively short period of time by engaging the same professional team, which generally implies repeatability and accuracy of the measurement.

Phantom

In all segments of this study, the heterogeneous phantom CIRS Thorax002LFC (Computerized Imaging Reference Systems Inc., Norfolk, Virginia) was used. The phantom anatomically represents the average human torso (30 cm long, 30 cm wide and 20 cm thick). It is made of plastic water, lungs (density 0.21 g/cm³) and bone-spinal cord (1.6 g/cm³), with 10 cylindrical inserts where the ionization chamber can be placed (Figure 1) and the dose measured at the particular place. The phantom also has a set of inserts (muscle, bone, lung and adipose equivalent tissue) of the known relative electron densities (RED)¹³.

Scanning the phantom on a CT simulator

The Thorax002LFC phantom was scanned on a sixteen-slice CT simulator LightSpeed (GE, Boston, Massachusetts). The gantry width bore 80 cm diameter, at a voltage in the X ray tube of 120 kV (thorax protocol). First, it was scanned with inserts of the known electron density in order to obtain the CT calibration curve that is the ratio between RED and Hounsfield units (HU). The materials used are in the range of -1000 for air, 0 for water and 1,000 HU for materials that simulate the bone. The obtained curve was compared with the “reference” curve in TPS, which was created by scanning the CIRS 062M phantom (25 cm long, 33 cm wide and 27 cm dense) that possesses 16 inserts with a known RED under the same conditions of the CT simulator. Acceptable difference RED for the same HU value, between curves, was ± 0.02 (ie. ± 20 HU for the same RED value, except for water ± 5 HU)⁴. The second time, the Thorax002LFC phantom was scanned (thorax protocol) with the cor-

responding cylindrical tissue inserts (Figure 1), for the making of a set of RT plans in the TPS.

The creation of clinical RT plans for dosimetric measurements

For study purposes, in the EBRT radiotherapy planning system Varian Eclipse 13.6 (Varian, Medical Systems, Palo Alto, California), six RT plans were made, four 3DCRT⁵, one IMRT and VMAT¹⁰. All plans were made for two photon energies 6 MV and 16 MV, as well as for two calculating algorithms: AAA and Acuros XB. This way, the isodose distribution in the phantom was obtained, ie. we got the absolute dose in different tissues (measuring points).

The beams geometry and the isodose distribution, as well as the position of the measuring points of the 3DCRT plans, are shown in Figure 2, while the detailed parameters of the plans are given in Table 1.

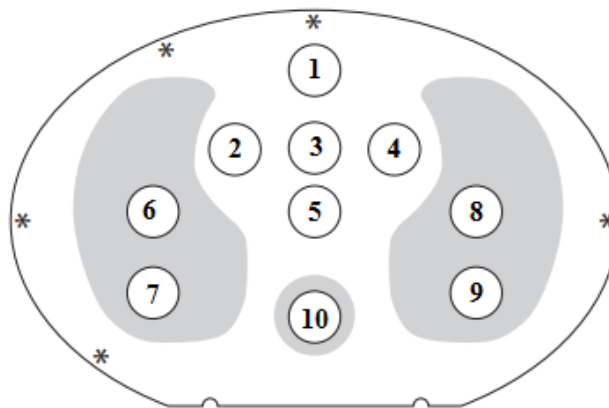


Fig. 1 – CIRS Thorax002LFC phantom with inserts for the soft tissue (1–5), lungs (6–9) and bone¹⁰.

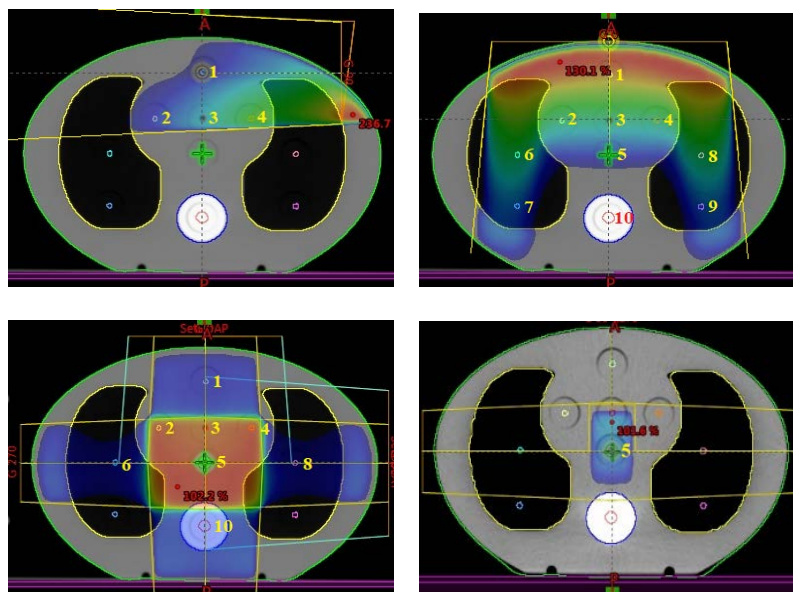


Fig. 2 – CIRS Thorax002LFC phantom with measuring points (1–10), beam geometry and isodose distribution for four 3DCRT RT plans (clinical tests 1–4).

For the purposes of making IMRT and VMAT RT plans, at the transverse CT slices of the CIRS Thorax002LFC phantom, planning target volume (PTV) and the heart are contoured at the length of 8 cm, while the lung and spinal cord are contoured to the entire length of the phantom (Figure 3)¹⁰. Detailed geometric-dosimetric parameters of these plans with dose limits for organs at risk (OAR) are given in Table 2.

Measurements on LINACs

The measurements were carried out on three Varian DHX LINACs (Varian Medical Systems, Palo Alto, California), with multi leaf collimator (MLC) Millennium120 and

nominal photon energies of 6 MV and 16 MV. One of the LINACs has no option of VMAT delivering.

To measure the absolute dose in the defined measuring positions of the Thorax002LFC phantom, we used the PTW-Semiflex 0.125 cm³ ionization chamber (Freiburg, Germany) with the SuperMax electrometer (Standard Imaging Inc., Middleton, Wisconsin). The ionization chamber and the electrometer were previously calibrated in the secondary standard dosimetry laboratory. Measurement uncertainty (for the measuring chain) is expressed as combined and expanded measurement uncertainty with expansion factor $k = 2$ (95%).

The absorbed dose at all the measuring points was determined based on the IAEA TRS 398 protocol¹⁴. In the lungs and materials equivalent to the bone, doses are meas-

Table 1

Geometric parameters of 3DCRT plans

Clinical test 1	Clinical test 2	Clinical test 3	Clinical test 4
SSD 100 cm	SAD, isocentre at point 1	SAD, isocentre at point 5	SAD, isocentre at point 5
1 direct field	1 tangential field	4 fields-box	3 non-coplanar fields
FS 20 × 10 cm ²	FS 15 × 10 cm ²	FS AP and PA 15 × 10 cm ²	FS 4 × 4 cm ² , G 30°, C 0°, Table 90°
G and C angle 0°	G and C 90°, wedge 60°	FS LatLeft and Right 15 × 8 cm ²	FS LatLeft 4 × 16 cm ² , G 90°, C 60°
Deliver 2 Gy to point 3	Deliver 2 Gy to point 1	Deliver 2 Gy to point 5	Deliver 2 Gy to point 5
Measurement points: 1–10	Measurement points: 1–4	Measurement points: 1–6, 8, 10	Measurement point: 5

FS - field size; G – gantry; C – collimator.

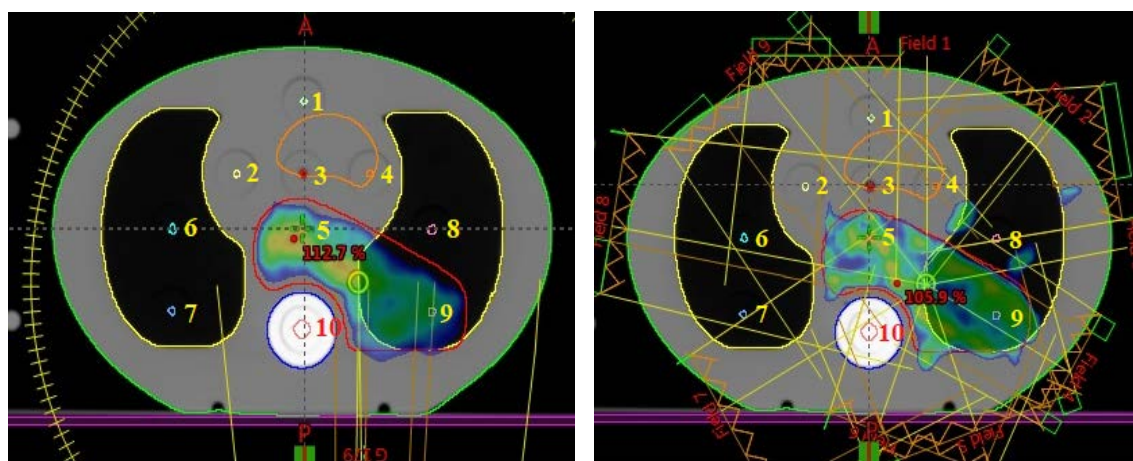


Fig. 3 – Intensity Modulated Radiotherapy (IMRT) and volumetric modulated arc therapy radiotherapy (VMAT RT) plans with beam geometry and isodose distributions, as well as the locations of measuring points (1–10).

Table 2

Geometric parameters of Intensity Modulated Radiotherapy (IMRT) and volumetric modulated arc therapy radiotherapy (VMAT RT) plans with dose limits for organ at risk (OAR)

Clinical test 5 IMRT	Clinical test 6 VMAT RT
SAD-9 IMRT fields	SAD-1 full arc
K 0°, G: 0, 40, 80, 120, 160, 200, 240, 260 and 320°	K 30°, G: 181–179°, clockwise
Deliver 2 Gy to PTV (100% at target mean)	
Dose constraints for OAR	
Spinal cord: $D_{\max} < 75\%$ of the prescribed dose	
Total lung: $D_{20\%} < 35\%$	
Heart: $D_{\max} < 55\%$ of the prescribed dose	
Measurement points: 1–10	

ured in small water volumes (the volume of ionization chamber) within these materials. Therefore, the measured doses in these points may have a larger error than the spots in plastic water. The influence of these small water volumes can be increasing the calculated dose up to 2% for a material equivalent to the lungs and 0.3% for a material equivalent to the bone¹⁵.

The total number of measuring points on three LINACs was 476, that is, 132 on LINAC 1 (92 for 3DCRT and 40 IMRT), 172 on LINAC 2 (92 3DCRT and 40 IMRT/VMAT) and 172 on LINAC 3 (92 3DCRT and 40 IMRT/VMAT). Divided by tissues, 280 measurements were done on soft tissue, 152 in the lungs, and 44 in the bone. Two hundred and thirty-eight measurements were done on photon beams 6 MV and 16 MV, as well as with calculating algorithms AAA and Acuros XB.

Statistical analysis

Due to a limited number of measuring positions in the Thorax002LFC phantom, the evaluation of the absolute dose values measured at each measuring position on LINAC (D_{meas}) and calculated on TPS (D_{cal}) was normalized with the dose measured at the reference point ($D_{\text{meas,ref}}$) for each test. Therefore, the equation for calculating the relative error is:

$$X (\%) = 100 * [(D_{\text{cal}} - D_{\text{meas}}) / D_{\text{meas,ref}}] \quad (1)$$

Allowed deviations for 3DCRT plans were 2–4%, while for IMRT/VMAT they were 3–4%.

Data are presented as arithmetic mean value with standard deviation (SD) or confidence interval (CI). The Kolmogorov-Smirnov test was applied to assess the normality of the studied continuous data.

Strength of the association between independent factors (accelerators, algorithms, tissues, photon energies, tests) and relative error data (dependent factor) were determined by using univariate and multiple linear regression analyses. Further detailed assessment was carried out using GLM univariate ANOVA (*post hoc* Bonferroni test) and Mann-Whitney *U* tests. All the analyses were estimated at minimal $p < 0.05$ level of statistical significance.

Complete statistical analysis of the data was done with the statistical software package SPSS Statistics 18 (USA).

Results

By measuring HU values for known RED values, we obtained the CT conversion curve for the CIRS Thorax002LFC phantom. The obtained curve was compared with the “reference” (TPS) curve, where the difference in the area of large electronic densities is seen, while in the lower density region, the match is within the allowed values. The RED values for bones (829 HU) differ by 3% while the difference in HU (RED 1.51) is 10% (Figure 4).

The differences between measured and TPS calculated doses at different measuring points (tissues) and RT plans (case 1–6), with values of tolerances (agreement criteria)

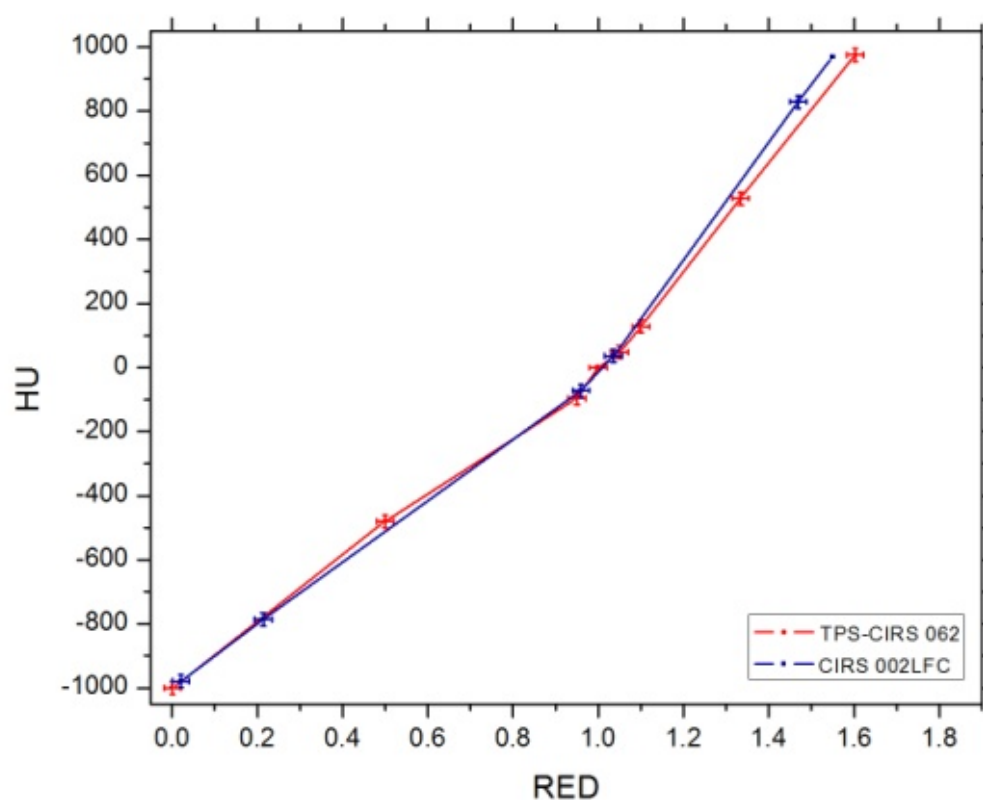


Fig. 4 – Shows of CT calibration curves obtained by CIRS Thorax002LFC and CIRS 062M phantom (“reference” curve located in treatment planning system –TPS).

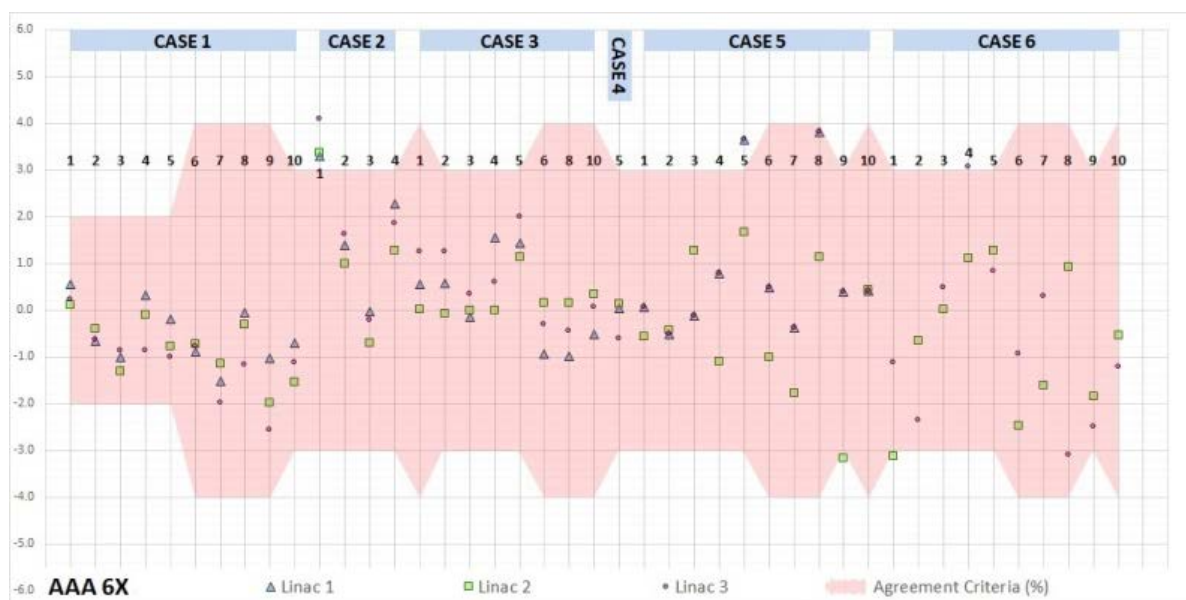
measured on three LINACs are presented in Figures 5 and 6. The results are grouped by calculating algorithms and photon beam energies.

Of the total 476 measuring points, the difference between measured and those TPS calculated doses greater than 4%, we had at 11 points (2.3%), 4–5% at 10 points (2.1%) and 5–6% at one position (0.2%). A 3–4% deviation was recorded at 19 measuring points (4%). The calculated (TPS) dose was in 353 cases (74.2%) lower than the measured and in 123 measurements (25.8%) higher.

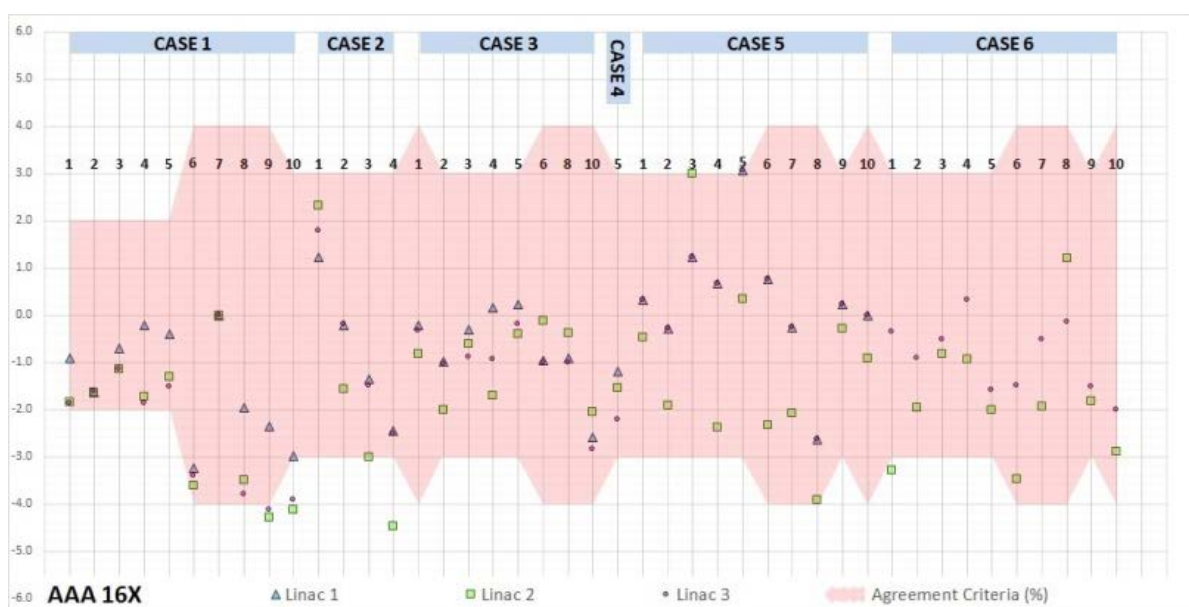
As Kolmogorov-Smirnov test revealed non-normal distribution of relative errors, some data transformation was necessary.

Firstly, negative sign marks obtained at any point, were corrected by adding corresponding fix value to all data. In this way, all relative errors have become positive. In the second part, these data were further transformed by applying $\log_{10}(X)$ transformation and used in all presented analyses.

Using the univariate and multivariate regression analyses, the effect of independent (explanatory) variables

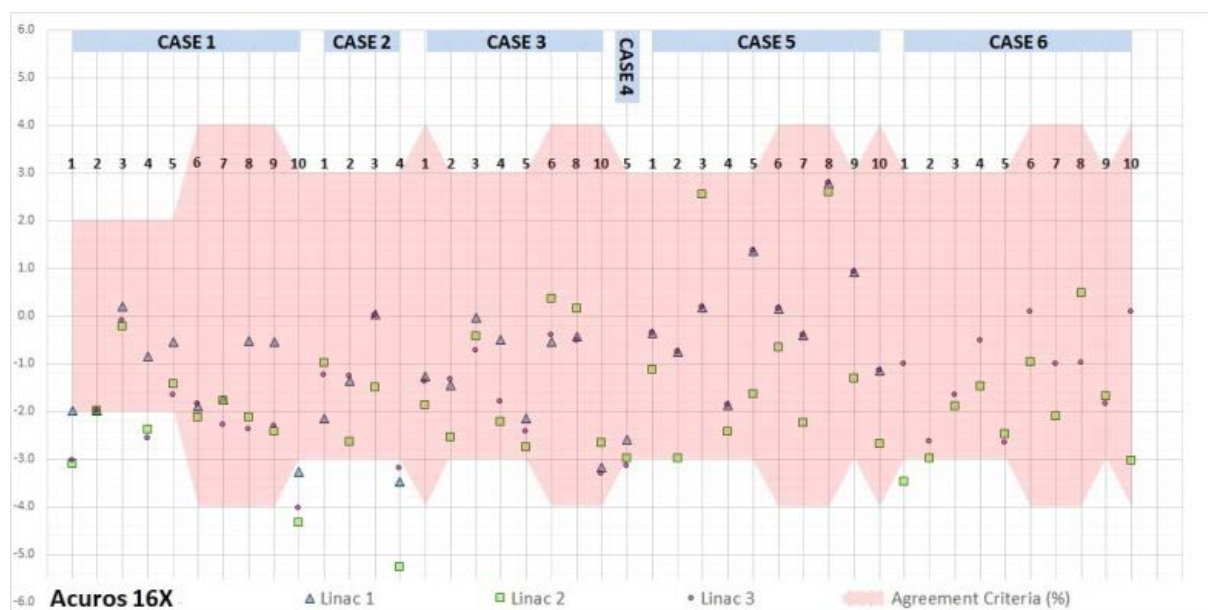


a)

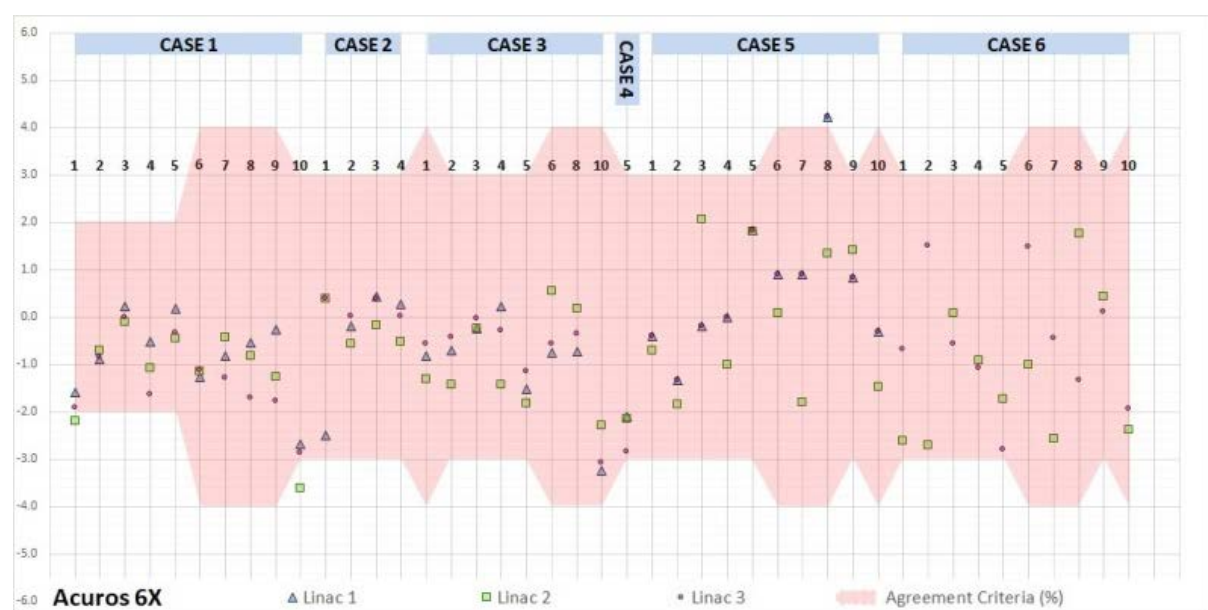


b)

Fig. 5 – Difference between measured and treatment planning systems (TPS) calculated doses in each of the tests (cases) and measuring points for the Analytical Anisotropic Algorithm (AAA) calculation algorithm:
a) 6 MV photon beam; b) 16 MV photon beam.



a)



b)

**Fig. 6 – Difference between measured and treatment planning systems (TPS) calculated doses in each of the tests (cases) and measuring points for the AcurosXB calculation algorithm:
a) 6 MV photon beam; b) 16 MV photon beam.**

on the relative errors X (%) was examined (Table 3).

Employing the univariate analysis of variance (GLM model, ANOVA), we examined the main effects of independent predictors on the relative error X (%), as it is presented in Table 4. Because of the large number of potential interactions of independent variables (total of 26), their effects on the measured results have not been shown.

For independent predictors, in which a statistically significant effect was found for the relative errors (devia-

tions), the significance of the differences between the mean values of the relative errors of certain categories was investigated, using the Bonferroni test (ie. steam comparisons). The overview of this analysis is given in Table 5.

In addition, we investigated the magnitude of the mean value of the relative errors, depending on the calculation algorithms and tissue types with the Mann-Whitney U test (Table 6).

Table 3**Univariate and multiple linear regression analysis of independent factors potentially associated with inaccurate dose calculation (measured vs. calculated).**

Independent variables	Univariate		Multiple	
	Beta (95% CI)	<i>p</i>	Beta (95% CI)	<i>p</i>
LINAC (1–3)	-0.013 (-0.018–0.013)	0.769	0.009 (-0.012–0.015)	0.825
Algorithm (AAA vs. Acuros XB)	0.112 (-0.006–0.054)	0.015	0.112 (0.009–0.052)	0.006
Tissue (soft vs. lung vs. bone)	0.259 (0.035–0.071)	< 0.001	0.272 (0.039–0.072)	< 0.001
Energy (6 MV vs 16 MV)	0.337 (-0.068–0.114)	< 0.001	0.337 (0.069–0.113)	< 0.001
Case (1–6)	-0.163 (0.005–0.018)	< 0.001	-0.183 (-0.007–0.019)	< 0.001

Beta – standardised regression coefficient; CI –confidence interval (unstandardized coefficient B).

Table 4**GLM univariate ANOVA (main effects of independent variables)**

Parameters	F	<i>p</i>
LINAC (1–3)	1.546	0.215
Algorithm (AAA vs. Acuros XB)	15.591	< 0.001
Tissue (soft tissue vs. lung vs. bone)	30.309	< 0.001
Energy (6 MV vs. 16 MV)	51.432	< 0.001
Case (1–6)	14.230	< 0.001

GLM – General Linear Model; AAA – Analytical Anisotropic Algorithm.

Table 5**Significance of differences in: calculating algorithms, tissue type, photon beam energy and radiation techniques (cases), using the Bonferroni test**

Parameters	Deviation (%), absolute values		<i>p</i> *
	n	mean ± SD	
Algorithm			
AAA (1)	238	1.36 ± 1.10	< 0.001 (1 : 2)
Acuros XB (2)	238	1.46 ± 1.06	
Tissue			
soft tissue (1)	280	1.26 ± 0.99	1.000 (1 : 2)
lung (2)	152	1.48 ± 1.10	< 0.001 (1 : 3)
bone (3)	44	2.10 ± 1.27	< 0.001 (2 : 3)
Photon beam energy			
6 MV (1)	238	1.12 ± 0.94	< 0.001 (1 : 2)
16 MV (2)	238	1.69 ± 1.13	
Case			
1	120	1.59 ± 1.15	< 0.001 (1 : 2)
2	48	1.51 ± 1.31	< 0.001 (1 : 3)
3	96	1.00 ± 0.87	< 0.001 (1 : 5)
4	12	1.80 ± 1.09	0.003 (1 : 6)
5	120	1.41 ± 1.07	0.033 (4 : 5)
6	80	1.50 ± 0.95	> 0.044 (5 : 6)

AAA – Analytical Anisotropic Algorithm; SD – standard deviation;

***post hoc Bonferroni test.**

Table 6**Algorithms and tissue depending differences**

Tissue	AAA		Acuros XB		<i>p</i> *
	Mean (%)	95% CI	Mean (%)	95% CI	
Soft	1.15	0.99–1.31	1.37	1.20–1.54	0.072
Lung	1.68	1.40–1.97	1.27	1.07–1.47	0.085
Bone	1.56	1.01–2.10	2.64	2.16–3.13	0.004

AAA – Analytical Anisotropic Algorithm; CI – confidence interval.

***Mann-Whitney *U* test.**

Discussion

Based on the comparison of the reference and measured conversion curves, we established a difference in the area of higher electronic densities (RED values for bones vary by 3%), while in lower density areas, the match is within the allowed values (Figure 4). However, it is estimated that the difference of 8 in the bone relative electron density affects dose TPS calculation accuracy less than 1%¹⁶.

Out of the total 476 measuring points, the deviation between TPS calculated and measured doses of 3–6% was obtained in 30 measuring points (6.3%) (Figures 5 and 6).

The measured dose was in 188 (79%) cases higher than TPS calculated for Acuros XB, while in the case of AAA the same was noticed in 165 (69.3%) cases.

Depending on the tissue type, the measured dose in bone was in 88.6% of the cases higher than the calculated one, for the lungs in 76.3% and soft tissue in 70.7% of the cases.

When the bone tissue is analyzed independently, the Acuros XB led in 95.5% of points to the increased measured dose in relation to the calculated (81.8% in the case of the AAA algorithm application).

Based on the univariate and multivariate regression analyses, we could notice a significant influence of calculating algorithms, tissue type, photon beam energy and test type (Cases 1–6) on the relative error (deviation) in both models (Table 3). These data indicate that these variables are significant independent predictors with an influence on the size of the relative error. Depending on the LINACs, there was no significant effect on the size of the relative error. Based on the value of the standardized Beta coefficient (Table 3), the greatest influence on the relative error was the photon beam energy (Beta = 0.337; 33.7%), then the tissue type (Beta = 0.272; 27.2), test types (Beta = -0.183; 18.3%) and the applied calculation algorithm (Beta = 0.112; 11.2%). The direction of the sign (+ or -) indicates that greater relative errors can be expected when using 16 MV in comparison to 6 MV (which is in accordance with the results of the studies by Rutonjski et al.¹⁵, Gershkevitch et al.¹⁷ and Knoos et al.¹⁸) in the bone tissue compared to the soft tissue and lungs, in tests cases 1 and 2 (compared to other cases) and in the application of the calculation algorithm Acuros XB vs. AAA.

Using the univariate analysis of variance (GLM model, ANOVA), this study confirmed significant effects on the relative error (previously obtained by univariate and multivariate regression analysis), depending on the applied calculation algorithm, type of tissue, photon beam energy and test type (Table 4).

If we focus on the specific research objectives of this study, the supplementary (*post hoc*) analysis (Bonferroni

test, Table 5) shows that the Acuros XB calculating algorithm leads to a statistically significant increase in the relative error compared to the AAA. The highest values of the relative error were registered for bone tissue (2.10 ± 1.27).

By comparing the AAA and Acuros XB calculating algorithms, a statistically significant difference in registered relative errors in the bone was shown (Table 6). The corresponding mean values and 95% of the confidence limit were 1.56% for the AAA algorithm and 2.64% for Acuros XB.

The fact that with the applied calculation algorithms there is no overlap of the 95% of confidence limits indicates a statistically significant difference for the bone. Applied calculating algorithms lead to approximately the same (statistically non-significant) relative errors in the soft tissue and lungs (which is opposite to the Schiefer et al.¹⁰ study, which established the same degree of accuracy of the two algorithms except for the lungs, where Acuros XB has a smaller relative error).

The design of the study also caused the appearance of certain weaknesses primarily in the statistical part of the examination. In the case of simultaneous examination of multiple independent variables (multiple regression analysis, GLM univariate ANOVA with multiple independent variables), ideally the highest reliability was obtained when the number of samples in each group was approximately the same. Phantom characteristics (the unequal number of measuring points related to the tissue type) significantly contributed to this problem.

The selected statistical methods due to their robustness and reliability, but also the fact that different statistical techniques confirm the results of the test, indicate that there is a large extent of correctness in our conclusions.

Conclusion

The performed End-to-End test on the heterogeneous phantom CIRS Thorax002LFC gives us a confirmation of the correct TPS dose calculation (for all EBRT techniques, photon beam energy, calculating algorithms and different tissue types) and delivery to a patient on LINAC in our RT center daily clinical practice. The mentioned phantom in practice can be used for control, but not for obtaining a reference calibration curve. The analysis of the results has showed that there is no statistically significant difference between the LINAC, but it exists between photon energies (greater relative errors can be expected when using 16 MV compared to 6 MV). In addition to the calculation algorithms (AAA vs Acuros XB), there were no significant differences in soft tissue and lung relative errors, but for the bone there was a difference in favor of AAA.

REFERENCES

1. International Atomic Energy Agency (IAEA). Lessons Learned from Accidental Exposures in Radiotherapy, Safety Reports Series No. 17. Vienna: IAEA; 2000.
2. IAEA. Investigation of an Accidental Exposure of Radiotherapy Patients in Panama. Vienna: IAEA. 2001.
3. Task Group on Accident Prevention and Safety in Radiation Therapy. Prevention of accidental exposures to patients undergoing radiation therapy. A report of the International Commission on Radiological Protection. Ann ICRP 2000; 30(3): 7–70.

4. Technical Reports Series No. 430. Commissioning and quality assurance of computerized planning systems for radiation treatment of cancer. Vienna: International Atomic Energy Agency; 2004.
5. IAEA-TECDOC-1583. Commissioning of radiotherapy treatment planning systems: testing for typical external beam treatment techniques. Report of the Coordinated Research Project (CRP) on Development of Procedures for Quality Assurance of Dosimetry Calculations in Radiotherapy. Vienna: International Atomic Energy Agency; 2008. (English, Russian)
6. Mijnheer B, Olszewska A, Florin C, Hartmann G, Knows T, Rosendale JC, et al. ESTRO Booklet No. 7. Quality assurance of treatment planning systems. Practical examples for non-IMRT photon beams. Brussels: ESTRO; 2005.
7. Fraass B, Doppke K, Hunt M, Kutcher G, Starkschall G, Stern R, et al. American Association of Physicists in Medicine Radiation Therapy Committee Task Group 53: quality assurance for clinical radiotherapy treatment planning. *Med Phys* 1998; 25(10): 1773–829.
8. AAPM. Report No. 055 – Radiation Treatment Planning Dosimetry Verification 1995. Alexandria, VA: AAPM American Association of Physicists in Medicine; 1995.
9. TG-119 IMRT Commissioning Tests Instructions for Planning, Measurement, and Analysis Version 10/21/2009. Alexandria, VA: AAPM American Association of Physicists in Medicine; 2009.
10. Schiefer H, Fogliata A, Nicolai G, Cozzi L, Selenga W, Born E, et al. The Swiss IMRT dosimetry intercomparison using a thorax phantom. *Med Phys* 2010; 37(8): 4424–31.
11. Gifford K, Followill D, Liu H, Starkschall G. Verification of the accuracy of a photon dose-calculation algorithm. *J Appl Clin Med Phys* 2002; 3(1): 26–45.
12. Brittan K, Rather S, Newcomb C, Murray B, Robinson D, Field C, et al. Experimental validation of the Eclipse AAA algorithm. *J Appl Clin Med Phys* 2007; 8(2): 76–92.
13. CIRS Tissue Simulation & Phantom Technology. IMRT Thorax phantom Model 002LFC, user guide. Available from: www.cirsinc.com/radiation-therapy
14. Technical Reports Series No. 398. Absorbed dose determination in external beam radiotherapy. An International Code of Practice for Dosimetry Based on Standards of Absorbed Dose to Water. Vienna: International Atomic Energy Agency; 2000.
15. Rutonjski L, Petrolić B, Baikal M, Teodorović M, Čudić O, Gershkevitch E, et al. Dosimetric verification of radiotherapy treatment planning systems in Serbia: national audit. *Radiat Oncol* 2012; 7(1): 155.
16. Thomas SJ. Relative electron density calibration of CT scanners for radiotherapy treatment planning. *Br J Radiol* 1999; 72(860): 781–6.
17. Gershkevitch E, Schmidt R, Velež G, Miller D, Korf E, Yip F, et al. Dosimetric verification of radiotherapy treatment planning systems: results of IAEA pilot study. *Radiother Oncol* 2008; 89(3): 338–46.
18. Knöös T, Wieslander E, Cozzi L, Brink C, Fogliata A, Albers D, et al. Comparison of dose calculation algorithms for treatment planning in external photon beam therapy for clinical situations. *Phys Med Biol* 2006; 51(22): 5785–807.

Received on April 11, 2020

Revised on April 18, 2020

Accepted on July 6, 2020

Online July, 2020



Selection of the optimal medical waste incineration facility location: A challenge of medical waste risk management

Izbor optimalne lokacije postrojenja za spaljivanje medicinskog otpada: izazov u upravljanju rizikom od medicinskog otpada

Kristina Stanojević*, Goran Radovanović†, Dragana Makajić-Nikolić*,
Gordana Savić*, Barbara Simeunović*, Nataša Petrović*

*University of Belgrade, Faculty of Organizational Sciences, Serbia; †University of
Defence, Rectorate, Belgrade, Serbia

Abstract

Background/Aim. Among the other challenges of the 21st century, medical waste (MW) has become an arising problem for both the environment and people because of its increasing amount, variety, and complexity. That is way MW management has become one of the very important ecological imperatives. Serbia with no potential for appropriate disposal of all MW is forced to export MW to countries with MW incineration facilities. Incineration lowers the possible risks of inappropriate disposal and the emission of environmental pollutants, but leads to the need for a “clever” choice of the incinerator facility location which has to meet diverse environmental, economic and technical criteria **Methods.** The criteria for the choice of optimal locations for a MW incinerator facility were as follows: the amount of MW that needs to be transported, the transport time from other locations, the current pollution of the location, the unemployment rate and the location safety in terms of natural disasters and accidents. By using the obtained results for seven efficient locations gained by Data Envelopment Analysis (DEA), we used a goal programming for the analysis of the most suitable location for a MW incineration facility. **Results.** In the proposed methodology on the chosen scenario and analysing the criteria relevant for selecting the most suitable location, using the DEA method, seven efficient locations for MW incineration facility were obtained. The optimal location was location 13. **Conclusion.** Based on the obtained results, we demonstrated that by the use of goal programming it is possible to develop a methodology for selection of optimal MW incineration facility location as one of the necessary activities of MW risk management.

Key words:

environment; incineration; medical waste; medical waste disposal; risk control.

Apstrakt

Uvod/Cilj. Među izazovima 21. veka, medicinski otpad (MO) je, imajući u vidu povećanje njegove količine, raznovrsnost i kompleksnost, postao rastući problem kako za životnu sredinu, tako i za ljude. Zbog toga je upravljanje MO postalo jedan od veoma važnih ekoloških imperativa. Srbija nema potencijala za adekvatno odlaganje celokupnog MO i mora da ga izvozi u zemlje koje imaju postrojenja za njegovo spaljivanje. Spaljivanje MO smanjuje moguće rizike prouzrokovane njegovim neodgovarajućim odlaganjem kao i emisije zagađivača životne sredine, ali rezultira potrebom za „pametnim” izborom lokacije za postrojenja za spaljivanje da bi bili ispunjeni različiti ekološki, ekonomski i tehnički kriterijumi. **Metode.** Za izbor optimalne lokacije postrojenja za spaljivanje MO korišćeni su sledeći kriterijumi: količina MO koja mora da se transportuje, vreme transporta između lokacija, trenutno zagađenje lokacije, stopa nezaposlenosti i bezbednost lokacije u odnosu na njenu izloženost prirodnim nepogodama i nesrećama. Korišćenjem rezultata za sedam efikasnih lokacija dobijenih metodom *Data Envelopment Analysis* (DEA), upotreбили smo model cilnog programiranja za dalju analizu izbora najpogodnije lokacije za postrojenje za spaljivanja MO. **Rezultati.** Primenom metode DEA za izabrani scenario i analize kriterijuma relevantnih za izbor najpogodnije lokacije, nađeno je sedam efikasnih lokacija za postrojenje za spaljivanje MO. Optimalna lokacija je bila lokacija 13. **Zaključak.** Na osnovu dobijenih rezultata, pokazali smo da je primenom cilnog programiranja moguće razviti metodologiju za selekciju optimalne lokacije za postrojenje za spaljivanje MO, kao jedne od neophodnih aktivnosti za upravljanje rizikom od MO.

Cljučne reči:

životna sredina; spaljivanje; medicinski otpad; medicinski otpad, odlaganje; rizik, kontrola.

Introduction

Over the past two decades, medical waste (MW) has become one of the most important topics, having in mind its negative impact on the health of the population and the environment¹⁻⁴. Several terms are used for MW both in literature as well as practice: “hospital waste”, “health care waste”, “infectious waste” or “pharmaceutical waste”². Since there is no single universal term for this type of waste, there is also no universally accepted definition of MW. The reason for this lies in the fact that MW is determined by various laws and regulations, resulting in the evidence that different countries, even different regions of the same country, imply different types of waste as MW^{2,5,6}. Knowing this, MW can be defined as: “waste resulting in the provision of health care services, which includes a variety of materials, of used needles and syringes, body parts, diagnostic samples, blood, chemicals, pharmaceuticals, medical devices and radioactive materials”⁷; “all medical, liquid or gaseous wastes which are generated from healthcare facilities, medical laboratories, research centers, pharmaceutical and veterinary factories, veterinary clinics, home nursing institutions; human and animal remnants, body fluids; blood and derivatives, human excreta, contaminated clothing, wipes, injectors, contaminated sharp tools, expired medicines and chemicals”⁸; “heterogenous mixture of communal waste, infectious, pathoanatomical, pharmaceutical and laboratory waste, disinfectants and packages, as well as chemical waste from health care institutions and veterinary organizations”⁹.

Having in mind that all of the various types of MW can imply different negative impacts, special attention has been given to appropriate treatment and disposal of MW, as well as necessary MW management (MWM)^{10,11}. Consequently, all types of health care institutions must be “in standby mode” in situations that include the possible creation of MW¹², especially when the generated MW can cause potential injuries to medical staff and the general public (directly in contact with MW or indirectly)^{5,12,13}. This is especially important given that according to the World Health Organization (WHO) and the USA Environmental Protection Agency, 10–25% of MW falls into the category of hazardous MW¹⁴, and that “the global trend in rising healthcare usage will result in more medical waste”⁵. Besides, inadequate MWM can lead to the risk of this waste, too^{5,15-19}. That is why research in the field of risks related to MW began in the 1990s. These MW risks include: “environmental pollution, such as water, air, soil, result in unpleasant odors, promoting the growth and multiplication of insects, rodents and vermin, and can lead to the transmission of diseases such as typhoid, cholera, human immunodeficiency virus (HIV) and hepatitis (B and C)”^{20,21}.

For these reasons, some authors use the general division of MW into medical general waste (or nonhazardous waste) and medical hazardous waste. The second type of waste is considered as medical risk waste²². Also, it is concluded that MWM, and medical waste risk management (MWRM) must be necessary parts of the management of any healthcare institutions/facilities, bearing in mind that “healthcare organi-

zations are routinely in a state of crisis management”²³. Interestingly, the modern concept of crisis originates from medical literature in which it indicates a dangerous state of health of the organism from which it can not recover without permanent damage, external intervention or without fundamental restructuring since the body's defense (immune) mechanisms are not enough to pull the organism out of the crisis. Social scientists have borrowed this basic medical metaphor to describe the crisis in economic, political, social, and cultural systems²⁴. Crisis management can be defined as an activity aimed at planning and implementing measures to resolve dangerous situations. As an area of action in the field of crisis resolution, whose goal is to overcome the crisis, crisis management has recently become a dominant area of interest in all organizations, including health institutions. Taking measures of crisis management in health care as an important area of functioning of human society is a specific subject of crisis management. The foundations of crisis management in healthcare are based on the creation of knowledge and the ability to respond to a crisis, and one of the goals of crisis management is both MWM and MWRM.

The main goal of health crisis management is to reduce the risk to the life of the population that has been imposed on potential crisis situations. The secondary goal is to reduce damage, ensure public safety during the crisis and the consequences of the crisis, and care for survivors and victims. It is certainly necessary to mention here the risk analysis, i.e. the assessment of vulnerability and risk that are complementary aspects of the same phenomenon; interactions of physical forces with human or environmental systems. Therefore, risk analysis and management in the MWM process include identification, hazard analysis as well as taking measures related to exposure to these hazards to prevent a crisis. This is extremely important because medical institutions have a special responsibility for making quality decisions based on quantitative methods, the results of which provide a comprehensive and exact basis for efficient MWM (where efficiency can be defined “by the phrase ‘do things right’”²⁵). Some of the most commonly used methods include Risk matrix, Failure Mode Effects Analysis (FMEA), Root Cause Analysis (RCA), Event tree analysis (ETA), Data Envelopment Analysis (DEA), Preliminary Hazard or Risk Analysis (PHA/PRA), Hazards and Operability Study (HAZOPs), Fault Tree Analysis (FTA), goal programming and others whose task is to identify, quantify, and mitigate the risks of MW²². Thus, obtained quantitative indicators in the process of crisis management, allow to align organizational resources with the goal of carrying out the mission of the organization as well as to improve the awareness of all involved stakeholders about the importance of MWM.

This is crucial nowadays, having in mind the current global COVID-19 pandemic and its rapid progress^{26,27} with the consequential rise of the amount of infectious MW and the need for improvements in the field of MW disposal, MWM, and MWRM to reduce the further spread of COVID-19 as well as other diseases.

Unfortunately, for the time being, there is no method of optimal MWM, treatment, or disposal of MW that eliminates

all of the risks caused by MW to humans or the environment²⁸. This is especially the case in Serbia, which produces a large amount of MW and there is no systematic presentation of data on the amount of MW generated in health care institutions. It is estimated that 48,000 tons of MW are generated annually in clinics and hospitals in Serbia, of which 9,600 tons are hazardous MW (of which 5,300 tons are generated in hospitals, 2,410 tons in health centers, 1,700 in other dispensaries, and 200 tons in health protection institutions)^{9,29}.

In health care facilities, where there was no possibility of sterilization of used syringes and needles, swabs, bandages, and other infectious waste, typical waste was mixed with municipal waste and referred to the city dump³⁰. Besides the installed autoclaves and shredders for sterilization of MW in Serbia, there are no other modern facilities for MW treatment, especially its incineration⁹. Knowing all that, it is no surprise that establishing MWM and incineration facilities is included within the goals of Waste Management Strategy for Serbia for the period 2010–2019⁹. The incineration of MW is one of the methods to reduce and remove MW. The main advantages of this type of MW treatment include a significant reduction in the quantity of waste, eliminating dangerous pathogens and organic matter, transforming waste into ash. A downside to this method of MW disposal is emissions of pollutants such as dioxins and furans [e.g. polychlorinated dibenzo-p-dioxins (PCDD), polychlorinated dibenzofurans (PCDF)], toxic metals, as well as particulate matter, which have negative impacts on the environment and human health^{30–32} because they “have been associated with a range of adverse health effects”⁷.

Under the framework of the European Commission's Guidelines for Waste and the National Strategy of the Republic of Serbia for waste management, the treatment of MW by incineration is carried out concerning all defined rules and

regulations regarding possible emissions to air, water and land^{9,33}. Nevertheless, the fact that waste incineration creates energy must be considered in the context of an integrated approach to waste management, which should include reduction, reusing, and recycling⁹.

These are the reasons why this study emphasizes adequate MWM, which involves solving the optimal location, routing and scheduling problems of MW collection, and incineration, as it is shown as good practice in other countries^{32–42}. This is especially significant today when authors like Yu et al.⁴³ prove the importance of MW and optimization of its disposal as one of the key tools in searching for possible solutions during the COVID-19 pandemic. Therefore, the aim of this study was to develop an appropriate methodology for selecting the optimal location for a MW incineration facility as one of the necessary activities of MWM and MWRM. For these reasons and due to the availability of data, the region of Šumadija and Western Serbia and one scenario were selected.

Methods

One of the long-term goals of the Strategy on Waste Management of Serbia is defined as the provision of capacity for MW incineration. This implies the necessary choice of most favorable location for it. The methodology presented in the study shows that it is first necessary to determine a region from which potential locations and criteria will be selected, which will then lastly provide us with the optimal location for the MW incineration facility. Selected efficient locations used in this research were obtained from the results of previous research of Stanojević et al.⁴⁴. The final results refer to the application of the DEA method and are used further on for choosing an optimal location by goal programming. The location selection process is presented in Figure 1

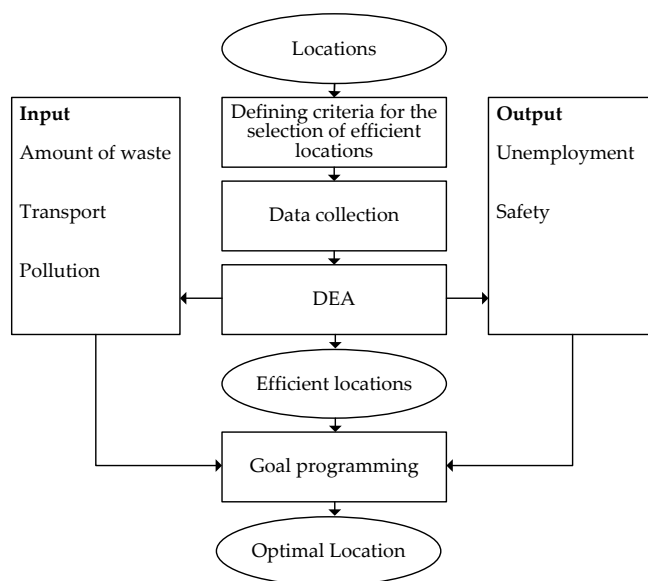


**Fig. 1 – The selection procedure for an efficient and optimal location.
DEA – Data Envelopment Analysis.**

(the results of Stanojević et al.⁴⁴ were complemented).

The first step of choosing a location was to consider the geo-economic map of Serbia, which is divided into 30 administrative areas, 29 cities, 30 urban municipalities, 149 municipalities, 6,158 villages, and 193 urban settlements⁴⁵. Regions according to the number of cities, population, area, the number of cities/municipalities with more than 40,000 inhabitants (this number is determined based on the city with the smallest population in Serbia, which is Prokuplje with 44,000 inhabitants⁴⁶) and the number of health facilities⁴⁷ are given in Table 1.

Table 1

Regions according to the number of cities, population, area, number of cities/municipalities with more than 40,000 inhabitants and the number of health facilities⁴⁴⁻⁴⁷

Parameter	Vojvodina	Belgrade	Šumadija and Western Serbia	South and Eastern Serbia	Kosovo and Metohija
Number of cities	8	1	10	9	1
Population	1,659,440	1,931,809	2,031,697	1,563,916	-
Area (km ²)	21,614	3,234	26,493	26,248	10,910
Population density per 1 km ²	89.40	513.10	76.70	59.60	-
Number of cities/municipalities with more than 40,000 inhabitants	13	17	14	12	-
Number of health institutions	92	54	101	93	-

Šumadija and Western Serbia occupy a central place in Serbia: the most registered medical institutions are located there, it is the largest area, with the most inhabitants, and with the most cities and the most towns/municipalities with more than 40,000 inhabitants. That is why it was elected as the region in which the efficient locations for the treatment of MW should be defined. Šumadija and Western Serbia, within the eight areas, have 14 towns/municipalities with more than 40,000 inhabitants⁴⁶. Featured cities are regarded as possible locations for effective MW treatment. In regions of Zlatibor and Kolubara, there is a city that has more than 40,000 inhabitants, while in other areas we have two potentially efficient locations. MW from municipalities and cities that are located within the same area, but have less than 40,000 inhabitants, “belong” to the city which is the closest to them.

Criteria for the selection of efficient locations within the region and determination of an optimal location were⁴⁴: the amount of generated MW that needs to be transported to a given location; duration of transport from all other locations to given locations; current pollution of each location; the unemployment rate; the safety of the location from natural disasters and accidents. The descriptions of criteria are given respectively: the amount of MW is in direct relation with the increase of the consequences of possible risk of the spillage of MW which can produce pollution of air, land, and water; duration of transport has impact to traffic and wherefore significant negative effects on the quality of air [emissions of CO₂, NO_x, CH₄, O₃, greenhouse gases (GHG) and their consequentially responsibilities “for acid deposition, stratospheric ozone depletion and climate change”]; this criterion is very important, having in mind that “incineration of medical waste involves the creation of certain gases such as CO₂, NO₂, CO and other gases, it is necessary to choose loca-

tions that have the least air pollution, specifically have the lowest risk of crossing the permissible limits of pollutants”⁴⁸; the unemployment rate has great importance as chosen criteria having in mind that this rate represents an important indicator in the evaluation of “socioeconomic development and welfare of countries”⁴⁹; consequences of natural disasters and accidents beside their devastating influence on people and material goods (infrastructure, households, firms, and plants) in the affected area with medical waste incineration facility, could be especially dangerous having in mind possible catastrophic emissions of MW of which 10–25% presents hazardous waste

with infectious, radioactive, or toxic characteristics¹⁴.

Accordingly, in the contest of the DEA method, inputs for given scenario were: the amount of generated MW, duration of transport, and pollution, while outputs were: the unemployment rate, and safety of the location from natural disasters and accidents. In the scenario of the methodology presented in this paper, all input and output criteria were equal (for the decision-makers). In other scenarios, weights of input and output criteria can be different according to the decision-makers' opinions. Consequently, efficient locations could be different.

Based on the chosen criteria, values, descriptions, and results obtained by using the DEA method, we further analysed gained efficient locations. To determine the optimal location, a model of goal programming, that integrates the same multiple criteria as the DEA method is created. Charnes and Cooper⁵⁰ illustrated how that deviation could be minimized by placing the variables that represent the deviation directly in the objective function of the model. This allows multiple (and sometimes conflicting) goals to be expressed in a model that will permit a solution to be found.

Let us suppose that N is a subset of efficient locations ($|N| \leq n$).

The parameters and variables used in a mathematical model of the proposed problem are following:

b_{rj} - normalized value r -th output for j -th location ($b_{rj} = y_{lmax} / r \in \{1, 2\}, j = 1, \dots, n$),

a_{lj} - normalized value l -th input for j -th location

($a_{lj} = x_{lj} / x_{lmin}, l \in \{1, 2, 3\}, j = 1, \dots, n$),

$z_j = \begin{cases} 1 & \text{if incineration facility is on the } j\text{-th location} \\ 0 & \text{otherwise} \end{cases}$

d_l^+ - deviation from the best value l -output,

d_r^- - deviation from the best value r -output.

The mathematical model of this problem has the following notation (1-5):

$$\min f(x) = \sum_{l=1}^3 d_l^+ + \sum_{r=1}^2 d_r^- \quad (1)$$

s.t.

$$\sum_{j=1}^n a_{lj} \cdot z_j - d_l^+ = 1, l \in \{1, 2, 3\}, \quad (2)$$

$$\sum_{j=1}^n b_{rj} \cdot z_j + d_r^- = 1, r \in \{1, 2\}, \quad (3)$$

$$\sum_{j=1}^n z_j = 1, \quad (4)$$

As it was mentioned before, it was assumed that all of the criteria (inputs and outputs) are equally important for the decision and that the only negative deviation is permitted, i.e. decreasing the input criteria:

$$(d_l^+ \geq 0, d_l^- = 0, i \in \{1, 2, 3\}, j = 1, \dots, n)$$

and the positive deviation, i.e. increasing output criteria:

$$(d_r^- \geq 0, d_r^+ = 0, i \in \{1, 2\}, j = 1, \dots, n).$$

Results

Efficient locations determined by the DEA method representd potential locations for the MW incineration facility and they are presented in Table 2.

The obtained results showed that there were seven efficient locations (the efficiency is equal to 1).

These locations were further analysed with aim to get an optimal solution which should have a minimal total deviation from an ideal location. The ideal location was obtained using the best input and output values, i.e. all criteria values of all observed locations. None of the selected locations had such values, so the goal was to find the location that deviates the least from the ideal one. The obtained values of inputs and outputs are given in Table 3.

After solving the above presented mathematical model, only for efficient locations ($n = 7$), the obtained values are shown in Tables 4 and Table 5.

The real deviation from the obtained ideal values and results of the authors Stanojević et al. ⁴⁴ are given in Table 5.

According to the obtained results, Location 13 was chosen as the optimal location for the building of MW incin-

Table 2

Efficiency of locations considered for medical waste incineration ⁴⁴

Location	Efficiency	Rank
Užice	1	1
Valjevo	0.9012	14
Loznica	0.9901	9
Šabac	0.917	13
Gornji Milanovac	1	1
Čačak	1	1
Jagodina	0.9832	10
Paraćin	0.9804	11
Kruševac	0.9945	8
Trstenik	1	1
Kraljevo	0.9225	12
Novi Pazar	1	1
Arandelovac	1	1
Kragujevac	1	1

Table 3

Values of inputs and outputs for various locations considered for medical waste incineration ⁴⁴

Location	Inputs		Outputs		
	Amount of waste (kg)	Transportation time (min)	Pollution	Unemployment	Safety
Užice	5,017.73	9,291	0.805	0.1894	0.9792
Valjevo	5,339.86	9,749	0.56333	0.1724	0.8939
Loznica	5,486.32	14,292	0.5975	0.3322	0.9459
Šabac	5,337.43	11,742	0.602	0.2126	0.9067
Gornji Milanovac	5,713.94	7,201	0.24044	0.1534	0.9387
Čačak	5,358.02	7,274	0.42333	0.1994	0.9441
Jagodina	5,468.85	9,260	0.3253	0.2634	0.8995
Paraćin	5,597.55	9,723	0.6675	0.2768	1.0000
Kruševac	5,316.27	9,829	0.43333	0.3006	0.8246
Trstenik	5,671.17	9,001	0.2263	0.2094	0.9898
Kraljevo	5,401.67	7,720	0.8775	0.2241	0.8922
Novi Pazar	5,392.39	13,514	0.26873	0.3687	0.9011
Arandelovac	5,644.52	8,910	0.24044	0.2439	0.9457
Kragujevac	5,195.40	7,636	0.6725	0.2829	0.9387

Table 4

The values of variables z_j for 7 most efficient locations considered for medical waste incineration

Location	z_j
Užice	0
Gornji Milanovac	0
Čačak	0
Trstenik	0
Kraljevo	0
Arandelovac	1
Kragujevac	0

Table 5

The values of deviations and objective function

Parameter	Amount of waste (kg)	Transport time (min)	Pollution	Unemployment	Safety
Deviation	626.79	1,709.00	0.01	-0.12	-0.04
Arandelovac	5,644.52	8,910.00	0.24	0.24	0.94
Ideal	5,017.73	7,201.00	0.23	0.36	0.98

eration facility. Regarding total transportation time, Location 13 was not the best solution (since it required more time than was calculated ideal value of 7,201 minutes). Even though Location 13 did not have an ideal value for any of the other criteria observed, it still proved as the most efficient location, given the reasons that the amount of MW (5,644.52 kg) which has to be transported to this location is much larger than the quantity that the other locations required, but the transportation time (8,910 minutes) and pollution (0.24044) are considerably lesser than at the other locations, namely, they are closer to the best values of these criteria. Safety (0.9457) and unemployment rate (0.2439) of this location were characterized by a relatively small deviation from the best value, so the minimum value of the objective function was equal to 0.807768.

Discussion

To reduce the risks that MW carries, developing countries, such as Serbia, must focus on solving this problem as soon as possible. The previous practice of sterilization and shredding MW and its disposal in a landfill or export abroad is a short-term solution. The consequences that may occur due to possible adverse events during MWM can be dangerous not only for human health but also for the entire ecosystem of the region. Therefore, the location, where it is possible and appropriate to dispose and treat MW, should be considered through the integration of different elements that meet environmental, social, economic, and technical criteria.

This study take into consideration the amount of waste that needs to be transported, the time of transport, the current pollution of the location, the unemployment rate, and the safety of the location of possible natural disasters and accidents. By the proposed methodology, these criteria were analyzed using the DEA method, and as the results, seven efficient locations for MW incineration facility were

obtained on the case of Serbia. In the presented research, it was used a goal programming model for further formulation and analysis to achieve an optimal location for the incineration of MW. In the chosen scenario, the location was Location 13.

The problem of MW and its disposal is growing rapidly throughout the world as a direct result of fast urbanization and population growth, requiring specialized treatment and management⁵¹. As it is mentioned before, poor MWM can potentially cause hazards such as exposed “health care workers, waste handlers, patients and the community at large to infection, toxic effects and injuries”⁷, as well as risks of environmental pollution and degradation. Bearing in mind that the limitation of the present research is related to the lack of adequate database on the amount of MW generated by each health institution, the future directions of research should include the promotion and creation of a single database of health facilities, their capacity, and resources at their disposal, which would allow better management of the health facilities, and would lead to an improvement of the process of MWM, as well as problems with which every institution of this type meets. Another limitation is related to the obtained location itself, which is the result of the assumption that all of the criteria (inputs and outputs) are equally important for the decision-makers. Namely, when it comes to the location of MW incineration, it must be noted “that selected sites should be located away from sensitive land uses, e.g. residential areas, educational and health services, etc.”⁵². This, consequently implies that the obtained location has to be carefully qualitatively reviewed to avoid unnecessary possible increase in pollution. Also, future research must consider different scenarios, with relation to different weights all of the criteria (inputs and outputs) for a goal programming model which in that case can give different results. Besides, cost-benefit analysis would show the long-term financial effects of such a decision.

Conclusion

The importance of MWM is reflected in the reduction of all possible negative impacts of MW both on the people and the environment. This problem can be solved by the right investment in the incinerator facility at the adequate location which will meet diverse multiple environmental, social, economic, and technical criteria to adequately manage

the final processing of MW, and provide proper MWRM. This adequate location, i.e. optimal location, can be obtained by methodology presented in this study using the DEA method and the goal programming.

Disclosure statement

All authors declare no conflicts of interest.

REFERENCES

1. Al-Habash M, Al-Zu'bi A. Efficiency and Effectiveness of Medical Waste Management Performance, Health Sector and its Impact on Environment in Jordan Applied Study. *World Appl Sci J* 2012; 19(6): 880–93.
2. Komilis DP. Issues on medical waste management research. *Waste Manag* 2016; 48: 1–2.
3. Makajic-Nikolic D, Petrovic N, Belic A, Rokvic M, Radakovic J-A, Tubic V. The fault tree analysis of infectious medical waste management. *J Clean Prod* 2016; 113: 365–73.
4. Mihailović O, Žarkić-Joksimović N, Petrović N, Makajić-Nikolić D, Radaković J-A. Economic and environmental effectiveness of infectious medical waste disposal system: A case study of the tertiary health-care institution. In: Čirović G, editor. SYM-OPIS 2017: Proceedings of XLIV Symposium on operational research International Regional Symposium; 2017 September; Civil Engineering and Geodesy high school, Zlatibor. Belgrade: Planeta Print; 2017. p. 35–40.
5. Windfeld ES, Brooks MS. Medical waste management - A review. *J Environ Manage* 2015; 163: 98–108.
6. Stanojević K, Petrović N, Drakulić M, Čirović M. Attitudes about Medical Waste Management in Serbia: A Case Study. In: Vasiljević D, Đorđević L, editors. SPIN'17: Proceedings of XI Symposium of entrepreneurs and scientists: Lean management of the Republic of Serbia resources, Belgrade. Belgrade: Faculty of Organizational Sciences; 2017. p. 286–92. (Serbian)
7. World Health Organization. Health-care waste. 2018 [cited 2020 Apr 04]. Available from: https://www.who.int/topics/medical_waste/en/.
8. Department of Health Service. Medical Waste Management. Management Act. 2004.
9. RS Official Gazette. Waste management strategy for the period 2010-2019. Nos. 29/2010. 2010 [cited 2020 Jan 28]. Available from: https://www.ekologija.gov.rs/?wpfb_dl=203. (Serbian)
10. Cheng YW, Sung FC, Yang Y, Lo YH, Chung YT, Li KC. Medical waste production at hospitals and associated factors. *Waste Manag* 2009; 29(1): 440–4.
11. Bokhoree C, Beeharry Y, Makoondlall-Chadee T, Doobah T, Soomary N. Assessment of environmental and health risks associated with the management of medical waste in Mauritius. *APCBEE Procedia* 2014; 9: 36–41.
12. Gómez-Mejía LR, Balkin DB, Cardy RL, Luis RG. Managing Human Resources. 5th ed. Phoenix, AZ: Arizona State University; 2014.
13. Birchard K. Out of sight, out of mind... the medical waste problem. *Lancet* 2002; 359(9300): 56.
14. Taghipour H, Mosafari M. Characterization of medical waste from hospitals in Tabriz, Iran. *Sci. Total Environ* 2009; 407(5): 1527–35.
15. Mohee R. Medical wastes characterization in healthcare institutions in Mauritius. *Waste Manag* 2005; 25(6): 575–81.
16. Baveja G, Muralidhar S, Aggarwal P. Hospital waste management—an overview. *Hospital Today* 2000; 5(9): 485–6.
17. Almunef M, Memish ZA. Effective medical waste management: it can be done. *Am J Infect Control* 2003; 31(3): 188–92.
18. Insa E, Zamorano M, Lopez R. Critical review of medical waste legislation in Spain. *Resour Conserv Recycl* 2010; 54(12): 1048–59.
19. Zhang L, Wu L, Tian F, Wang Z. Retrospection-Simulation-Revision: Approach to the Analysis of the Composition and Characteristics of Medical Waste at a Disaster Relief Site. *PLoS One* 2016; 11(7): e0159261.
20. Pruss A, Girault E, Rushbrook P. Safe Management of Wastes from Healthcare Activities. Geneva: World Health Organization; 1999.
21. Ribeiro Paulo JM, de Lemos T, Chaleira A. Risk Management in Medical Waste. 2013 [cited 2020 Feb 18]. Available from: https://www.researchgate.net/profile/Teresa_Lemos/publication/282099580_Risk_Management_in_Medical_Waste_-_Case_Study_of_the_Ilha_do_Pico_-_Azores/links/5602c12e08aeaf867fb759bf/Risk-Management-in-Medical-Waste-Case-Study-of-the-Ilha-do-Pico-Azores.pdf.
22. Sefouli L, Kalla M, Bahmed L, Aouragh L. The risk assessment for the healthcare waste in the hospital of Batna city, Algeria. *Int J Environ Sci Dev* 2013; 4(4): 442–5.
23. Nemeth C, Wears RL, Patel S, Rosen G, Cook R. Resilience is not control: healthcare, crisis management, and ICT. *Cogn Technol Work* 2011; 13(3): 189–202.
24. Kešetović Ž, Toth I. Crisis management problems - a scientific monograph. Velika Gorica: Veleučilište Velika Gorica; 2012. (Croatian)
25. Marković V, Stajić Lj, Stević Ž, Mitrović g, Novarić B, Radojičić Z. A Novel Integrated Subjective-Objective MCDM Model for Alternative Ranking in Order to Achieve Business Excellence and Sustainability. *Symmetry* 2020; 12(1): 164.
26. Klemesš JJ, Van Fan Y, Tan RR, Jiang P. Minimising the present and future plastic waste, energy and environmental footprints related to COVID-19. *Renew Sust Energ Rev* 2020; 127: 109883.
27. MacKenzie D. How bad will it get? *New Sci* 2020; 245(3269): 7.
28. Ministry of Health of the Republic of Serbia. National guide for safe medical waste management. 2008 [cited 2020 Jan 28]. Available from: http://www.kbs.co.rs/pdf/vodic_medicinski_otpad.pdf. (Serbian)
29. Bera M, Mihajlov A, Hodolić J, Agarski B. Analysis of situation of hazardous waste from medical institutions in Serbia and world. *Kvalitet* 2008; 18(11–12): 38. (Serbian)
30. Coutinho M, Pereira M, Rodrigues R, Borrego C. Impact of medical waste incineration in the atmospheric PCDD/F levels of Porto, Portugal. *Sci Total Environ* 2006; 362(1–3): 157–65.
31. Lee CC, Huffman GL. Medical waste management/incineration. *J Hazard Mater* 1996; 48(1–3): 1–30.
32. RS Official Gazette. The rule book for Medical Waste Management. Nos. 48/2019. 2019 [cited 2020 Feb 23]. Available from: <https://www.paragraf.rs/propisi/pravilnik-o-upravljanju-medicinskim-otpadom.html>. (Serbian)

33. *Eiselt HA*. Locating landfills - Optimization vs. reality. *Eur J Oper Res* 2007; 179(3): 1040–9.
34. *Alumur S, Kara BY*. A new model for the hazardous waste location-routing problem. *Comput Oper Res* 2007; 34(5): 1406–23.
35. *Erkut E, Neuman S*. Analytical models for locating undesirable facilities. *Eur J Oper Res* 1989; 40(3): 275–91.
36. *Sinany-Stern Z, Mebrez A, Tal AG, Shemuel B*. The location of a hospital in a rural region: the case of the Negev. *Locat Sci* 1995; 3(4): 255–66.
37. *Chen YT, Chen CC*. The privatization effect of MSW incineration services by using data envelopment analysis. *Waste Manag* 2012; 32(3): 595–602.
38. *Alçada-Almeida L, Coutinho-Rodrigues J, Current J*. A multiobjective modeling approach to locating incinerators. *Socio-Econ Plan Sci* 2009; 43(2): 111–20.
39. *Faizal UM, Jayachitra R, Vijayakumar P, Rajasekar M*. Optimization of inbound vehicle routes in the collection of bio-medical wastes. *Materials Today Proceed* 2021; 45(2):692–9.
40. *Wichapa N, Khokhajaikiat P*. A Hybrid Multi-Criteria Analysis Model for Solving the Facility Location–Allocation Problem: A Case Study of Infectious Waste Disposal. *J Eng Technol Sci* 2018; 50(5): 698–718.
41. *Budak A, Ustundag A*. Reverse logistics optimisation for waste collection and disposal in health institutions: the case of Turkey. *Int J Logist Res Appl* 2017; 20(4): 322–41.
42. *Alshraideh H, Qdais HA*. Stochastic modeling and optimization of medical waste collection in Northern Jordan. *J Mater Cycles Waste Manag* 2017; 19(2): 743–53.
43. *Yu H, Sun X, Solvang WD, Zhao X*. Reverse logistics network design for effective management of medical waste in epidemic outbreaks: Insights from the coronavirus disease 2019 (COVID-19) outbreak in Wuhan (China). *Int J Environ Res Public Health* 2020; 17(5): 1770.
44. *Stanojević K, Makajić-Nikolić D, Savić G*. Selection of efficient locations for medical wastes incineration plants. In: Jaško O, Marinković S, editors. *SymOrg* 2016: Reshaping the Future through Sustainable Business Development and Entrepreneurship; 2016 Jun 10–13; Faculty of Organizational Sciences; Zlatibor, Srbija. Belgrade: Faculty of Organizational Sciences; 2016. p. 577–84.
45. *Statistical Office of the Republic of Serbia*. Statistical yearbook of the Republic of Serbia. 2019 [cited 2020 Feb 09]. Available from: <http://webzrzs.stat.gov.rs/WebSite/userFiles/file/Aktuelnosti/God2015.pdf>. (Serbian)
46. *Statistical Office of the Republic of Serbia*. Population by ethnicity and sex, by municipalities and cities. 2011 [cited 2020 Feb 04]. Available from: http://popis2011.stat.rs/?page_id=2162. (Serbian)
47. *Ministry of Health of the Republic of Serbia*. Register of medical institutions. 2020 [cited 2020 Feb 05]. Available from: <https://www.rfzo.rs/index.php/linkovi/zdravstvene-ustanove>. (Serbian)
48. *Stanković S, Vasković V, Petrović N, Radojić Z, Ljubojević M*. Urban traffic air pollution: Case study of Banja Luka. *Environ Eng Manag J* 2015; 14(12): 2783–91.
49. *Isjmović S, Jeremić V, Petrović N, Radojić Z*. Colouring the socio-economic development into green: I-distance framework for countries' welfare evaluation. *Qual Quant* 2015; 49(2): 617–29.
50. *Charnes A, Cooper WW*. Programming with linear fractional functionals. *Nav Res Logist Q* 1962; 9(3–4): 181–6.
51. *Hassaan MA*. A gis-based suitability analysis for siting a solid waste incineration power plant in an urban area case study: Alexandria governorate, Egypt. *J Geogr Inf Syst* 2015; 7: 643–57.
52. *Koros K*. Kenya: Sweet poison - Illegal ripening of fruits exposes millions of Kenyans to cancer. In *AllAfrica. The Star*. 2014. [cited 2020 Jun 15]. Available from: <https://allafrica.com/stories/201411111021.html>.

Received on May 21, 2020

Revised on July 6, 2020

Accepted on July 7, 2020

Online First July, 2020



Simultaneous and alternative IgG seroreactivity against *Helicobacter pylori* antigens VacA, 30 kDa and 50 kDa is a better biomarker approach for the outcome of infection than VacA and 50 kDa alone

Istovremena i alternativna IgG seroreaktivnost protiv *Helicobacter pylori* antigena VacA, 50 kDa i 30 kDa je bolji biomarkerski model ishoda infekcije nego VacA i 50 kDa pojedinačno

Nebojša Manojlović^{*†}, Ivana Tufegđić^{†‡}, Elizabeta Ristanović^{†§},
Dubravko Bokonić^{†¶}

Military Medical Academy, ^{*}Clinic for Gastroenterology and Hepatology, [†]Institute for Pathology, [§]Institute for Microbiology, [¶]National Poison Control Center, Belgrade, Serbia; [‡]University of Defence, Faculty of Medicine of the Military Medical Academy, Belgrade, Serbia

Abstract

Background/Aim. In our previous study, IgG seropositivities against *Helicobacter (H) pylori* antigens VacA, 50 kDa, 30 kDa, and 26 kDa were highlighted as biomarkers for the specific outcome of infection. We designed and conducted this study in order to investigate whether synchronous and/or alternative seroreactivity against *H. pylori* antigens VacA, 50 kDa, 30 kDa and 26 kDa in patients with gastric cancer and peptic ulcers exhibit stronger association than with dyspepsia and *vice versa*. **Methods.** In order to determine IgG antibodies to *H. pylori* antigens, a Western blot test was performed in 123 patients: 31 with gastric cancer, 31 with duodenal ulcer, 31 with gastric ulcer and 30 with functional dyspepsia. We analyzed IgG seroreactivity against four *H. pylori* antigens (VacA, 50 kDa, 30 kDa, 26 kDa) in their synchronous/alternative combination as well as seroreactivity to synchronous and alternative combinations of *H. pylori* antigens between a group with functional dyspepsia and others. The analysis of diagnostic characteristics of the best synchronous and alternative seroreactivity combination was

done, and tested *versus* VacA as biomarker for gastric cancer and peptic ulcer, and 50 kDa as a biomarker for dyspepsia. **Results.** VacA seropositivity or 50 kDa seronegativity ($p = 0.015$) and VacA seropositivity or 50 kDa and 30 kDa seronegativity ($p = 0.044$) had the better diagnostic characteristics with statistically significantly better fraction correct than VacA seropositivity alone. VacA seronegativity along with 50 kDa and 30 kDa seropositivity ($p = 0.003$), 50 kDa seropositivity ($p = 0.01$), 30 kDa seropositivity ($p = 0.015$) and 50 kDa or 30 kDa seropositivity ($p = 0.02$) had better diagnostic characteristics and significantly better fraction correct than 50 kDa seropositivity alone. **Conclusion.** Simultaneous and alternative IgG seroreactivity/unreactivity against *H. pylori* antigens VacA, 50 kDa and 30 kDa have stronger association with the specific infection outcome, considering gastric cancer and peptic ulcer, or dyspepsia, than VacA and 50 kDa IgG seropositivity alone.

Key words: antigens; biomarkers; duodenal ulcer; helicobacter pylori; stomach neoplasms; stomach ulcer.

Apstrakt

Uvod/Cilj. U našoj prethodnoj studiji IgG seropozitivnosti prema *Helicobacter (H) pylori* antigenima VacA, 50 kDa, 30 kDa i 26 kDa označene su kao biomarkeri specifičnog ishoda infekcije. Cilj ovog rada bio je da se istraži da li istovremena i/ili alternativna seroreaktivnost protiv *H. pylori* antigena VacA, 50 kDa, 30 kDa i 26 kDa ima jaču povezanost sa karcinomom želuca i peptičkim ulkusima nego sa dispepsijom, i suprotno. **Metode.** U cilju određivanja IgG antitela specifičnih prema *H. pylori* antigenima primenjen je *Western blot* test kod 123 ispitanika: 31 sa karcinomom želuca, 31 sa ulkusom duodenuma,

31 sa ulkusom želuca i 30 sa funkcionalnom dispepsijom. Analizirana je seroreaktivnost protiv četiri *H. pylori* antigena (VacA, 50 kDa, 30 kDa, 26 kDa) u njihovim istovremenim/alternativnim kombinacijama kao i istovremena i alternativna seroreaktivnost protiv *H. pylori* antigena u grupi ispitanika sa dispepsijom, u odnosu na druge grupe ispitanika. Uradjena je analiza dijagnostičkih karakteristika najboljih kombinacija istovremenih i alternativnih seroreaktivnosti i testiranje u odnosu na VacA kao biomarker karcinoma želuca i peptičkog ulkusa i 50 kDa kao biomarker dispepsije. **Rezultati.** Seropozitivnost prema VacA ili seronegativnost prema 50 kDa ($p = 0,015$) i seropozitivnost prema VacA i seronega

tivnost prema 50 kDa ili 30 kDa ($p = 0,044$) imali su bolje dijagnostičke karakteristike sa statistički značajno boljom tačnom frakcijom u odnosu na seropozitivnost na sam VacA. Seronegativnost prema VacA zajedno sa 50 kDa i 30 kDa seropozitivnošću ($p = 0,003$), 50 kDa seropozitivnošću ($p = 0,01$), 30 kDa seropozitivnošću ($p = 0,015$), 50 kDa ili 30 kDa seropozitivnošću ($p = 0,02$) imale su bolje dijagnostičke karakteristike i statistički značajno bolju tačnu frakciju u odnosu na samu 50 kDa seropozitivnost. **Zaključak.** Istovremena i alternativna

IgG seroreaktivnost/nereaktivnost protiv *H. pylori* antigena VacA, 50 kDa i 30 kDa ima jaču povezanost sa specifičnim ishodom infekcije kod karcinoma želuca i peptičkih ulkusa ili dispepsije, u odnosu na pojedinačnu IgG seropozitivnost prema VacA i 50 kDa.

Ključne reči:

antigeni; biološki pokazatelji; duodenum, ulkus; helicobacter pylori; želudac, neoplazme; želudac, ulkus.

Introduction

Because of the differences in bacterial epitopes and host characteristics, infections with *Helicobacter (H) pylori* induce different immune responses¹. Immune response against *H. pylori* shows variability in gastric diseases in the sense of different seroreactivity to some of *H. pylori* antigens. *H. pylori* isolates from gastric tumoral mucosa and nontumoral gastric mucosa do not display the same antigens². In our previous article, we reported IgG seroreactivity against *H. pylori* VacA as a potential biomarker for gastric cancer (GCA), gastric ulcer (GU) and duodenal ulcer (DU). On the other hand, IgG seroreactivity against *H. pylori* 50 kDa antigen could be a biomarker for functional dyspepsia (FD), IgG seroreactivity against *H. pylori* 30 kDa antigen could be a biomarker for antrum predominant gastritis while IgG seroreactivity against *H. pylori* Urease A 26 kDa antigen could be a biomarker for pancreatitis³. Synchronous seropositivity and seronegativity to two or three *H. pylori* antigens were associated with the infection outcome.

The synchronous presence of IgG against 19 kDa and 35 kDa⁴, 19.5 kDa and 136 kDa⁵, 19.5 kDa along with 33 kDa and 136 kDa⁵, 116 kDa and 89 kDa⁶, the absence of 19 kDa and 35 kDa seroreactivity⁷, the presence of 120 kDa and 85 kDa⁸, all were associated with GCA. The synchronous seropositivity to 87 kDa and 35 kDa⁹, 125 kDa along with 87 kDa and 35 kDa⁹, CagA and 35 kDa¹⁰ all were associated with peptic ulcer (PU). On the other hand, synchronous seropositivity to 120 kDa, 33 kDa, 30 kDa and 19 kDa was associated with the intensity of antral inflammation¹¹.

We conducted this study with the aim to investigate the association of synchronous and alternative seroreactivity to VacA, 50 kDa, 30 kDa and 26 kDa. VacA and 26 kDa seropositivity were considered as a biomarker for the serious outcome of infection in patients with GCA and PU, and, on the other hand, seronegativity was considered as a biomarker for FD. 50 kDa seropositivity was considered as a biomarker for FD and 30 kDa, and, as opposed to that, seronegativity was considered as a biomarker for the serious outcome of infection. At the same time, it was interesting to compare the degree of association of VacA seropositivity and 50 kDa seropositivity with the specific outcome of infection vs. synchronous and alternative seroreactivity to two or three *H. pylori* antigens.

Methods

The study was conducted during 2009 at the Clinic for Gastroenterology and Hepatology of the Military Medical

Academy (MMA), Institute of Pathology of the MMA and Institute of Microbiology of the MMA, Belgrade, Serbia. We selected and enrolled the patients with dyspeptic symptoms, different underlying disease (GCA, DU, GU and gastritis), and actual *H. pylori* infection confirmed by histopathological examination and anti-*H. pylori* IgG positive ViraBlot.

We took medical history from all patients and performed a physical examination, abdominal ultrasound (US) or computer tomography (CT), esophagogastroduodenoscopy (EGDS), complete blood count (CBC), liver and renal chemistry. The inclusion criteria were: 1) the presence of dyspepsia symptoms, 2) previously untreated patients due to *H. pylori* infection, 3) without treatment with proton pump inhibitors and H2 blockers in the last two weeks, 4) the absence of malignancy except for GCA, 5) the absence of any immunological disorder, 6) informed consent of the patient for: a) EGDS and biopsy, b) blood sample for analyses, c) participation in the study, 7) endoscopic and histopathological diagnosis of one of the following diseases: GCA, DU, GU, gastritis; 8) confirmed histopathological diagnosis of *H. pylori* infection, 9) Western blot detection system (ViraBlot) IgG positive for *H. pylori* infection.

EGDS was performed in all our patients in the endoscopy section using Olympus (GIFQ165, SN: 2207997, Olympus corporation, Tokyo) forward viewing EGDS under local application of Xylocaine spray. A minimum of four gastric mucosal tissue biopsies (two of them from the antrum and corpus) and additional biopsies from any endoscopically visible lesion were taken. All patients were examined for findings that indicated endoscopic gastritis, such as erythema, hyperemia, atrophy, and mucosal nodularity according to the criteria of the Houston-updated Sydney grading system, and for gastric tumor, DU and GU.

Blood samples were obtained from all of them and frozen at -20 °C degree. Using the ViraBlot, IgG anti Vacuolating cytotoxin A (VacA) 87 kDa, Cytotoxin associated with gene A (CagA) 136 kDa, Urease B 66 kDa (UreB 66), Heat shock protein 60 kDa (Hsp60), Flagellin 55 kDa (Fla 55), 50 kDa, 30 kDa, Urease A 26 kDa (UreA 26) and 24 kDa *H. pylori* antigens were identified. *H. pylori* antigens of ViraBlot represent a combination of German patient isolates of highly antigenic *H. pylori* strains. Bands for diagnosis of *H. pylori* infection were divided into highly specific as CagA 136 kDa, VacA 87 kDa, 30 kDa, UreA 26 kDa, 24 kDa and less specific as Hsp 60 kDa and 50 kDa. According to the manufacturer's guideline for use, the test was considered negative if there were no bands or there were nonspecific bands such as

UreB 66 kDa, Hsp 66 kDa, Fla 55 kDa, 50 kDa. The test was possibly positive if there was one clear specific band of 30 kDa, UreaA 26 kDa, 24 kDa. The test was positive if there was at least one band of following two specific CagA 136 kDa or VacA 87 kDa or at least one clear band of 30 kDa, UreaA 26 kDa, 24 kDa or one clear band of 30 kDa, UreaA 26 kDa, 24 kDa and one clear band of Hsp60 kDa, and 50 kDa. In this study we used the data from our previous study³, considering only ViraBlot IgG against VacA, 50 kDa, 30 kDa and 26 kDa.

The diagnosis of GCA was established in 31 patients, DU in 31 patients, and GU in 31 patients, while in 30 patients gastritis with FD was diagnosed.

All patients included in the study were analyzed in several ways. Firstly, the patients were analyzed according to the baseline diagnosis: GCA, GU, DU and dyspepsia. Subsequently, groups with GCA and PU were joined in one group and tested vs. the group of dyspepsia.

In the first analysis, we searched for combination seropositivity as a biomarker for the serious outcome of infection in baseline groups in the following combinations: VacA seropositivity along with the absence of 50 kDa seropositivity; VacA seropositivity along with the absence of 30 kDa seropositivity; VacA seropositivity along with 26 kDa seropositivity; the absence of both 50 and 30 kDa seropositivity; the absence of 50 kDa and presence of 26 kDa seropositivity; the absence 30 kDa and presence of 26 kDa seropositivity.

In the second part of the first analysis, we searched for combination seropositivity as a biomarker for FD: the absence of VacA seropositivity and the presence of 50 kDa seropositivity; the absence of VacA and the presence of 30 kDa seropositivity; the absence of VacA and the presence of 50 and 30 kDa seropositivity; the presence of 50 kDa and 30 kDa seropositivity together.

In the second analysis, we searched for alternative combination of seropositivity/negativity as biomarkers for the serious outcome in baseline groups in the following combinations: VacA seropositivity or 50 kDa seronegativity; VacA seropositivity or 50 kDa and 30 kDa seronegativity; VacA seropositivity along with 26 kDa seropositivity and 50 kDa seronegativity; VacA seropositivity, 26 kDa seropositivity, 30 kDa seronegativity.

In the second part of the second analysis, we searched for the alternative combination of seropositivity/negativity as a biomarker for FD in the following combinations: VacA seronegativity along with 50 kDa or 30 kDa seronegativity;

50 kDa or 30 kDa seropositivity.

In the third analysis, we joined groups with GCA, GU and DU and tested vs. FD with the same criteria as in the first and second analysis.

We performed statistical analysis of the frequency of the previously mentioned combinations in baseline groups GCA, GU, DU vs. FD and GCA and PU group vs. FD group.

In the fourth analysis, accuracy and discriminative ability of various seropositive/seronegative combination against investigated *H. pylori* antigens in the prediction of the outcome of infection were estimated with Sensitivity (Se), Specificity (Sp), Positive predictive value (PPV), Negative predictive value (NPV), Fraction correct (FC) and Clinical utility index (CUI) in the form of Case-finding utility or Positive utility index (CUI Ve+) and Screening utility or Negative utility index (CUI Ve-). $CUI\ Ve+ = Se \times PPV$ and $CUI\ Ve- = Sp \times NPV$ represent important indexes for clinicians estimating both accuracy and discriminative ability of the test.

Statistical analysis

Complete statistical data analysis was done with the statistical software package, SPSS Statistics 18. Most of the variables were presented as the frequency of certain categories, so *t*-test of proportion or cross-tabulation analysis (odds ratio, confidence intervals) were done for the calculation of statistical significance of the differences between groups. In case of continuous data, variables were presented as median, minimal and maximal values (range). All the analyses were estimated at minimal $p < 0.05$ level of statistical significance.

Results

Four groups of patients with GCA, DU, GU and upper FD were comparable regarding gender and age (Table 1).

Seroreactivity against synchronous combinations of *H. pylori* antigens VacA, 50 kDa, 30 kDa and 26 kDa is shown in Table 2.

Seropositivity to VacA and seronegativity to 50 kDa taken together were significantly more frequent in GCA ($p = 0.045$), GU ($p = 0.02$) and DU ($p = 0.045$) than in FD.

Seronegativity to both 30 kDa and 50 kDa was significantly more frequent in GCA ($p = 0.006$), GU ($p = 0.006$) than in FD, but with only trend to significance in comparison with DU ($p = 0.056$).

Table 1

Demographic and clinical characteristics of the examined patients

Parameters	Groups of patients				Total (n = 123)
	GCA (n = 31)	DU (n = 31)	GU (n = 31)	FD (n = 30)	
Gender, n					
male	10	13	12	13	48
female	21	18	19	17	75
Age (years),					
median (range)	65 (40–85)	54 (21–87)	67.5 (34–81)	63.5 (21–80)	63 (21–87)

GCA – gastric cancer; DU – duodenal ulcer; GU – gastric ulcer; FD – upper functional dyspepsia.

Table 2

**Seroreactivity against synchronous combinations of *H. pylori* antigens
VacA, 50 kDa, 30 kDa and 26 kDa in four groups of patients**

WB IgG	Groups, n (%)					FD vs. others		
	GCA 31 (100)	DU 31 (100)	GU 31 (100)	FD 30 (100)		GCA	DU	GU
VacA+ 50 kDa-	8 (26)	8 (26)	9 (29)	2 (7)	<i>p</i> OR CI	0.045	0.045	0.02
VacA+ 30 kDa-	5 (16)	4 (13)	7 (23)	3 (10)	<i>p</i> OR CI	ns	ns	ns
VacA+ UreA26+	15 (48)	17 (55)	15 (48)	10 (30)	<i>p</i> OR CI	ns	ns	ns
VacA- 50 kDa+	6 (19)	5 (16)	6 (19)	15 (50)	<i>p</i> OR CI	0.01 4.2 1.3–13.1	0.005 5.2 1.6–17.2	0.01 4.2 1.3–13.1
VacA- 30 kDa+	5 (16)	10 (32)	4 (13)	16 (53)	<i>p</i> OR CI	0.002 5.9 1.8–19.6	ns	0.0008 7.7 2.2–27.5
VacA- 50 kDa+ 30 kDa+	2 (6)	5 (16)	3 (10)	11 (37)	<i>p</i> OR CI	0.005	ns	0.02
50 kDa+ 30 kDa+	12 (39)	12 (39)	7 (23)	17 (57)	<i>p</i> OR CI	ns	ns	0.006 0.22 0.09–0.68
50 kDa- 30 kDa-	10 (32)	6 (19)	10 (32)	1 (3)	<i>p</i> OR CI	0.006	ns	0.006
50 kDa- 26 kDa+	9 (29)	14 (45)	14 (45)	4 (13)	<i>p</i> OR CI	ns	0.01	0.01
30 kDa- 26 kDa+	11 (35)	5 (16)	10 (32)	6 (20)	<i>p</i> OR CI	ns	ns	ns

WB – Western blot; OR – odds ratio; CI – confidence intervals; ns – non significant.

For other abbreviations see under Table 1.

Seronegativity to 50 kDa along with 26.5 kDa seropositivity was significantly more frequent in DU ($p = 0.01$) and GU ($p = 0.01$) than in FD, but not in GCA.

Seronegativity to VacA along with 50 kDa seropositivity was significantly more frequent in FD than in GCA ($p = 0.01$), GU ($p = 0.01$), and DU ($p = 0.005$).

Seronegativity to VacA along with 30 kDa seropositivity was significantly more frequent in FD than in GCA ($p = 0.002$) and GU ($p = 0.0008$), but not than in DU.

Seronegativity to VacA along with 50 kDa and 30 kDa seropositivity was significantly more frequent in FD than in GCA (0.005) and GU ($p = 0.02$), but showed only trend to significance in comparison with DU ($p = 0.068$).

Seropositivity to both 50 kDa and 30 kDa was significantly more frequent in FD than in GU ($p = 0.006$), but not as frequent as in GCA and DU.

The other synchronous seropositivity combinations were not different among the investigated groups (Table 2).

All alternative seropositivity/seronegativity combinations, apart from 50 kDa or 30 kDa seropositivity, which is significantly more frequent in FD than in GCA ($p = 0.006$) and GU ($p = 0.006$), but not as frequent as in DU, were sig-

nificantly more frequent in GCA, PU, GU groups than in FD or *vice versa* depending on the intention of the test (Table 3).

Synchronous seropositivity to VacA with seronegativity to 50 kDa ($p = 0.014$), synchronous seronegativity to both 50 kDa and 30 kDa ($p = 0.0024$), and 26 kDa seropositivity with seronegativity to 50 kDa ($p = 0.013$) were significantly more frequent in GCA and PU than in FD. Synchronous combinations of VacA seronegativity with 50 kDa seropositivity ($p = 0.001$), 30 kDa seropositivity ($p = 0.01$), 50 kDa and 30 kDa seropositivity ($p = 0.01$) were significantly more frequent in FD than in GCA and PU. In addition to that seropositivity combination of 50 kDa and 30 kDa was significantly more frequent in FD ($p = 0.039$) (Table 4).

All alternative combinations, except for VacA seropositivity or 26 kDa seropositivity, had a significantly more different frequency than the comparison group. Other VacA seropositive combination whatever companion (50 kDa seronegativity, 30 kDa seronegativity, both 50 kDa and 30 kDa seronegativity, 26 kDa seropositivity with either 50 kDa or 30 kDa seronegativity) were significantly more frequent in GCA than in FD. VacA seronegativity along with 50 kDa or 30 kDa seropositivity ($p = 0.0001$), and 50 kDa or 30 kDa

Table 3

Seroreactivity against alternative combination of *Helicobacter pylori* antigens VacA, 50 kDa, 30 kDa and 26 kDa in four groups of patients

WB IgG	Groups, n (%)					FD vs others		
	GCA 31 (100)	DU 31 (100)	GU 31 (100)	FD 30 (100)		GCA	DU	GU
VacA + or 50kDa-	24 (77)	26 (84)	25 (81)	14 (47)	<i>p</i>	0.013	0.002	0.006
					OR	3.92	5.91	4.76
					CI	1.3–11.3	1.8–19.6	1.51–14.95
VacA+ or 50kDa- 30kDa-	24 (77)	20 (65)	24 (77)	10 (32)	<i>p</i>	0.0005	0.015	0.0005
					OR	6.86	3.63	6.86
					CI	2.2–21.3	1.6–10.47	2.2–21.3
VacA+ or 26kDa+ 50kDa-	21 (68)	24 (77)	23 (74)	12 (40)	<i>p</i>	0.03	0.003	0.007
					OR	3.15	5.14	4.31
					CI	1.1–9	1.7–15.7	1.45–12.8
VacA+ or 26kDa+ 30kDa-	23 (74)	20 (65)	23 (74)	11 (37)	<i>p</i>	0.003	0.03	0.003
					OR	4.96	3.14	4.96
					CI	1.67–14.84	1.1–8.93	1.67–14.84
VacA- 50kDa+ or 30kDa+	8 (26)	10 (32)	6 (19)	18 (60)	<i>p</i>	0.007	0.03	0.001
					OR	4.3	3.2	6.3
					CI	1.5–12.8	1.1–9	2–19.8
50kDa+ or 30kDa+	21 (68)	26 (84)	21 (68)	29 (97)	<i>p</i>	0.006	ns	0.006
					OR			
					CI			

WB – Western blot; OR – odds ratio; CI – confidence intervals; ns – non significant.

For other abbreviations see under Table 1.

Table 4

Seroreactivity against synchronous combination of *Helicobacter pylori* antigens in patients with gastric cancer (GCA) and peptic ulcers (PU), and functional dyspepsia (FD)

WB IgG	Patients, n (%)		<i>p</i>	OR	CI (95%)
	GCA and PU 93 (100)	FD 30 (100)			
CagA + VacA+	50 (54)	9 (30)	0.023	2.71	1.1–6.5
VacA+ 26kDa+	47 (50)	10 (30)	ns		
VacA+ 50kDa- 30kDa-	25 (27)	2 (7)	0.03	5.1	1.1–23
VacA+ 30kDa- 50kDa+	16 (17)	3 (10)	ns		
VacA- 50kDa+ 30kDa+	17 (18)	15 (50)	0.0006	4.5	1.8–10.9
VacA- 30kDa+ 50kDa+	19 (20)	16 (53)	0.0006	4.5	1.9–10.7
VacA- 50kDa+ 30kDa+	10 (11)	11 (37)	0.001	4.8	1.8–12.9
50kDa+ 30kDa+	31 (33)	17 (57)	0.03	2.6	1.1–6.1
50kDa- 30kDa-	26 (28)	1 (3)	0.004	11.2	1.5–87
26kDa+ 50kDa-	37 (40)	4 (13)	0.01	4.5	1.4–13.3

WB – Western blot; OR – odds ratio; CI – confidence intervals; ns – non significant.

Table 5

Seroreactivity against alternative combination of *Helicobacter pylori* antigens in patients with gastric cancer (GCA) and peptic ulcers (PU), and functional dyspepsia (FD)

WB IgG	Patients, n (%)		<i>p</i>	OR	CI (95%)
	GCA and PU 93 (100)	FD 30 (100)			
VacA+ or 50kDa-	74 (80)	14 (47)	0.0005	4.45	1.85–10.7
VacA+ or 26kDa+	82 (88)	27 (90)	ns		
VacA+ or (50kDa-)+(30kDa-)	68 (73)	10 (32)	0.0002	5.44	2.24–13.2
VacA+ or (26kDa+)+(50kDa-)	68 (73)	12 (40)	0.002	4.08	1.7–9.67
VacA+ or (26kDa+)+(30kDa-)	66 (71)	11 (37)	0.0016	4.22	1.77–10.05
(VacA-)+(50kDa+) or (30kDa+)	24 (26)	20 (67)	0.0001	5.8	2.4–14
30kDa+ or 50kDa+	68 (73)	29 (97)	0.031	10.7	1.4–82

WB – Western blot; OR – odds ratio; CI – confidence intervals; ns – non significant.
For other abbreviations see under Table 1.

Table 6

Diagnostic characteristics of IgG against 50 kDa, synchronous and alternative combination of VacA, 50 kDa, 30 kDa for functional dyspepsia (FD)

WB bands antigen seroreactivity	GCA and PU, n (%), (n = 93)	FD, n (%) (n = 30)	Sn	Sp	PPV	NPV	CUI+ (VP)	CUI- (P)	Fraction correct
50 kDa	44 (47)	23 (77)	77	53	34	87	0.26 (VP)	0.46 (P)	61
VacA- 50 kDa+ 30 kDa+	10 (11)	11 (37)	37	89	52	81	0.19 (VP)	0.73 (G)	76**
VacA- 50 kDa+ 30 kDa+	17 (18)	15 (50)	50	82	47	83	0.23 (VP)	0.68 (G)	74**
VacA- 30 kDa+ 50 kDa+	19 (20)	16 (53)	53	80	46	84	0.24 (VP)	0.67 (G)	73*
VacA- 50 kDa+ or 30 kDa+	24 (26)	20 (67)	67	74	45	87	0.30 (VP)	0.65 (G)	72.4*

p* < 0.05; *p* < 0.01 vs. 50 kDa group.

Sn – sensitivity; Sp – specificity; PPV – positive predictive value; NPV – negative predictive value; CUI – clinical utility index.

For other abbreviations see under Table 1.

A qualitative interpretation of the clinical utility index: (E) => 0.81 excellent; (G) => 0.64 good; (SA) => 0.49 satisfactory/adequate; (P) => 0.36 poor; (VP) < 0.36 very poor.

seropositivity (*p* = 0.031) were significantly more frequent in FD than in GCA and PU (Table 5).

Among synchronous and alternative seropositivity/seronegativity combinations, we selected those with the most pronounced probability and/or odds ratio and compared their diagnostic characteristics with 50 kDa or VacA. VacA seropositivity or 50 kDa seronegativity (*p* = 0.015) and VacA seropositivity or 50 kDa and 30 kDa seronegativity (*p* = 0.044) had bet-

ter diagnostic characteristics with statistically significant better fraction correct than VacA seropositivity alone (Table 6).

VacA seronegativity along with either 50 kDa or 30 kDa seropositivity (*p* = 0.003), 50 kDa seropositivity (*p* = 0.01), 30 kDa seropositivity (*p* = 0.015), 50 kDa or 30 kDa seropositivity (*p* = 0.02) had better diagnostic characteristics and significantly better fraction correct than 50 kDa seropositivity alone (Table 7, Figure 1).

Table 7

Diagnostic characteristics of IgG against VacA, synchronous and alternative combination of VacA, 50 kDa, 30 kDa for GCA and PU

WB bands antigen seroreactivity	GCA and PU, n (%), (n = 93)	FD, n (%), (n = 30)	Sn	Sp	PPV	NPV	CUI+	CUI-	Fraction correct
VacA	53 (57)	10 (33)	57	67	84	33	0.48 (P)	0.22 (VP)	59
VacA+ or 50 kDa-	75 (82)	14 (47)	81	53	84	47	0.68 (G)	0.25 (VP)	74*
VacA+ or 50 kDa- 30 kDa-	68 (73)	10 (33)	73	67	87	44	0.64 (G)	0.3 (VP)	71.5*
VacA+ or 26 kDa+ 50 kDa-	68 (73)	12 (40)	73	60	85	42	0.62 (SA)	0.25 (VP)	69.9
VacA+ or 26 kDa+ 30 kDa -	66 (71)	11 (37)	71	63	86	41	0.61 (SA)	0.26 (VP)	69

* $p < 0.05$ vs. VacA group.

Sn – sensitivity; Sp – specificity; PPV – positive predictive value; NPV – negative predictive value; CUI – clinical utility index. For other abbreviations see under Table 1.

A qualitative interpretation of the clinical utility index: (E) => 0.81 excellent; (G) => 0.64 good; (SA) => 0.49 satisfactory/adequate; (P) => 0.36 poor; (VP) < 0.36 very poor.

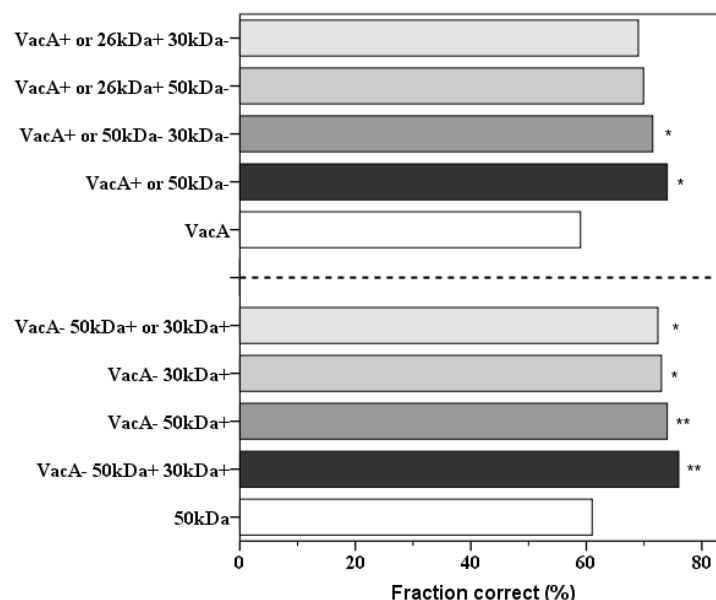


Fig. 1 – Fraction correct of different seroreactivity combination against *Helicobacter pylori* VacA, 50 kDa, 30 kDa and 26 kDa in comparison with 50 kDa and VacA alone.

* $p < 0.05$; ** $p < 0.01$ vs. corresponding 50 kDa (VacA) group.

Discussion

Difference in immune response with preferences to specific antigens was observed in young children¹², but in GCA and PU also, with different results^{3–11}. Our analysis of synchronous seropositivity/seronegativity IgG combinations as a candidate biomarker for the serious outcome of the infection showed that VacA+50 kDa- is significantly more frequent in patients with GCA and PU than in FD due to very low frequency in FD (7%).

At the same time, the frequency of this combination in GCA and PU group was also relatively low (27%), and its

application in clinical practice seems implausible. Seronegativity to both 50 kDa and 30 kDa had similar results.

Alternative seropositivity/seronegativity combination could offer the manifestation of the existing differences. For example, VacA seronegativity was present in 25% of patients with either GCA or PU with synchronous 50 kDa seronegativity. If we applied criteria for VacA seropositivity or 50 kDa seronegativity, we would increase the percent of true positive finding for 25%, and, at the same time, the specificity would decrease due to 13.3% false positive results in FD. The analysis of an alternative seropositivity/seronegativity candidate biomarker for the serious outcome showed more

interesting results with 4 promising combination of VacA+ or 50 kDa- ($p = 0.0005$; OR = 4.45); 50 kDa+ and 30 kDa- ($p = 0.0002$; OR = 5.54); 26 kDa+ and 50 kDa-, and 26 kDa+ and 30 kDa-. These results were notably interesting, giving us the idea to test their diagnostic abilities. When we analyzed diagnostic characteristics of the above-mentioned combinations, two of them VacA+ or 50 kDa- ($p = 0.015$) and VacA+ or 50 kDa+ and 30 kDa- ($p = 0.044$) showed significantly better results than VacA alone. VacA+ or 50 kDa- had the highest sensitivity (81%), lower specificity than VacA+ or 50 kDa- and 30 kDa- (53% vs. 67% vs. 67%, respectively); lower PPV than VacA+ or 50 kDa- and 30 kDa- (84 vs. 87, respectively); highest NPV (47 vs. 33 vs. 44, respectively), and the highest CUI+ (0.68 vs. 0.48 vs. 0.64, respectively). CUIVE+ of both tests can be considered as good, but CUIVE- is very poor for both. These two tests may perspective have a good role in clinical practice^{13, 14}. The analysis of synchronous and alternative seropositivity/seronegativity of VacA, 50 kDa, 30 kDa, 26 kDa antigen combinations regarding a biomarker for functional dyspepsia showed four significant results. VacA seronegativity along with 50 kDa seropositivity ($p = 0.006$, OR = 4.5), 30 kDa seropositivity ($p = 0.0006$, OR = 4.5), 50 kDa and 30 kDa seropositivity ($p = 0.001$, OR = 4.8), and, apart from that, 50 kDa and 30 kDa seropositivity together, were more frequent in FD than in GCA and PU groups. Two alternative combinations have been analyzed, VacA- along with 50 kDa+ or 30 kDa+ ($p = 0.0001$, OR = 5.8), 50 kDa+ or 30 kDa+ ($p = 0.031$, OR = 10.7), both being significantly more frequent in FD than in GCA.

The four combinations with the best results as a biomarker for FD: VacA- along with either 50 kDa+ and 30 kDa+, 50 kDa+ and 30 kDa+, 50 kDa+ or 30 kDa+ have significantly better diagnostic characteristics than 50 kDa seropositivity alone. When we compared diagnostic characteristics of these four tests with 50 kDa seropositivity, we found that sensitivity and NPV were the highest in 50 kDa. Specificity, PPV and CUIVE- were the highest in VacA- along with 50 kDa+ and 30 kDa+ combination. NPV and CUIVE+ were the highest in VacA- along with 50 kDa+ or 30 kDa+. It is interesting that all four combinations have CUIVE- at the level of "good", but at the same time all CUIVE+ were "very poor". This implies possible application of these seroreactivity combinations as a test with good screening utility.

Alternative seropositivity/seronegativity combination led to the improvement of sensitivity, with no significant deterioration of specificity.

Previously published results highlighted the association of 19 kDa or 19.5 kDa seropositivity with 35 kDa⁴, 136 kDa⁵, 136 kDa along with 33 kDa⁵ and GCA. Contrary to the previous, Chua et al.⁷ reported that the seronegativity of 19 kDa and 35 kDa were associated with GCA. According to the study of Karami et al.⁶ 126 kDa and 89 kDa seropositivity are associated with GCA, but Janulaityte-Günther et al.⁸ reported only the synchronous seropositivity of 120 kDa and 85 kDa associated with GCA, while with the absence of one seropositivity, the association with GCA disappeared. According to the published results, PU is associated with 35 kDa seropositivity along with either 87 kDa seropositivity, 87 kDa or 125 kDa seropositivity⁹, and CagA seropositivity¹⁰. In our study, we did not use 19 kDa, 19.5 kDa and 35 kDa antigens. Shafai et al.¹⁵ reported that multiplex serology assay using synchronously more *H. pylori* antigens was able not only to detect subjects with current *H. pylori* infection, but it could also screen dyspeptic patients for the presence of gastric atrophy. This simple and cost-efficient method can supplement routine screening ELISAs to increase the chances of detecting current infections, as well as atrophic gastritis.

The limitations of our study were a relatively small number of participants, and German ViraBlot with *H. pylori* isolates from German patients.

Conclusion

In our study combined seropositivity/seronegativity of *H. pylori* antigens VacA, 50 kDa and 30 kDa had a significantly stronger association with either GCA and PU or FD than previously reported single seropositivity against VacA and 50 kDa. It could be interesting to analyze diagnostic abilities of the observed shift in response to *H. pylori* antigens VacA, 50 kDa and 30 kDa related to the severity of gastric mucosal lesion. Synchronous and/or alternative seropositivity/seronegativity to *H. pylori* antigens VacA, 50 kDa and 30 kDa may be investigated as a diagnostic test, and in our further analysis it would be justified to be tested vs. and along with alarm features in patients with dyspeptic symptoms, in order to select the patients with the uninvestigated dyspepsia who are candidates for early EGDS.

REFERENCES

1. Song H, Michel A, Nyrén O, Ekström AM, Pawlita M, Ye W. A CagA-independent cluster of antigens related to the risk of noncardia gastric cancer: associations between *Helicobacter pylori* antibodies and gastric adenocarcinoma explored by multiplex serology. *Int J Cancer* 2014; 134(12): 2942–50.
2. Yokota S, Amano K, Hayashi S, Kubota T, Fujii N, Yokochi T. Human antibody response to *Helicobacter pylori* lipopolysaccharide: presence of an immunodominant epitope in the polysaccharide chain of lipopolysaccharide. *Infect Immun* 1998; 66(6): 3006–11.
3. Manojlović N, Tufegđić I, Ristanović E, Bokunjić D. Serum IgG antibodies against *Helicobacter pylori* low molecular weight antigens 50kDa, 30kDa and Urease A 26 kDa, along with Vacuolating cytotoxin A are associated with the outcome of infection. *Vojnosanit Pregl* 2020; 77(4): 405–12.
4. Chomvarin C, Ottivet O, Hahnvajanawong C, Intapan PM, Wongvajanana S. Seroreactivity to specific antigens of *Helicobacter pylori* infection is associated with an increased risk of the dyspeptic gastrointestinal diseases. *Int J Infect Dis* 2009; 13(5): 647–54.
5. Schumann C, Triantafilou K, Rasche FM, Möricke A, Vogt K, Triantafilou M, et al. Serum antibody positivity for distinct *Helicobacter pylori* antigens in benign and malignant gastroduodenal disease. *Int J Med Microbiol* 2006; 296(4–5): 223–8.

6. Karami N, Talebkhan Y, Saberi S, Esmaili M, Oghalaie A, Abdirad A, et al. Seroreactivity to *Helicobacter pylori* antigens as a risk indicator of gastric cancer. *Asian Pac J Cancer Prev* 2013; 14(3): 1813–7.
7. Chua TS, Fock KM, Chan YH, Dhamodaran S, Sim CS, Ng TM, et al. Seroreactivity to 19.5-kDa antigen in combination with absence of seroreactivity to 35-kDa antigen is associated with an increased risk of gastric adenocarcinoma. *Helicobacter* 2002; 7(4): 257–64.
8. Janulaityte-Günther D, Kupcinskas L, Pavilonis A, Valuckas K, Wadström T, Andersen LP. Combined serum IgG response to *Helicobacter pylori* VacA and CagA predicts gastric cancer. *FEMS Immunol Med Microbiol* 2007; 50(2): 220–5.
9. Aucher P, Petit ML, Mannant PR, Pezennec L, Babin P, Fauchere JL. Use of immunoblot assay to define serum antibody patterns associated with *Helicobacter pylori* infection and with *H. pylori*-related ulcers. *J Clin Microbiol* 1998; 36(4): 931–6.
10. Lamarque D, Gilbert T, Roudot-Thoraval F, Deforges L, Chaumette MT, Delchier JC. Seroprevalence of eight *Helicobacter pylori* antigens among 182 patients with peptic ulcer, MALT gastric lymphoma or non-ulcer dyspepsia. Higher rate of seroreactivity against CagA and 35-kDa antigens in patients with peptic ulcer originating from Europe and Africa. *Eur J Gastroenterol Hepatol* 1999; 11(7): 721–6.
11. Filipčec Kanizaj T, Katić M, Presecki V, Gasparov S, Colić Cvrle V, Kolaric B, et al. Serum antibodies positivity to 12 *Helicobacter pylori* virulence antigens in patients with benign or malignant gastroduodenal diseases-cross-sectional study. *Croat Med J* 2009; 50(2): 124–32.
12. Kindermann A, Konstantopoulos N, Lehn N, Demmelmaier H, Koletzko S. Evaluation of two commercial enzyme immunoassays, testing immunoglobulin G (IgG) and IgA responses, for diagnosis of *Helicobacter pylori* infection in children. *J Clin Microbiol* 2001; 39(10): 3591–6.
13. Mitchell AJ. Sensitivity \times PPV is a recognized test called the clinical utility index (CUI+). *Eur J Epidemiol* 2011; 26(3): 251–2; author reply 252.
14. Bossuyt PM, Reitsma JB, Linnert K, Moons KG. Beyond diagnostic accuracy: the clinical utility of diagnostic tests. *Clin Chem* 2012; 58(12): 1636–43.
15. Shafaie E, Saberi S, Esmaili M, Karimi Z, Najafi S, Tashakoripoor M, et al. Multiplex serology of *Helicobacter pylori* antigens in detection of current infection and atrophic gastritis - A simple and cost-efficient method. *Microb Pathog* 2018; 119: 137–44.

Received on January 16, 2020

Accepted on July 13, 2020

Online First July, 2020



Analysis of structural and vascular changes of the optic disc and macula in different stages of primary open angle glaucoma

Analiza strukturnih i vaskularnih promena optičkog diska i makule u različitim stadijumima primarnog glaukoma otvorenog ugla

Maja Petrović*, Mirko Resan^{†‡}, Gordana Stanković Babić[§], Tatjana Šarenac Vuločić^{||}, Marija Radenković*, Aleksandar Veselinović*, Marija Trenkić[§], Marija Cvetanović*

*Clinical Center Niš, Eye Clinic, Niš, Serbia ; [†]Military Medical Academy, Eye Clinic, Belgrade, Serbia; [‡]University of Defence, Faculty of Medicine of the Military Medical Academy, Belgrade, Serbia; [§]University of Niš, Faculty of Medicine, Niš, Serbia; ^{||}University of Kragujevac, Faculty of Medicine, Kragujevac, Serbia

Abstract

Background/Aim. It is possible that patients with open-angle glaucoma be asymptomatic in the early stage of the disease. The aim of this study was to determine the structural and vascular changes of the optic disc (OD) and macula in healthy and primary open-angle glaucoma (POAG) eyes, detected by optical coherence tomography (OCT) and optical coherence tomography angiography (OCTA) as well as the correlation of the OCT and OCTA measurements and their association with the presence of POAG. **Methods.** A total of 196 eyes were included and classified into four groups, out of them 48 were healthy eyes, 51 eyes were with mild POAG, 50 eyes with moderate POAG, and 47 eyes with advanced glaucoma. All subjects underwent standard ophthalmic examination. OCT measured the mean, superior and inferior retinal nerve fiber layer (RNFL) thickness and macular ganglion cell complex (GCC). OCTA evaluated the vessel capillary density (VCD) in OD, foveal avascular zone (FAZ) and macular vessel density (VD) in the superficial (SL) and deep (DL) retinal vascular plexus. **Results.** Patient characteristics were similar except for

decreased visual acuity, thinner corneas, higher intraocular pressure and higher cup/disc ratio in POAG patients. OCT results showed that RNFL and GCC thickness gradually decreased according to POAG severity. Within the assessment conducted by OCTA, VCD's value in OD also diminished with the progression of POAG, having the lowest value in patients with advanced glaucoma. The same pattern was observed in vessel density around FAZ and VD values. Comparing the structural and vascular changes, a significant positive correlation was found between RNFL thickness and VCD inside OD, and GCC and VD SL in the macular zone. **Conclusion.** OCT and OCTA allow of a noninvasive quantification of the structural and vascular changes in OD and the macular zone and accurately distinguish between healthy eyes and eyes with POAG, showing an association with the presence and progression of glaucoma.

Key words: angiography; disease progression; glaucoma, open-angle; macula lutea; optic disc; tomography, optical coherence.

Apstrakt

Uvod/Cilj. U ranoj fazi bolesti, bolesnici sa glaukomom otvorenog ugla ne moraju imati simptome. Cilj rada je bio da se utvrde strukturne i vaskularne promene optičkog diska (OD) i makule u zdravim očima i očima kod bolesnika sa primarnim glaukomom otvorenog ugla (PGOU), koje su registrovane optičkom koherentnom tomografijom (OKT) i optičkom koherentnom tomografskom angiografijom (OKTA), kao i korelacija između OKT i OKTA parametara i njihova povezanost sa prisustvom PGOU. **Metode.** Ukupno je analizirano 196 očiju podeljenih u četiri grupe: 48 zdravih očiju, 51 sa blagim glaukomom, 50 sa umerenim glaukomom i

47 očiju sa uznapredovalim glaukomom. Svi ispitanici pregledani su standardnim oftalmološkim pregledom. Pomoću OKT merena je debljina prosečnog, gornjeg i donjeg sloja nervnih vlakana mrežnjače (SNVM) i ganglijskog ćelijskog kompleksa (GČK) makule, a pomoću OKTA analizirala je gustina kapilarnih krvnih sudova (GKS) u OD, fovealna avaskularna zona (FAZ) i gustina krvnih sudova (GS) makule u površinskoj (P) i dubokoj (D) retinalnoj vaskularnoj mreži. **Rezultati.** Bolesnici sa PGOU imali su smanjenu oštrinu vida i smanjenu debljinu rožnjače, povišeni očni pritisak (OP) kao i povećani *cup/disc* (C/D) odnos. Rezultati OKT pokazali su da je prosečna debljina SNVM, kao i debljina GČK smanjena kod bolesnika sa PGOU, posebno u kasnoj fazi bolesti. Ana

lizom OKTA utvrđeno je da se vrednosti GKS u OD takođe smanjuju sa napredovanjem PGOU, pokazujući najnižu vrednost kod bolesnika sa uznapredovalim glaukomom. Isto je zapaženo putem OKTA pregleda makule i praćenjem gustine krvnih sudova oko FAZ i vrednosti GS makule. Upoređivanjem strukturnih i vaskularnih promena, utvrđena je značajna pozitivna korelacija između debljine SNVM i GKS unutar OD, kao i GKS i GS makule u P retinalnoj vaskularnoj mreži. **Zaključak.** Primena OKT i OKTA

omogućuje neinvazivnu kvantifikaciju strukturnih i vaskularnih promena u OD i makularnom predelu i precizno razlikovanje zdravih očiju od očiju sa PGOU, pokazujući povezanost sa prisustvom i progresijom glaukoma.

Ključne reči:

Angiografija; bolest, progresija; glaukom otvorenog ugla; žuta mrlja; optički disk; tomografija, optička, koherentna.

Introduction

Glaucoma represents the second leading cause of blindness worldwide ¹. It is a progressive optic neuropathy leading to preventable but irreversible visual defects ². It remains unclear whether the decreased retinal blood flow is the cause or result of an optic nerve glaucomatous damage ³. However, there is growing evidence that vascular hypothesis, supported by reduced retinal blood flow and vessel diameter seen in glaucoma patients, can depict the pathogenesis of glaucoma ^{4,5}.

Recently, scholars have suggested that the vascular dysfunction in the optic disc (OD), also termed as optic nerve head, may have a crucial role in the development and progression of the open angle glaucoma (OAG) ⁶. Considering the possibility for patients with glaucoma to be asymptomatic in the early stages, there is a serious risk for them to remain undiagnosed until the symptoms occur ⁴. We hypothesize that it is important to visualize retinal microcirculation in order to confirm the diagnose and treat patients accordingly. The optical coherence tomography angiography (OCTA) was introduced as a reliable, non-invasive, rapid diagnostic procedure providing assessment of perfusion separately in various retinal layers, as well as in the OD ⁷. Recent studies showed a reduced papillary vessel density (VD) in glaucomatous eyes ⁸ and suggested a possible correlation between the diameter of the retinal arterioles and the optic nerve damage ⁵. Additionally, measuring the macular perfusion has the potential for detecting a reduced metabolic rate in dysfunctional retinal ganglion cells before they undergo apoptosis and cause the ganglion cell complex (GCC) to become thinner ⁹.

Structural changes in glaucoma patients can be detected using optical coherence tomography (OCT) as one of the noninvasive imaging technologies. OCT is designed to assess morphology and thickness of retinal layers, such as the innermost layers of the retina, which include the retinal nerve fiber layer (RNFL), ganglion cell layer, and inner plexiform layer. Diagnostic accuracy for glaucoma can be improved when macular OCT measurements focus particularly on the GCC ⁹, since it provides detailed information of retinal structure ¹⁰. Both OCT and OCTA differentiate between healthy and glaucomatous eyes ¹¹. Nerve fiber layer and vessel diameter changes are pathophysiological manifestations of OAG without a strict cause-effect relationship in terms of which one appears first ⁴. However, some studies confirmed their correlation showing OD blood flow decrease and RNFL thickness reduction are directly correlated in glaucoma patients ³. Similar findings were observed within healthy subjects, showing retinal

VD directly correlating with the RNFL thicknesses ¹⁰. Furthermore, vessel density within the RNFL was lower in patients suffering from OAG ¹².

The aim of this study was to evaluate structural and vascular changes of the OD and macula in healthy and OAG eyes, detected by OCT and OCTA, and to examine correlation of OCT and OCTA measurements and their association with the presence and stage of OAG.

Methods

This investigation was designed as a cross-sectional study. We examined a total of 196 eyes from 196 adult primary OAG (POAG) or POAG suspected patients examined at the Eye Clinic, Clinical Center Niš, Serbia from June 2019 to February 2020. The study was conducted according to the Declaration of Helsinki and the protocol was approved by the local Ethics Committee of the Clinical Center Niš.

Participants were enrolled after obtaining the informed consent and were divided into four groups. Group 1 consisted of 48 healthy eyes; group 2 had 51 eyes with stage 1 POAG; group 3 had 50 eyes with stage 2 POAG; and group 4 had 47 eyes with advanced glaucoma. Staging of POAG was performed by Hodapp-Parrish classification of severity of visual field defect. All subjects underwent standard ophthalmologic examination including visual acuity (VA) assessment, intraocular pressure (IOP) measurement using Goldmann applanation tonometry and a standard anterior segment slit lamp examination. Central Corneal Thickness (CCT) was measured by Pachymetry on Optical biometer and topography-keratometer OA-2000 Tomey.

All OCT and OCTA examinations were performed at Optovue apparatus, AngioVue Comprehensive Imaging system, using two patented technologies: Split Spectrum Amplitude Decorrelation Angiography (SSADA protocol) and Motion Correction Technology for reduction of artifacts by using software volume-based projection artifact removal (3D PAR). The vessel density measurements were determined with PAR correction only. The SSADA method is used to compare the consecutive B scans at the same location to capture the dynamic motion of the red blood cells using motion contrast. A trained examiner reviewed all the OCTA scans and only the images with good clarity, a signal strength index (SSI) of more than 50, with no residual motion were included for the analysis. Image cropping or local weak signal resulting from vitreous opacity or segmentation errors that could not be corrected were rejected.

The OCT measurement parameters in OD were RNFL defined as the thickness in micrometers and Cup/Disc area

(C/D) in mm^2 . RNFL thickness was determined in OD mode in which data, along a 3.45-mm-diameter circle around the OD, was mapped using 12 concentric rings and 24 radial scans. Mean, superior, and inferior RNFL thicknesses were computed. The GCC scan covered a square grid of 6×6 mm on the central macula and was centered 1 mm temporal to the fovea. The GCC thickness was measured from the inner limiting membrane (ILM) to the posterior boundary of the inner plexiform layer. Mean, superior, and inferior GCC thicknesses were acquired.

During OCTA and retinal structure assessment, vessel capillary density (VCD) and vascular network density were evaluated in OD. Whole image (WI), inside disc (ID) and peripapillary density (PP) were acquired. In the foveal avascular zone (FAZ), OCTA analysed the following parameters: FAZ area, FAZ perimeter and foveal density (FD) – vessel density of the 300μ width ring surrounding the FAZ, macular vessel density (VD) in the superficial (SL) and deep (DL) retinal vascular plexus with a 6×6 mm² macula scan were determined. Vessel density was calculated as the percent area occupied by flowing blood vessels in the selected region.

The retinal layers of each scan were segmented automatically by the AngioVue software to visualize the superficial retinal capillary plexuses in a slab from ILM to the inner plexiform layer (IPL) minus $10 \mu\text{m}$. For this study, whole *en face* image VD (wiVD) was derived from the entire 6×6 mm² scan, and perifoveal VD was measured in an annular region centered on the fovea with an inner diameter of 1 mm and outer diameter of 3 mm.

The visual field was tested by the Standard Automatic Perimetry (SAP) 24-2 threshold test, at the Optopol PTS perimeter.

We included patients aged above 40 years with a confirmed diagnosis of glaucoma, without any chronic disease (diabetes, neurological disorders, cataracts, except the ones with the level of <1 according to Lens Opacity Classification System) or medication use that could influence OCT and OCTA results. Other exclusion criteria were subjects with false positive and negative errors $> 15\%$ and fixation loss $> 33\%$, on SAP, low signal intensity on OCT and poorly centered scan, anomalies in the anterior segment of the eye, trauma, chronic inflammation, retinal diseases, previously surgical and/or laser eye surgery. Pregnant women and women in the period of the lactation were also not considered.

Furthermore, eyes with a history of intraocular surgery (except uncomplicated cataract surgery or uncomplicated glaucoma surgery), coexisting retinal pathologic features, nonglaucomatous optic neuropathy, uveitis, or ocular trauma

were also excluded from the study, as were individuals with a diagnosis of Parkinson's disease, Alzheimer's disease, or dementia and a history of stroke or diabetic or hypertensive retinopathy.

Data analysis and sample size determination

A total sample size was calculated *a priori* based on the G*Power software. A predicted effect size of 0.7 was smaller compared to the literature data where the difference in RNFL thickness between healthy subjects and glaucoma patients was 1.6482, the statistical power of 90% and significance level of 5%. We used a one-tailed *t*-test. Under these circumstances, a minimum of 82 patients (41 per group) were needed for this study.

In order to analyze the collected data, we used the standard methods of descriptive statistics. The differences between the mean values of continuous variables with normal distribution were assessed by a parametric ANOVA test. We used a nonparametric Kruskal Wallis H test for variables whose values did not follow a normal distribution. *Post hoc* analysis was done by a parametric Student's *t*-test and for variables whose values did not follow a normal distribution we used a non-parametric Mann-Whitney *U* test. To determine the differences in the incidence of certain categories, we used a χ^2 test or Fisher's test of the real likelihood for low frequencies. The presence of a relation between the variables of interest was analyzed by standard correlation analysis using the Pearson's correlation coefficient to determine the direction and strength of the connection/correlation. Binary logistic regression models were used to evaluate the association between OCT and OCTA parameters with the presence of POAG. In all analyses, *p*-value of less than 0.05 was considered as statistically significant.

Results

There were 76 (38.8%) males and 120 (61.2%) females, aged 66.4 ± 8.2 years (46–89 years), without a significant difference in average age between genders (66.7 ± 8.5 years male and 66.4 ± 8.0 years female).

Analysis was done between groups of glaucoma patients [148 (76.5%)] and healthy subjects [48 (24.5%)] with similar gender proportion and average age in both groups. The patients with glaucoma were divided according to glaucoma stage. There was a similar average age between the groups. The IOP was the highest and CCT the lowest in the third stage of glaucomatous eyes. Clinical characteristics of the examined groups of patients are shown in Table 1.

Table 1

Baseline characteristics of patients

Characteristics	Healthy subjects	Patients with glaucoma		
		first stage	second stage	third stage
Patients, n (%)	48 (24.5)	51 (26.0)	50 (25.5)	47 (24.0)
Male/female, n/n	13/35	17/33	23/27	23/24
Age (years), mean \pm SD	64.1 ± 9.2	66.7 ± 7.6	67.4 ± 8.4	67.6 ± 7.6
Visual acuity, mean \pm SD	0.99 ± 0.05	$0.91 \pm 0.18^*$	$0.85 \pm 0.24^*$	$0.69 \pm 0.3^{**}$
IOP (mmHg), mean \pm SD	17.9 ± 3.5	17.4 ± 3.3	18.6 ± 6.2	$23.2 \pm 11.9^*$
CCT (μm), mean \pm SD	543.0 ± 32.2	541.5 ± 24.3	537.1 ± 32.5	$510.4 \pm 34.5^{**}$

IOP – intraocular pressure; CCT – central corneal thickness; SD – standard deviation.

Statistical analysis included Kruskal Wallis test: $*p < 0.05$ vs. other groups; $**p < 0.01$ vs. other groups.

Analysis of the OCT parameters of OD and macula are shown in Tables 2 and 3. All examined OCT parameters, including average, superior and inferior RNFL thickness, were significantly lower in patients with glaucoma. Also, the glaucoma patients in the third stage had a substantial decrease in all values compared to the first stage. The C/D area was significantly higher in glaucoma patients and, among them, it was significantly higher in patients with the

third stage of glaucoma, compared to other stages.

All OCT measurements of the macula were significantly higher in the healthy subjects compared to glaucoma patients. GCC differed significantly between stages, being highest in the first and lowest in the third stage (Table 3).

Analysis of the OCTA at the level of macula and OD are shown in Tables 4 and 5. All examined OCTA

Table 2

Optical coherence tomography measurement of optic disc

Parameter	Healthy subjects	Patients with glaucoma		
		first stage	second stage	third stage
RNFL (μm), mean \pm SD	100.7 \pm 6.9*	87.6 \pm 10.2	84.2 \pm 10.3	67.9 \pm 14.2 [†]
RNFL sup. (μm), mean \pm SD	103.2 \pm 6.7*	89.5 \pm 9.7	86.4 \pm 10.4	70.3 \pm 16.5 [†]
RNFL inf. (μm), mean \pm SD	98.3 \pm 7.8*	85.9 \pm 11.2	81.4 \pm 11.7	66.2 \pm 15.2 [†]
C/D area (mm^2), mean \pm SD	0.34 \pm 0.1*	0.44 \pm 0.1	0.55 \pm 0.2	0.72 \pm 0.1 [#]

RNFL –retinal nerve fiber layer; sup. – superior; inf. – inferior; C/D – Cup/Disc area; SD – standard deviation.

Statistical analysis included Kruskal Wallis test or ANOVA: * $p < 0.01$ vs. all stages glaucoma; # $p < 0.01$ vs. other glaucoma stages; [†] $p < 0.01$ vs. first stage (*post hoc* analysis).

Table 3

Optical coherence tomography measurement of macula

Parameter	Healthy subjects	Patients with glaucoma		
		first stage	second stage	third stage
GCC (μm), mean \pm SD	96.3 \pm 5.2*	89.5 \pm 8.8 [#]	84.9 \pm 10.6 [#]	69.8 \pm 12.8
GCC sup (μm), mean \pm SD	95.6 \pm 5.2*	89.5 \pm 8.7 [#]	85.2 \pm 11.0 [#]	69.8 \pm 14.2
GCC inf (μm), mean \pm SD	97.1 \pm 5.4*	89.6 \pm 9.1 [#]	84.7 \pm 12.3 [#]	69.3 \pm 15.2

GCC – ganglion cell complex; sup. – superior; inf. – inferior.

Statistical analysis included Kruskal Wallis test or ANOVA: * $p < 0.01$ vs. all stages glaucoma; # $p < 0.01$ vs. other glaucoma stages (*post hoc* analysis).

Table 4

Optical coherence tomography angiography measurement of small vessels in optic disc

Parameter	Healthy subjects	Patients with glaucoma		
		first stage	second stage	third stage
WI VCD, mean \pm SD	51.03 \pm 1.89*	47.18 \pm 3.24	46.28 \pm 3.44	38.08 \pm 6.42 [#]
ID VCD, mean \pm SD	51.45 \pm 5.08*	46.70 \pm 6.46	47.57 \pm 5.78	43.36 \pm 8.45 [#]
PP VCD, mean \pm SD	53.62 \pm 2.26*	50.12 \pm 3.87	48.59 \pm 3.91 [#]	38.04 \pm 8.45 [#]
PP sup. VCD, mean \pm SD	54.08 \pm 2.55*	50.09 \pm 3.73	48.96 \pm 3.85	38.74 \pm 9.17 [#]
PP inf. VCD, mean \pm SD	53.36 \pm 2.27*	50.05 \pm 4.45	48.09 \pm 5.05	37.64 \pm 9.11 [#]

WI– whole image; VCD – vessel capillary density; ID – inside disc; PP – peripapillary; sup. – superior; inf. – inferior.

Statistical analysis included Kruskal Wallis test or ANOVA: * $p < 0.01$ vs. glaucoma; # $p < 0.01$ vs. other glaucoma stages (*post hoc* analysis).

Table 5

Optical coherence tomography angiography measurement of macula

Parameter	Healthy subjects	Patients with glaucoma		
		first stage	second stage	third stage
FAZ area (mm^2), mean \pm SD	0.24 \pm 0.09*	0.33 \pm 0.14	0.34 \pm 0.11	0.35 \pm 0.12
FAZ perimeter (mm), mean \pm SD	1.99 \pm 0.46*	2.33 \pm 0.87	2.38 \pm 0.53	2.58 \pm 0.78
FD (%), mean \pm SD	51.46 \pm 4.06*	45.29 \pm 8.34	46.02 \pm 6.97	45.53 \pm 6.14
VD SL (%), mean \pm SD	47.38 \pm 3.24*	41.51 \pm 6.39	42.03 \pm 4.82	37.44 \pm 6.08 [#]
VD SL sup. (%), mean \pm SD	47.64 \pm 3.77*	40.58 \pm 5.99	41.96 \pm 4.95	37.66 \pm 6.14 [#]
VD SL inf. (%), mean \pm SD	47.36 \pm 3.42*	41.17 \pm 5.87	41.75 \pm 5.19	36.90 \pm 6.57 [#]
VD DL (%), mean \pm SD	52.89 \pm 3.25*	50.08 \pm 4.71	48.46 \pm 5.14	46.23 \pm 6.00 [†]
VD DL sup. (%), mean \pm SD	53.11 \pm 3.17*	50.19 \pm 4.85	48.68 \pm 5.34	46.86 \pm 6.03 [†]
VD DL inf. (%), mean \pm SD	52.66 \pm 3.58*	50.01 \pm 5.00	48.13 \pm 5.64	45.78 \pm 6.61 [†]

FAZ – foveal avascular zone; FD – vessel density of the 300 μ width ring surrounding the FAZ; VD – macular vessel density in the superficial (SL) and deep (DL) retinal vascular plexus; sup. – superior; inf. – inferior.

Statistical analysis included Kruskal Wallis test or ANOVA: * $p < 0.01$ vs. glaucoma; # $p < 0.01$ vs. other glaucoma stages; [†] $p < 0.01$ vs. first stage (*post hoc* analysis).

parameters were significantly higher in healthy subjects. All variables were notably lower in patients with the third stage of glaucoma compared to the first stage. Value of peripapillary (PP) VCD differed substantially between all stages, being highest in the first and lowest in the third stage (Table 4).

All examined OCTA parameters (FAZ area and perimeter, FD, VD SL and VD DL) were significantly higher in healthy subjects compared to glaucoma. All VD in superficial layers were substantially lower in the third stage compared to the first and second stages. VD in deep layer was significantly lower in patients with the third stage of glaucoma only compared to the first stage (Table 5).

Pearson correlation coefficient showed significant positive correlation between GCC and VD in superficial retinal vascular plexus, while other OCT and OCTA parameters did not show significant interrelation. Contrary, in glaucoma patients, significant correlation was shown between VD in the superficial and deep retinal vascular plexuses with GCC (Table 6).

The Pearson's correlation coefficient showed significant positive correlation only between RNFL average and whole image VD ($r = 0.314$, $p < 0.05$) in OD of healthy subjects. All OCT and OCTA parameters showed strong and significant positive correlation in patients with glaucoma (Table 7).

Association of OCT and OCTA measurements of macula and OD with presence of glaucoma were analyzed by

binary logistic regression model (Enter model). For the binary logistic regression dependent variable was coded as 0-no glaucoma and 1-presence of glaucoma, while independent variables were OCTA and OCT measurements of macula or OD.

The analysis showed significant association of ID VCD – inside disc vessel capillary density with presence of glaucoma [ExpB 0.66; 95% confidence interval (CI) 0.46–0.93]. The increase of this OCTA parameter for one unit reduced odd for glaucoma appearance for 34%. All other parameters of OD did not show significant association with glaucoma. Other performed analysis of macula parameters showed significant association of OCT parameters: GCC superior (ExpB 0.51; 95% CI 0.29–0.90) and GCC inferior (ExpB 0.46; 95% CI 0.24–0.85). Increasing these parameters for one unit reduced the odds for glaucoma for about 50%. OCTA showed significant association of FD with glaucoma (ExpB 0.76; 95% CI 0.63–0.91) and reduction of odd for 24% for one unit increase.

Discussion

Long-standing mechanical approach to glaucomatous OD damage blames increased intraocular pressure as the main reason for visual impairment. With the introduction of novel techniques capable of measuring vascular density and blood flow, a new vascular theory in the pathogenesis of glaucoma was revealed. One of these techniques, the OCTA,

Table 6

Pearson's correlation coefficient between optical coherence tomography (OCT) and OCT angiography (OCTA) parameters of macula

OCT parameters	OCTA parameters	Healthy subjects	Glaucoma patients
GCC total	FAZ area	-0.257	-0.108
	FAZ perimeter	-0.225	-0.136
	FD	0.241	0.016
	VD SL	0.491**	0.449**
	VD DL	0.226	0.394**
GCC superior	VD SL superior	0.577**	0.390**
	VD DL superior	0.223	0.322**
GCC inferior	VD SL inferior	0.289*	0.538**
GCC inferior	VD DL inferior	0.166	0.222**

GCC – ganglion cell complex; FAZ – foveal avascular zone; FD – vessel density of the 300 μ width ring surrounding the FAZ; VD – vessel density; DL – deep layer; SL –superficial layer.

* $p < 0.05$; ** $p < 0.01$.

Table 7

Pearson's correlation coefficient between optical coherence tomography (OCT) and OCT angiography (OCTA) parameters of optical disc

OCT parameters	OCTA parameters	Healthy subjects	Glaucoma patients
RNFL average	WI VCD	0.284	0.698**
	ID VCD	0.276	0.165*
	PP VCD	0.136	0.719**
	WI VD all vessels	0.314*	0.644**
	ID VD all vessels	0.248	0.293**
	PP VD all vessels	0.200	0.727**
RNFL superior	PP VCD superior	0.169	0.664**
RNFL superior	PP VCD superior all vessels	0.134	0.688**
RNFL inferior	PP VCD inferior	0.123	0.707**
RNFL inferior	PP VD inferior all vessels	0.237	0.719**

RNFL –retinal nerve fiber layer; WI – whole image; VCD – vessel capillary density; ID – inside disc; PP – peripapillary; WI – whole *en face* image; VD – vessel density.

* $p < 0.05$; ** $p < 0.01$.

is a noninvasive, high-resolution depiction of the vascular structure in the retina. With this as a measurement, the Fechtner and Weinreb¹³ theory was established, arguing that the change in blood flow in OD is the pathogenic factor leading to visual field loss, and that macular involvement had significant influence in glaucoma pathogenesis. In this prospective study, we evaluated the characteristics of OCT and OCTA findings in healthy and OAG eyes.

This study confirms the finding of other authors that corneal thickness and IOP play an important part in the diagnosis and understanding of various types of glaucoma¹⁴. In patients with POAG, all examined OCT parameters in OD and macula differ significantly from those found in healthy subjects and among different stages of POAG. This clearly indicates structural damage in glaucomatous eyes registered by the OCT. Glaucoma leads to progressive damage of retinal ganglion cells and their axons in the RNFL presented with thinning. Clinical follow-up and evaluation of glaucoma needs sensitive methods for detecting progression and preventing visual field loss. OCT and OCTA enable multiple parameters to be used for monitoring disease progression¹⁵. However, predicting this disease progression, especially in advanced stages of POAG, is challenging because of the existence of a so-called “floor effect”, after which no further structural change can be detected in OCT-based RNFL thickness measurements and due to an increase in variability of VF measurements¹⁶. RNFL in whole and both superior and inferior position was significantly lower in glaucomatous eyes. Literature data indicate that RNFL thinning and rate of average RNFL loss detected by OCT were connected with visual field loss. This stands for both glaucoma suspects and glaucomatous eyes^{17, 18}. In line with these results, examined glaucomatous eyes had significantly deteriorated VA and parameters of visual field. Previous studies have already established regional correlations between RNFL loss, GCC loss, and visual field deficits in glaucomatous eyes, showing concomitant structural damages in macula as seen in OD¹⁹.

The importance of the spatial structure of RNFL thickness map data over conventional average circumpapillary RNFL thickness in diagnosing glaucoma was clearly demonstrated in a *post hoc* study of 93 eyes from Los Angeles Latino Eye Study (LALES). Superior diagnostic performance was shown for all models using full RNFL thickness maps²⁰. In patients with glaucoma, all sectors and average RNFL showed significant association with the development of glaucoma. In developed glaucomatous eyes, standard determination of RNFL has high clinical value but its determination is primarily connected with prediction of visual field loss.

All examined OCTA parameters at the level of OD and macula showed significant differences in healthy subjects and patients with glaucoma, indicating presence of vascular damage, alongside structural impairment. This is in line with the data from a similar study confirming that VCD is diminished in glaucomatous eyes^{21–23}. Some literature data present that all the OD VD parameters except the inside disc VD were significantly lower in glaucomatous eyes than in control eyes²⁴. Other results indicate the VCD in the radial

papillary capillaries layer and in the nerve head layer of glaucomatous eyes was significantly lower than in age-matched control eyes¹. The same authors presented results that VCD in all peripapillary segments was higher than in NHL, similarly to our findings.

All examined macular OCTA parameters in superficial and deep layers differentiated in glaucoma presence and the stage of the disease. This highlights a role of vascular factors in the pathogenesis of glaucoma. In a prospective study examining change rate of GCC thickness and macular VD in healthy and OAG eyes, scholars presented results that glaucomatous eyes showed a faster decrease in macular VD than GCC thinning. Faster macular VD decrease rate was significantly associated with the severity of glaucoma, however, the association between GCC thinning rate and glaucoma severity was insignificant²⁵. Recent longitudinal study found that rate of change in macula whole *en face* VD was substantially quicker in OPG (-2.23% per year) than in healthy eyes (0.29% per year). Conversely, the rate of change in GCC thickness was not significantly different from zero, and no significant differences in the rate of GCC change among diagnostic groups were found¹⁶. This indicates that vascular changes in macula have a better predictive role for development of OAG than structural changes. Literature data showed that projection-resolved OCTA algorithm, used to remove flow projection artifacts, and superficial vascular complex density in macula, showed high accuracy in detection of glaucoma and glaucoma stages. This could be useful in the clinical evaluation⁹. OCTA could be a promising tool for monitoring glaucoma progression, particularly for patients with advanced glaucoma. This is consistent with a previous study showing that OCTA measurement does not have a detectable floor in the glaucoma continuum, whereas GCC thickness reached the estimated floor at a late stage²⁶.

To assess a linear correlation between several variables measured by OCT and OCTA in the glaucomatous and healthy eyes, we used the Pearson's correlation. In healthy eyes, there was no correlation between structural changes in OD detected by OCT and vascular changes detected by OCTA. But, in patients with glaucoma, VCD and VD in all examined segments showed a significant and strong positive correlation with RNFL measurements. A similar study demonstrated that peripapillary VCD but not inside disc, had strong correlation with the severity of glaucoma, determined by the measurement of the RNFL²⁷. This is also confirmed in the study by Lommatzsch et al.¹ where papillary VCD showed high correlation with RNFL average and rim area.

Macular GCC correlated only with superficial VD in healthy eyes. Contrary, in glaucoma patients, GCC correlated with the thickness of superficial and deep retinal vascular plexuses. The results did not reveal significant correlation between structural and vascular parameters in healthy eyes, but strong positive correlation of all those parameters in glaucomatous eyes indicating close connection between vascular and structural changes. This implicates the importance of vascular disorders in development and progression of glaucoma. In line with this are results that

compared with age-matched control subjects, vascular density of the parafoveal retina decreased in the OAG subjects²⁸. It remains unclear whether the reduced microcirculation in glaucoma patients induces the neuronal damage or arises through reduced circulation requirements in damaged tissue. Due to cross-sectional design of the study, we could not conclude if vascular changes precede papillary disc damage, but regression analysis gives us some insight into this question.

This study found that VD in macula and OD predict the development of glaucoma. In a group model, inside disc capillary density and VD of ring surrounding the FAZ showed significant association with presence of glaucoma. OCTA measurements in macula and OD and OCT measurements in macula can predict glaucoma presence, however this is not found in OCT analysis of OD. According

to this, it can be assumed that vascular changes in different regions of the retina could be a better predictor for glaucoma development than structural changes.

Conclusion

The analysis of OCT bands and OCTA vascular plexuses may be complementary for the noninvasive quantification of the structural and vascular changes in OD and macula, and accurately distinguishes between healthy and diseased eyes, showing association with presence and development of POAG. Our study demonstrated that reduced VD in glaucomatous eyes correlated with functional and structural changes at the OD and macula in glaucoma. Vascular parameters could be a useful adjunct tool to evaluate/diagnose glaucoma.

REFERENCES

1. Lommatzsch C, Rothaus K, Koch JM, Heinz C, Grisanti S. Vessel density in OCT angiography permits differentiation between normal and glaucomatous optic nerve heads. *Int J Ophthalmol* 2018; 11(5): 835–43.
2. Van Melkebeke L, Barbosa-Breda J, Huygens M, Stalmans I. Optical Coherence Tomography Angiography in Glaucoma: A Review. *Ophthalmic Res* 2018; 60(3): 139–51.
3. Lee EJ, Lee KM, Lee SH, Kim T-W. OCT Angiography of the Peripapillary Retina in Primary Open-Angle Glaucoma. *Invest Ophthalmol Vis Sci* 2016; 57(14): 6265–70.
4. Kawasaki R, Wang JJ, Rochtchina E, Lee AJ, Wong TY, Mitchell P. Retinal Vessel Caliber Is Associated with the 10-year Incidence of Glaucoma. *Ophthalmology* 2013; 120(1): 84–90.
5. De Leon JM, Cheung CY, Wong T-Y, Li X, Hamzah H, Aung T, et al. Retinal vascular caliber between eyes with asymmetric glaucoma. *Graefes Arch Clin Exp Ophthalmol* 2015; 253(4): 583–9.
6. Chan KKW, Tang F, Tham CCY, Young AL, Cheung CY. Retinal vasculature in glaucoma: a review. *BMJ Open Ophthalmol* 2017; 1(1): e000032.
7. Holló G. Optical Coherence Tomography Angiography in Glaucoma. *Turk J Ophthalmol* 2018; 48(4): 196–201.
8. Akagi T, Zangwill LM, Shoji T, Sub MH, Saunders LJ, Yarmohammadi A, et al. Optic disc microvasculature dropout in primary open-angle glaucoma measured with optical coherence tomography angiography. *PLoS One* 2018; 13(8): e0201729.
9. Takasagawa HL, Liu L, Ma KN, Jia Y, Gao SS, Zhang M, et al. Projection-Resolved Optical Coherence Tomography Angiography of Macular Retinal Circulation in Glaucoma. *Ophthalmology* 2017; 124(11): 1589–99.
10. Yu J, Gu R, Zong Y, Xu H, Wang X, Sun X, et al. Relationship Between Retinal Perfusion and Retinal Thickness in Healthy Subjects: An Optical Coherence Tomography Angiography Study. *Invest Ophthalmol Vis Sci* 2016; 57(9): OCT204–10.
11. Brusini P. OCT Glaucoma Staging System: a new method for retinal nerve fiber layer damage classification using spectral-domain OCT. *Eye (Lond)* 2018; 32(1): 113–9.
12. Chen CL, Zhang A, Bojikian KD, Wen JC, Zhang Q, Xin C, et al. Peripapillary Retinal Nerve Fiber Layer Vascular Microcirculation in Glaucoma Using Optical Coherence Tomography-Based Microangiography. *Invest Ophthalmol Vis Sci* 2016; 57(9): OCT475–85.
13. Fechtner RD, Weinreb RN. Mechanisms of optic nerve damage in primary open angle glaucoma. *Surv Ophthalmol* 1994; 39(1): 23–42.
14. Bechmann M, Thiel MJ, Roesen B, Ullrich S, Ulbig MW, Ludwig K. Central corneal thickness determined with optical coherence tomography in various types of glaucoma. *Br J Ophthalmol* 2000; 84(11): 1233–7.
15. Dong ZM, Wollstein G, Schuman JS. Clinical Utility of Optical Coherence Tomography in Glaucoma. *Invest Ophthalmol Vis Sci* 2016; 57(9): OCT556–67.
16. Moghimi S, Bowd C, Zangwill LM, Pentado RC, Hasenstab K, Hou H. Measurement Floors and Dynamic Ranges of OCT and OCT Angiography in Glaucoma. *Ophthalmology* 2019; 126(7): 980–8.
17. Niles PI, Greenfield DS, Sehi M, Bhardvaj N, Iverson SM, Chung YS. Advanced Imaging in Glaucoma Study Group. Detection of progressive macular thickness loss using optical coherence tomography in glaucoma suspect and glaucomatous eyes. *Eye (Lond)* 2012; 26(7): 983–91.
18. Miki A, Medeiros FA, Weinreb RN, Jain S, He F, Sharpsten L, et al. Rates of retinal nerve fiber layer thinning in glaucoma suspect eyes. *Ophthalmology* 2014; 121(7): 1350–8.
19. Le PV, Tan O, Chopra V, Francis BA, Ragab O, Varma R, et al. Regional correlation among ganglion cell complex, nerve fiber layer, and visual field loss in glaucoma. *Invest Ophthalmol Vis Sci* 2013; 54(6): 4287–95.
20. An G, Omodaka K, Hashimoto K, Tsuda S, Shiga Y, Takada N, et al. Glaucoma Diagnosis with Machine Learning Based on Optical Coherence Tomography and Color Fundus Images. *J Healthc Eng* 2019; 2019: 4061313.
21. Shin JW, Lee J, Kwon J, Choi J, Kook MS. Regional vascular density-visual field sensitivity relationship in glaucoma according to disease severity. *Br J Ophthalmol* 2017; 101(12): 1666–72.
22. Rao HL, Kadambi SV, Weinreb RN, Puttaiah NK, Pradhan ZS, Rao DA, et al. Diagnostic ability of peripapillary vessel density measurements of optical coherence tomography angiography in primary open-angle and angle-closure glaucoma. *Br J Ophthalmol* 2017; 101(8): 1066–70.
23. Sub MH, Zangwill LM, Manalastas PI, Belghith A, Yarmohammadi A, Medeiros FA, et al. Optical coherence tomography angiography vessel density in glaucomatous eyes with focal lamina cribrosa defects. *Ophthalmology* 2016; 123(11): 2309–17.
24. Hou TY, Kuang TM, Ko YC, Chang YF, Liu CJ, Chen MJ. Optic Disc and Macular Vessel Density Measured by Optical Coherence Tomography Angiography in Open-Angle and Angle-Closure Glaucoma. *Sci Rep* 2020; 10(1): 5608.
25. Hou H, Moghimi S, Proudfoot JA, Ghabari E, Pentado RC, Bowd C, et al. Ganglion Cell Complex Thickness and Macular Vessel

- Density Loss in Primary Open-Angle Glaucoma. *Ophthalmology* 2020; 127(8): 1043–52.
26. Shoji T, Zangwill LM, Akagi T, Saunders LJ, Yarmohammadi A, Manalastas PI, et al. Progressive Macula Vessel Density Loss in Primary Open-Angle Glaucoma: A Longitudinal Study. *Am J Ophthalmol* 2017; 182: 107–17.
27. Chen CL, Bojikian KD, Gupta D, Wen JC, Zhang Q, Xin , et al. Optic nerve head perfusion in normal eyes and eyes with glaucoma using optical coherence tomography-based microangiography. *Quant Imaging Med Surg* 2016; 6(2): 125–33.
28. Tao A, Liang Y, Chen J, Hu H, Huang Q, Zheng J, et al. Structure-function correlation of localized visual field defects and macular microvascular damage in primary open-angle glaucoma. *Microvasc Res* 2020; 130: 104005.

Received on May 26, 2020

Accepted on August 4, 2020

Online First August, 2020



Degree of cognitive impairment in patients with carotid stenosis in relation to cerebral ischemic lesions

Stepen kognitivnog oštećenja u odnosu na cerebralne ishemijske lezije kod bolesnika sa karotidnom stenozom

Elena Joveva*, Gordana Djordjević†, Vuk Milošević†, Anita Arsovska‡, Miroslava Živković‡

*University Goce Delčev, Faculty of Medical Sciences, Clinical Hospital of Štip, Štip, Republic of North Macedonia; †Clinical Center Niš, Clinic of Neurology, Niš, Serbia;

‡University Clinic of Neurology, Skopje, Republic of North Macedonia

Abstract

Background/Aim. Carotid stenosis is a risk factor for cognitive impairment. The aim of the study was to evaluate the degree of cognitive impairment in patients with asymptomatic and symptomatic carotid stenosis and correlate it with the presence, location, and extent of cerebral ischemic lesions. **Methods.** A prospective analysis of 180 patients aged 50–70 years, divided into three groups (asymptomatic carotid stenosis, symptomatic carotid stenosis, and controls) was made. We assessed demographic characteristics, vascular risk factors, ultrasound examination of the carotid arteries, computerized tomography (CT), magnetic resonance imaging (MRI) of the brain, and neuropsychological testing. **Results.** The brain CT findings on admission showed ischemic lesions in the left hemisphere in 13.3% of patients in the asymptomatic group and in 41% of those in the symptomatic group. In the right hemisphere, lesions were registered in 10% of the asymptomatic patients and in 46.7% of the symptomatic patients. The difference between groups was statistically significant. The lesion volumes measured on CT and MRI scans were significantly different ($p < 0.001$) between groups with asymptomatic and symptomatic carotid stenosis. The degree of cognitive impairment, measured by the Addenbrooke's Cognitive Examination Revised (ACE-R), was significantly different between the groups ($p < 0.05$), with the most severe deficit in the symptomatic group. **Conclusion.** Our study has shown that cognitive impairment was more severe in patients with symptomatic carotid stenosis, compared to the patients with asymptomatic carotid stenosis.

Key words:

cognition disorders; carotid stenosis; diagnosis; magnetic resonance imaging; severity of illness index; risk factors; x-ray computed tomography.

Apstrakt

Uvod/Cilj. Karotidna stenoza je faktor rizika od razvoja poremećaja kognitivnih funkcija. Cilj ovog istraživanja je bio da ispita stepen kognitivnog poremećaja kod bolesnika sa asimptomatskom i simptomatskom karotidnom stenozom i njegove povezanosti sa postojanjem, lokacijom i veličinom cerebralnih ishemijskih lezija. **Metode.** Prospektivnom analizom obuhvaćeno je 180 bolesnika starosti od 50 do 70 godina, podeljenih u tri grupe (asimptomatska i simptomatska karotidna stenoza i osobe bez stenoze karotidnih arterija – kontrolna grupa). Procenjene su demografske karakteristike i vaskularni faktori rizika, izvršeni su ultrazvučni pregled karotidnih arterija, kompjuterizovana tomografija (KT), magnetna rezonanca (MR) mozga, kao i neuropsihološko testiranje. **Rezultati.** Nalazi KT mozga na prijemu pokazali su lezije u levoj hemisferi kod 13,3% asimptomatskih bolesnika i 41% bolesnika u simptomatskoj grupi. U desnoj hemisferi registrovane su lezije kod 10% bolesnika u asimptomatskoj i 46,7% bolesnika u simptomatskoj grupi. Razlika između grupa bila je statistički značajna. Zapremina lezija, merena metodama KT i MR, statistički značajno se razlikovala ($p < 0,001$) između grupa sa asimptomatskom i simptomatskom karotidnom stenozom. Step kognitivnih oštećenja, meren Adenbrukovim revidiranim testom kognitivne procene (ACE-R), bio je značajno različit između grupa ($p < 0,05$) sa najizraženijim deficitom u simptomatskoj grupi. **Zaključak.** Naše istraživanje je pokazalo da je kognitivno oštećenje kod bolesnika sa simptomatskom karotidnom stenozom značajno višeg stepena od onog kod bolesnika sa asimptomatskom karotidnom stenozom.

Ključne reči:

saznanje, poremećaji; aa. carotis, stenoza; dijagnoza; magnetska rezonanca, snimanje; bolest, indeks težine; faktori rizika; tomografija, kompjuterizovana, rendgenska.

Introduction

The presence of carotid stenosis is a potential risk factor for cognitive impairment, which has been proven by several studies^{1–4}. The underlying mechanisms are embolization and hypoperfusion that can cause lacunary or silent brain infarcts, associated with an increased risk of dementia. Cognitive impairment might also be present in asymptomatic high-grade carotid stenosis, without evidence of infarction on magnetic resonance imaging (MRI), connected with microangiopathy and vascular risk factors⁴.

The aim of our study was to evaluate the degree of cognitive impairment in asymptomatic and symptomatic carotid stenosis patients, and correlate it with the presence, location, and extent of cerebral ischemic lesions.

Methods

A prospective analysis included 180 patients aged 50–70 years, divided into three groups: asymptomatic patients with carotid stenosis, without transient ischemic attack (TIA)/stroke; symptomatic patients, with carotid stenosis and TIA/stroke; and a control group of patients with headache/vertigo and normal carotid arteries on a computed tomography (CT) scan. Written consent was obtained from the patients/their families and the study was approved by the local Ethics Committee.

Exclusion criteria were: aphasia, intracerebral hemorrhage, vascular malformations, tumors, multiple sclerosis, or other diseases on neuroimaging, severe stroke with the National Institutes of Health Stroke Scale (NIHSS) score > 15.

We assessed demographic characteristics and vascular risk factors. Ultrasound examination of the carotid arteries was performed using B-mode ultrasonography with a 7.5 MHz probe according to the Atherosclerosis Risk in Communities (ARIC) protocol⁵. The patients were stratified according to the degree of stenosis as follows: no stenosis; low (0–49%); moderate (50–69%); and a high degree of stenosis ($\geq 70\%$)⁶. Cognitive functions were evaluated using

the Addenbrooke's Cognitive Examination Revised (ACE-R) score⁷. We analyzed temporal and spatial orientation, attention, calculation, speech, memory, and visuospatial abilities. The test was carried out six months after hospitalization in patients with symptomatic stenosis, and six months after initial examination in patients with asymptomatic carotid stenosis and in the control group. CT of the brain was performed on admission and at 24 h to 72 h thereafter, analyzing the size and location of acute ischemic lesions. MRI of the brain was performed within six months after the initial examination of all patients. The severity of stroke was estimated using the NIHSS, ranging from 0–30. Stroke was classified as mild (≤ 8), moderate (9–15), and severe (> 15)⁸. Patients with severe stroke (NIHSS > 15) were excluded from this study. Statistical analysis was performed using STATISTICA 7.1 and SPSS 17.0 statistical software.

Results

On admission, CT of the brain showed no structural lesions in 60% of patients in the asymptomatic group, 10% of patients in the symptomatic group, and 100% of patients in the control group. The difference between asymptomatic carotid stenosis (ACS) and symptomatic carotid stenosis (SCS) patients was statistically significant ($p < 0.001$). On the control CT, structural lesions were seen in 40% of ACS patients and in all SCS ones.

In the CT findings on admission, lesions in the left hemisphere were registered in 13.3% of ACS patients, and in 41% of SCS patients. The difference between the two groups was statistically significant ($p < 0.001$).

In the CT findings on admission, lesions in the right hemisphere were registered in 10.0% of ACS patients, and in 46.7% of SCS patients. The difference was statistically significant ($p < 0.001$).

The ischemic lesion volumes (cm^3) measured on CT and MRI scans were significantly different ($p < 0.001$) between ACS patients and SCS patients (Figure 1).

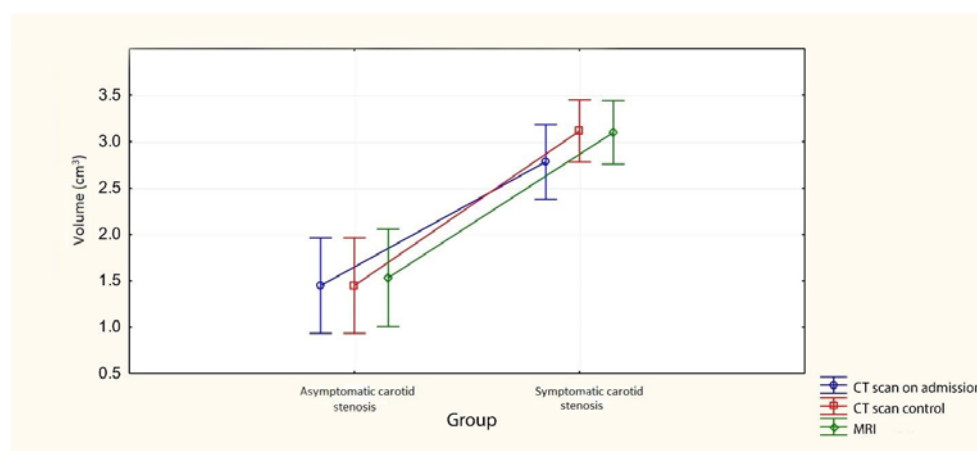


Fig. 1 – Ischemic lesion volumes (cm^3) in the asymptomatic carotid stenosis group and in the symptomatic carotid stenosis group.
CT – computed tomography; MRI – magnetic resonance imaging.

Ischemic brain lesions were registered on the follow-up MRI examination in 60% of ACS patients and in all SCS patients. Control subjects had no ischemic brain lesions on MRI.

MRI examination showed lesions in the left hemisphere in 13.3% of ACS patients and 45% of SCS patients ($p < 0.001$), and lesions in the right hemisphere in 10% of ACS patients and 53.3% of SCS patients ($p < 0.001$). The locations of structural lesions on CT and MRI are shown in Table 1.

Table 1

Location of structural brain lesions according to CT scan on admission and control CT and MRI scans

Location of lesion	ACS patients n (%)	SCS patients n (%)
CT scan on admission		
no lesion	36 (60.0)	6 (10.0)
frontal	1 (1.7)	4 (6.7)
parietal	6 (10.0)	19 (31.7)
temporal	5 (8.5)	11 (18.3)
occipital	1 (1.7)	8 (13.3)
basal ganglia	11 (18.3)	
Control CT scan		
no lesion	36 (60)	0
frontal	1 (1.7)	4 (6.7)
parietal	6 (10.0)	21 (35.0)
temporal	5 (8.5)	13 (21.7)
occipital	1 (1.7)	8 (13.3)
basal ganglia	11 (18.3)	14 (23.3)
MRI		
no lesions	36 (60)	0
frontal	1 (1.7)	5 (8.3)
parietal	6 (10.0)	20 (33.3)
temporal	5 (8.5)	13 (21.7)
occipital	1 (1.7)	8 (13.3)
basal ganglia	11 (18.3)	14 (23.3)

Note: CT of the brain was performed on admission and at 24 h to 72 h thereafter; MRI of the brain was performed within six months after the initial examination of all patients.

CT – computed tomography; MRI – magnetic resonance imaging; ACS – asymptomatic carotid stenosis; SCS – symptomatic carotid stenosis.

Impairment of temporal and spatial orientation was registered in 16.7% of patients in the SCS group ($p < 0.05$). Impairment of attention was recorded in 48.3% of ACS patients, 71.7% of SCS patients, and 25.0% of control subjects. There was a statistically significant difference regarding ACS patients compared to SCS patients and the control subjects ($p = 0.01$, $p = 0.009$, respectively). Impairment of calculation abilities was registered in 43.3% of ACS patients, 78.3% of SCS patients, and 13.3% of control subjects. The difference was statistically significant regarding SCS patients compared to the ACS patients and the control group, respectively ($p < 0.001$). Language impairment was seen in 3.3% of ACS patients, 58.3% of SCS patients, and in none in the control group. The difference between ACS patients and SCS patients was significant ($p < 0.001$), and nonsignificant between ACS patients and the controls ($p > 0.05$). Memory impairment was recorded in 75% of ACS patients, 91.7% of SCS patients, and in 28.3% of patients in the control group. The differences between ACS patients, SCS patients, and controls were significant ($p = 0.02$, $p < 0.001$, respectively).

The average ACE-R scores were 78.7 ± 4.6 in ACS patients, 65.6 ± 3.9 in SCS patients, and 96.5 ± 2.9 in the control subjects (Figure 2). Analysis of variance showed the statistically significant differences in the average scores in the three groups ($p < 0.001$). The *post hoc* Tukey HSD test showed a statistically significant difference between ACS patients, SCS patients, and the control group ($p < 0.001$).

The relation between the degree of cognitive impairment and the location of lesions on the initial CT, control CT, and MRI examinations in ACS patients and SCS patients is shown in Tables 2, 3, and 4, respectively. There was no statistically significant correlation between lesion location on admission, control scans and MRI findings, and the level of cognitive impairment found on the ACE-R test ($p > 0.05$).

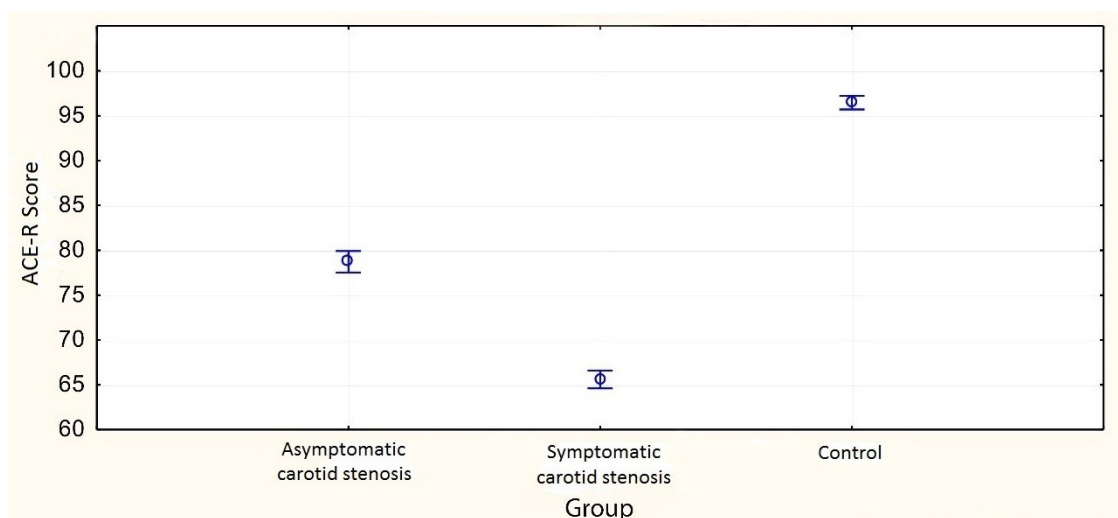


Fig. 2 – Average ACE-R score in the asymptomatic carotid stenosis group, the symptomatic carotid stenosis group, and the control group.

ACE-R – Addenbrooke's Cognitive Examination Revised.

Table 2

Number of patients according to the location of lesions on CT scans on admission and the degree of cognitive impairment (CI)

Location of lesion	Asymptomatic carotid stenosis			Total	Symptomatic carotid stenosis			Total
	mild CI	moderate CI	severe CI		mild CI	moderate CI	severe CI	
No lesions	35	13	0	48	0	5	1	6
Frontal lobe	0	0	0	0	0	3	1	4
Parietal lobe	1	0	0	1	0	9	10	19
Temporal lobe	1	2	0	3	0	7	4	11
Occipital lobe	1	0	0	1	0	5	3	8
Basal ganglia	3	4	0	7	0	7	5	12
Total	41	19	0	60	0	36	24	60

CT – computed tomography.

Table 3

Number of patients according to the location of lesions on control CT scans (24-72 h after initial examination) and the degree of cognitive impairment (CI)

Location of lesion	Asymptomatic carotid stenosis			Total	Symptomatic carotid stenosis			Total
	mild CI	moderate CI	severe CI		mild CI	moderate CI	severe CI	
No lesions	35	13	0	46	0	0	0	0
Frontal lobe	0	0	0	0	0	3	1	4
Parietal lobe	1	0	0	1	0	11	10	21
Temporal lobe	2	2	0	4	0	9	4	13
Occipital lobe	1	0	0	1	0	5	3	8
Basal ganglia	4	4	0	8	0	8	6	14
Total	41	19	0	60	0	36	24	60

CT – computed tomography.

Table 4

Number of patients by the location of lesion registered on MRI scans and degree of cognitive impairment (CI)

Location of lesion	Asymptomatic carotid stenosis			Total	Symptomatic carotid stenosis			Total
	mild CI	moderate CI	severe CI		mild CI	moderate CI	severe CI	
No lesions	26	9	0	35	0	0	0	0
Frontal lobe	1	0	0	1	0	3	2	5
Parietal lobe	4	2	0	6	0	11	9	20
Temporal lobe	3	2	0	5	0	9	4	13
Occipital lobe	1	0	0	1	0	5	3	8
Basal ganglia	6	6	0	12	0	8	6	14
Total	41	19	0	60	0	36	24	60

MRI – magnetic resonance imaging.

Discussion

The results of our study are in accordance with the data found in the literature. The study by Moreau et al. ⁹ directly compared the sensitivity of CT and MRI scans in patients with TIA and/or mild strokes with acute ischemic lesions. CT and MRI were performed within 24 h after symptom onset. Acute ischemic lesions were compared on CT and MRI, while the acute lesion volume was measured on MRI. The study showed that MRI exhibited higher sensitivity compared to CT in identifying small acute ischemic lesions. MRI also showed lesions with smaller volumes that were missed on CT scans. In TIA or lacunar stroke patients, acute ischemic lesions were identified on MRI in 35–50% of the patients, while the same lesions were found in only 10% when CT scans were performed. The same results were found in the study by Forster et al. ¹⁰ where the percentage of acute strokes proven on MRI after negative CT scans was greater than 33%. This difference is mostly the consequence

of the size, i.e. the volume of the stroke because the sensitivity of CT in recognizing ischemic lesions smaller than 1 cm³ is weak ¹¹. The limitation of our study is that CT and MRI scans were not performed simultaneously, and the time between the symptom onset and MRI scans was longer compared to the timing of CT scans. As early ischemic changes become more prominent with time, this fact goes potentially in favor of the MRI diagnostics ⁹. The percentage of visualized lesions on MRI was higher in the asymptomatic carotid stenosis group.

A study by Tomlinson et al. ¹² suggests that the volume of stroke is correlated to the appearance and development of cognitive impairment. Stroke can cause vascular dementia when the volume of stroke is greater than 100 mL ¹². A survey by Zekry et al. ¹³ suggests that the total volume of stroke can explain only a small portion of cognitive impairment in stroke patients. It finds that strokes in strategic areas play an important role in the cognitive disorder mechanism, and that they are connected with the severity of

dementia. These strategic regions are: cortical limbic regions, frontal cortex, and white mass. There are limitations due to the fact that many patients who have brain damage, usually have motor difficulties that adversely affect their performance on the test (eg. drawing), and often have a language difficulty^{14, 15}. In our study too, there was no statistically significant correlation between the lesion location on admission and in control CT and MRI scans in the examined groups of patients, compared to the level of cognitive impairment seen on the ACE-R test. In our study, we chose neuropsychological testing which is necessary for the screening of patients with dementia after stroke or patients with carotid stenosis, without the anamnestic data for stroke and its identification in the early stages of the disease, which would enable early intervention and possibly, with proper cognitive rehabilitation¹⁵, delay cognitive impairment development. The study by Lees et al.¹⁵ examined the usefulness of the ACE-R test in detecting cognitive impairment after stroke. The test yields data for the patient's cognitive profile, and as a screening method it can speed up the cognitive deficit diagnostic procedure after stroke¹⁴. It was shown that the ACE-R has a significant connection with other neuropsychological tests that examine

only a certain domain. Assessment of memory by ACE-III is associated with two classic neuropsychological memory tests – Free and Cued Selective Reminding Test and the Rey Auditory Verbal Learning Test^{14, 15}. Speech and verbal fluency, which were tested using ACE-R, were in correlation with the tests that assess attention and executive functions (the trail making test, memory span, Stroop test)¹⁵. In the study by Al-Qazzaz et al.¹⁶, it was found that stroke increases the risk of cognitive impairment, where 21% of the stroke survivors experienced cognitive function decline after the third month¹⁶. This research showed that demographic characteristics of stroke patients, including age and gender, are related to cognitive impairment and dementia. Cognitive impairment increased with age due to decreased cerebral flow.

Conclusion

We did not find a statistically significant connection between the locations of the cerebral ischemic lesions and the degree of cognitive impairment. However, the results of the study confirmed that cognitive impairment was more severe in the patients with stroke and SCS compared to the patients with ACS.

R E F E R E N C E S

- Hofman A, Ott A, Breteler MM, Bots ML, Slooter AJ, van Harskamp F, et al. Atherosclerosis, apolipoprotein E, and prevalence of dementia and Alzheimer's disease in the Rotterdam Study. *Lancet* 1997; 349(9046): 151–4.
- Johnston SC, O'Meara ES, Manolio TA, Lefkowitz D, O'Leary DH, Goldstein S, et al. Cognitive impairment and decline are associated with carotid artery disease in patients without clinically evident cerebrovascular disease. *Ann Intern Med* 2004; 140(4): 237–47.
- Mathiesen EB, Waterloo K, Joakimsen O, Bakke SJ, Jacobsen EA, Bonna KH. Reduced neuropsychological test performance in asymptomatic carotid stenosis: The Tromso Study. *Neurology* 2004; 62(5): 695–701.
- Pettigrew LC, Thomas N, Howard VJ, Veltkamp R, Toole JF. Low mini-mental status predicts mortality in asymptomatic carotid arterial stenosis. Asymptomatic Carotid Atherosclerosis Study investigators. *Neurology* 2000; 55(1): 30–4.
- Wang J, Wu J, Zhang S, Zhang L, Wang C, Gao X, et al. Elevated fasting glucose as a potential predictor for asymptomatic cerebral artery stenosis: a cross-sectional study in Chinese adults. *Atherosclerosis* 2014; 237(2): 661–5.
- von Reutern GM, Goertler MW, Bornstein NM, Del Sette M, Evans DH, Hetzel A, et al. Grading Carotid Stenosis Using Ultrasonic Methods. *Stroke* 2012; 43(3): 916–21.
- Larner AJ, Mitchell AJ. A meta-analysis of the accuracy of the Addenbrooke's Cognitive Examination (ACE) and the Addenbrooke's Cognitive Examination-Revised (ACE-R) in the detection of dementia. *Int Psychogeriatr*. 2014; 26(4): 555–63.
- Kvab LK, Diong J. National Institutes of Health Stroke Scale (NIHSS). *J Physiother* 2014; 60(1): 61.
- Moreau F, Asdaghi N, Modi J, Goyal M, Coutts S. Magnetic Resonance Imaging versus Computed Tomography in Transient Ischemic Attack and Minor Stroke: The More You See the More You Know. *Cerebrovasc Dis Extra* 2013; 3(1): 130–6.
- Forster A, Gass A, Kern R, Ay H, Chatzikonstantinou A, Hennerici MG, et al. Brain imaging in patients with transient ischemic attack: a comparison of computed tomography and magnetic resonance imaging. *Eur Neurol* 2012; 67(3): 136–41.
- Castle J, Mlynash M, Lee K, Canfield AF, Wofford C, Kemp S, et al. Agreement regarding diagnosis of transient ischemic attack fairly low among stroke-trained neurologists. *Stroke* 2010; 41(7): 1367–70.
- Tomlinson BE, Blessed G, Roth M. Observations on the brains of demented old people. *J Neurol Sci* 1970; 11(3): 205–42.
- Zekry D, Duyckaerts C, Belmin J, Geoffre C, Herrmann F, Moulia R, et al. The vascular lesions in vascular and mixed dementia: the weight of functional neuroanatomy. *Neurobiol Aging* 2003; 24(2): 213–9.
- Fedorova D, Krulova P, Ressler P, Jarekova V, Slonkova J, Bar M, et al. Addenbrooke's cognitive examination in nondemented patients after stroke. *Neuropsychiatry* 2018; 8(2): 505–12.
- Lees RA, Hendry BA, Broomfield N, Stott D, Larner AJ, Quinn TJ. Cognitive assessment in stroke: feasibility and test properties using differing approaches to scoring of incomplete items. *Int J Geriatr Psychiatry* 2017; 32(10): 1072–8.
- Al-Qazzaz NK, Ali HS, Ahmad SA, Islam S. Cognitive assessments for the early diagnosis of dementia after stroke. *Neuropsychiatr Dis Treat* 2014; 10: 1743–51.

Received on May 2, 2020

Revised on August 12, 2020

Accepted on August 20, 2020

Online First August, 2020



Evaluation of mechanical properties of three commonly used suture materials for clinical oral applications: an *in vitro* study

Procena mehaničkih svojstava tri najčešće korišćena šavna materijala za oralnu primenu u kliničkoj stomatologiji – *in vitro* studija

Shahabe Saquib Abullais*, Nabeeh Abdullah Al-Qahtani*, Talib Amin
Naqash†, Abdul Ahad Khan‡, Suraj Arora§, Shaeesta Bhavikatti*

King Khalid University, College of Dentistry, *Periodontics and Community Dental Sciences,
Research Center for Advanced Materials Sciences, †Prosthetic Dentistry, ‡Department of Oral
and Maxillofacial Surgery, §Restorative Dental Sciences, Abha, KSA

Abstract

Background/Aim. Appropriate selection of suture materials is a crucial step in oral, maxillofacial and periodontal surgery for uneventful healing. We have scarcity of comprehensive studies comparing mechanical properties of commonly used suture material in oral surgery. The present *in vitro* study sought to evaluate the effect of saliva on the strength, elongation and stiffness of the commonly used suture material over a period of two weeks. **Methods.** Three suture materials, silk (SL), polyglactin 910 (PG) and polypropylene (PP), were used in 4–0 gauge. A total of 120 suture samples (40 from each material) were used for the investigation. Artificial saliva was mixed with human serum in 1:1 ratio and maintained at pH of 7.4 to 8.1 to simulate oral environment. All samples were tested at pre-immersion (baseline), as well as on the 3rd, 7th and 14th day in the post-immersion period. A universal testing machine was used to test the selected mechanical properties. The collected data were subjected to statistical analysis. **Results.** The distribution of mean baseline strength and percentage elongation was significantly higher in the PP group ($p < 0.001$), whereas

stiffness score was the highest in the SL group ($p < 0.001$). Inter-group comparison revealed that the PP group had maximum tensile strength compared to the PG and SL groups at all time points. When percentage elongation was compared, the PP and PG groups showed the highest values on the 7th and 14th day, respectively. The PP group exhibited the highest stiffness values compared to the SL and PG groups on the 7th and 14th day in the post-immersion period ($p < 0.001$). Intra-group comparison showed that all suture materials had significant difference in mechanical properties when pre-immersion values were compared to the 14th day post-immersion values ($p < 0.001$). **Conclusion.** PP sutures are the strongest and have the highest tensile strength and elongation property. PP seems to sustain its tensile strength better than SL and PG at the end of the 14th day. Controlled clinical studies are necessary to verify this finding in an *in vivo* setting.

Key words:
materials testing; polymers; polypropylenes; saliva, artificial; silk; sutures; tensile strength.

Apstrakt

Uvod/Cilj. Izbor odgovarajućeg šavnog materijala je presudan korak za bezbedno zarastanje rane u oralnoj, maksilofacijalnoj i parodontalnoj hirurgiji. Sveobuhvatne studije koje bi upoređivale mehanička svojstva šavnih materijala koji se često koriste u oralnoj hirurgiji su malobrojne. Ova *in vitro* studija imala je za cilj da proceni efekat pljuvačke na čvrstoću, izduženje i krutost šavnog materijala koji se uobičajeno koristi tokom perioda od dve nedelje. **Metode.** Korišćena su tri šavna materijala debljine 4–0: svila (SL), poliglaktin 910 (PG) i polipropilen (PP). Za ispitivanje je korišćeno ukupno 120 uzoraka (po 40 od svakog materijala). Veštačka pljuvačka je bila pomešana sa humanim serumom u odnosu 1:1 i održavana na pH od 7,4 do 8,1 kako bi se simuliralo okruženje u

usnoj duplji. Svi uzorci su bili testirani pre potapanja u pljuvačku (bazalni nivo), kao i 3., 7. i 14. dana nakon potapanja. Za ispitivanje odabranih mehaničkih svojstava korišćena je univerzalna mašina za testiranje. Urađena je statistička analiza prikupljenih podataka. **Rezultati.** Prosečna vrednost čvrstoće pre potapanja u veštačku pljuvačku, kao i procenat izduženja bili su značajno viši kod PP materijala ($p < 0,001$), dok je krutost bila najviša kod uzoraka SL ($p < 0,001$). Međusobnim poređenjem ispitivanih materijala, ustanovljeno je da je PP u svim vremenskim tačkama imao maksimalnu čvrstoću vlakana u odnosu na PG i SL. Kada se poredilo procentualno izduženje, PP i PG su pokazali najviše vrednosti 7. (PP) i 14. dana (PP). Materijal PP je imao veće vrednosti krutosti u poređenju sa SL i PG 7. i 14. dana nakon potapanja u veštačku pljuvačku ($p < 0,001$). Poređenje vrednosti

posmatranih mehaničkih svojstava unutar pojedinih vrsta šavnog materijala pokazalo je da je kod svih materijala postojala značajna razlika u tim parametrima 14. dana nakon potapanja u veštačku pljuvačku u odnosu na bazalne vrednosti ($p < 0,001$). **Zaključak.** Šavni materijal PP je najčvršći i ima najveću zateznu čvrstoću i svojstvo izduženja. Čini se da PP zadržava čvrstoću vlakana bolje od SL i PG na kraju 14. dana

od potapanja u veštačku pljuvačku. Neophodne su kontrolisane kliničke studije da bi se ovaj nalaz potvrdio u uslovima *in vivo*.

Ključne reči:
materijali, testiranje; polimeri; polipropileni; pljuvačka, veštačka; svila; šavovi; čvrstoća, zatezna.

Introduction

Important concerns of periodontal, oral and maxillofacial surgeons refer to the selection of proper suture material. The suture material should be biocompatible and easy to use. Also, it should form a proper knot, have the property of elongation, be biodegradable in some circumstances and resist breakage during its use¹. The mechanical properties of the suture materials play an important role in regulating their behavior.

Placing sutures in the oral cavity is challenging due to varied functions of mastication, speech, swallowing and high tissue vascularization along with continuous pooling of saliva². Suitable sutures must possess specific physical and mechanical properties, amongst which the tensile strength is one of the most important properties. The function of the suture while in use is controlled by its elasticity, stiffness and tensile strength³.

The flap edges should remain in close approximation after suturing of the surgical site to assist primary healing, failure of which can have a negative effect on the desired results of the surgery. Tensile strength is an important feature that is required to be maintained because the suture material tends to lose between 70% and 80% of its original strength. Therefore, the required original tensile strength must always be maintained to avoid breakage of the suture material^{4,5}. Moreover, a compromise with the strength of the suture material can result in incomplete coaptation of the flap and consequent healing by secondary intention⁶. Most of the published studies related to mechanical properties discussed mainly a breaking force. There are very few reports that actually compare other useful aspects, like failure elongation, failure stress/strain and stiffness across suture materials. However, exhaustive studies that are cited on suture materials are comparatively less pertinent to materials used for oral and periodontal surgical procedures^{7,8}.

A distinct suture material shows discrete behavior in the oral cavity⁹. Various experimental researches indicated that the suture tensile strength could be affected by saliva, various solutions or consumed fluids. It has been found that there is a reduction in the strength of Vicryl® after it is immersed in saliva, bovine milk, and soy milk for 35 days¹⁰. Another study described remarkable reduction in the strength of two different suture types (Vicryl® and Monocryl®) after they

were submerged in artificial saliva, chlorhexidine and essential oil mouth rinse¹¹.

Of the various commercially available suture materials, silk (SL) and polyglactin (PG) are most often used in oral and periodontal surgery. Silk is the most frequently used natural suture material, due to its better handling properties¹².

Consequently, the aim of this study is to assess and compare the tensile strength, percentage elongation and stiffness of SL, polyglactin 910 (PG) and polypropylene (PP) suture material in an environment simulating the oral cavity (immersed in artificial saliva) and a pre-immersion dry condition for an interval of fourteen days. The results mentioned in the present study are meant to provide a baseline data for oral surgeons and periodontist by assembling the mechanical and physical properties of these sutures under controlled conditions. So, this data will help in the selection of suitable suture material depending upon the required area of surgical procedure.

Methods

The present *in vitro* experimental study design was approved by the King Khalid University Ethical Review Committee (ERC), Abha, Saudi Arabia (SRC/ETH/2017-18/090). The study was conducted in the period from November 2018 to February 2019. Three distinct suture materials were involved in the current study and their physical properties were evaluated: SL, which is observed by many surgeons as a benchmark due to its easy handling¹², PG (Vicryl®), which is a multifilament absorbable synthetic suture comprised of a copolymer of glycolide and L-lactide, and PP monofilament, non-absorbable material made of an isotactic crystalline stereoisomer of polypropylene (Table 1). Suture materials were divided into the control (pre-immersed) and the test group (immersed in artificial saliva – Table 2). All the test suture materials were exposed to thermo-cycling (alternate temperature change from 5 °C to 55 °C), so as to simulate the challenges in the oral cavity.

A total of 120 suture samples were collected from commercially available unexpired stocks. Forty samples were obtained from each suture material type. All the suture samples were measured at a uniform length of 18 cm. Ten specimens from each group were tested for tensile strength before immersing into artificial saliva and referred

Table 1

Description of the suture material used in the study

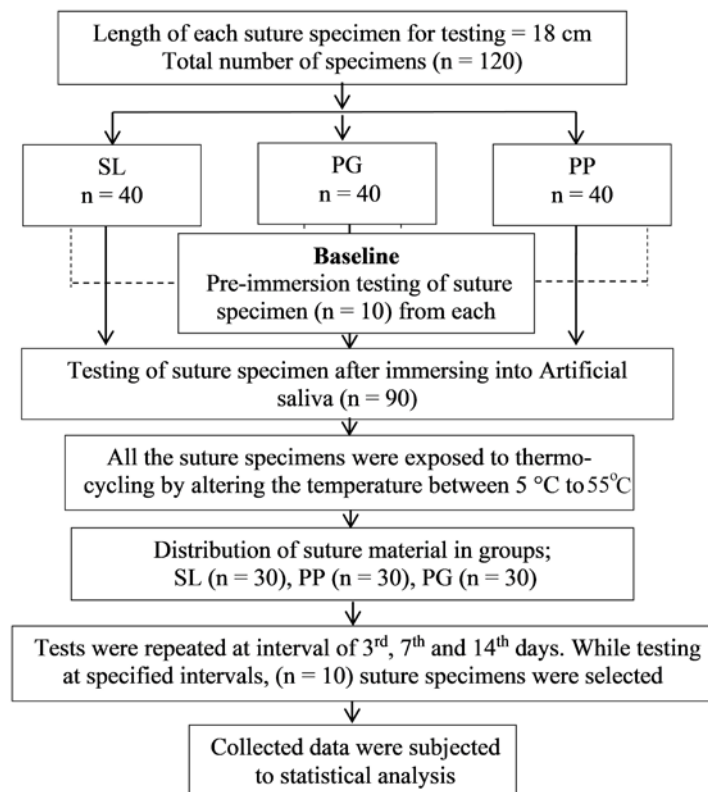
Suture material	Brand	Manufacturer	Degradation
Silk (SL)	Mersilk®	Ethicon, Johnson & Johnson Pvt. Ltd. India	non-absorbable
Polyglactin 910 (PG)	Vicryl®	Ethicon, Johnson & Johnson Pvt. Ltd. India	absorbable
Polypropylene (PP)	Prolene®	Ethicon, Johnson & Johnson Pvt. Ltd. India	non-absorbable

Table 2**Chemical composition of artificial saliva**

Chemical components	Concentration (g/L)
Sodium chloride (NaCl)	0.125
Potassium chloride (KCl)	0.963
Potassium thiocyanate (KSCN)	0.189
Monopotassium phosphate (KH ₂ PO ₄)	0.654
Urea (CH ₄ N ₂ O)	0.200
Sodium sulfate decahydrate (Na ₂ SO ₄ 10H ₂ O)	0.763
Ammonium chloride (NH ₄ Cl)	0.178
Calcium dchloride dihydrate (CaCl ₂ , 2H ₂ O)	0.227
Sodium bicarbonate (NaHCO ₃)	0.630

to as a control group. Remaining suture specimens were kept in artificial saliva until exposed to an experimental procedure (Figure 1). A detailed description of the study protocol has been described in Figure 2.

Artificial saliva was formulated by mixing the compounds shown in Table 2 in one liter of distilled water¹³. To prevent any chemical changes, the prepared mixture was kept secured in an amber color bottle until used for the ex-

**Fig. 1 – Different suture specimens immersed in artificial saliva.****Fig. 2 – Flowchart of the study design.**

SL – silk; PG – polyglactin 910; PP – polypropylene.

periment. During the experiment, the prepared artificial saliva was mixed with human serum in 1:1 ratio, to simulate oral environment. This biologic mixture was kept at a pH of 7.4 to 8.1 in an incubator at 37 °C¹⁴.

The setup of the experiment and the testing machine are shown in Figure 3.

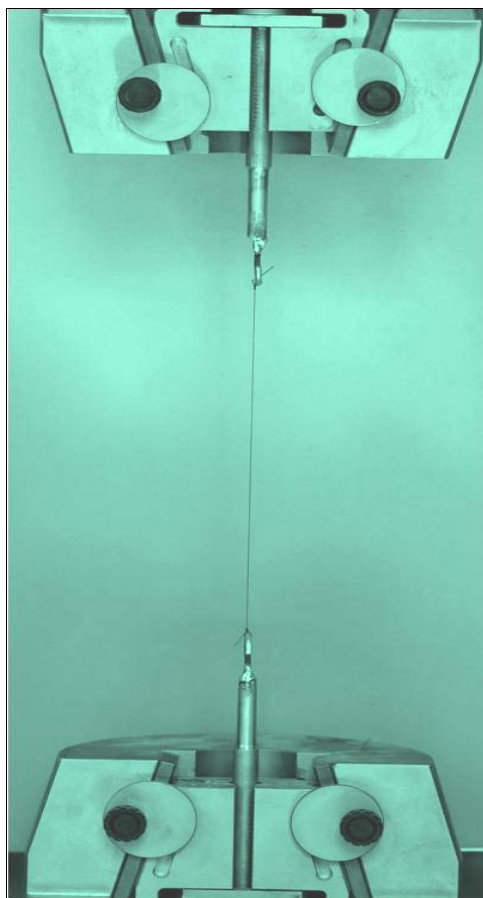


Fig. 3 – Experiment setup showing suture material tied to the hook of the separating arms of a universal testing machine.

Measurements were recorded for tensile strength, percentage elongation and stiffness. Tensile strength was defined as maximum load that can be applied to a suture material before the suture breaks; it was measured in Newtons (N). Elongation was defined as cumulative displacement exhibited by a suture material before it breaks when a gradual load is delivered and it was measured in millimeters (mm). Stiffness was defined as a measurement of the capacity of a suture material to elongate by the application of gradually increasing load before it breaks and it was measured in N per millimeter (N/mm). The stiffer materials would exhibit lesser elongation.

The data on continuous variables is presented as mean and standard deviation (SD) across the study groups. Statistical test analysis of variance (ANOVA) was used for the inter-group and intra-group comparison. In the entire study, the *p*-values less than 0.05 were considered to be statistically significant. All the hypotheses were formulated using two-tailed alternatives against each null hypothesis (hypothesis of no difference). The entire data was statistically analyzed using Statistical Package for Social Sciences (SPSS version 21.0, IBM Corporation, USA) for MS Windows.

Results

Baseline (pre-immersion) comparison of mean tensile strength, percentage elongation and stiffness are presented in Table 3. The distribution of mean baseline strength and percentage elongation was significantly higher in the PP group, followed by the PG group and the least with the SL group (*p*-value < 0.001 for all). However, stiffness score was the highest with the SL group compared to the PP and PG groups, respectively (*p* < 0.001 for all).

Table 4 shows the distribution and comparison of mean tensile strength among three suture groups on the 3rd, 7th and 14th day after the immersion in the saliva. The PP group exhibited the maximum tensile strength when compared to the PG and SL groups at all points in time (*p* < 0.001).

Table 3

Tensile strength, percentage elongation and stiffness of different suture material groups at baseline (pre-immersion)

Suture material	Tensile strength (N)	Elongation (%)	Stiffness (N/mm)
	mean ± SD	mean ± SD	mean ± SD
Silk (SL)	10.60 ± 1.26	4.5 ± 0.54	1.33 ± 0.22
Polyglactin 910 (PG)	14.50 ± 1.27	12.11 ± 1.39	0.67 ± 0.07
Polypropylene (PP)	20.40 ± 1.26	16.78 ± 0.76	0.68 ± 0.06
<i>p</i> -value	0.001***	0.001***	0.001***

SD – standard deviation.

****p*-value – highly significant.

Table 4

Inter-group comparison of tensile strength (in N) pre- and post-immersion in saliva

Time of immersion	Silk (SL)	Polyglactin 910 (PG)	Polypropylene (PP)	<i>p</i> -value (Inter-group)		
	mean ± SD	mean ± SD	mean ± SD	SL vs. PG	SL vs. PP	PG vs. PP
Pre-immersion	10.60 ± 1.26	14.50 ± 1.27	20.40 ± 1.26	0.001***	0.001***	0.001***
Post-immersion in saliva						
3rd day	9.75 ± 1.21	12.80 ± 1.64	19.40 ± 1.39	0.05**	0.001***	0.001***
7th day	8.80 ± 0.83	11.80 ± 1.10	18.15 ± 1.59	0.05**	0.001***	0.001***
14th day	8.25 ± 1.07	10.80 ± 1.76	15.40 ± 1.27	0.05**	0.001***	0.001***

SD – standard deviation.

p*-value – significant; *p*-value – highly significant.

Table 5 shows the distribution and comparison of mean percentage elongation among three suture groups on the 3rd, 7th and 14th day after the immersion in the saliva. The PP group exhibited the maximum percentage elongation when compared to the PG and SL groups at baseline and on the 7th day after the immersion ($p < 0.05$ and $p < 0.001$), whereas the PG group exhibited the highest percentage elongation compared to the SL and PP groups on the 3rd and 14th day after the immersion ($p < 0.05$ and $p < 0.001$).

Table 6 shows the distribution and comparison of mean stiffness among three suture groups on the 3rd, 7th and 14th day after the immersion in the saliva. The highest stiffness was recorded by the SL group, followed by the PP and PG groups at baseline and on the 3rd day after the immersion ($p < 0.001$), whereas the PP group exhibited higher stiffness compared to the SL and PG groups on the 7th and 14th day after the immersion ($p < 0.001$).

Table 7 presents intra-group comparison of different suture material with respect to different variables (strength, percentage of elongation and stiffness) from pre-immersion to the 14th day after the immersion. All three suture material showed a significant difference in strength, percentage of elongation and stiffness when mean values from baseline (pre-immersion) were compared to the 14th day after the immersion.

Discussion

The key step of surgery is a meticulous wound closure. The main purpose of a wound closure is eradication of dead space, apposition of wound margins to generate a closed secure environment and preservation of tensile strength at the wound margins till the tissue tensile strength becomes satisfactory to bear external load¹⁵. Previously, materials like animal hair, natural fibers, silk, nylon and gut mucosa were used to seal the surgical sites¹⁶. A surgeon always desires for better handling characteristics and tensile strength of a suture while choosing appropriate suture material. The tensile strength of a suture material is an essential property that helps suture material to bear the tissue traction at the flap margin¹⁷. Suture materials manifesting low tensile strength are more liable to break during the healing phase because of pull created by edema and tissue tension.

Suture materials are mainly categorized as absorbable and nonabsorbable, natural and synthetic, braided polyfilament and monofilament fibers¹⁸. Distinct suture materials bearing the same diameter size may differ significantly in their tensile strength. Most of the reported studies on mechanical properties of sutures are done on skin and subcutaneous tissues^{18–20}. In these exploratory studies, sutures were

Table 5

Inter-group comparison of percentage elongation pre- and post-immersion in saliva

Time of immersion	Silk (SL)	Polyglactin 910 (PG)	Polypropylene (PP)	<i>p</i> -value (Inter-group)		
	mean \pm SD	mean \pm SD	mean \pm SD	SL vs. PG	SL vs. PP	PG vs. PP
Pre-immersion	4.5 \pm 0.54	12.11 \pm 1.39	16.78 \pm 0.76	0.001***	0.001***	0.001***
Post-immersion in saliva						
3rd day	8.67 \pm 0.78	20.78 \pm 6.33	17.89 \pm 0.82	0.001***	0.001***	0.05**
7th day	13.67 \pm 1.87	16.44 \pm 2.31	19.22 \pm 1.78	0.05**	0.001***	0.05**
14th day	15.95 \pm 2.12	18.22 \pm 1.44	13.33 \pm 1.30	0.05**	0.001***	0.001***

SD – standard deviation.

p*-value – significant; *p*-value – highly significant.

Table 6

Inter-group comparison of stiffness (in N/mm) pre- and post-immersion in saliva

Time of immersion	Silk (SL)	Polyglactin 910 (PG)	Polypropylene (PP)	<i>p</i> -value (Inter-Group)		
	mean \pm SD	mean \pm SD	mean \pm SD	SL vs. PG	SL vs. PP	PG vs. PP
Pre-immersion	1.33 \pm 0.22	0.67 \pm 0.07	0.68 \pm 0.06	0.001***	0.001***	0.657 ^{ns}
Post-immersion in saliva						
3rd day	0.69 \pm 0.07	0.36 \pm 0.02	0.63 \pm 0.04	0.001***	0.576 ^{ns}	0.05**
7th day	0.38 \pm 0.09	0.42 \pm 0.07	0.55 \pm 0.05	0.05**	0.001***	0.001***
14th day	0.38 \pm 0.12	0.39 \pm 0.04	0.68 \pm 0.07	0.875 ^{ns}	0.001***	0.001***

SD – standard deviation.

p*-value – significant; *p*-value – highly significant; ^{ns}*p*-value – statistically non-significant.

Table 7

Intra-group comparisons of tensile strength, percentage of elongation and stiffness of different suture materials from pre-immersion (baseline) to the 14th day

Baseline to the 14 th day comparison	Silk (SL)	Polyglactin 910 (PG)	Polypropylene (PP)
Tensile strength	0.001***	0.001***	0.001***
% elongation	0.001***	0.001***	0.001***
Stiffness	0.001***	0.001***	0.001***

****p*-value – highly significant.

exposed to few environmental conditions that can influence physical and mechanical properties of the sutures. Studies associated with oral cavity present a number of difficulties, like the presence of saliva, reflux gastric juice, pressure from the surrounding soft tissues and occlusal forces that can markedly change the properties of suture materials ^{21, 22}.

In the present study the suture gauge designation was fixed at 4–0 in order to help in comparisons of a single gauge of suture. For most of the intraoral surgeries the commonly used gauges are in the range of 3–0 to 4–0, with an increasing number of zeros making the diameter smaller and the suture weaker, confirming that as the diameter decreases the suture becomes weaker. For the current study silk, polygalactin 910 and polypropylene suture materials were used because of their demand in various oral surgical procedures ²³. Sutures were immersed in artificial saliva to be used as a control group as previous studies indicated its possible harmful effect on the mechanical properties of suture materials ^{24, 25}. To the best of authors' knowledge, it is the first original study that assesses the mechanical properties of different suture materials used intraorally by simulating a natural environment.

All the experiments were done by a single investigator to circumvent any inter-examiner error. The time frame and test frequencies of the present study were in accordance with the clinical relevance of the frequent oral and periodontal surgical procedures. Different studies have found a positive correlation between the reduction in tensile strength and resorption rates of distinct suture materials under controlled experimental conditions ^{10, 26, 27}. A prime element that can influence the resorption rate of suture materials is the variation in pH of the solution. It has been well documented that a decrease in the pH increases the resorption rate of the sutures ²⁴. The pH of the current study was kept between 7.4 and 8.1 by checking it regularly for stability and changing the solution every 2 days.

The outcome of the current study exhibits that the PP group manifested maximum tensile strength and percentage elongation in contrast to the PG and SL group, whereas the PP group manifested the lowest stiffness. The elongation capacity of the material is inversely proportional to the stiffness, the stiffer sutures exhibit less elongation. Since no comprehensive study had been done *in vitro* to assess the mechanical properties of the PP suture material compared to the PG and SL in the oral environment, we chose this material in our study design. In one study different gauge of sutures were used to evaluate the mechanical properties of strength, elongation and stiffness of the PP suture material ²⁸. The test values for 4–0 gauge suture were analogous to the values recorded at baseline (pre-immersion) in the present study.

Earlier studies on the PG sutures exhibited good handling properties, high initial tensile strength, and less tissue

reactions during healing ^{29, 30}. A strong correlation between suture degradation and tensile strength has been described in various studies under controlled *in vitro* and *in vivo* settings. PG degradation *in vivo* is mostly due to proteolytic enzymes. The PG sutures preserved more than two-thirds of their initial tensile strength on the 14th day of the post-immersion period ³¹. The results of the present study were similar to this result of previous study. Some studies state that, when PG is immersed in saliva, it shows a fast tensile strength loss, especially after 7 days ¹⁰. This is in contradiction to the findings of the present experimental study.

SL is the most frequently used suture material in the surgical procedures even though it exhibits inferior mechanical properties. Even though SL is said to be a non-resorbable suture but acknowledged to be subject to proteolytic degradation over a longer period ³². Studies indicate that SL is one of the most vulnerable sutures to the differences in pH conditions ²⁴. In the present study, it was found that mechanical properties of the SL sutures diminished on the 14th day after the immersion. These outcomes are in accordance with the respites presented by Banche et al. ¹² where tensile strength of SL declined upon exposure to saliva.

As the present study design is *in vitro*, it has certain constraints as mentioned below. The outcome of the current experiment may not be completely similar to the oral clinical situations. There are various possible confounding factors, such as diet, habits, occlusal forces and medications in the oral cavity that may affect the oral environment and cause variation in the mechanical properties of sutures. More information can be collected by performing molecular interpretation of the selected suture materials upon their reaction with saliva. However, this was beyond the scope of the current experimental study.

Conclusion

The present study affirms that the suture materials tend to lose a significant amount of tensile strength when exposed to oral environment. The PP sutures showed highest mechanical properties when compared to the PG, and SL suture. Under the limitation of the present study, the authors conclude that PP is the best suture material for wound closure after oral and periodontal surgeries, followed by PG and SL, respectively.

Acknowledgment

The authors extend their appreciation to the deanship of scientific research at King Khalid University for funding this work through the general research project under grant number (GRP-168-42).

REFERENCES

1. Nalenay SE, Lear W, Krnjic JJ, Maughan CB. Mechanical properties of suture materials in general and cutaneous surgery. J Biomed Mater Res B Appl Biomater 2015; 103(4): 735–42.
2. Vasantha A, Satheesh K, Hoopes W, Lucaci P, Williams K, Rapley J. Comparing suture strengths for clinical applications: a novel *in vitro* study. J Periodontol 2009; 80(4): 618–24.

3. Burkhart SS, Wirth MA, Simonich M, Salem D, Lanctot D, Athanasios K. Knot security in simple sliding knots and its relationship to rotator cuff repair: How secure must the knot be? *Arthroscopy* 2000; 16(2): 202–7.
4. Arce J, Palacios A, Alvitez-Temoche D, Mendoza-Azpur G, Romero-Tapia P, Mayta-Tovalino F. Tensile Strength of Novel Nonabsorbable PTFE (Teflon(R)) versus Other Suture Materials: An *In Vitro* Study. *Int J Dent* 2019; 2019: 7419708.
5. Hiatt WH, Stallard RE, Butler E, Badgett B. Repair following mucoperiosteal flap surgery with full gingival retention. *J Periodontol* 1968; 39(1): 11–6.
6. Burkhardt R, Lang NP. Coverage of localized gingival recessions: comparison of micro- and macrosurgical techniques. *J Clin Periodontol* 2005; 32(3): 287–93.
7. Chu CC. Mechanical-properties of suture materials—An important characterization. *Ann Surg* 1981; 193(3): 365–71.
8. von Fraunhofer JA, Storey RJ, Masterson BJ. Tensile properties of suture materials. *Biomaterials* 1988; 9(4): 324–7.
9. Racey G, Wallace W, Cavalaris C, Marguard J. Comparison of a polyglycolic-poly-lactic acid suture to black silk and plain catgut in human oral tissues. *J Oral Surg* 1978; 36(10): 766–70.
10. Ferguson RE Jr, Schuler K, Thornton BP, Vasconez HC, Rinker B. The effect of saliva and oral intake on the tensile properties of sutures: an experimental study. *Ann Plast Surg* 2007; 58(3): 268–72.
11. Alsarhan M, Alnofaie H, Ateeq R, Almahdy A. The Effect of Chlorhexidine and Listerine® Mouthwashes on the Tensile Strength of Selected Absorbable Sutures: An *In Vitro* Study. *BioMed Res Int* 2018; 2018: 8531706.
12. Banche G, Roana J, Mandras N, Amasio M, Gallesio C, Allizon V, et al. Microbial adherence on various intraoral suture materials in patients undergoing dental surgery. *J Oral Maxillofac Surg* 2007; 65(8): 1503–7.
13. Gal JY, Fovet Y, Adib-Yadzi M. About a synthetic saliva for *in vitro* studies. *Talanta* 2001; 53(6): 1103–15.
14. Vasanthan A, Satheesh K, Hoopes W, Lucasi P, Williams K, Rapley J. Comparing suture strengths for clinical applications: a novel *in vitro* study. *J Periodontol* 2009; 80(4): 618–24.
15. Lai SY, Becker DG, Edlich RF. Sutures and needles. 2009. Available from: <http://www.eMedicine.com> [accessed 2010 October].
16. Pillai C, Sharma CP. Review paper: absorbable polymeric surgical sutures. Chemistry, production, properties, biodegradability, and performance. *J Biomater Appl* 2010; 25: 291–366.
17. von Fraunhofer JA, Storey RS, Stone IK, Masterson BJ. Tensile strength of suture materials. *J Biomed Mater Res* 1985; 19(5): 595–600.
18. Edlich RF, Panek PH, Rodeheaver GT, Turnbull VG, Kurtz LD, Edgerton MT. Physical and chemical configuration of sutures in the development of surgical infection. *Ann Surg* 1973; 177(6): 679–688.
19. Moy R L, Lee A, Zalka A. Commonly used suture materials in skin surgery. *Am Fam Physician* 1991; 44(6): 2123–8.
20. Ketchum LD. Suture materials and suture techniques used in tendon repair. *Hand Clin* 1985; 1(1): 43–53.
21. Karabulut R, Sonmez K, Turkyilmaz Z, Bagbanci B, Basaklar AC, Kale N. An *in vitro* and *in vivo* evaluation of tensile strength and durability of seven suture materials in various pH and different conditions: an experimental study in rats. *Indian J Surg* 2010; 72(5): 386–90.
22. McCaul LK, Bagg J, Jenkins WM. Rate of loss of irradiated polyglactin 910 (vicryl rapide) from the mouth: A prospective study. *Br J Oral Maxillofac Surg* 2000; 38(4): 328–30.
23. Siervo S. *Suturing Techniques in Oral Surgery*. 1st ed. Berlin, Germany: Quintessence Publication Co. 2008.
24. Chu CC, and Moncrief G. An *in vitro* evaluation of the stability of mechanical properties of surgical suture materials in various pH conditions. *Ann Surg* 1983; 198(2): 223–8.
25. Mohammed A, Hourya A, Ravan A, Ahmed A. The Effect of Chlorhexidine and Listerine® Mouthwashes on the Tensile Strength of Selected Absorbable Sutures: An *In Vitro* Study. *BioMed Res Int* 2018; 2018: 8531706.
26. Alsbehri MA, Baskaradoss JK, Geevarghese A, Ramakrishnaiah R, Tatakis DN. Effects of myrrh on the strength of suture materials: an *in vitro* study. *Dent Mater J* 2015; 34(2): 148–153.
27. Arcuri C, Cecchetti F, Dri M, Muggi F, Bartoli FN. Suture in oral surgery. A comparative study. *Minerva Stomatol* 2006; 55(1–2): 17–31.
28. Debus ES, Geiger D, Sailer M, Ederer J, Thiede A. Physical, biological and handling characteristics of surgical suture material: a comparison of four different multifilament absorbable sutures. *Eur Surg Res* 1997; 29(1): 52–61.
29. Rashid RM, Sartori M, White LE, Villa MT, Yoo SS, Alam M. Breaking strength of barbed polypropylene sutures: a blinded, controlled comparison with nonbarbed sutures of various calibers. *Arch Dermatol* 2007; 143(7): 869–72.
30. Yaltirik M, Dedeoglu K, Bilgic B, Koray M, Ersev H, Issever H, et al. Comparison of four different suture materials in soft tissues of rats. *Oral Dis* 2003; 9(6): 284–6.
31. Hochberg J, Meyer KM, Marion MD. Suture choice and other methods of skin closure. *Surg Clin North Am* 2009; 89(3): 627–41.
32. Altman GH, Diaz F, Jakuba C, Calabro T, Horan RL, Chen J, et al. Silk-based biomaterials. *Biomaterials* 2003; 24(3): 401–16.

Received on January 14, 2020

Revised on August 5, 2020

Accepted on August 10, 2020

Online First August, 2020



Application of P16, P63, cyclin D1 immunostaining and nuclear morphometric analysis for assessment of cervical dysplasia

Primena imunohistohemijskih markera P16, P63, ciklin D1 i morfometrijske analize u proceni težine displazije grlića materice

Biserka Vukomanović Djurdjević^{*†}, Bojana Andrejić Višnjić[‡],
Aleksandar Perić[§], Dane Nenadić[¶], Nenad Baletić[§]

Military Medical Academy, ^{*}Institute for Pathology, [§]Clinic of Otorhinolaryngology, [¶]Department of Gynecology, Belgrade, Serbia; [†]University of Defence, Faculty of Medicine of the Military Medical Academy, Belgrade, Serbia; [‡]University of Novi Sad, Faculty of Medicine, Department of Histology and Embryology; Novi Sad, Serbia

Abstract

Background/Aim. Human papilloma virus (HPV) infection is the main etiological factor for the development of cervical precancerous dysplastic squamous intraepithelial lesions (SIL). The virus oncoproteins affect several proteins included in cell proliferation. The aim of this study was to evaluate application of immunohistochemical markers related to proteins of the cell cycle and, also, application of nuclear morphometric analysis for assessment of cervical dysplasia. **Methods.** Retrospective study included 78 women with detection of presence of high-risk HPV by polymerase chain reaction (PCR), with histopathology diagnosis low-grade SIL (LSIL) or high-grade SIL (HSIL). Immunohistochemical staining for p16, p63, cyclin D1 and morphometric analysis of the nuclear surface area were performed. The control group consisted of ten women without SIL and without HPV infection. This study was conducted in

accordance with the Helsinki Declaration. **Results.** Comparing immunohistochemical expression of p16 and p63, highly statistically significant differences ($p < 0.001$) were established among the control, LSIL and HSIL groups, while cyclin D1 showed significant statistical difference ($p < 0.05$). Great variations were observed in nuclear morphology and nuclear surface area that had highly statistically significant differences ($p < 0.001$) among the control, LSIL and HSIL groups. **Conclusion.** This study demonstrated that immunohistochemical analysis of p16, p63 and cyclin D1 are important for diagnosis of dysplastic changes in cervical epithelium. Also, morphometric analysis of the nuclear surface area demonstrated a high significance for diagnosis of cervical dysplasia.

Key words:

diagnosis; immunohistochemistry; ovarian neoplasms; papilloma viridae; polymerase chain reaction; severity of illness index.

Apstrakt

Uvod/Cilj. Infekcija humanim papiloma virusima (HPV) je glavni etiološki faktor za razvoj displastičnih, skvamoznih intraepitelih lezija (SIL) grlića materice. Virusni onkoproteini utiču na gene i proteine koji su uključeni u deobu ćelije. Cilj istraživanja je bio da se ispita efekat primene imunohistohemijskih markera koji se odnose na proteine uključene u ćelijski ciklus, kao i primene morfometrijske analize jedara u proceni težine displazije grlića materice. **Metode.** U retrospektivno istraživanje je bilo uključeno 78 žena kod kojih je potvrđeno prisustvo visoko rizičnih tipova humanih papiloma virusa (HPV) metodom *polymerase chain reaction* (PCR), a histološki je dijagnostikovana

SIL niskog (LSIL) ili visokog (HSIL) stepena. Izvršene su imunohistohemijske analize p16, p63 i *cyclin* D1 i morfometrijska analiza površine jedara. Kontrolnu grupu činilo je 10 žena kod kojih nije potvrđeno prisustvo HPV virusa, niti SIL lezije. Studija je sprovedena uz poštovanje principa Helsinške deklaracije. **Rezultati.** Ustanovljena je statistički visoko značajna razlika u imunohistohemijskoj ekspresiji markera p16 i p63 ($p < 0,001$) između kontrolne grupe i LSIL i HSIL grupa i statistički značajna razlika u ekspresiji *cyclin* D1 ($p < 0,05$) između ovih grupa. Morfometrijska analiza površina jedara pokazala je visoko statistički značajnu razliku ($p < 0,001$) između ispitivanih grupa. **Zaključak.** Studija je pokazala da imunohistohemijske analize p16, p63 i *cyclin* D1 imaju

značaja u dijagnostici SIL grlića materice. Takođe, pokazano je da je morfometrijska analiza jedara cervikalnih ćelija veoma značajna u dijagnostici displazije.

Ključne reči:

dijagnoza; imunohistohemija; jajnik, neoplazme; papiloma virus, humani; polimeraza, reakcija stvaranja lanaca; bolest, indeks težine.

Introduction

One of the most common diseases of modern age is the cervical cancer and dysplasia of epithelium of cervical mucosa. Squamous cell carcinoma of the cervix in Serbia is among cancers with very high incidence and mortality^{1, 2}. Preventive examinations of this disease decreased morbidity drastically. Health education of young people with information about risk factors also gives good results in the prevention of this serious disease.

Human papilloma virus (HPV) infection is the main etiological factor for the development of precancerous dysplastic squamous intraepithelial lesions (SIL) and cervical carcinoma. HPV is a large group of viruses specific for their tropism for epithelium. The different levels of oncogenic potential of HPV viruses are very important characteristic for research. In this moment, we know that a persistent infection in high-risk type of HPV, have a high tendency of dysplastic or neoplastic progress³. Typing of HPV may be performed as a big prognostic factor by several laboratory techniques, but the polymerase chain reaction (PCR) has been mostly used. HPV typing provides information relevant to the patient's clinical treatment⁴.

One of the crucial pathogenic problem and characteristics of HPV is its ability to integrate itself in the human genome. This event is the main cause of cervical epithelial dysplasia. Cervical dysplasias are among the most common histopathological diagnoses of the females. In those cases, the virus affects cells structure and functions. Depending on the area affected, we have a diagnosis of low grade and/or high grade SIL (LSIL and HSIL, respectively). At the beginning of the pathogenesis of dysplasia, there are low-grade dysplasias. That level of pathophysiological and pathological changes occur at the level of the lower third of the full epithelial thickness. If dysplastic cells are present in the epithelial thickness greater than one third of the total epithelial thickness, then we are talking about severe dysplasia. The nuclei of dysplastic cells are irregular in many morphologic characteristics. Nuclei have different shape, larger area. Also nuclei are hyperchromatic and occupy a significant part of the cell volume like bigger nuclear than cytoplasmatic volume. Due to the specific pathophysiologic and genetic mechanisms in the cytoplasm, perinuclear clearance of the cytoplasm, called koilocytosis, can be seen morphologically. In cells with dysplasia, there is a disturbance of the cell cycle and maturation. Inadequate genetic regulation results morphologically like a stratification disorder. As well as, we can notice as very important morphological disorder, the presence of a pathological mitoses. The index of pathological mitoses determines the severity of dysplasia^{5, 6}. It is interesting that on microscopic preparations we can notice zones of reg-

ular epithelium that directly extend to the epithelium with dysplasia. A p16 protein is very important "regulator" of cell-cycle. Normally, it prevents progression of cell cycle. That protein has the important role for inhibiting cyclin D-dependent protein kinases. After the integration of HPV into the nuclei of squamous cell genome, some of tumor suppressor genes are lost and cell cycle is deregulated. The progression from a transient to a transforming HPV infection is characterized by a strong increase of HPV E6/E7 mRNA and protein expression. Viral oncoprotein E7 disrupts pRb in transforming HPV infections. The disturbance of the Rb pathway leads to a compensatory overexpression of p16. It works by a negative feedback loop. p16-overexpression in cells is considered as a surrogate marker for deregulated E7 expression and hence for transforming HPV infections. Overexpression and cellular accumulation of p16 may be evaluated immunohistochemically and studies show that immunopositivity to p16 is an important marker^{6, 7}.

p63 is one of the members of the group of p53 genes. It participates in determining the proliferation of epithelial cells. p63 inhibits the cell cycle at a determined point and induces apoptosis. In that way, its influence is the inhibition of oncogenic mutations⁸. According to data from molecular cell biology, genetic models and clinic research, it appears that p63 may act as either an oncogene or a tumor suppressor gene in different scenarios. The role in promotion of tumorigenesis is by promoting cell proliferation and survival, and it depends of the whole p53 family⁹.

Cyclin D1 is associated with the cyclin-dependent kinases (CDKs). It inhibits the retinoblastoma (RB) protein, and induces proliferation. Many additional factors have positive or negative effects on the control of cellular proliferation. Many researches have shown changes within the RB-p16-cyclin D1 pathways. Relatively few studies have investigated cyclin D1 expression within the normal cervix or SIL changes, and most of the latter have focused on the more common *in situ* and invasive squamous lesions¹⁰.

The use of computer programs in the analysis of dysplastic nuclei is an imperative of the 21st century. This is a way of objectifying the process of assessing the degree of dysplasia. It is of special importance when the dysplasia reaches the junction/border of the lower with the middle third of the epithelium: the border of mild and severe dysplasia. For pathologist in routine practice, it plays a big role in the differential diagnosis in many different cases: dysplasia and immature squamous metaplasia with atypia, reactive atypia in atrophic epithelium is also unambiguous. Morphometric analysis is performed by analyzing morphometric software for cellular structures. For dysplasia of the cervical epithelium, the most important component is the analysis of cell nuclei. Comparison of numerical values of diameter,

volume and surface of nuclei and cytoplasm gives the possibility of easier diagnostics, especially since numerical values can be used. In addition, the advantage of morphometry is that the nuclei from the dysplasia zone can be compared by computer with the nuclei that are not dysplastic, which further verifies the diagnosis.

Methods

The study was retrospective and included 88 patients treated during a period of 30 months. Of the selected specimens, 10 women were in the control group. The rest of the subjects ($n = 78$) who formed dysplasia group, entered the study after meeting the following criteria: 1) primary lesion that had not been treated before; 2) colposcopic finding suggestive of dysplasia; 3) Papanikolau (PAPA) test result (according to Bethesda criteria) showing some of the following – LSIL, HSIL, atypical squamous cells of undetermined significance (ASCUS); 4) performed PCR HPV typing, with proven presence of one of the following types: 16, 18, 31 or 33. The study did not include women with previously diagnosed and treated dysplasia, as well as women with squamous cell carcinoma.

The control group consisted of women who did not have HPV infection, nor dysplasia or any clinical data indicating the possibility of dysplastic process. These patients had symptoms of uterine myomas and due to that had underwent hysterectomy. The final histopathological findings of the control group cervix tissue denied any signs of dysplasia, and verified only mild nonspecific inflammation.

Biopsy samples of all patients who met the entry criteria underwent standard histological tissue processing, hematoxylin-eosin staining, immunohistochemical staining and morphometric tissue analysis. Histological diagnoses were established under the light microscope, according to the latest World Health Organization (WHO) classification criteria and were classified as LSIL or HSIL, and upon that, additional two groups were formed: LSIL group ($n = 48$) and HSIL ($n = 30$)¹¹.

Following antibodies were used for immunohistochemical staining: p16 (CINtec® E6H4 Histology Kit, Ventana), p63 (DAK-p63, DAKO), cyclin D1 (EP12, Cell marque, Milipore Sigma). Staining was performed according to manufacturers instructions (having internal and external control tissue), and interpreted as positive or negative staining according to reference guidelines: positive p16 staining was interpreted as nuclear and/or cytoplasmic⁷. p63 nuclear staining is considered as immunohistochemical positivity⁹. Cyclin D1–nuclear staining is considered as immunohistochemical positivity¹⁰.

Morphometric analysis was performed using Image J software on digital microphotographs. Analysis was performed in the zone of the most intense dysplasia. The surface of the nucleus was analyzed, since its characteristics are the most important diagnostic criterion for diagnosing dysplasia and that the most important changes in dysplasia take place at the nuclear area.

The obtained results were compared among control group and dysplasia group. Statistical significance of the obtained results was analyzed by the methodology of analytical and descriptive statistics. A χ^2 -test was used for statistical analysis of immunohistochemical results. The Kruskal Wallis test was used to analyze the morphometric results of the nuclei. The results are presented in images, numerically and graphically.

Results

Using the χ^2 -test, it was verified that there is a highly statistically significant difference ($\chi^2 = 14.841$, $p = 0.001$) in p16 expression between patients without cervical epithelial dysplasia (control group), and those with LSIL and HSIL (Figures 1 and 2).

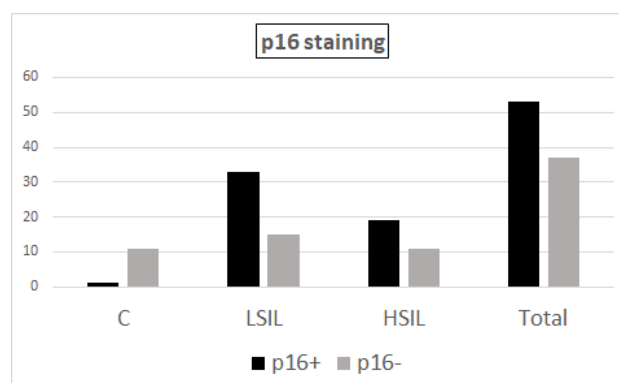


Fig. 1 – Results of p16 immunohistochemical staining (y-axis – number of women). LSIL – low-grade squamous intraepithelial lesions (SIL); HSIL – high-grade SIL.

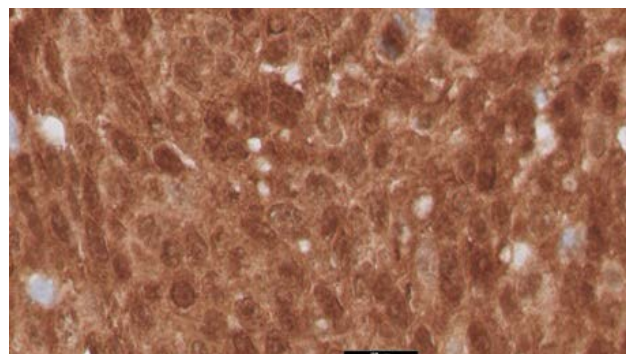


Fig. 2 – Positivity of p16 in cervical squamous cells (hematoxylin-eosin, $\times 60$).

Expression of p63 showed highly statistically significant difference ($\chi^2 = 17.639$, $p = 0.000$) among the control, LSIL and HSIL groups, when compared by χ^2 -test (Figures 3 and 4).

In patients without cervical epithelial dysplasia (control group), compared with those in the LSIL and HSIL groups, χ^2 -test revealed statistically significant difference in cyclin D1 expression ($\chi^2 = 7.483$, $p = 0.024$) (Figures 5 and 6).

Kruskal Wallis test revealed highly statistically significant difference ($p < 0.001$) in the nuclear surface area

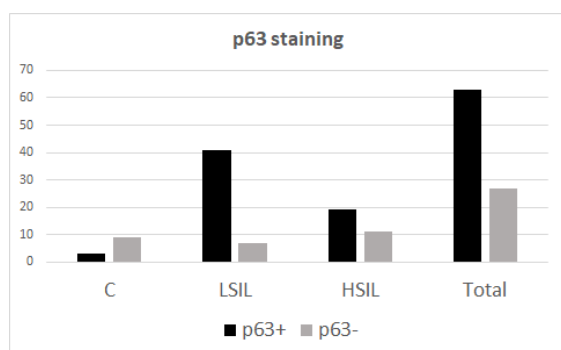


Fig. 3 – Results of p63 immunohistochemical staining (y-axis – number of women). LSIL – low-grade squamous intraepithelial lesions (SIL); HSIL – high-grade SIL.

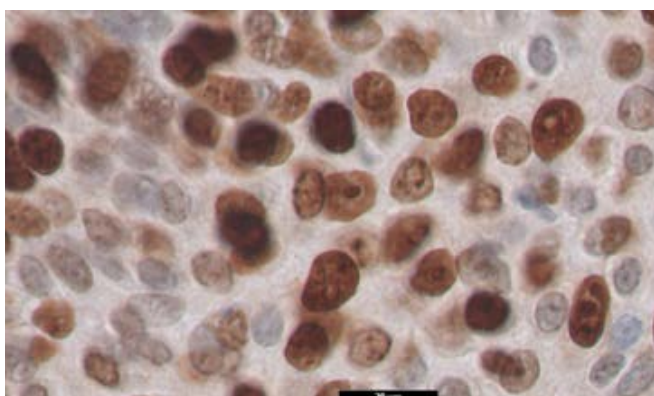


Fig. 4 – Positivity of p63 in cervical squamous cells (hematoxylin-eosin, ×60).

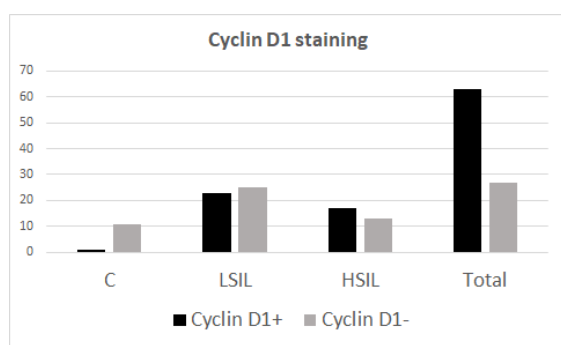


Fig. 5 – Results of cyclin D1 immunohistochemical staining (y-axis – number of women). LSIL – low-grade squamous intraepithelial lesions (SIL); HSIL – high-grade SIL.

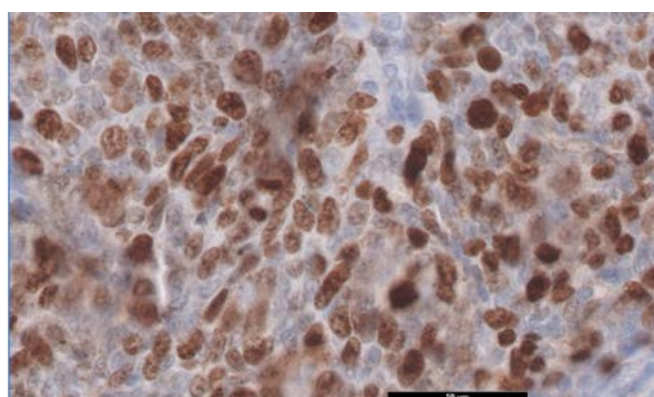


Fig. 6 – Positivity of cyclin D1 in cervical squamous cells (hematoxylin-eosin, ×40).

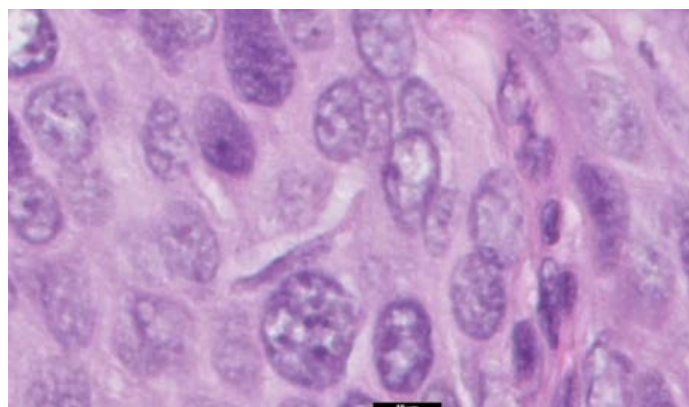


Fig. 7 – Nuclear characteristics and enlargement in squamous intraepithelial lesions (SIL) (hematoxylin-eosin, ×80).

of the cervical epithelial cells among examined groups. Morphological changes on epithelial cells with dysplasia were clearly visible (Figure 7).

Discussion

Cervical cancer is one of the most common deadly diseases in female population. Also, in 21st century, it is a disease with a poor prognosis. High-stadium of the disease is a bad prognostic factor. HPV is the main etiological factor for

the disease. But cervical cancer is final pathological event. LSIL and HSIL are without symptoms. They occur from the moment of HPV infection and can be present for many years before the cancer develops. Developing a methodology for histopathological diagnosis of these lesions and recognizing prognostic factors for the development of HPV-induced lesions are very important. They provide information of the necessary treatment of precancerous lesion. This prevents cancer. Intraepithelial lesions are treated with both classical and modern technological methods ⁴.

The epithelium of cervix is stratified squamous, or columnar. The region where cylindrical epithelium continues with squamous epithelium is the most fragile location for pathologic process, especially for dysplasias. This is the place where the most frequent premalignant lesions occur. But as with all viral infections, the effect of the virus depends on both general immunity and local immunity. Protection against non-HPV sexually transmitted disease and the presence of normal microflora in the female reproductive organs also make prevention of cervical epithelial dysplasia and cervical cancer development. It is also easier to diagnose dysplasia if there is no associated inflammation and infection with non-HPV microbiological etiological factors. Reparative atypia and various forms of metaplasia can be a factor of complication in the diagnosis of cervical epithelial dysplasia.

The use of immunohistochemical markers in modern pathology is imperative. This includes the diagnosis of pathological conditions of the cervix. Immunohistochemically, analyzed markers in nondysplastic epithelial cervical cells – p16, p63 and cyclin D1, if are positive, depending on the marker used (except p63), are present in a small percentage of cells located in basal layers. This results in accordance with literature data ¹⁰⁻¹⁴.

The p16ink4a/RB pathway is of a great significance. As a result, its malfunctions can be a good diagnostic marker for making prognosis of premalignant lesions ¹⁵. Some authors who studied immunoexpression of p16 showed a linear increase in this expression from LSIL to HSIL ^{12, 13}.

In our study, it was verified that there is a highly statistically significant difference in p16 expression in patients without cervical epithelial dysplasia, with LSIL and with HSIL. Our results are similar to above mentioned, and many other stating that p16 expression increases with the progression of dysplastic changes in cervical squamous epithelium. From other experimental and literature data and review articles, following should be kept in mind, regarding p16 expression – its level can both increase or decrease depending on tissue. There are great variations in interpretation of what p16 positivity is in some studies. Therefore, it is important to find panel of biomarkers necessary for the diagnosis of cervical epithelial dysplasia especially for the differential diagnosis of the degree of dysplasia in cases borderline from LSIL to HSIL ^{4, 14-17}. Our result show that p16 expression is one of the most significant biomarkers and diagnostic methods for HPV. This was confirmed both in accordance with the fact that p16 can rarely be positive in the cervical epithelium without dysplasia, but in a different percentage and a different microscopic image of the visualization of it. That is why we have to be very careful with interpretations of this immunohistochemical marker. Also, we have to find the best supplemental markers ^{13, 17}.

HPV by producing E6 and E7 oncoproteins affects tumor suppressor genes in the cell. Several of those genes are genes of p63, cyclin-dependent kinase inhibitors (p21, p27, p16) and retinoblastoma (pRb). That promotes malfunction of normal cell cycle and inhibits the repair of DNA damage.

Some of the consequences of this happening may induce proliferation or cell apoptosis ¹⁸.

According to the literature, we may conclude that p63 expression is evidently increased in cervical intraepithelial neoplasia ⁸. Our study did not deviate from those literature data. Expression of p63 showed highly significant statistical difference among the control group, and LSIL and HSIL groups. p63 positivity in the control group was smallest, compared to the LSIL and HSIL groups, which is also in accordance with theoretical and experimental scientific data. When comparing number of positive and negative cases among all analyzed cases, and just in the LSIL and HSIL groups, we observed predominance of p63 positive cases in dysplastic cells, which showed to be statistically highly significant. Functional and biochemical alterations of cell cycle components are one of the crucial pathogenesis mechanisms of this virus ¹⁹. The expression of p63 is a significant marker for diagnostics of cervical carcinomas ⁸.

HPV induced deviations of E2F referred before, in concept of p53 family deregulation, stimulates the activation of cyclin-dependent kinase inhibitor ¹⁸. The malfunction of RB-p16-cyclin D1 pathways results in abnormalities in cell cycle. The mechanism of occurrence is by increasing activity of cyclin-D1 ¹⁰. Some authors have shown correlation between degree of dysplasia of cervical epithelial cells and cyclin E ¹³. Some authors have shown immunoexpression of cyclin D1 in dysplastic cells and found that in contrast to p16, immunoreactivity of cyclin D1 is decreased in relation to the degree of dysplasia ¹². Our study showed statistically significant difference in cyclin D1 expression between the group of patients without cervical epithelial dysplasia and the LSIL and HSIL group. Our results show predominance of cyclin D1 positive cases when observing total sample, as well as when comparing number of positive and negative cases among the control and LSIL or HSIL groups, which was proven statistically highly significant. The number of positive cases in our HSIL group showed slight decline, compared to the LSIL group, but still it was significantly higher compared to controls. It appears that in some other cervical lesions, expression of cyclin D1 decreases as the dysplastic process progression occurs ¹⁰. The explanation may be in different immune statuses – general and local. An explanation should also be in gene mutations. Laboratory standardization also plays a huge role in research results.

Morphological changes on epithelial cells with dysplasia are clearly visible. They exist in the nucleus and in the cytoplasm. The nuclear cytoplasmic ratio has also changed. The architecture of epithelial cell stratification in dysplasia is disturbed. Increased mitotic count and koilocytosis were presented also. The differential diagnosis of dysplasia in relation to reparative processes and inflammation is sometimes difficult. Also, metaplasia together with inflammation makes it difficult to diagnose dysplasia and gradation of dysplasias. Exclusion of the subjective component of the pathologist in the diagnosis is the basic goal of the pathology. The 21st century provides an opportunity to use software that can help a pathologist in the process of excluding the subjective component in making a diagnosis.

Morphometric analyzes of different types are applied and improved. Their improvement is a promising factor for the accuracy of pathological diagnosis.

Histologically, dysplasias were classified as LSIL or HSIL, according to its nuclear and cytoplasmatic features and the thickness of epithelium that was affected. In the LSIL group, changes were present in lower third of epithelium, while in the HSIL group, it involved whole epithelial thickness. Our results showed highly statistically significant difference between the nuclear surface area of the cervical epithelial cells in the LSIL and HSIL groups and epithelium without dysplasia. Out of total number of analyzed cases, 10 were in the control group, 48 in the LSIL group and 30 in the HSIL group. In specimens of the LSIL and HSIL groups,

standard histopathological examination detected nuclear changes that were proven by morphometric analysis. Nuclear surface area increased significantly compared to the control samples. The research results, the economic factor and the availability of morphometry makes this methodology most promising.

Conclusion

This study demonstrated that immunohistochemical analysis of p16, p63 and cyclin D1 is important for diagnosis of dysplastic changes in cervical epithelium. Also, morphometric analysis of the nuclear surface area demonstrated its high importance for diagnosis of cervical dysplasia.

R E F E R E N C E S

- Mihajlović J, Pechlivanoglou P, Miladinov-Mikov M, Zivković S, Postma MJ. Cancer incidence and mortality in Serbia 1999–2009. *BMC Cancer* 2013; 13: 18.
- Naumović T, Miljusić D, Djorđević M, Zivković S, Perisic Z. Mortality from cervical cancer in Serbia in the period 1991–2011. *JBUON* 2015; 20(1): 231–4.
- Izadi-Mood N, Asadi K, Shojaei H, Sarmadi S, Ahmadi SA, Sani S, et al. Potential diagnostic value of P16 expression in premalignant and malignant cervical lesions. *J Res Med Sci* 2012; 17(5): 428–33.
- Balasubramaniam S, Balakrishnan V, Ein Oon C, Kaur G. Key Molecular Events in Cervical Cancer Development. *Medicina* 2019; 55: 384.
- Cooper DB, McCatbray CE. Cervical Dysplasia. StatPearls (Internet). Treasure, Island (FL): StatPearls Publishing; 2019. Available from: <https://www.ncbi.nlm.nih.gov/books/NBK430859/>
- Sabasrabuddhe VV, Luhn P, Wentzensen N. Human papillomavirus and cervical cancer: biomarkers for improved prevention efforts. *Future Microbiol* 2011; 6(9): 1083–98.
- Zhu Y, Ren C, Yang L, Zhang X, Liu L, Wang Z. Performance of p16/Ki67 immunostaining, HPV E6/E7 mRNA testing, and HPV DNA assay to detect high-grade cervical dysplasia in women with ASCUS. *BMC Cancer* 2019; 19(1): 271.
- Houghton O, McCluggage WG. The expression and diagnostic utility of p63 in the female genital tract. *Adv Anat Pathol*. 2009; 16(5): 316–21.
- Chen Y, Peng Y, Fan S, Li Y, Xiao ZX, Li C. A double dealing tale of p63: an oncogene or a tumor suppressor. *Cell Mol Life Sci* 2018; 75(6): 965–73.
- Little L, Stewart CJ. Cyclin D1 immunoreactivity in normal endocervix and diagnostic value in reactive and neoplastic endocervical lesions. *Mod Pathol* 2010; 23(4): 611–8.
- Zheng W, Fadare O, Quick CM, Shen D, Guo D. *Gynecologic and obstetric pathology*. Singapore: Springer; 2019.
- Portari EA, Russomano FB, de Camargo MJ, Machado Gayer CR, da Rocha Guillobel HC, Santos-Rebouças CB, et al. Immunohistochemical expression of cyclin D1, p16Ink4a, p21WAF1, and Ki-67 correlates with the severity of cervical neoplasia. *Int J Gynecol Pathol* 2013; 32(5): 501–8.
- Keating JT, Cviko A, Riethdorf S, Riethdorf L, Quade BJ, Sun D, et al. Ki-67, cyclin E, and p16INK4 are complimentary surrogate biomarkers for human papilloma virus-related cervical neoplasia. *Am J Surg Pathol* 2001; 25(7): 884–91.
- Krishnappa P, Mohamad IB, Lin YJ, Barua A. Expression of P16 in high-risk human papillomavirus related lesions of the uterine cervix in a government hospital, Malaysia. *Diagn Pathol* 2014; 9: 202.
- Witkiewicz AK, Knudsen KE, Dicker AP, Knudsen ES. The meaning of p16(ink4a) expression in tumors: functional significance, clinical associations and future developments. *Cell Cycle* 2011; 10(15): 2497–503.
- Nam EJ, Kim JW, Hong JW, Jang HS, Lee SY, Jang SY, et al. Expression of the p16 and Ki-67 in relation to the grade of cervical intraepithelial neoplasia and high-risk human papillomavirus infection. *J Gynecol Oncol* 2008; 19(3): 162–8.
- Li Y, Liu J, Gong L, Sun X, Long W. Combining HPV DNA load with p16/Ki-67 staining to detect cervical precancerous lesions and predict the progression of CIN1-2 lesions. *Virol J* 2019; 16(1): 117.
- Schiffman M, Castle PE, Jeronimo J, Rodriguez AC, Wacholder S. Human papillomavirus and cervical cancer. *Lancet* 2007; 370(9590): 890–907.
- Conesa-Zamora P, Doménech-Peris A, Orantes-Casado FJ, Ortiz-Reina S, Sabuquillo-Frías L, Acosta-Ortega J, et al. Effect of human papillomavirus on cell cycle-related proteins p16, Ki-67, Cyclin D1, p53, and ProEx C in precursor lesions of cervical carcinoma: a tissue microarray study. *Am J Clin Pathol* 2009; 132(3): 378–90.

Received on August 18, 2020

Accepted on August 27, 2020

Online First August, 2020



Beneficial effects of liraglutide on peripheral blood vessels

Korisni efekti liraglutida na periferne krvne sudove

Xueyang Zhang*, Yongbo Wang*, Simengge Yang†, Junwei Zong†, Xuejiao Wang*, Ran Bai*

The First Affiliated Hospital of Dalian Medical University, *Department of Endocrinology, †Department of Orthopedics, Dalian, Liaoning, PR China

Abstract

Background/Aim. Macroangiopathy is the major cause of death and disability in type 2 diabetic patients. Studies have shown that liraglutide, a glucagon-like peptide 1 (GLP-1) receptor agonist, can protect cardiovascular system by inhibiting chronic inflammation of diabetes. However, a study about the effects of liraglutide on peripheral blood vessels and peripheral blood leukocytes has not been reported yet. The aim of this study was to determine vasculoprotective effect, vascular protection and mechanism of action of liraglutide in addition to its hypoglycemic effect. **Methods.** A total of 60 hospitalized patients with type 2 diabetes were recruited from December 2013 to December 2014 at the First Affiliated Hospital of Dalian Medical University, PR China. Before the treatment with liraglutide, height and weight were measured to calculate body mass index (BMI). Blood urea nitrogen (BUN) and so on were detected. Homeostasis model assessment of insulin resistance (HOMA-IR) and islet β cell function (HOMA- β) were computed. After applying liraglutide for three months, all indexes were measured again. The effects of liraglutide on these indexes were analyzed by paired sample *t*-test. **Results.** After the treatment with liraglutide, values of glycosylated hemoglobin –

HbA1c (8.46 ± 1.62 vs. $7.26 \pm 1.40\%$) and 2h postprandial blood glucose – 2hPBG (11.95 vs. 9.6 mmol/L) decreased significantly ($p < 0.05$). Body weight (87.3 vs. 82.5 kg) and BMI (30.37 vs. 28.63 kg/m²) decreased by 5.5% and 5.7%, respectively ($p < 0.05$). Also, levels of triglycerides (TG) (2.57 ± 1.54 vs. 1.81 ± 0.70 mmol/L) and LDL-cholesterol (2.92 ± 0.78 vs. 1.89 ± 0.66 mmol/L) reduced significantly ($p < 0.05$). Ankle-brachial index (ABI) decreased from 1.24 ± 0.10 to 1.14 ± 0.06 cm/s by 8%, while brachial-ankle pulse wave velocity (ba-PWV) decreased from $1,442.15 \pm 196.26$ to $1,316.85 \pm 146.63$ cm/s by 8.7%, and both differences were statistically significant ($p < 0.001$). **Conclusion.** Liraglutide, with a good hypoglycemic effect, can significantly reduce postprandial blood glucose and HbA1c, but cannot significantly improve fasting plasma glucose, insulin resistance and islet β cell function. It also considerably decreased body weight, BMI and TG. Liraglutide can significantly lower ba-PWV and ABI to protect peripheral blood vessels.

Key words:

ankle-brachial index; arterioles; blood vessels; body mass, index; capillaries; diabetes mellitus, type 2; leukocytes; lipids; liraglutide; venules.

Apstrakt

Uvod/Cilj. Makroangiopatija je glavni uzrok smrti i invalidnosti kod bolesnika sa dijabetesom tipa 2. Studije su pokazale da liraglutid, agonist *glucagon-like peptide 1* (GLP-1) receptora, može zaštititi kardiovaskularni sistem inhibicijom hroničnog zapaljenja prouzrokovanog dijabetesom. Međutim, efekti liraglutida na periferne krvne sudove i leukocite u perifernoj krvi nisu opisani do sada. Cilj ovog rada bio je da se, pored hipoglikemijskog dejstva liraglutida, ispita i njegov vaskuloprotektivni efekat, kao i mehanizam tog dejstva. **Metode.** U studiju je bilo uključeno 60 bolesnika sa dijabetesom tipa 2 hospitalizovanih od decembra 2013. do decembra 2014. godine u Prvoj bolnici Medicinskog univerziteta Dalian iz Kine. Pre početka terapije liraglutidom, svim bolesnicima su izmerene visina i telesna masa da bi se izračunao indeks telesne mase (ITM). Takođe, određene su i vrednosti uree u krvi (BUN) i drugi biohemijski parametri.

Izračunate su vrednosti HOMA-IR (*Homeostasis model assessment of insulin resistance*) i HOMA- β (*Homeostasis model assessment of islet β cell function*) indeksa. Posle tri meseca primene liraglutida, ponovo su određeni svi indeksi. Efekti liraglutida na te indekse analizirani su *t*-testom zavisnih uzoraka. **Rezultati.** Posle tromesečnog lečenja liraglutidom, vrednosti glikoziliranog hemoglobina A1c – HbA1c ($8,46 \pm 1,62\%$ vs. $7,26 \pm 1,40\%$) i nivoa glukoze u krvi 2 časa posle obroka (2hPBG) ($11,95$ mmol/L vs. $9,6$ mmol/L) značajno su se smanjili ($p < 0,05$). Telesna masa ($87,3$ kg vs. $82,5$ kg) i ITM ($30,37$ kg/m² vs. $28,63$ kg/m²) smanjili su se 5,5%, odnosno 5,7% ($p < 0,05$). Nivoi triglicerida ($2,57 \pm 1,54$ mmol/L vs. $1,81 \pm 0,70$ mmol/L) i LDL-holesterola ($2,92 \pm 0,78$ mmol/L vs. $1,89 \pm 0,66$ mmol/L) takođe su se značajno smanjili ($p < 0,05$). *Ankle-brachial index* (ABI) smanjio se sa $1,24 \pm 0,10$ cm/s na $1,14 \pm 0,06$ cm/s ili za 8%, a *brachial-ankle pulse wave velocity* (ba-PWV) sa $1\,442,15 \pm 196,26$ cm/s na $1\,316,85 \pm 146,63$ cm/s ili za 8,7%, što je u oba slučaja

bilo statistički značajno smanjenje ($p < 0,001$). **Zaključak.** Liraglutid, sa dobrim hipoglikemijskim efektom, može značajno smanjiti nivo glukoze u krvi nakon obroka i vrednost HbA1c, ali ne utiče značajno na nivo glukoze u plazmi natašte, insulinsku rezistenciju i funkciju β ćelija Langerhansovih ostrvaca pankreasa. Takođe, lek značajno smanjuje telesnu masu, ITM i nivo triglicerida kao i vred-

nosti ba-PWV i ABI, pokazatelje zaštite perifernih krvnih sudova.

Ključne reči:

brahijalni indeks gležnja; arteriole; krvni sudovi; telesna masa, indeks; kapilari; diabetes mellitus, tip 2; leukociti; lipidi; liraglutid; venule.

Introduction

The China Chronic Diseases and Risk Factors Surveillance in 2013 showed that the prevalence of diabetes mellitus (DM) in people aged 18 or older was 10.4%¹. DM is an independent risk factor for cardiovascular and cerebrovascular diseases². The key to the treatment of type 2 DM (T2DM) is long-term stable control of blood glucose to prevent or delay the occurrence and development of chronic complications of diabetes. Epidemiological studies have found that T2DM patients have a 2–4 times higher risk of developing myocardial infarction and stroke than normal people have^{3,4}. The prevention and treatment of diabetic macroangiopathy should be based on the control of blood sugar, blood pressure, blood lipids, body weight and other factors. The deposition of advanced glycosylation end products caused by persistent hyperglycemia, insulin resistance, hypertension and hyperlipidemia lead to an increase in oxidative stress, promotion of aggregation of blood mononuclear macrophages, and release of proinflammatory cytokines, that further damage vascular endothelium leading to atherosclerosis^{5,6}.

Glucagon-like peptide 1 (GLP-1) receptor agonists are a newer generation of hypoglycemic drugs. In addition to controlling blood sugar, they have good effects on reducing body weight, improving insulin resistance, treating fatty liver and protecting cardiovascular system^{7–9}. Liraglutide is a glucagon-like peptide 1 (GLP-1) analogue produced by yeast using genetic recombination¹⁰. In the Liraglutide Effect and Action in Diabetes: Evaluation of cardiovascular outcome Results (LEADER) study, liraglutide was confirmed to have the effects of lowering blood sugar and glycosylated hemoglobin (HbA1c), improving insulin resistance, protecting islet function, decreasing blood lipids and body weight, and reducing vasoconstriction pressure^{11–18}. Liraglutide has been shown to protect cardiovascular function at both cellular models and animal models¹⁹. Liraglutide has also been proven to reduce cardiovascular events in diabetic patients during clinical trials and to protect cardiovascular system by managing cardiovascular risk factors²⁰.

Atherosclerosis is a systemic disease, which often involves multiple blood vessels such as carotid arteries, lower extremity arteries, and renal arteries in addition to coronary arteries and cerebral arteries²¹. Because the carotid and lower extremity arteries are superficial and easy to examine, they are often considered to be the windows of systemic atherosclerotic disease. Epidemiological investigations have shown that peripheral arteriosclerotic diseases seriously affect the prognosis of other cardiovascular and cerebrovascular diseases. With the advancement of inspection techniques, high-sensitivity nonin-

vasive vascular examinations have been used in clinical practice. Pulse wave velocity (PWV) and ankle-brachial index (ABI) are two important evaluation indicators in these examinations. As an indicator of arterial stiffness, PWV can independently predict the risk of cardiovascular and cerebrovascular disease development and death²². ABI can be used for an early diagnosis of lower extremity obstructive disease²³. These two examinations can evaluate vascular arteriosclerosis from both function and structure of the blood vessels. Arteriosclerosis often changes vascular function first and then it changes vascular structure. Increased PWV can occur in a variety of diseases associated with atherosclerosis, such as DM, high blood pressure, dyslipidemia and severe kidney disease. Depending on selected arteries, PWV can be divided into carotid-femoral PWV, carotid-radial PWV, carotid-brachial PWV, and brachial-ankle PWV (ba-PWV). The study found that ba-PWV was a better predictor of T2DM macrovascular complications than carotid PWV²⁴. Ba-PWV of more than 1,400 cm/s usually suggests an increase in vascular stiffness. ABI is the ratio of systolic pressure of the ankle to systolic pressure of the arm, which reflects the degree of the openness of peripheral blood vessels. The normal value of ABI is 0.9–1.3. ABI of more than 0.9 often indicates peripheral obstructive vascular disease, while ABI that is less than 1.3 often points out arterial calcification and weakened vasoconstriction. A systematic retrospective study manifested that ABI could be used to predict the occurrence of cardiovascular diseases²⁵.

Inflammation and insulin resistance are thought to be the basis of atherosclerosis in T2DM²⁶. Studies have shown that increased white blood cells can worsen insulin sensitivity and predict the development of DM²⁷. Mononuclear cells in blood infiltrate into the intima and differentiate into macrophages. Infiltrating macrophages phagocytose oxidatively modified low-density lipoproteins and gradually get transformed into foam cells. This leads to the development of atherosclerosis. Adherence of mononuclear cells to vascular endothelial cells is considered to be one of the earliest events in the complex mechanism of atherosclerosis²⁸. Inflammatory mediators associated with the pathogenesis include interleukin 6 (IL-6), C-reactive protein (CRP), and tumor necrosis factor alpha (TNF- α). CRP is an inflammatory factor in the development and progression of atherosclerosis. Any high concentration of CRP is closely related to the occurrence of cardiovascular diseases. CRP can increase the expression of cell adhesion molecules and monocyte chemoattractant protein 1 (MCP-1), promote the production of matrix metalloproteinase 1 (MMP-1), activate the complement system to promote the production of arteriosclerosis, and reduce the expression of nitric oxide synthetase mRNA and bioactive activity of nitric oxide in endothelium²⁹.

Methods

Patients

The study included T2DM patients with poor glycemic control admitted to the Department of Endocrinology at the First Affiliated Hospital of Dalian Medical University from December 2013 to December 2014, aged between 18 and 70 years, with fasting C-peptide (FCP) > 1 ng/mL, HbA1c 7–11%. The T2DM diagnosis meets the diagnostic and classification criteria approved by the World Health Organization (WHO) in 1999.

Those patients who met any of the following criteria were excluded from the study: severe renal dysfunction, creatinine clearance (CCR) < 60 mL/min; abnormal liver function, alanine aminotransferase (ALT) or aspartate aminotransferase (AST) > 120 U/L combined with severe acute complications of DM and stress; infection and malignancy; severe history of cardiovascular and cerebrovascular disease in previous 3 months; pregnancy, preparing pregnancy and lactation period in women; various diseases with a significant effect on blood sugar; using drugs other than hypoglycemic drugs that affect blood sugar, such as hormones; a history of pancreatitis and a history or family history of medullary thyroid carcinoma.

Exit criteria were as follows: violation of inclusion criteria or compliance with exclusion criteria; serious adverse drug reactions; drug allergic reactions; loss of patients during follow-up.

Experimental drugs and administration methods

Liraglutide (6 mg/mL), produced by Danish Novo Nordisk, is subcutaneously injected once a day. The drug can be injected at any time without depending on meal time. The patients were recommended to get injections at the same time every day when it was the most convenient for them.

Those patients who met the inclusion criteria were given diabetic education and informed about the role and possible side effects of liraglutide. They filled in the informed consent form and were adjusted to the treatment plan.

General information

Age, sex and medical history of the enrolled patients were recorded in detail. Height and body weight were measured according to standard protocols to calculate body mass index (BMI) for each patient.

The patients were taken blood from in the early morning after 12 hours of overnight fasting. An automated biochemical analyzer measured urea nitrogen (BUN), creatinine (Cr), glycosylated hemoglobin A1c (HbA1c), fasting venous blood glucose (FPG), fasting C-peptide (FCP), alanine aminotransferase (ALT), aspartate aminotransferase (AST), white blood cells (WBC), monocytes (M), total cholesterol (TC), triglycerides (TG), high-density lipoprotein cholesterol (HDL-C), low-density lipoprotein cholesterol (LDL-C), and

CRP. Fingertip 2h postprandial blood glucose (2hPBG) was measured by the Roche blood glucose meter.

Parameter calculation formula

Parameter calculation formulas were as follows:

$CCR = [(140 - \text{age}) \times \text{body weight (kg)}] / 0.818 \times Cr$ ($\mu\text{mol/L}$); homeostasis model assessment of insulin resistance ($HOMA-IR$) = $1.5 + FPG$ (mmol/L) \times FCP (pmol/L) / 2,800; homeostasis model assessment of islet β cell function ($HOMA-\beta$) = $0.27 \times FCP$ (pmol/L) / [FPG (pmol/L) - 3.5]; BMI = body weight (kg) / height² (m²).

Experiment process

The temperature of the examination room was kept at 22–25 °C, and the other parameters were taken 5 minutes before the measurement. The patients took off their heavy clothing and removed the socks to reveal the heel. They were lying in the supine position on the bed, with the upper arm and ankle strapped for the electrocardiography (ECG) clip and heart sound map sensor. Heart sound map, heart rate value, left arm blood pressure, left arm pulse wave, right arm blood pressure value, right arm pulse wave, left ankle blood pressure value, left ankle pulse wave, right ankle blood pressure value, and right ankle pulse wave data were collected. The process allowed the acquisition to be completed, so the instrument automatically calculated ba-PWV and ABI after the cuffs were filled and deflated twice.

The enrolled patients recorded general information in detail and signed informed consent on the day of their admission. They were measured according to the above given indicators and the next day for noninvasive peripheral blood vessel testing. The starting dose of liraglutide was 0.6 mg once a day for subcutaneous injecting, and the patients were observed for adverse drug reactions. If there was no obvious adverse reaction after 3–7 days, the dose was increased to 1.2 mg once daily. If there was a significant gastrointestinal reaction after the drug addition, the dose could be reduced back to 0.6 mg/day, and the dose was increased after the low-dose administration time was extended. The dose was increased to 1.8 mg/day from 1.2 mg/day after a week for the patients with poor hypoglycemic effect.

Statistical analysis

The normality of continuous variables was verified by S-K test. Variables that conform to normal distribution are expressed as mean \pm standard deviation (SD) and the difference between the before and after liraglutide treatment was analyzed by the paired *t*-test. The non-normal distribution variables were expressed by quartile, and the differences were compared by the nonparametric Wilcoxon test. Significant variables screened by univariate analysis were further analyzed by multiple regression analysis to prove independent factors. SPSS 25.0 software was used for statistical analysis. A double-tailed *p*-value less than 0.05 was considered statistically significant.

Results

In this study, 64 patients with type T2DM were initially enrolled. Four of them dropped out during the follow-up, so 60 patients were finally enrolled (Table 1). Among them, there were 31 males and 29 females. They were 46.85 ± 7.60 years old, with the disease history of 8 (3–10) years. Twenty one of them had complications and 10 had chronic complications of DM. Noninvasive angiography was performed in 13 cases. After the use of liraglutide, the patients had adverse reactions such as nausea and loss of appetite in varying degrees, but they were tolerable. Later on, the patients' nausea and other discomfort gradually disappeared. No patients were withdrawn because of severe gastrointestinal reactions. There were no allergies at the injection sites. One patient had a marked hypoglycemia due to liraglutide, but it was tackled after a prompt symptomatic treatment.

It can be concluded that liraglutide can considerably reduce body weight and BMI.

TG decreased from 2.57 ± 1.54 mmol/L to 1.81 ± 0.70 mmol/L with the decrease of 29.6%. LDL-C decreased by 35.3% from 2.92 ± 0.78 mmol/L to 1.89 ± 0.66 mmol/L and both differences were statistically noteworthy ($p < 0.001$). TC and HDL-C decreased by 12% and 4.8%, respectively, yet without any significant difference ($p > 0.05$), suggesting that liraglutide may effectively bring down the levels of TG and LDL-C.

After the liraglutide treatment, M, CRP and WBC all decreased in varying degrees, but the differences were not statistically relevant.

ABI and ba-PWV are important indexes reflecting the level of peripheral vascular stiffness. Three months after the treatment, ABI decreased from 1.24 ± 0.10 cm/s to 1.14 ± 0.06 cm/s by 8%, while ba-PWV decreased from $1,442.15 \pm 196.26$ cm/s

Table 1

Baseline data for the patients		
Parameter	mean \pm SD/quartile	(minimum, maximum)
Gender (M/F), n	31/29	
Age Δ (years)	46.85 ± 7.60	(32, 66)
History $\#$ (years)	8 (3~10)	(0.038, 17)
Biochemistry analysis		
ALT Δ (U/L)	39.42 ± 18.93	(7, 95)
AST $\#$ (U/L)	21 (17, 31)	(9, 64)
Urea $\#$ (μ mol/L)	5.69 (5.21~6.51)	(3.34, 8.85)
Cr Δ (μ mol/L)	60.22 ± 13.26	(32, 98)
CCR Δ (mL/min)	178.46 ± 48.34	(81.11, 319.53)
Comorbidity, n	21	-
Chronic complications, n	10	-
Side effects, n		
gastric reaction	25	-
hypoglycemia	1	-
allergic reactions	0	-

Δ Variables are shown as mean \pm standard deviation (SD) if the variable was conformed to normal distribution by S-K test; $\#$ Variables are shown as quartile 50% (25%~75%) if the variable was not conformed to normal distribution by S-K test; M – male; F – female; ALT – alanine aminotransferase; AST – aspartat aminotransferase; Cr – creatinine; CCR – creatinine clearance.

The data about diabetic blood lipid inflammation and vascular measurements in patients before and after liraglutide administration are given in Table 2.

After the 3-month treatment with liraglutide, the levels of HbA1c and 2hPBG decreased significantly ($p < 0.05$), indicating the notable hypoglycemic effect of liraglutide. Although FPG and FCP decreased in varying degrees with no significant difference, HOMA-IR and HOMA- β showed no distinct difference, suggesting the insignificant effects on improving insulin resistance and islet function.

Body weight decreased by 5.5% from 87.3 (80–101) kg to 82.5 (76–93) kg, while BMI decreased by 5.7% from 30.37 (29.43 – 31.83) kg/m² to 28.63 (27.78 – 30.80) kg/m², and both differences were statistically significant ($p < 0.001$).

to $1,316.85 \pm 146.63$ cm/s by 8.7%, thus revealing that liraglutide may improve peripheral vascular stiffness effectively.

Multivariate regression analysis for ba-PWV is shown in Table 3.

Multiple regression analysis showed that increment of ABI – in-ABI (increment = difference between values of a variable: 3rd month vs. baseline), in-HbA1c and in-TG were independent risk factors for in-ba-PWV. The contributions to ba-PWV are in-ABI, in-HbA1c and in-TG in turn. According to the correlation coefficient, the following regression equation is constituted:

$$\text{in-ba-PWV} = 40.975 + 524.447 \times \text{in-ABI} + 16.287 \times \text{in-HbA1c} + 18.79 \times \text{in-TG}$$

Table 2

**Comparing diabetic, blood lipid, inflammatory and vascular stiffness data
in patients before and after liraglutide administration**

	Baseline	3rd month	<i>t</i>	<i>p</i>
HbA1c ^Δ (%)	8.46 ± 1.62	7.26 ± 1.40	5.234**	< 0.001
FPG [#] (mmol/L)	8.3 (7.24~8.84)	7.46 (6.52~8.67)	-1.612	0.107
2hPBG [#] (mmol/L)	11.95 (10.15~13.4)	9.6 (8.425~11.05)	-5.913**	< 0.001
FCP ^Δ (ng/mL)	3.24 ± 1.37	3.05 ± 0.77	1.198	0.236
HOMA-IR ^Δ	4.60 ± 1.39	4.25 ± 0.87	1.813	0.075
HOMA-β ^Δ	62.47 ± 33.02	69.78 ± 39.09	-1.711	0.092
BW [#] (kg)	87.3 (80~101)	82.5 (76~93)	-5.974**	< 0.001
BMI [#] (kg/m ²)	30.37 (29.43~31.83)	28.63 (27.78~30.80)	-5.865**	< 0.001
TC [#] (mmol/L)	5.09 (4.03~5.67)	4.48 (3.74~5.36)	-1.612	0.107
TG ^Δ (mmol/L)	2.57 ± 1.54	1.81 ± 0.70	4.083**	< 0.001
LDL-C ^Δ (mmol/L)	2.92 ± 0.78	1.89 ± 0.66	18.936**	< 0.001
HDL-C ^Δ (mmol/L)	1.24 ± 0.24	1.18 ± 0.24	1.614	0.112
M [#] (× 10 ⁹ /L)	0.43 (0.38~0.55)	0.43 (0.34~0.54)	-1.937	0.053
WBC ^Δ (× 10 ⁹ /L)	7.03 ± 1.32	6.88 ± 1.39	0.615	0.541
CRP ^Δ (mg/dL)	5.38 ± 2.45	5.16 ± 2.45	1.863	0.067
ABI ^Δ (cm/s)	1.24 ± 0.10	1.14 ± 0.06	7.941**	< 0.001
ba-PWV ^Δ (cm/s)	1,442.15 ± 196.26	1,316.85 ± 146.63	8.599**	< 0.001

HbA1c – glycosylated hemoglobin; **FPG** – fasting venous blood glucose; **PBG** – postprandial blood glucose; **FCP** –fasting C-peptides; **HOMA-IR** – homeostasis model assessment of insulin resistance; **HOMA-β** – homeostasis model assessment of β cell function; **BW** – body weight; **BMI** – body mass index; **TC** – total cholesterol; **TG** – triglycerides; **LDL-C** – low-density lipoprotein cholesterol; **HDL-C** – high-density lipoprotein cholesterol; **M** – monocytes; **WBC** – white blood cells; **CRP** – C-reactive protein; **ABI** – ankle-brachial index; **ba-PWV** – brachial-ankle pulse wave velocity.

Δ Variables are shown as mean ± standard deviation (SD) and paired *t*-test was carried out if the variable was conformed to normal distribution by S-K test; **#** Variables are shown as quartile 50% (25%~75%) and paired nonparametric Wilcoxon test was carried out if the variable was not conformed to normal distribution by S-K test; * *p* < 0.05; ** *p* < 0.001.

Table 3

Multivariate Regression Analysis for increment of ba-PWV (3rd month vs. baseline)

Parameter	Unstandardized		Standardized β	<i>t</i>	<i>p</i>	Collinearity	
	β	SD				tolerance	VIF
Constant	40.975	22.014		1.861	0.068		
in-ABI (cm/s)	524.447	141.401	0.437	3.709	< 0.001	0.919	1.088
in-HbA1c (%)	16.287	7.227	0.256	2.254	0.028	0.986	1.015
in-TG (mmol/L)	18.790	9.181	0.240	2.047	0.045	0.929	1.076

ABI – ankle-brachial index; **HbA1c** – glycosylated hemoglobin; **TG** – triglycerides; **SD** – standard deviation; **In** – increment (difference between values of a variable: 3rd month vs. baseline); **VIF** – variance inflation factor.

Discussion

Macroangiopathy is one of serious complications of T2DM. Prevention of the occurrence and development of macroangiopathy requires comprehensive control. Therefore, new hypoglycemic drugs are particularly important for the role of diabetic macroangiopathy. This study observed 60 cases, including 13 cases of noninvasive vascular examination. The comparison between the before and after use of liraglutide showed that liraglutide could not only effectively reduce postprandial blood glucose, HbA1c, body weight, BMI, TG, but it could also reduce ba-PWV and ABI.

HbA1c guides diabetes treatment, shows blood sugar control levels, adjusts hypoglycemic regimens, influences the quality of care and predicts diabetes complications. Foreign studies have shown that HbA1c was closely related to diabetes complicated by cardiovascular and cerebrovascular diseases³⁰. The UK Prospective Diabetes Study (UKPDS) confirmed that for every 1% decrease in HbA1c, the risk of any endpoint associated with DM was reduced by 21% and the risk of developing myocardial infarction was reduced by 18%. In Chinese Type 2 Diabetes Guidelines (2017), HbA1c control targets should be < 6.5% for patients with T2DM who have a shorter course, no complications and a longer life expectancy without a cardiovascular disease. In this research,

HbA1c decreased significantly from $8.46 \pm 1.62\%$ to $7.26 \pm 1.40\%$, which was consistent with the results of the LEADER studies. The LEADER series of studies showed that liraglutide significantly reduced HbA1c in patients with T2DM and was superior to glimepiride and rosiglitazone^{13–18}. However, the average level of HbA1c in some patients in this study still did not meet the standard (HbA1c $< 7\%$) considering the higher levels of HbA1c before the application of liraglutide, the shorter follow-up time, and the smaller dose of liraglutide. 2hPBG decreased significantly from 11.94 ± 3.17 mmol/L before the treatment to 9.63 ± 1.53 mmol/L ($p < 0.05$) 3 month later, but there was no significant difference between the before and after FPG ($p > 0.05$), suggesting that liraglutide can effectively reduce postprandial blood glucose, but it can only limitedly control fasting blood glucose. GLP-1 receptor agonists cause the hypoglycemic effect by delaying gastric emptying, promoting insulin secretion, inhibiting glucagon and somatostatin secretion, so this drug has an advantage in controlling postprandial blood glucose^{31,32}.

Progressive failure of islet function and insulin resistance is considered to be the main pathological basis of T2DM. Long-term hyperglycemia and insulin resistance can cause atherosclerosis caused by the damage of vascular endothelium. Insulin resistance index can be expressed by HOMA-IR. It is generally believed that HOMA-IR increases with the increase of insulin resistance. HOMA-IR is a HOMA-IR formula fitted with C-peptide. Studies have confirmed that this formula could also be used to assess an individual's insulin resistance³³. HOMA-IR and HOMA- β were calculated using this formula in our study. HOMA-IR and FCP decreased, while HOMA- β increased, but there was no statistical significance ($p > 0.05$). These results were different from other studies. The LEADER-2 study showed that islet function was assessed by the ratio of proinsulin to insulin, and liraglutide improved islet beta cell function compared to glimepiride¹⁵. In the LEADER-3 study, HOMA-IR evaluated insulin resistance, and liraglutide significantly improved insulin resistance in comparison with glimepiride¹⁴. The LEADER-4 studies have shown that liraglutide significantly increased islet function if compared with gliclazide, on the basis of HOME- β and proinsulin-to-insulin ratios evaluating islet beta cells function¹⁶. Moreover, liraglutide had the effect of reducing body weight, and the decrease in body weight also indirectly improved insulin resistance. In this study, the negative results of liraglutide for insulin resistance and islet function improvement might be related to fewer cases and shorter observation time.

T2DM is often accompanied by obesity. DM accompanied by obesity increases the risk of cardiovascular diseases. Current hypoglycemic drugs (such as insulin, sulfonylureas, thiazolidinediones) can cause an increase in body weight and GLP-1 receptor agonists inhibit food intake by directly acting on the hypothalamus. Weight loss is achieved by inhibiting gastric emptying through the autonomic nervous system. Liraglutide was confirmed not to increase body weight in phase II clinical trial and showed a

weight-reducing effect in phase III clinical trial. Liraglutide 1.8 mg/day, individually or in combination with other hypoglycemic agents, had a significant weight-reducing effect in the LEADER-1 to 5 series of studies^{12–17}. It was found that liraglutide could reduce visceral fat by using computed tomography to analyze body composition in the LEADER-2 and LEADER-3 studies. Body weight decreased significantly from 87.3 (80–101) kg to 82.5 (76–93) kg and BMI decreased significantly from 30.37 (29.43–31.83) kg/m² to 28.63 (27.78–30.80) kg/m² ($p < 0.05$) in this study, which again confirmed that liraglutide could reduce patients' body weight and BMI. Liraglutide was confirmed to have the effect on reducing visceral fat in another study conducted in parallel with this.

Blood lipids are one of cardiovascular risk factors, including TC, TG, HDL-C, LDL-C and free fatty acids (FFAs). GLP-1 receptor agonists can directly act, inhibit gastric emptying, promote insulin secretion and increase the clearance of chylomicrons, and promote and enhance intestinal lipoprotein catabolism. Liraglutide reduces the levels of TC, LDL-C, TG, HDL-C and FFAs in the LEADER-4 study^{13–14}. In this study, TG and LDL-C decreased significantly after the treatment with liraglutide, while there was no significant difference between TC and HDL-C that decreased after using liraglutide.

T2DM is often accompanied by systemic complications that show no early symptoms and are difficult to detect through symptoms. Early diagnosis, early intervention and prevention of progression of diabetes complications are particularly important in the management of DM. Diabetic macroangiopathy is the leading cause of death and disability in T2DM, so it is necessary to establish an early diagnosis of macroangiopathy. Arteriosclerosis is the main pathophysiological basis of diabetic macroangiopathy. Arterial stiffness is related to arteriosclerosis and can be used to predict cardiovascular and cerebrovascular diseases. ABI and ba-PWV are indicators of atherosclerosis. Ba-PWV is a vascular functional test for the detection of early atherosclerosis. ABI is a structural examination of blood vessels that can be used to understand the openness of blood vessels in the lower extremities and whether there is occlusion. A large number of clinical trials have demonstrated that liraglutide can reduce the occurrence of cardiovascular adverse events and protect cardiovascular function. However, the impact of liraglutide on peripheral blood vessels has not been reported yet. In this study, the effects of liraglutide on ba-PWV were statistically significant ($p < 0.05$), indicating that liraglutide reduced peripheral vascular stiffness and protected peripheral blood vessels. ABI > 1.3 suggests vascular calcification and reduced vasoconstriction, while ABI < 0.9 indicates arterial stenosis. In this group study, ABI declined significantly from 1.24 ± 0.10 cm/s to 1.14 ± 0.06 cm/s after the drug administration, which suggested the vasoconstriction was better than before the treatment. The decrease of ABI value also predicted the improvement of arteriosclerosis by liraglutide treatment.

The mechanism of liraglutide in improving arteriosclerosis in patients with T2DM is not fully understood and

may be the result of a combination of inhibition of inflammation and non-inflammation. Noyan-Ashraf et al.³⁴ fed C57BI6 mice for 32 weeks on a high-fat diet (45% of calories from fat) and a normal diet, and randomly divided the two groups into two subsegments during the last week of feeding. In the subgroups, liraglutide (30 µg/kg, 2 times/day) and placebo were injected respectively³⁴. It was found that high-fat diet induced an increase in serum TNF-α, while treatment with liraglutide for 1 week was effective in reducing high-fat diet-induced elevation of TNF-α. It was detected that liraglutide could reduce expression of intercellular adhesion molecule 1 (ICAM-1) and vascular cell adhesion molecule 1 (VCAM-1) in culture of human vascular endothelial cells *in vitro*³⁵. In human umbilical vein endothelial cells (HUVEC) cultured *in vitro*, it was discovered that liraglutide intervention induced the synthesis of nitric oxide (NO), and the concentration of NO increased in a dose-dependent manner with liraglutide. At the same time, it was observed that 1 µg/mL liraglutide could enhance the activity of endothelial nitric oxide synthase (eNOS) and restore the expression of eNOS at mRNA level induced by cytokines. The studies in human umbilical vein endothelial cells (HCAEC) have also unearthed that liraglutide could increase eNOS phosphorylation and NO production by activating the AMP-activated protein kinase (AMPK) pathway³⁵. Torres et al.³⁶ have confirmed that liraglutide could increase the release of calcium ions from endoplasmic network in vascular smooth muscle cells and increase mitochondrial calcium ion uptake through mitochondrial fusion protein-2, a key factor in mitochondrial-endoplasmic reticulum coupling, to enhance mitochondrial activity. Liraglutide can reduce endoplasmic reticulum stress induced by high glucose in HUVEC and also inhibit the expression of p53 up-regulated modulator of apoptosis. Liraglutide can prevent endoplasmic reticulum-dependent apoptosis of vascular endothelial cells through mitochondrial modulation.

The concept that atherosclerosis is an immune-mediated inflammatory lesion has been widely accepted. In this study, inflammatory related indicators, such as WBC, M and CRP, were detected in the vascular protection mechanism. Increased peripheral blood leukocytes can be used to predict the development of DM. M and macrophages are prototype cells of innate immune system and they are present in various stages of atherosclerosis. Studies on apoE-deficient mice have revealed that liraglutide significantly reduced the area of aortic atherosclerosis by inhibiting M/macrophage aggregation and reducing foam cell formation to prevent the occurrence of atherosclerosis³⁷. The clinical study of liraglutide on peripheral blood leukocytes and M has not been reported yet. Since the aim of this research was to discuss the effects of liraglutide on WBC and M in peripheral blood vessels so as to explore the possible mechanism of liraglutide on vascular protection, the analysis of WBC and M before and after the treatment showed

that WBC dropped from $7.03 \pm 1.32 \times 10^9/L$ to $6.88 \pm 1.39 \times 10^9/L$, and M went down from $0.43 (0.38-0.55) \times 10^9/L$ to $0.43 (0.34-0.54) \times 10^9/L$, but the differences were not statistically significant. Therefore, the examination of the impact of liraglutide on WBC and M in peripheral blood vessels may require a larger sample size and longer follow-up studies. CRP is an important marker of inflammation and studies have shown that GLP-1 receptor agonists can reduce the inflammatory response in diabetic patients and reduce the level of CRP in the body. This study found that there was no significant difference in CRP before and after the treatment with liraglutide, which was also inconsistent with the results of other studies. Van Raalte et al.³⁸ divided 69 T2DM patients with poor glycaemic control treated by metformin into two groups, each of those receiving exenatide and insulin glargine respectively for 1 and 3 years. The results of the study showed that exenatide reduced significantly serum high-sensitivity CRP when compared with glargine. A meta-analysis also suggested that liraglutide significantly reduced serum CRP levels³⁹. The negative results of CRP in this study may be related to fewer cases and large dispersion before the treatment. Hence, the effect of liraglutide on chronic inflammation in T2DM patients still requires further large-scale studies.

There were three limitations in this study. Firstly, the sample size included in this study was rather small. Secondly, no control group was used for comparative study results. Thirdly, follow-up time was short.

Conclusion

This study provides a new clinical basis for the beneficial effects of liraglutide on peripheral blood vessels. Liraglutide protects peripheral blood vessels in addition to its lowering blood sugar, reducing body weight and lowering blood lipids. Therefore, the results of this study may be the most beneficial to the treatment of patients with diabetic macroangiopathy or risk factors for diabetic macroangiopathy.

Liraglutide, with a good hypoglycemic effect, can significantly reduce postprandial blood glucose and HbA1c, but cannot considerably improve fasting plasma glucose, insulin resistance and islet function. It also significantly decreased body weight, BMI and TG. Liraglutide can significantly lower ba-PWV and ABI to protect peripheral blood vessels, but its effects on peripheral blood leukocytes, M and CRP need further research that may benefit from expanding the sample size and prolonging the treatment time.

Acknowledgement

This study was supported by the National Science Foundation of Liaoning Province of PR China (No. 2015020310).

R E F E R E N C E S

1. Wang L, Gao P, Zhang M, Huang Z, Zhang D, Deng Q, et al. Prevalence and ethnic pattern of diabetes and prediabetes in China in 2013. *JAMA* 2017; 317(24): 2515–23.
2. Gerstein HC, Colhoun HM, Dagenais GR, Diaz R, Lakshmanan M, Pais P, et al. Dulaglutide and renal outcomes in type 2 diabetes: an exploratory analysis of the REWIND randomised, placebo-controlled trial. *Lancet* 2019; 394(10193): 131–8.
3. Nakamura J, Kamiya H, Haneda M, Inagaki N, Tanizawa Y, Araki E, et al. Causes of death in Japanese patients with diabetes based on the results of a survey of 45,708 cases during 2001–2010: Report of the Committee on Causes of Death in Diabetes Mellitus. *J Diabetes Investig* 2017; 8(3): 397–410.
4. Ceriello A, Gavin JR 3rd, Boulton AJM, Blickstead R, McGill M, Raz I, et al. The Berlin Declaration: call to action to improve early actions related to type 2 diabetes. How can specialist care help? *Diabetes Res Clin Pract* 2018; 139: 392–9.
5. Kattoor AJ, Pothineni NVK, Palagiri D, Mehta JL. Oxidative stress in atherosclerosis. *Curr Atheroscler Rep* 2017; 19(11): 42.
6. Rehman K, Akash MSH. Mechanism of generation of oxidative stress and pathophysiology of type 2 diabetes mellitus: how are they interlinked? *J Cell Biochem* 2017; 118(11): 3577–85.
7. Thomas MC. The potential and pitfalls of GLP-1 receptor agonists for renal protection in type 2 diabetes. *Diabetes Metab* 2017; 43(Suppl 1): 2S20–2S27.
8. Scheen AJ. GLP-1 receptor agonists and heart failure in diabetes. *Diabetes Metab* 2017; 43 Suppl 1: 2S13–2S19.
9. Petit JM, Vergès B. GLP-1 receptor agonists in NAFLD. *Diabetes Metab* 2017; 43 Suppl 1: 2S28–2S33.
10. Iepsen EW, Torekov SS, Holst JJ. Liraglutide for type 2 diabetes and obesity: a 2015 update. *Expert Rev Cardiovasc Ther* 2015; 13(7): 753–67.
11. Marso SP, Daniels GH, Brown-Frandsen K, Kristensen P, Mann JF, Nauck MA, et al. Liraglutide and cardiovascular outcomes in type 2 diabetes. *N Engl J Med* 2016; 375(4): 311–22.
12. Athyros VG, Katsiki N, Tentolouris N. Editorial: Do some glucagon-like-peptide-1 receptor agonists (GLP-1 RA) reduce macrovascular complications of type 2 diabetes mellitus. A commentary on the liraglutide effect and action in diabetes: evaluation of cardiovascular outcome results (LEADER) trial. *Curr Vasc Pharmacol* 2016; 14(5): 469–73.
13. Marso SP, Poulter NR, Nissen SE, Nauck MA, Zinman B, Daniels GH, et al. Design of the liraglutide effect and action in diabetes: evaluation of cardiovascular outcome results (LEADER) trial. *Am Heart J* 2013; 166(5): 823–30.e5.
14. Steinberg WM, Nauck MA, Zinman B, Daniels GH, Bergenstal RM, Mann JF, et al. LEADER 3–lipase and amylase activity in subjects with type 2 diabetes: baseline data from over 9000 subjects in the LEADER Trial. *Pancreas* 2014; 43(8): 1223–31.
15. Daniels GH, Hegedüs L, Marso SP, Nauck MA, Zinman B, Bergenstal RM, et al. LEADER 2: baseline calcitonin in 9340 people with type 2 diabetes enrolled in the liraglutide effect and action in diabetes: evaluation of cardiovascular outcome results (LEADER) trial: preliminary observations. *Diabetes Obes Metab* 2015; 17(5): 477–86.
16. Petrie JR, Marso SP, Bain SC, Franek E, Jacob S, Masmiquel L, et al. LEADER-4: blood pressure control in patients with type 2 diabetes and high cardiovascular risk: baseline data from the LEADER randomized trial. *J Hypertens* 2016; 34(6): 1140–50.
17. Masmiquel L, Leiter LA, Vidal J, Bain S, Petrie J, Franek E, et al. LEADER 5: prevalence and cardiometabolic impact of obesity in cardiovascular high-risk patients with type 2 diabetes mellitus: baseline global data from the LEADER trial. *Cardiovasc Diabetol* 2016; 15: 29.
18. Rutten GE, Tack CJ, Pieber TR, Comlekci A, Ørsted DD, Baeres FM, et al. LEADER 7: cardiovascular risk profiles of US and European participants in the LEADER diabetes trial differ. *Diabetol Metab Syndr* 2016; 8: 37.
19. Terasaki M, Nagashima M, Hirano T. A glucagon-like peptide-1 analog liraglutide suppresses macrophage foam cell formation and atherosclerosis. *Peptides* 2014; 54: 19–26.
20. Lambadiari V, Pavlidis G, Kousathana F, Varoudi M, Vlastos D, Maratou E, et al. Effects of 6-month treatment with the glucagon like peptide-1 analogue liraglutide on arterial stiffness, left ventricular myocardial deformation and oxidative stress in subjects with newly diagnosed type 2 diabetes. *Cardiovasc Diabetol* 2018; 17(1): 8.
21. Libby P, Buring JE, Badimon L, Hansson GK, Deanfield J, Bittencourt MS, et al. Atherosclerosis. *Nat Rev Dis Primers* 2019; 5(1): 56.
22. Munakata M. Brachial-ankle pulse wave velocity in the measurement of arterial stiffness: recent evidence and clinical applications. *Curr Hypertens Rev* 2014; 10(1): 49–57.
23. Felício JS, Koury CC, Abdallah Zahalan N, de Souza Resende F, Nascimento de Lemos M, Jardim da Motta Corrêa Pinto R, et al. Ankle-brachial index and peripheral arterial disease: An evaluation including a type 2 diabetes mellitus drug-naïve patients cohort. *Diab Vasc Dis Res* 2019; 16(4): 344–50.
24. Hwang IC, Jin KN, Kim HL, Kim YN, Im MS, Lim WH, et al. Data on the clinical usefulness of brachial-ankle pulse wave velocity in patients with suspected coronary artery disease. *Data Brief* 2017; 16: 1078–82.
25. Xu L, He R, Hua X, Zhao J, Zhao J, Zeng H, et al. The value of ankle-brachial index screening for cardiovascular disease in type 2 diabetes. *Diabetes Metab Res Rev* 2019; 35(1): e3076.
26. Christen T, Trompet S, Rensen PCN, Willems van Dijk K, Lamb HJ, Jukema JW, et al. The role of inflammation in the association between overall and visceral adiposity and subclinical atherosclerosis. *Nutr Metab Cardiovasc Dis* 2019; 29(7): 728–35.
27. Karakaya S, Altay M, Kaplan Efe F, Karadağ İ, Ünsal O, Bulur O, et al. The neutrophil-lymphocyte ratio and its relationship with insulin resistance in obesity. *Turk J Med Sci* 2019; 49(1): 245–8.
28. Sanmarco LM, Eberhardt N, Ponce NE, Cano RC, Bonacci G, Aoki MP, et al. New insights into the immunobiology of mononuclear phagocytic cells and their relevance to the pathogenesis of cardiovascular diseases. *Front Immunol* 2018; 8: 1921.
29. Castro AR, Silva SO, Soares SC. The use of high sensitivity C-reactive protein in cardiovascular disease detection. *J Pharm Pharm Sci* 2018; 21(1): 496–503.
30. Kimura T, Kaneto H, Kanda-Kimura Y, Shimoda M, Kamei S, Anno T, et al. Seven-year observational study on the association between glycemic control and the new onset of macroangiopathy in Japanese subjects with type 2 diabetes. *Intern Med* 2016; 55(11): 1419–24.
31. Anderson J. The pharmacokinetic properties of glucagon-like peptide-1 receptor agonists and their mode and mechanism of action in patients with type 2 diabetes. *J Fam Pract* 2018; 67(6 suppl): S8–S13.
32. Rodbard HW. The clinical impact of GLP-1 receptor agonists in type 2 diabetes: focus on the long-acting analogs. *Diabetes Technol Ther* 2018; 20(Suppl 2): S233–41.
33. Tang Q, Li X, Song P, Xu L. Optimal cut-off values for the homeostasis model assessment of insulin resistance (HOMA-IR) and pre-diabetes screening: Developments in research and prospects for the future. *Drug Discov Ther* 2015; 9(6): 380–5.
34. Noyan-Ashraf MH, Shikata EA, Schukki I, Mukovozov I, Wu J, Li RK, et al. A glucagon-like peptide-1 analog reverses the molecular pathology and cardiac dysfunction of a mouse model of obesity. *Circulation* 2013; 127(1): 74–85.
35. Di Tomo P, Lanuti P, Di Pietro N, Baldassarre MP, Marchisio M, Pandolfi A, et al. Liraglutide mitigates TNF- α induced pro-

- atherogenic changes and microvesicle release in HUVEC from diabetic women. *Diabetes Metab Res Rev* 2017; 33(8): doi: 10.1002/dmrr.2925.
36. *Torres G, Morales PE, García-Miguel M, Norambuena-Soto I, Cartes-Saavedra B, Vidal-Peña G*, et al. Glucagon-like peptide-1 inhibits vascular smooth muscle cell dedifferentiation through mitochondrial dynamics regulation. *Biochem Pharmacol* 2016; 104: 52–61.
37. *Jojima T, Uchida K, Akimoto K, Tomotsune T, Yanagi K, Iijima T*, et al. Liraglutide, a GLP-1 receptor agonist, inhibits vascular smooth muscle cell proliferation by enhancing AMP-activated protein kinase and cell cycle regulation, and delays atherosclerosis in ApoE deficient mice. *Atherosclerosis* 2017; 261: 44–51.
38. *van Raalte DH, Bunck MC, Smits MM, Hoekstra T, Cornér A, Diamant M*, et al. Exenatide improves β -cell function up to 3 years of treatment in patients with type 2 diabetes: a randomised controlled trial. *Eur J Endocrinol* 2016; 175(4): 345–52.
39. *Mazidi M, Karimi E, Rezaie P, Ferns GA*. Treatment with GLP1 receptor agonists reduce serum CRP concentrations in patients with type 2 diabetes mellitus: A systematic review and meta-analysis of randomized controlled trials. *J Diabetes Complications* 2017; 31(7): 1237–42

Received on April 23, 2020

Revised on August 7, 2020

Accepted on August 31, 2020

Online First September, 2020



Comparative analysis of operation time and intraoperative fluoroscopy time in intramedullary and extramedullary fixation of trochanteric fractures

Uporedna analiza trajanja operacije i intraoperativne fluoroskopije kod intramedularne i ekstramedularne fiksacije trohanternih preloma

Milan M. Mitković^{*†}, Saša Milenković^{*†}, Ivan Micić^{*†}, Predrag Stojiljković^{*†},
Igor Kostić^{*}, Milorad B. Mitković[†]

^{*}Clinical Center Niš, Clinic for Orthopedics and Traumatology, Niš, Serbia; [†]University of Niš, Faculty of Medicine, Niš, Serbia

Abstract

Background/Aim. Cephalomedullary and extramedullary methods are used for the internal fixation of trochanteric fractures. The usage of the third generation Gamma Nail (GN) is a gold standard in this kind of treatments. Self-dynamisable Internal Fixator (SIF) is an extramedullary implant for trochanteric fractures' treatment. The aim of this study was to compare these two methods regarding operation time and intraoperative fluoroscopy time. **Methods.** A total of 89 patients with a surgical treatment of a trochanteric fracture were included in this study. There were two groups of patients – GN group (43 patients) and SIF group (46 patients). **Results.** Average operation times were 67.5 min (GN group) and 56.0 min (SIF group). Average intraoperative fluoroscopy times were 84.8 s (GN group) and 36.7 s (SIF group). The difference between the groups was statistically significant for both of the given parameters ($p < 0.05$). The correlation between operation time and intraoperative fluoroscopy time was confirmed in the SIF group ($p < 0.05$; $r = 0.405$),

while it was not confirmed in the GN group ($p > 0.05$). There was a higher variability in the GN method than in the SIF method regarding the duration and type of repeated surgical maneuvers followed by X-ray checks. **Conclusion.** The number of planned surgical interventions per day could depend on the type of trochanteric fracture internal fixation (intramedullary or extramedullary). Certain additional analyses including radiation dose assessment are desirable to clarify if shorter intraoperative fluoroscopy time in the SIF method can have the influence regarding intraoperative X-ray protection clothing. If there is the need to activate dynamization in long femoral axis after initial static fixation in that axis, the SIF method provides its spontaneous activation several weeks after the surgery without the need neither for additional surgery nor for additional intraoperative fluoroscopy.

Key words:

external fixators; femoral fractures; fluoroscopy; internal fixators; intraoperative period; orthopedic procedures.

Apstrakt

Uvod/Cilj. Zbrinjavanje trohanternih preloma butne kosti se najčešće vrši metodama intramedularne i ekstramedularne unutrašnje fiksacije. Primena Gama klina (GK) treće generacije, kao intramedularne metode, se smatra zlatnim standardom u ovoj oblasti. Samodinamizirajući unutrašnji fiksator (SUF) predstavlja ekstramedularni implantat koji se, između ostalog, koristi u lečenju trohanternih preloma. Cilj rada je bio da se uporede navedene metode fiksacije u pogledu dužine trajanja operacije i intraoperativne fluoroskopije. **Metode.** Studijom je bilo obuhvaćeno 89 bolesnika sa hirurški zbrinutim trohanternim prelomom. Ispitanici su bili podeljeni u dve grupe – GK grupu (43 bolesnika) i SUF grupu (46 bolesnika). **Rezultati.** Prosečno trajanje

operacije iznosilo je 67,5 min (GK grupa), odnosno 56,0 min (SUF grupa). Prosečno trajanje intraoperativne fluoroskopije iznosilo je 84,8 s (GK grupa) i 36,7 s (SUF grupa). Između grupa ispitanika je postojala značajna statistička razlika u pogledu oba navedena parametra ($p < 0,05$). Povezanost između trajanja operacije i trajanja intraoperativne fluoroskopije bila je potvrđena u SUF grupi ($p < 0,05$; $r = 0,405$), ali ne i u GK grupi ($p > 0,05$). GK metoda je pokazala veću varijabilnost u odnosu na SUF metodu po pitanju trajanja i vrste repetitivnih hirurških manevara koji zahtevaju rendgensku proveru. **Zaključak.** Broj planiranih operacija u jednom danu može biti određen vrstom unutrašnje fiksacije trohanternih preloma (intramedularna ili ekstramedularna). Potrebne su dodatne analize koje uključuju i procenu doze

zračenja kako bi se proverilo da li prosečno kraća intraoperativna fluoroskopija kod SUF metode može uticati na korišćenje opreme za zaštitu od rendgenskog zračenja od strane medicinskog osoblja. Ukoliko je poželjno postoperativno aktivirati inicijalno blokiranu dinamizaciju u uzdužnoj osi butne kosti, SUF metoda omogućava da se to ostvari bez potrebe za naknadnom

hirurškom intervencijom sa dodatnom intraoperativnom fluoroskopijom.

Ključne reči:

fiksatori, spoljni; femur, prelomi; fluoroskopija; fiksatori, unutrašnji; intraoperativni period; ortopedske procedure.

Introduction

Trochanteric fractures are osteoporotic fractures, mainly occurring in the elderly^{1,2}. These fractures are an important socioeconomic factor influencing life quality³. The relation between trochanteric and femoral neck fractures, as a type of osteoporotic hip fractures, is a variable in different parts of the world, confirming the influence of genetic and environmental factors in their incidence. Femoral neck fractures are more present in Northern Europe, while trochanteric fractures more occur in Central and Southern Europe⁴. Horii et al.⁵ found that trochanteric fractures incidence rapidly grows in relation to femoral neck fractures after the eighth decade of life.

Internal fixation is the most common type of trochanteric fractures treatment. The analysis of operation time can be useful both in the daily planning of operative programs (number of operations) and in anesthesia administration. Intraoperative fluoroscopy time is important to be analyzed, primarily regarding the adequate protection of medical staff who are exposed to X-rays daily. There are different data in the bibliography about comparative analysis of intramedullary and extramedullary trochanteric fractures fixation concerning operation time and intraoperative fluoroscopy time. These data mainly refer to the comparison between cephalomedullary methods and Dynamic Hip Screw (DHS).

Gold standard in trochanteric fractures' internal fixation is the usage of the third generation of Gamma Nail (GN), as an intramedullary method with a cannulated lag screw⁶⁻⁹. Trochanteric fractures with pertrochanteric component (i.e. fracture line extending in lower-medial direction from the greater trochanter) require the use of lag screws^{6,9}. Self-dynamisable Internal Fixator (SIF) is an extramedullary implant being in routine use at many centers, predominantly for femoral fractures fixation. There are diverse types of SIF implants. The type having a "trochanteric unit" includes the use of lag screws for femoral neck and head¹⁰⁻¹³. The "trochanteric unit" is available in two modes – the mode with multiple thinner non-cannulated lag screws and the mode with one wider cannulated lag screw.

The aim of this study was to compare an intramedullary and an extramedullary method of pertrochanteric fractures' internal fixation – the third generation GN and SIF with two non-cannulated lag screws in terms of operation time and intraoperative fluoroscopy time.

Methods

Two groups of patients with a unilateral trochanteric fracture having a pertrochanteric component were analyzed

in this study – 43 patients treated by the third generation GN (GN group) and 46 patients treated by SIF with two lag screws (SIF group). Regarding the AO Foundation/Orthopaedic Trauma Association (AO/OTA) classification based on preoperative and intraoperative X-ray analysis by the authors, all cases included 31-A1 and 31-A2 fractures, but also 31-A3 fractures accompanied by a pertrochanteric fracture line. Both groups included consecutive cases treated at the Clinic for Orthopaedics and Traumatology in Clinical Center Niš (Niš, Serbia) by all working surgeons from the Clinic after January 1st, 2012. There were 67% female and 33% male patients. The average age of the patients was 73.4 years in the GN group and 76.2 in the SIF group. The fixation method used (intramedullary or extramedullary) depended on every surgeon's preference for the method he was more familiar with.

GN used in this study was the third generation short GN. The type of SIF used had a "trochanteric unit" with three holes for non-cannulated lag screws. In all cases with this implant, the proximal fracture fragment was fixed by two lag screws. Three lag screws can be used in patients with a very wide femoral neck, but there was no such case in this study. When using just two lag screws, the triangular configuration of these holes gives an opportunity for the surgeon to make the choice for the more adequate of the two possible positions for the lower lag screw after the application of the first (upper) lag screw. Fixation of the distal fracture fragment included one screw passing the hole of the clamp and another screw (antirotation screw) passing the oblong hole in the implant body. The main role of the clamp is expressed when the lateral cortex is fractured distally to the lag screws and if the dynamisation in the long femoral axis is advisable. A fully screwed screw for the clamp initially blocks that dynamisation, while local biomechanical forces can spontaneously unlock the clamp several weeks after the surgery, thus spontaneously activating the dynamisation in the long femoral axis (Figure 1). Locking of the GN can be performed initially in dynamic or in static mode (the surgeon can sometimes assess that initially dynamic mode cannot provide sufficient initial fracture stability). If there is the need to transform the GN fixation postoperatively from the initially rigid (static) to a dynamic mode in the long femoral axis, some additional surgery of locking screw removal has to be performed.

Operation time (min) and intraoperative fluoroscopy time (s) were analyzed in patient groups. Operation time was measured as the time between the initial surgical incision and final suture. Intraoperative fluoroscopy was read on the screen of the C-arm used.

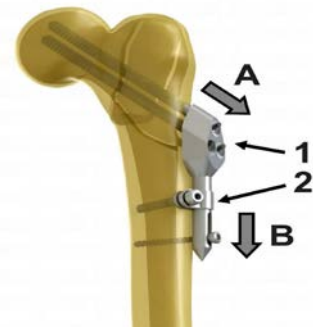


Fig. 1 – Self-dynamisable Internal Fixator (SIF) in a trochanteric fracture.

1 – trochanteric unit; 2 – clamp; A – dynamization in the femoral neck axis; B – dynamization in the long femoral axis, which is spontaneously activated after delayed unlocking of the clamp by local biomechanical forces if the contact between fracture fragments is insufficient.

The operative technique of SIF in trochanteric fractures treatment was followed by fluoroscopy in three phases of the surgery – checking the position of the K-wire for femoral neck and head, checking the first lag screw position and the final check of the fixation (Figure 2).

The GN method was succeeded by intraoperative fluoroscopy checks in all of the phases mentioned above, but also in additional phases such as checking the elastic guide-wire position and checking the vertical level of implant body before the K-wire admission to the femoral neck and head.

Statistics for average values comparing included *t*-test and Mann-Whitney *U* test. Bivariate correlation, by Spearman's correlation coefficient, was analyzed between the given parameters ¹⁴.

Results

In relation to the SIF group, average operation time and intraoperative fluoroscopy time were significantly higher in the GN group ($p < 0.05$) (Table 1).

The highest values of operation time and intraoperative fluoroscopy time (115 min; 176 s) were in the GN group, while the lowest values (20 min; 16 s) were in the SIF group.

The correlation between operation time and intraoperative fluoroscopy time was confirmed in the SIF group ($p < 0.05$) and this correlation was low positive ($0.3 < r < 0.5$). The correlation was not confirmed in the GN group ($p > 0.05$) (Table 2).

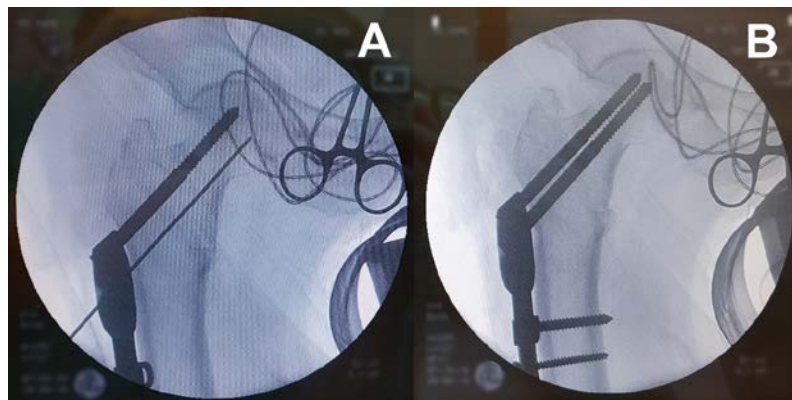


Fig. 2 – Intraoperative fluoroscopy is required in three phases of trochanteric fracture surgery by Self-dynamisable Internal Fixator (SIF): A) checking the position of just a K-wire and implant body, checking the position of the first lag screw and a K-wire with implant body; B) final check of the fixation.

Table 1

Operation time and intraoperative fluoroscopy time in trochanteric fractures' treatment by the third generation Gamma Nail (GN) and by Self-dynamisable Internal Fixator (SIF)

Parameter	GN group (mean \pm SD)	SIF group (mean \pm SD)	t/z	p
Operation time (min)	67.5 \pm 17.1	56.0 \pm 17.0	3.195	0.002*
Intraoperative fluoroscopy time (s)	84.8 \pm 30.2	36.7 \pm 19.8	-7.079	< 0.001†

**t*-test; †Mann-Whitney *U* test; SD – standard deviation.

Table 2

Correlations between operation time and intraoperative fluoroscopy time in trochanteric fractures' treatment by the third generation Gamma Nail (GN) and by Self-dynamisable Internal Fixator (SIF)

Statistical parameter	GN group	SIF group
Spearman's correlation coefficient (r)	0.267	0.405
Significance (p)	0.173	0.005

Discussion

Longer average operation time in the GN group could be explained by a more frequent need for intraoperative fluoroscopy in an intramedullary method than in an extramedullary method due to the reduced visual exposure of the implant position. Also, the fixation by GN includes more guiding instruments than the fixation by SIF. Every guiding instrument involves additional manual maneuvers of the surgeon, thus prolonging the operation time. Rimming of the medullary canal is a maneuver specific to intramedullary fixation, which is a factor for longer operation time as well.

Shorter average intraoperative fluoroscopy time in the SIF group could be explained by a more frequent need for intraoperative fluoroscopy in intramedullary methods than in extramedullary methods of fixation, as explained for the longer operation time too. Namely, as above-mentioned, the SIF method in trochanteric fractures treatment is followed by fluoroscopy in three phases of the surgery – checking the position of the K-wire for femoral neck and head, checking the first lag screw position and the final check of the fixation. The GN method is also succeeded by intraoperative fluoroscopy checks in these three phases, but also in additional phases such as checking the elastic guide-wire position, as well as checking the vertical level of implant body before the K-wire admission to the femoral neck and head.

Correlation between operation time and intraoperative fluoroscopy time was confirmed in the SIF group. The correlation was low positive, i.e. longer intraoperative fluoroscopy is expected to be followed by longer operation time and vice versa, but there was no high proportion in this relation. On the other hand, the correlation was not confirmed in the GN group. This could be explicated by the assumption that, in cephalomedullary fixation, the need for repetitive X-ray checks is variable depending on the phases of the surgery. This means that repetitive X-rays are in some cases more needed, e.g. during a K-wire setting, while in other cases they are more needed in elastic guiding wire admission, etc. Different phases of the surgery are followed by different durations of appropriate surgical maneuvers and hence by different time required for its repetitive performance. Furthermore, that additional time is sometimes not significant considering total operation time or very short duration of the maneuver. The surgical procedure of the SIF method in the trochanteric fractures treatment is followed by the requirement for repetitive X-ray checks mostly in the first phase (checking the position of the K-wire for femoral neck and head), while the second and third phases are mostly not followed by the necessity for repetitive fluoroscopy (the second phase can be followed mostly by one additional X-ray check due to the possible need for the first lag screw correction). The variation in the requirement for repetitive X-ray checks regarding surgical phases thus could be considered as lower in the SIF than in the GN method, which explains the difference in the correlations of operation time and intraoperative fluoroscopy time between the groups.

Alonso et al.¹⁵ analyzed scatter radiation around the C-arm and they found that the lead protection is a must within 2 m of the C-arm unit. Operative technique of trochanteric fractures fixation by SIF allows the surgeon to stay at the distance of 2 meters and more from the C-arm while performing intraoperative fluoroscopy in all phases of the surgery. However, some phases of the GN method, as in other cephalomedullary methods, require the surgeon to be next to the operating table and C-arm (during entry point positioning, elastic guiding wire admission or the phases with very short repetitive maneuvers)^{16, 17}. Based on the point of view above¹⁵, we could infer that X-ray protective clothes (protective apron, thyroid shield) are not strictly to be used in trochanteric fractures fixation by the SIF implant, while it is strictly recommended during the GN fixation.

Kelly et al.¹⁸ found that trochanteric fractures' internal fixation (including both intramedullary and extramedullary methods) was accompanied by significantly higher doses of radiation if cumulative intraoperative fluoroscopy time exceeded 50 seconds and if operation lasted longer than one hour¹⁸. Having obtained the results of average operation time and average intraoperative fluoroscopy time, we may assume that the average dose of radiation could be expected to be significantly higher in the GN group than in the SIF group. This statement, if accepted as true, could contribute to the deductions derived above about X-ray protective clothing. However, additional studies including the dose of radiation analysis are recommended so as to verify this statement.

Dynamisation in the femoral neck axis is important in trochanteric fractures with a pertrochanteric component, providing significant interfragmentary transfer of the load¹⁹. This dynamisation does not have to be blocked at the first postoperative time due to a lot of cancellous bone in the fracture area. In other trochanteric fractures, it may be beneficial to provide dynamization in the long femoral axis. When the implant with a lag screw is used, the dynamization in the long femoral axis can be achieved if the fracture has the line extending laterally below the entry point of a lag screw²⁰. Furthermore, this line can sometimes be overlooked if standard X-rays are used and a comminutive trochanteric fracture can be misconsidered as just a pertrochanteric fracture (31-A1 or 31-A2)²¹. In some cases with a trochanteric fracture fixation which is primarily rigid in the long femoral axis (as in static locking of a short GN), the need to transform the fixation into longitudinally dynamic mode can be manifested in the weeks after the surgery²¹. The transformation of the GN fixation into longitudinally dynamic mode requires some additional surgery in terms of the intervention with the locking screw including additional fluoroscopy, too. When SIF is used, initially blocked longitudinal dynamisation can be activated by spontaneous partial unlocking of the clamps as the result of local biomechanical forces^{22, 23}, thus excluding the need for additional surgery and for additional intraoperative fluoroscopy^{21, 24}. The amount of biomechanical forces' energy passing through the clamp is greater if the fracture healing is prolonged, i.e. if the fracture fragments' contact is

insufficiently long. The clamp can be unlocked if this energy exceeds its specific amount, so SIF can be considered as an “intelligent implant” that “recognizes” the need for dynamization in the long femoral axis, providing its activation “by itself”, thus being the only implant with this feature today^{10–13, 24}.

Regarding the bibliographic data about the third generation GN, Sim et al.²⁵ found the average operation time was 85 min, while Kelly et al.¹⁸ found the average intraoperative fluoroscopy time was 116 s. Furthermore, Wu et al.²⁶, Unger et al.²⁷ and Arirachakaran et al.²⁸ found average operation times were 67 min, 56 min and 62 min, respectively, while average intraoperative fluoroscopy times were 52 s, 62 s and 109 s, respectively which implies that all these intraoperative fluoroscopies were longer than 50 s.

The similarity between DHS and SIF may be attributed to extramedullary principles in both methods. Kelly et al.¹⁸ analyzed DHS fixation of trochanteric fractures, where intraoperative fluoroscopy time was 39 s, almost identical as in the SIF group in our study. Muller et al.²⁹ and Arirachakaran et al.²⁸ found that average operation times in DHS fixation of trochanteric fractures were 63 min and 54 min, respectively. These results are similar to the ones for

SIF in our study (average operation time in the SIF group held the value between the two above mentioned average results for DHS).

Conclusion

Operation time and intraoperative fluoroscopy time are expected to be longer if the third generation GN is used as an intramedullary method in relation to the use of SIF as an extramedullary method. Operation time duration can have the influence in the number of surgical interventions per day. Additional analyses including radiation dose assessment are desirable in order to clarify if shorter intraoperative fluoroscopy time in the SIF method can influence the choice of medical staff X-ray protection clothing during the surgery of trochanteric fractures fixation.

Acknowledgement

This work is a part of the project “Virtual human osteoarticular system and its application in preclinical and clinical practice” (No. III41017) funded by the Ministry of Education, Science and Technological Development of the Republic of Serbia.

R E F E R E N C E S

1. Han J, Hahn MH. Proximal femoral geometry as fracture risk factor in female patients with osteoporotic hip fracture. *J Bone Metab* 2016; 23(3): 175–82.
2. Melton LJ 3rd. Epidemiology of hip fractures: implications of the exponential increase with age. *Bone* 1996; 18(3 Suppl): 121S–5S.
3. Ström O, Borgström F, Kanis JA, Compston J, Cooper C, McCloskey EV, et al. Osteoporosis: burden, health care provision and opportunities in the EU: a report prepared in collaboration with the International Osteoporosis Foundation (IOF) and the European Federation of Pharmaceutical Industry Associations (EFPIA). *Arch Osteoporos* 2011; 6: 59–155.
4. Scheerlinck T, Opdevegh L, Vaes P, Opdecam P. Hip fracture treatment: outcome and socio-economic aspects. A one-year survey in a Belgian University Hospital. *Acta Orthop Belg* 2003; 69(2): 145–56.
5. Horii M, Fujiwara H, Ikeda T, Ueshima K, Ikoma K, Shirai T et al. Urban versus rural differences in the occurrence of hip fractures in Japan's Kyoto prefecture during 2008–2010: a comparison of femoral neck and trochanteric fractures. *BMC Musculoskelet Disord* 2013; 14: 304.
6. Saarenpää I, Heikkinen T, Ristiniemi J, Hyvönen P, Leppilähti J, Jalovaara P. Functional comparison of the dynamic hip screw and the Gamma locking nail in trochanteric hip fractures: a matched-pair study of 268 patients. *Int Orthop* 2009; 33(1): 255–60. (English, French)
7. Borbjerg PE, Larsen MS, Madsen CF, Schønnemann J. Failure of short versus long cephalomedullary nail after intertrochanteric fractures. *J Orthop* 2019; 18: 209–12.
8. Kempf I, Taglang G. The Gamma Nail – historical background. *Osteo Trauma Care* 2005; 13: 2–6.
9. Shu WB, Zhang XB, Lu HY, Wang HH, Lan GH. Comparison of effects of four treatment methods for unstable intertrochanteric fractures: A network meta-analysis. *Int J Surg* 2018; 60: 173–81.
10. Mitković MB, Milenković S, Micić I, Mladenović D, Mitković MM. Results of the femur fractures treated with the new selfdynamisable internal fixator (SIF). *Eur J Trauma Emerg Surg* 2012; 38(2): 191–200.
11. Mitković MM, Milenković S, Micić I, Kostić I, Stojiljković P, Mitković MB. Operation time and intraoperative fluoroscopy time in different internal fixation methods for subtrochanteric fractures treatment. *Srp Arh Celok Lek* 2018; 146(9–10): 543–8.
12. Micić ID, Mitković MB, Park IH, Mladenović DB, Stojiljković PM, Golubović ZB, et al. Treatment of subtrochanteric femoral fractures using selfdynamisable internal fixator. *Clin Orthop Surg* 2010; 2(4): 227–31.
13. Mitković MB, Bumbaširević M, Golubović Z, Mladenović D, Milenković S, Micić I, et al. New biological method of internal fixation of the femur. *Acta Chir Jugosl* 2005; 52(2): 113–6.
14. Mukaka MM. Statistics corner: A guide to appropriate use of correlation coefficient in medical research. *Malawi Med J* 2012; 24(3): 69–71.
15. Alonso JA, Shaw DL, Maxwell A, McGill GP, Hart GC. Scattered radiation during fixation of hip fractures. Is distance alone enough protection? *J Bone Joint Surg Br* 2001; 83(6): 815–8.
16. Mahajan A, Samuel S, Saran AK, Mahajan MK, Mam MK. Occupational radiation exposure from C arm fluoroscopy during common orthopaedic surgical procedures and its prevention. *J Clin Diagn Res* 2015; 9(3): RC01–4.
17. Chen J, Zuo CH, Zhang CY, Yang M, Zhang PX. Comparison of the effects of two cephalomedullary nails (zimmer natural nail and proximal femoral nail antirotation) in treatment of elderly intertrochanteric fractures. *Beijing Da Xue Xue Bao Yi Ban* 2019; 51(2): 283–7. (Chinese)
18. Kelly GA, Rowan FE, Hurson C. Factors influencing radiation exposure during internal fixation of hip fractures. *Eur J Orthop Surg Traumatol* 2017; 27(5): 637–41.
19. Bogosavljević M, Stokić D, Frisčić Z, Ristić BM. Unstable intertrochanteric fractures: how to prevent uncontrolled impaction

- and shortening of the femur. *Vojnosanit Pregl* 2011; 68(5): 399–404.
20. Hao Y, Zhang Z, Zhou F, Ji H, Tian Y, Guo Y, et al. Risk factors for implant failure in reverse oblique and transverse intertrochanteric fractures treated with proximal femoral nail antirotation (PFNA). *J Orthop Surg Res* 2019; 14(1): 350.
21. Kostić I, Mitković MM, Mitković MB. Treatment of stable and unstable intertrochanteric fractures with selfdynamisable internal fixator (concept of double dynamization). *Vojnosanit Pregl* 2015; 72(7): 576–82.
22. Soro N, Attar H, Brodie E, Veidt M, Molotnikov A, Dargusch MS. Evaluation of the mechanical compatibility of additively manufactured porous Ti-25Ta alloy for load-bearing implant applications. *J Mech Behav Biomed Mater* 2019; 97: 149–58.
23. Kim DO, Kim YM, Choi ES. Repeated Metal Breakage in a Femoral Shaft Fracture with Lateral Bowing – A Case Report. *J Korean Fract Soc* 2012; 25(2): 136–41.
24. Milenković S. Hip fractures. Niš: Faculty of Medicine of University of Niš; 2011. (Serbian)
25. Sim JC, Kim TH, Hong KD, Ha SS, Lee JS. Comparative Study of Intertrochanteric Fracture Treated with the Proximal Femoral Nail Anti-Rotation and the Third Generation of Gamma Nail. *J Korean Fract Soc* 2013; 26(1): 37–43. (Korean)
26. Wu K, Xu Y, Zhang L, Zhang Y, Xu W, Chu J, et al. Which implant is better for beginners to learn to treat geriatric intertrochanteric femur fractures: A randomised controlled trial of surgeons, metalwork, and patients. *J Orthop Translat* 2019; 21: 18–23.
27. Unger AC, Wilde E, Kienast B, Jurgens C, Schulz AP. Treatment of trochanteric fractures with the Gamma3 Nail – methodology and early results of a prospective consecutive monitored clinical case series. *Open Orthop J* 2014; 8: 466–73.
28. Arirachakaran A, Amphansap T, Thanindrarn P, Piyapittayanun P, Srisawat P, Kongtharvonskul J. Comparative outcome of PFNA, Gamma nails, PCCP, Medoff plate, LISS and dynamic hip screws for fixation in elderly trochanteric fractures: a systematic review and network meta-analysis of randomized controlled trials. *Eur J Orthop Surg Traumatol* 2017; 27(7): 937–52.
29. Muller F, Dobliger M, Kottmann T, Fuchtmeyer B. PFNA and DHS for AO/OTA 31-A2 fractures: radiographic measurements, morbidity and mortality. *Eur J Trauma Emerg Surg* 2020; 46(5): 947–53.

Received on May 16, 2020

Revised on August 7, 2020

Accepted on September 23, 2020

Online First September, 2020



Distance visual acuity in air force pilots and student pilots when exposed to + Gz acceleration in human centrifuge

Oštrina vida na daljinu kod pilota borbene avijacije i studenata pilota izloženih + Gz ubrzanju u humanoj centrifugi

Danijela Randjelović*, Sunčica Srećković^{†‡}, Tatjana Šarenac Vulović^{†‡},
Nenad Petrović^{†‡}

*Aero Medical Institute, Zemun, Serbia; [†]Clinical Center Kragujevac, Clinic of Ophthalmology, Kragujevac, Serbia; [‡]University of Kragujevac, Faculty of Medical Sciences, Department of Ophthalmology, Kragujevac, Serbia

Abstract

Background/Aim. High speeds that modern aircraft develop during take-off, flight and landing place an additional strain on the organ of vision. Owing to its considerable practical implementation in air combat, the effect of +Gz acceleration on the organ of vision is considered increasingly important for research. Substantial changes in visual functions may occur during high acceleration onset rates. However, it is important for a pilot to maintain visual acuity in order to be able to monitor new functional displays for rapid orientation, scan the configuration of terrain, display of weapons systems and enemy aircraft and deal with additional issues of the complexity of spatial orientation. The aim of the investigation was to establish whether distance visual acuity in air force pilots and student pilots is affected when exposed to +Gz acceleration. **Methods.** The study was performed on a defined population consisting of 95 respondents from 21 to 45 years of age divided into two groups. The first group included 65 air force pilots and the second group comprised of 30 student pilots, all of whom were exposed to an acceleration of +5.5 Gz. The testing was per-

formed in a human centrifuge, which mimics conditions of real Gz acceleration, in the Department of Biodynamics in Aero Medical Institute (Zemun, Serbia). We examined the obtained differences in distance visual acuity before and after exposure to acceleration. **Results.** After the testing, all respondents in the group of air force pilots had distance visual acuity of 1.0, while in the group of student pilots a statistically significant difference in distance visual acuity was observed after being exposed to +Gz acceleration. **Conclusion.** Transient changes in distant visual acuity were more pronounced in the group of student pilots in comparison with the changes in visual acuity in the air force pilots when exposed to the same acceleration values (+5Gz acceleration). Since change in distance visual acuity is the most sensitive physiological indicator when exposed to high acceleration, individual physiological pilot training in the human centrifuge increases tolerance to accelerations, which is important for flight safety in both peacetime and combat conditions.

Key words:

acceleration; aerospace medicine; pilots; students; visual acuity.

Apstrakt

Uvod/Cilj. Velike brzine prilikom poletanja, tokom letenja i prilikom sletanja modernih letilica predstavljaju dodatni napor za organ vida. Zbog njihove velike praktične primene u vazdušnoj borbi, uticaj +Gz ubrzanja na organ vida je veoma važan za istraživanje. Kod visokog početnog stepena ubrzanja mogu se javiti značajne promene u vidnim funkcijama. Pri tome je važno održati oštrinu vida kako bi mogli da se prate novi funkcionalni displeji za brzu orijentaciju pilota, konfiguracija reljefa terena, prikaz oružanih sistema i protivničkih aviona i uspešno savladaju svi dodatni zahtevi orijentacije u prostoru. Cilj rada je bio da se utvrdi da li postoji uticaj na

oštrinu vida na daljinu kod pilota borbene avijacije i studenata pilota usled izlaganja +Gz ubrzanju. **Metode.** Ispitivanje je sprovedeno na definisanoj populaciji, 95 ispitanika starosti od 21 do 45 godina podeljenih u dve grupe. Prvu grupu činilo je 65 pilota borbene avijacije, a drugu 30 studenata pilota. Svi ispitanici su bili izlagani ubrzanju od +5,5 Gz. Ispitivanje je vršeno u Odeljenju za biodinamiku Vazduhoplovno medicinskog instituta (Zemun, Srbija), na humanoj centrifugi u kojoj postoje uslovi realnog Gz ubrzanja. Posmatrali smo dobijene razlike u oštrini vida na daljinu pre i nakon izlaganja ubrzanju. **Rezultati.** U grupi pilota borbene avijacije, svi ispitanici su posle testa imali oštrinu vida na daljinu 1.0, a u grupi studenata uočena je statistički značajna razlika u

oštrini vida na daljinu nakon izlaganja +Gz ubrzanju. **Zaključak.** Prolazne promene oštine vida na daljinu, veće su kod studenata pilota nego kod pilota borbene avijacije kada su izloženi ubrzanju istih vrednosti (+5Gz ubrzanju). Budući da je promena oštine vida na daljinu najosetljiviji fiziološki pokazatelj u uslovima izlaganja visokom ubrzanju, individualna fiziološka trenaza pilota u humanoj

centrifugi poboljšava toleranciju na ubrzanja što je važno za bezbednost letenja u mirnodopskim uslovima kao i u borbenim manevrima.

Ključne reči:

ubrzanje; medicina, vazduhoplovna; piloti; studenti; vid, oština.

Introduction

Visual acuity (VA) is the ability of the eye to distinguish separate objects of observation in the outside world and is defined as the ability of the eye to see two separate points at the smallest angle. VA is better if the observed angles are closer and if the visual angle of each eye is smaller. It is dependent on the dioptric apparatus of the eye, transparency of the media, health of the retina, especially the central part of the yellow spot, the visual pathway and the central nervous system. VA of 1.0 is characteristic only of the centre of the foveola¹.

The ability to differentiate between two separate points is characteristic of the whole field of vision but it decreases significantly as the distance from the foveola increases. If a picture is formed outside the foveola, VA decreases sharply, so in the horizontal meridian it is 0.1 already at 20 degrees. VA is tested by an optotype. Most optotypes are designed in the way that the symbol to be recognised is formed of segments, the visual angle of which is 1', and that the whole figure comprises five segments. All optotypes are based on the fact that normal central VA understands the size of the picture on the retina of 0.004 mm and the visual angle of 1', and that the histological structure of the macula, especially its central part – the foveola, enables quick noticing of the object of observation. The mean diameter of the plug in the macular area is 0.004 mm, which is also the distance between two plugs separated by a third. This angle is at the same time the smallest angle separating the two observed points, it is invariable and is 1' of the visual angle¹.

Optotypes must be standardised so that obtained results can be compared. The contrast between the black optotype symbols on the bright surface should be 80–90%, and the brightness of the background 85 cd/m². The optotype symbols must be at a minimum distance of 3 cm. The Landolt Optotype is considered physiologically as the most accurate. It is a circle drawn within a 5' square, the thickness of its circular line being 1'. There is a 1'-long gap at one point on the circular line, forming a 1' x 1' opening in the shape of a square that faces different sides. The ratio between the size of the test and the size of the inner circle, thickness of the circular line and dimensions of the gap is 5 : 3 : 1. Constructed in this way, it is black on a white base. The Landolt ring is the only device that can test the real minimum separable. In European countries, VA is most often expressed in linear decimal values from 0.05 to 1.0. VA testing results must be written clearly, comprehensively and always in the same manner, and contain the following elements: vision – right eye (VOD) or vision – left eye

(VOS) score for the examined eye and VA without sight correction (sc), expressed in decimals (0.50) or fractions (30/60).

In aviation physiology, spatial disorientation can be overcome most efficiently by means of physiological training². Massive human and material losses compelled aviation physiology scientists in the 1920s to focus on investigating physiological mechanisms that may be a cause of crash and try and find solutions or at least mitigate the problem. Training is based on theoretical knowledge of the physiological effects of speed and acceleration, as well as of factors that increase or reduce the body's tolerance to the effect of dynamic flight factors³. Training is carried out in the human centrifuge, the aim being to enable the pilot to improve his tolerance to acceleration in the conditions of real G load, as well as learning about his body's potential response to excessive G stress⁴. Practically, the device is a combined gravity-altitude laboratory which simulates various flight conditions (+Gz load) and conditions of high-altitude flying (lower atmospheric pressure) with gradual or sudden change in cabin altitude (explosive compression). The structure of the device allows the maximum possible acceleration of up to +30Gz, but where people are involved, the given acceleration goes up to +9Gz, and with technical material up to +25Gz.

Air force pilots flying supersonic planes of the third, fourth and fifth generations, may be exposed to high values of +Gz load even while performing regular flight tasks. The most sensitive part of the organism to positive acceleration is the cardiovascular system. Blood as liquid tissue moves and retracts into lower body parts and, as a result, symptoms and outages of different organ systems occur, such as visual effects or loss of consciousness⁵.

In flight, accelerations occurring due to changes in flight direction of high-speed planes exceed the normal gravitational force and cause various changes in the functioning of the whole organism, particularly the visual function. Exposure to +Gz acceleration brings about worsening of vision before any disorder of consciousness takes place⁶. Exposure to an acceleration of +4.5 Gz usually leads to a complete loss of vision – the "black curtain". At lower rates of acceleration, it causes loss of peripheral vision while central vision is maintained – the "grey curtain". Rates of acceleration causing loss of peripheral vision differ largely from person to person, and depend on the brightness of both the visual field and the object of observation, as well as on the degree of fatigue. Visual disorders occurring due to positive acceleration are caused by retinal ischemia⁷. The eye receives blood by means of the central retinal artery (*arteria centralis retinae*). Intraocular pressure is normally 22 mmHg and for blood to

circulate in the retina the pressure in the retinal artery must be above 20 mmHg, so that blood flow can be maintained. When exposed to positive acceleration, the pressure inside the eye is reduced by about 22 mmHg *per* 1 G, and an increase in acceleration leads to an interruption in the supply of oxygen to the retina, causing visual disorders known as the “grey and black curtains”. The “grey curtain” is a result of progressive reduction in blood flow in the blood vessels of the retina, while the “black curtain” is caused by complete stalling of blood flow in the blood vessels of the retina. The “grey curtain” is the first sign of non-compensated G stress and is a common symptom known to any air force pilot. One study claims that 98% of pilots in the Royal Air Force of Australia have experienced this phenomenon⁸. With an increase in acceleration up to +4Gz and +5Gz, the pressure in the *arteria centralis retinae* decreases below the level of intraocular pressure, which causes a complete loss of vision, and the “black curtain” occurs when arterial pressure in the eye drops below 22 mmHg. The pilot’s consciousness is still unimpaired and he is capable of maneuvering the plane, using radio connection and communicating with flight control. There is an interval of 4–6 s from the interruption of retinal blood flow until a complete loss of vision occurs, which is conditioned by an oxygen reserve in the retinal artery. Recovery of vision occurs as soon as the oxygen reserves are replenished and the pressure in the retinal artery rises above 20 mmHg. The “black curtain” has been observed in 29% of pilot respondents in the Royal Air Force of Australia⁸. A study involving Brazilian Air Force states that 20% of their pilots have experienced a complete loss of vision⁹. Examining the eye bottom by ophthalmoscope, one notices that the arteries and arterioles are pale, completely empty. The interval between a sudden drop in pressure and loss of vision is 4–6 s thanks to a small reserve of oxygen that is diluted in the extravascular retinal fluid. Vision is only restored when this oxygen reserve in the retina is replenished and when the pressure of the oxygen diluted in the extravascular fluid rises above the minimum necessary for normal functioning of vision. Exposure to acceleration also causes reduced eye movement, which in some research papers is taken as a highly reliable indicator of partial or complete loss of vision¹⁰. The “grey” and “black curtain” are deemed a subjective experience by individual pilots.

Methods

The research included 95 pilots from 21 to 45 years of age. All of the respondents were highly selective, had no history of ocular diseases or system disorders, they were provided information about the scientific research and each of them filled in and signed a consent form to participate in the research. Depending on the years of flying experience and flight hours, the pilots were classified into two groups: a group of air force pilots, comprising of 65 pilots, and a group of 30 student pilots. Both groups were exposed to an acceleration of +5.5 Gz.

We observed the prevalence of exposure to positive acceleration, examining the effect of acceleration on distance VA in these two groups of respondents. The investigation

was conducted in a gravity-altitude laboratory (human centrifuge).

We examined the obtained differences in distance VA at a particular rate of acceleration between the two group of respondents, thus obtaining our own significant indicator of the condition of visual functions at the beginning of professional career and after years of flying. Before testing in the centrifuge, the respondents were checked by methods that are part of the standard medical-psychological expertise procedure, and underwent control check-ups to establish whether there were any pathological conditions that could affect the pilots’ tolerance to acceleration (increased body temperature, upper respiratory track infections, or a subjective feeling of the pilot himself). Two hours before the testing, the respondents were asked to have a light meal. One should always consider the adrenalin reaction instigated by apprehension in the face of possible failure of testing, by being subjected to testing, as well as accompanying disturbances of the vegetative function. Safety of respondents and their comfort in the cockpit must never be compromised.

The respondents were exposed to prolonged acceleration in the centrifuge, from 9.00 to 11.00 in the morning. A linear increase in acceleration test was used with both groups of respondents, meaning that acceleration was increased up to +5.5Gz without anti-G protection, the acceleration gain being 0.1 G/s. The first step in testing was exposing the respondents to an acceleration of +2Gz increasing to +5.5Gz, and then reducing it back to +2Gz. While being exposed to increases in acceleration from +2Gz to +5. Gz, the respondents were required to respond to the light signals in the cockpit by pressing the stick switch. If the respondent did not press the switch, the acceleration decreased. After a one-minute intermission, the respondent would leave the centrifuge cabin.

The pilots’ distance VA was tested upon entering and exiting the cabin. It was carried out by a subjective method using the Landolt optotype. The testing was carried out monocularly, the right eye first, and then the left, at the distance of 6 m from the optotype (direct method of testing VA). The investigated pilots were tasked with naming the position of the ring opening (Latin letter “C”), starting with the biggest to the smallest. The size of the opening and the test as a whole are designed in such a way that if the pilot has normal VA, he should be able to see clearly all the symbols from a certain distance, meaning, see the biggest symbols from the distance of 60 m, to the smallest ones that he would be able to notice from the distance of 6 m. VA was expressed in decimal numbers. If VA is normal, a pilot can see the tenth line on the optotype and that is expressed as 1.0.

Results

Before the test, all the respondents, both in the student pilot group and the group of air force pilots, had distance VA of 1.0. After the test of linear increase in acceleration, a statistically significant difference in VA ($p = 0.000$) was noticed in both groups. In the group of air force pilots all of the respondents also had distance VA of 1.0 after the test. In the student pilot group, after the test, in 66.7% of cases

Table 1

Visual parameters in student pilots and air force pilots				
Distance visual acuity		Student pilots n (%)	Air Force pilots n (%)	<i>p</i>
Before the test	1.0	30 (100)	65 (100)	0.000*
After the test	0.8	3 (10.0)	0 (0)	
	0.9	7 (23.3)	0 (0)	
	1.0	20 (66.7)	65 (100)	
<i>p</i>		0.002 [†]	/	

* – statistically significant difference between student pilots and air force pilots;

[†] – statistically significant difference before vs. after the test within observed groups of respondents (χ^2 -test).

distance VA was 1.0, in 23.3% it was 0.9 and in the remaining 10% it was 0.8. By analysing the frequency of respondents with a difference in distance VA before and after the test, a statistically significant difference ($p = 0.002$) was noticed in the student pilot group (Table 1).

Discussion

Aviation medicine includes a wide range of tasks, the end goal of which is continuous creation of measures and procedures which would best equip the pilot for flight and performance of duties he has been entrusted with, at the same time reducing risks to life, health and material resources to a minimum. In aviation medicine, the journey from theory to practice is somewhat longer since any research calls for complex technical innovations and high level of security for their verification¹¹. The pilot profession is a job involving optimum mental and physical fitness, full personal integrity and excellent health. It is one of few professions in which work capacity is under permanent scrutiny. Pilots are a highly selective population that undergoes regular controls throughout their flight experience, as any functional deficiency might compromise the safety of flight¹². In the field of physiology of acceleration, notable variations in tolerance to G acceleration have been noticed. Most pilots start their flight experience with a grey curtain at +3Gz to +3.5Gz and near loss of consciousness at +4.5Gz to +5.0Gz, while there are those who lose consciousness immediately upon acceleration exceeding +3.0Gz, as well as those who tolerate +7.0Gz and +7.5Gz accelerations¹³. Apart from medical significance, high sensitivity to G acceleration also has a high operational significance in military aviation because, when a pilot takes command of the plane, there is a potential risk to his life, the lives of the crew and the plane. In comparison with other systems of the human body, the circulatory system is the one most significantly affected by positive G acceleration. Progression of symptoms, from a minimal reduction in vision to a black curtain, to loss of consciousness, is to be expected due to the reduction of blood flow in the upper body parts. If acceleration is high enough to cause a black curtain or other visual symptoms, it will manifest itself a few seconds after arterial pressure has reached its lowest value¹¹. As the system pressure rises, vision may be restored, but full recovery is delayed for a few seconds until circulation has been restored thanks to the oxygen reserve in the retina in the period of anemia. In the works by Feigl et al.¹³ and Tsai et

al.¹⁴, it is shown that after being exposed to +Gz acceleration, the depth of the eye chamber increases and energy reserves in the retina and the central nervous system enable the brain and the visual apparatus to keep on functioning for a few seconds longer after blood flow to the brain has been cut off. This enables tolerance to sudden high increases in G acceleration over a short period of time, usually for about 5 seconds¹⁵. With high acceleration onset rate, significant changes in visual functions may occur. However, maintaining distance visual acuity is of considerable importance for a pilot to be able to orientate himself in space rapidly, visually scan the configuration of the terrain, display of weapons systems and enemy aircraft and deal with additional issues of the complexity of spatial orientation³. Tolerance to +Gz accelerations, and the ensuing changes in visual acuity, may be compromised if pilots do not experience high +Gz accelerations over a longer period of time¹⁶. This is why there is a question of how much air combat training a pilot needs in order to maintain good tolerance. It is a known fact that a pilot who flies in air combat conditions at least once a week tolerates +Gz acceleration better than pilots who do this once in two weeks or once a month^{17, 18}. When exposed to an acceleration of +5.5Gz, the air force pilots showed greater tolerance to acceleration compared to the student pilots, as there were statistically significant distance visual acuity differences. We have not found any similar data in available literature.

Conclusion

There was a considerable degree of transient loss of distance visual acuity in the student pilots in comparison with the air force pilots upon exposure to high +Gz acceleration. In the student pilots, a transient reduction in distance visual acuity occurred upon exposure to a +5Gz acceleration, whereas visual acuity of the air force pilots remained unchanged before and after exposure to the acceleration of the same value. One of the most sensitive physiological indicators when exposed to high acceleration is a change in distance visual acuity. Individual pilot training in the human centrifuge mimicking real G acceleration conditions improves tolerance to acceleration and brings about only minor changes in visual acuity upon exposure to acceleration. In this way, pilots become familiar with their body's response to increased G accelerations, which is important for flight safety both in peacetime and combat conditions.

R E F E R E N C E S

1. Čolić J. Determination of visual acuity using different types of optotypes. Expertal work paper. Novi Sad: Faculty of Sciences, Department of Physics; 2016. (Serbian)
2. Davis JR., Johnson R, Stepanek J, Fogarty JA. Fundamentals of Aerospace Medicine. 4th ed. New York, NY: Lippincott Williams & Wilkins (LWW); 2008.
3. Wolkanowski M, Truszczyński O, Wojtkowiak M. New method of visual disturbances assessment in pilots during tests in the Polish human centrifuge. *Int J Occup Med Environ Health* 2007; 20(1): 44–7.
4. Rudnjanin S, Arsic-Komljenovic G, Pavlovic M, Vujnovic J. Loss of consciousness as criterion of +Gz tolerance at Institute of Aviation Medicine MMA during +Gz acceleration selective test. *Acta Physiol Hung* 2006; 93(4): 371–6.
5. Harrison MF, Coffey B, Albert WJ, Fischer SL. Night vision goggle-induced neck pain in military helicopter aircrew: a literature review. *Aerosp Med Hum Perform* 2015; 86(1): 46–55.
6. Agarwal A, Werchan PM, Lessard C. Neurovestibular effects of +Gz. *Ind J Aerosp Med* 2002; 46: 34–41.
7. Norsk P. Cardiovascular and fluid volume control in humans in space. *Curr Pharm Biotechnol* 2005; 6(4): 325–30.
8. Rickards CA, Newman DG. G-induced visual and cognitive disturbances in a survey of 65 operational fighter pilots. *Aviat Space Environ Med* 2005; 76(5): 496–500.
9. Horis JK, Pilecki N. Simulated night vision goggle wear and colored aftereffects. *Aviat Space Environ Med* 2013; 84(3): 206–11.
10. Pattarini JM, Blue RS, Castleberry TL, Vanderploeg JM. Preflight screening techniques for centrifuge-simulated suborbital space-flight. *Aviat Space Environ Med* 2014; 85(12): 1217–21.
11. Curdt Christiansen C, Drageger J, Kriebel J. Principles and Practice of Aviation Medicine. 1st ed. London: World Scientific Publishing Company; 2009.
12. DeHart RL. Fundamentals of Aerospace Medicine. Philadelphia, PA: Lea & Febiger 2003. P. 398–410.
13. Feigl B, Zele AJ, Stewart IB. Mild systemic hypoxia and photopic visual field sensitivity. *Acta Ophthalmol* 2011; 89(2): e199–e204.
14. Tsai ML, Horng CT, Liu CC, Shieh P, Hung CL, Lu DW, et al. Ocular responses and visual performance after emergent acceleration stress. *Invest Ophthalmol Vis Sci* 2011; 52(12): 8680–5.
15. Dalecki M, Bock O, Guardiera S. Simulated flight path control of fighter pilots and novice subjects at +3 Gz in a human centrifuge. *Aviat Space Environ Med* 2010; 81(5):484–8.
16. Feigl B, Stewart I, Brown B. Experimental hypoxia in human eyes: implications for ischaemic disease. *Clin Neurophysiol* 2007; 118(4): 887–95.
17. Tsai ML, Liu CC, Wu YC, Wang CH, Shieh P, Lu DW, et al. Ocular responses and visual performance after high- acceleration force exposure. *Invest Ophthalmol Vis Sci* 2009; 50(10): 4836–9.
18. Yu CS, Wang EM, Li WC, Braithwaite G. Pilots' visual scan patterns and situation awareness in flight operations. *Aviat Space Environ Med* 2014; 85(7): 708–14.

Received on June 7, 2020

Revised on July 8, 2020

Accepted on July 13, 2020

Online First July 2020



The use of piezoelectric instrumentation and platelet rich fibrin matrix in septorhinoplasty: report of two cases

Primena piezoelektričnih instrumenata i fibrina bogatog trombocitima u septorinoplastici

Aleksandar Dimić*, Vladimir Stojiljković†, Tamara Vujačić†

*Military Medical Academy, Clinic for Otorhinolaryngology, Belgrade, Serbia;

†VS Clinic and Beauty, Belgrade, Serbia

Abstract

Introduction. Rhinoplasty is one of the most commonly performed surgeries in the area of aesthetic surgery. Surgical instruments, which are used in traditional rhinoplasty, like saws, chisels and osteotomes are relatively imprecise and their usage can lead to uncontrolled fractures of the bone and consequently to inadequate final results. Piezoelectric-powered ultrasonic instruments (PEI) are currently the most innovative instrumentation available for minimally traumatic reshaping of the bony vault and lateral walls. There are many studies which have shown positive effects of platelet-rich fibrin (PRF) in postoperative course of rhinoplasty patients. **Case report.** We presented two innovative approaches in rhinoplasty combined PEI and PRF matrix through two case reports. In both patients, satisfying results were achieved by use of PEI technique. Also, usage of PRF membrane provided good healing and small postoperative edema. **Conclusion.** Based on our experience, the use of of PEI technique has many benefits. It is safe, practical and effective method and it demonstrates valuable and favourable results in osteotomies. Also, usage of PRF membrane helps patients in better healing and less postoperative edema.

Key words:

osteotomy; platelet-rich fibrin; otorhinolaryngologic surgical procedures; piezosurgery; rhinoplasty.

Apstrakt

Uvod. Rinoplastika je jedna od najčešće izvođenih operacija u polju estetske hirurgije. Hirurški instrumenti koji se koriste u tradicionalnoj rinoplastici, poput dleta, čekića i osteotoma, relativno su neprecizni i njihova upotreba može dovesti do nekontrolisanih fraktura kostiju i, posledično, do neadekvatnog krajnjeg rezultata. Piezoelektrični ultrazvučni instrumenti (PEI) predstavljaju trenutno najnapredniju raspoloživu tehniku za minimalno traumatsko preoblikovanje nosnih kostiju. Postoje mnoge studije koje su dokazale pozitivne efekte fibrina bogatog trombocitima (PRF) u postoperativnom toku kod pacijenta sa prethodno učinjenom rinoplastikom. **Prikaz bolesnika.** Prikazana je kombinacija ova dva inovativna pristupa u rinoplastici (PEI i PRF) kod dva pacijenta. U oba slučaja, primenom PEI tehnike postignuti su zadovoljavajući rezultati. Takođe, upotreba PRF obezbedila je dobro zarastanje i mali postoperativni edem. **Zaključak.** Na osnovu našeg iskustva, PEI tehnika ima mnoge prednosti kao bezbedna, praktična i efikasna metoda sa naročito značajnim i povoljnim rezultatima u osteotomijama. Takođe, upotreba PRF membrane pomaže pacijentima u boljem zarastanju i formiranju značajno manjeg postoperativnog edema

Ključne reči:

osteotomija; fibrin obogaćen trombocitima; hirurgija, otorinolaringološka, procedure; piezohirurgija; rinoplastika.

Introduction

Rhinoplasty is one of the most commonly performed surgeries by otolaryngologists and plastic surgeons in the area of aesthetic surgery. Since nose takes central position and gives every face a definition, any alterations in this region can make huge difference in the appearance of a person. Therefore, it is crucial that surgeons who perform

rhinoplasty have thorough knowledge of nose anatomy¹. Regarding visibility of nose anatomy, it is our opinion that open rhinoplasty could be considered golden standard, since it allows best visibility and much easier reconstruction.

Surgical instruments, which are used in traditional rhinoplasty, like saws, chisels and osteotomes are relatively imprecise and their usage can lead to uncontrolled fractures of the bone and consequently to inadequate final results. Piezoelec

tric-powered ultrasonic instruments (PEI) are currently the most innovative instrumentation available for minimally traumatic reshaping of the bony vault and lateral walls². The first use of PEI for rhinoplasty was first published by Robiony et al.³ in 2007. It is based on piezoelectric micrometric ultrasonic vibrations, which can be applied for bone incisions through various tips, depending on what is being done – osteotomy or osteoplasty. Just ten years ago, it was almost unimaginable for surgeons to have such kind of atraumatic device at disposal, with which they can safely reshape the bone, without breaking it, but also simultaneously prevent damaging of surrounding mucosa, soft tissues and ligaments. As a result, patients have faster recovery and more natural looking results, with less bleeding, bruising, scarring, ecchymosis and edema^{4,5}.

There are many studies which have shown positive effects of platelet-rich fibrin (PRF) in postoperative rhinoplasty patients^{6,7}. PRF is developed and published by Choukroun et al.^{8,9} and first, it was mostly used in oral and orthopedic surgery for bone regeneration and in plastic surgery for chronic wound healing. PRF is produced from venous blood which is withdrawn in special epruvets without anticoagulants and then centrifuged. After centrifugation, final product is separated in three parts and PRF is created in the middle one as a complex fibrin matrix which can be pulled out and put on bony and cartilaginous vault of the nose^{8,9}. Gode et al.⁷ applied PRF membrane on bony dorsum and supratip area and observed positive outcome on skin thickness and postoperative edema, especially in early postoperative period.

We presented two innovative approaches in rhinoplasty combined PEI and PRF matrix through two case reports.

Case report

Case 1

A 21-year-old female came to us complaining about the size of her nose and wide and large nostrils. She also reported some light breathing difficulties. Finding on nasal analysis included presence of dorsal hump, bulbous nasal tip with asymmetric alar cartilages and thick sebaceous skin which requested refinement of her nasal tip. Septal deviation and wide lateral walls of the nose were also present. The operative plan included open rhinoplasty approach through an inverted V shaped transcolumellar incision and dissection with extended soft tissue elevation, allowing a complete visual assessment of the entire osteocartilaginous vault. After that dorsal hump removal was preformed with a blade tip, additional remodelling of nasal dorsum was made with diamond burr (Figure 1). Whichever instrument is being used, an open roof never occurred, because underlying cartilages and mucosa were unharmed through PEI. After this, a septoplasty with cartilaginous graft harvesting was done. Then a "low to low" lateral osteotomy was performed with an angulated saw. Fracture line started from the pyriform aperture and continued along the nasofacial angle. This osteotomy was combined with transverse osteotomy with great caution to preserve Webster triangle. Medial osteotomy was not performed because the narrow of bone pyramid was enough.



Fig. 1 – The bony cap was removed as preoperatively planned to lower the dorsal profile line.

Cephalic trimming of alar cartilages left them symmetric with a 6-mm rim strip. For tip complex stability and correction of medial crural asymmetry interdomal and transdomal sutures were placed together with columellar graft from septum harvesting. Finally, PRF membrane was placed on bony and cartilaginous vault of the nose (Figures 2 and 3). One month postoperative results are shown in Figure 4. The patient was satisfied with aesthetic result, although there was still some swelling present.



Fig. 2 – Platelet-rich fibrin (PRF) membrane ready for placing on nasal and cartilaginous dorsum.

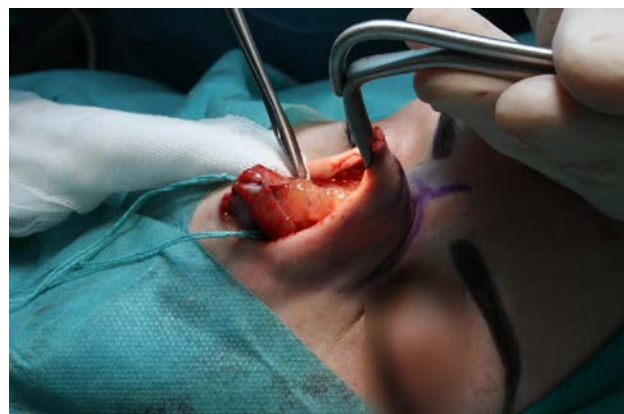


Fig. 3 – Platelet-rich fibrin (PRF) membrane being placed on dorsum.



Fig. 4 – Preoperative (up) and postoperative (down) views (one month after) of the patient in Case 1.

Case 2

A 35-year-old female patient presented with complaints about her nasal breathing, dorsal hump and droopy nose. After analysis we agreed that dorsal hump reduction is needed as well as septoplasty and nose tip reinforcement. The operative plan included the following: open rhinoplasty approach through a transcolumellar incision with supraperichondrial, submusculoaponeurotic plane in order to avoid injury to the arterial, venous and lymphatic supply as much as possible. Then a septoplasty with cartilaginous graft harvesting was done. Septum was trimmed and totally realised in caudal part. Dorsal hump reduction was performed with a blade tip, additional remodelling of nasal dorsum was done with diamond burr. After lateral osteotomies with PEI, alar cartilages were trimmed in their horizontal and vertical parts leaving symmetric alar cartilages. Columellar graft was sutured to caudal septum, interdomal and transdomal sutures for nose tip. PRF membrane was placed on bony and cartilaginous vault of the nose for better wound healing and less postoperative swelling and hematoma (Figure 5). The patient was very satisfied with the aesthetic result and all of her complaints were settled. One month postoperative period results are shown on Figure 6.

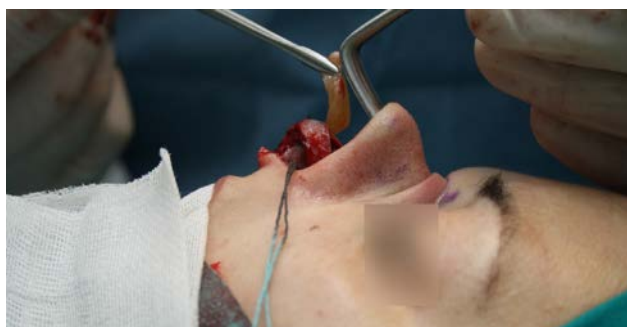


Fig. 5 – Platelet-rich fibrin (PRF) membrane being placed.



Fig. 6 – Preoperative (up) and postoperative (down) views (1 one month after) of the patient in Case 2.

Discussion

The field of rhinoplasty is well studied and the current literature is full of various techniques. Since the osteotomy is fundamental step in rhinoplasty, multiple different techniques have been employed to overcome postoperative morbidities like ecchymosis, edema, pain, and bleeding. Involvement of PEI in rhinoplasty was definitely a breakthrough moment and represents a significant step forward in rhinoplasty surgery. It provided precise osteotomies without causing unstable and undesirable fractures, comminution, and bony instability and at the same time minimizing soft tissue disruption and postoperative morbidities^{10–12}.

With traditional chisels, a substantial amount of force is being passed to the incision line and soft tissue surrounding it. Since the chisels are being "blindly" used, nasal soft tissue and vessels may be lacerated which increases the risk of bleeding, but also prolongs operation duration and patient recovery time. Comparing to this, PEI requires minimal external pressure and no need for hammer hits^{4, 12}.

We consider that regardless of the technique of performing an osteotomy, it is very important to point out the necessity of preserve Webster's triangle. This triangle represents a small area on the caudal part of the maxillary frontal process. It is a support for respiratory valvular and is crucial for the primacy of functional nasal airway obstruction and internal valvular collapse.

Meta-analysis from 2019, published by Mirza et al.¹³, proved that PEI causes less ecchymosis, edema and pain than conventional osteotomy, without extending the duration of surgery. It included six randomized clinical trials from 2015 to 2019 and additionally proved that PEI has no longer duration in surgery, unlike some previous trials have suggested. The study by Otake et al.¹⁴ was the first to prove the clinical advantage of PEI in the soft tissue. In most studies reporting the superiority of piezosurgery, the evaluations are mostly

based on clinical observations. But, there are also few studies which followed the histopathological effects on bone and periosteum. They showed better osteocyt survival, less damage to the peripheral tissue and periosteum^{15, 16}. Labanca et al.¹⁷ shared that usage of PEI induces the release of bone morphogenetic proteins with a controlled inflammatory process and triggers the bone remodelling earlier.

After tissue damage platelets and inflammatory cells are first to come to damaged place. The fibrin network captures circulating cells and activates vascularization in the wound area. It is known that fibrin matrix directly activates angiogenesis¹⁸. Thrombocytes contain growth factors and cytokines that initiate wound healing. PRF matrix contains all growth factors which are wantable in the wound, like endothelial growth factor and vascular endothelial growth factor. It promotes fibroblastic proliferation and induce angiogenesis and at the same time collecting circulating stem cells in blood and promoting osteoblastic activity⁸. Some studies also reported antimicrobial and antifungal activities of PRF matrix against *Escherichia coli*, *Staphylococcus aureus*, *Candida albicans*, and *Cryptococcus neoformans*¹⁹.

Gode et al.⁷ investigated effects of PRF on postoperative edema and wound healing with ultrasonography as an objective evaluation method and they

found positive effects of PRF on postoperative edema, especially in the early postoperative period. Patients who have thicker skin have bigger tendency of forming „dead space“ which can later be filled with scar tissue, which consequently leads to persistent edema and bad cosmetic outcome. It is our opinion that PRF membrane should be used mandatory in this kind of cases.

Conclusion

Based on our experience adoption of PEI technique has many benefits. It is safe, practical and effective method and it demonstrates valuable and favourable results in osteotomies. Also in our observation usage of PRF membrane helps patients in better healing and less postoperative edema. We hope that our results with piezosurgery combined with PRF matrix will encourage other surgeons who perform rhinoplasty to start its use.

Conflict of interest

The authors declared no potential conflicts of interest with respect to the research, authorship, and publication of this article.

REFERENCES

1. Ishii LE, Tollefson TT, Basura GJ, Rosenfeld RM, Abramson PJ, Chaiet SR, et al. Clinical Practice Guideline: Improving Nasal Form and Function after Rhinoplasty. *Otolaryngol Head Neck Surg* 2017; 156(2 Suppl): S1–S30.
2. Manbachi A, Cobbold RSC. Development and application of piezoelectric materials for ultrasound generation and detection. *Ultrasound* 2011; 19(4): 187–96.
3. Robiony M, Polini F, Costa F, Toro C, Politi M. Ultrasound piezoelectric vibrations to perform osteotomies in rhinoplasty. *J Oral Maxillofac Surg* 2007; 65(5): 1035–8.
4. Gerbault O, Daniel RK, Kosins AM. The Role of Piezoelectric Instrumentation in Rhinoplasty Surgery. *Aesthet Surg J* 2016; 36(1): 21–34.
5. Goksel A, Saban Y. Open Piezo Preservation Rhinoplasty: A Case Report of the New Rhinoplasty Approach. *Facial Plast Surg* 2019; 35(1): 113–8.
6. Guler I, Kum RO, Yilmaz YF. Application Of Platelet Rich Fibrin Matrix (PRFM) In Septorhinoplasty. *ENT Updates* 2019; 9(1): 53–8.
7. Gode S, Ozturk A, Kismali E, Berber V, Turbal G. The Effect of Platelet-Rich Fibrin on Nasal Skin Thickness in Rhinoplasty. *Facial Plast Surg* 2019; 35(4): 400–3.
8. Choukroun J, Diss A, Simonpieri A, Girard MO, Schoeffler C, Dohan SL, et al. Platelet-rich fibrin (PRF): a second-generation platelet concentrate. Part IV: clinical effects on tissue healing. *Oral Surg Oral Med Oral Pathol Oral Radiol Endod* 2006; 101(3): e56–60.
9. Choukroun J, Adda F, Schoeffler C, Vervelle A. An opportunity in perio-implantology: The PRF. *Implantodontie* 2001; 42: 55–62. (French)
10. Gonzalez-Lagunas J. Is the piezoelectric device the new standard for facial osteotomies? *J Stomatol Oral Maxillofac Surg* 2017; 118(4): 255–8.
11. Kocak I, Dogan R, Gokler O. A comparison of piezosurgery with conventional techniques for internal osteotomy. *Eur Arch Otorhinolaryngol* 2017; 274(6): 2483–91.
12. Singh P, Dhar S, Singh E, Vijayan R, Mosabehi A. Piezoelectric Ultrasound Rhinoplasty. *Aesthet Surg J* 2020; 40(2): NP63–NP64.
13. Mirza AA, Alandjani TA, Al-Sayed AA. Piezosurgery versus conventional osteotomy in rhinoplasty: A systematic review and meta-analysis. *Laryngoscope* 2020; 130(5): 1158–65.
14. Otake Y, Nakamura M, Henmi A, Takahashi T, Sasano Y. Experimental Comparison of the Performance of Cutting Bone and Soft Tissue between Piezosurgery and Conventional Rotary Instruments. *Sci Rep* 2018; 8(1): 17154.
15. Kurt Yazgar S, Serin M, Rakici IT, Sirvan SS, Irmak F, Yazgar M. Comparison of piezosurgery, percutaneous osteotomy, and endonasal continuous osteotomy techniques with a caprine skull model. *J Plast Reconstr Aesthet Surg* 2019; 72(1): 107–13.
16. Stoetzer M, Magel A, Kampmann A, Lemound J, Gellrich NC, von See C. Subperiosteal preparation using a new piezoelectric device: a histological examination. *GMS Interdiscip Plast Reconstr Surg DGPW* 2014; 3: Doc18. doi: 10.3205/iprs000059.
17. Labanca M, Azgola F, Vinci R, Rodella LF. Piezoelectric surgery: Twenty years of use. *Br J Oral Maxillofac Surg* 2008; 46(4): 265–9.
18. Nu Nurden AT. Platelets, inflammation and tissue regeneration. *Thromb Haemost* 2011; 105 Suppl 1: S13–33.
19. Szczepanski T, Król W, Wielkoszynski T. Antibacterial effect of autologous platelet gel enriched with growth factors and other active substances: an in vitro study. *J Bone Joint Surg Br* 2007; 89(3): 417–20.

Received on July 9, 2019

Revised on July 10, 2020

Accepted on July 13, 2020

Online First July, 2020



Imaging findings of familial adenomatous polyposis-associated aggressive mesenteric fibromatosis: A case report

Agresivna mezenterijalna fibromatoza udružena sa familijarnom adenomatoznom polipozom – karakteristike dobijene primenom *imaging* tehnika snimanja

Srdjan Stošić, **Slavica Sotirović-Seničar**

University Clinical Center of Vojvodina, Center for Radiology, Novi Sad, Serbia

Abstract

Introduction. Aggressive fibromatosis, also known as desmoid type fibromatosis (DF) is a locally aggressive fibroblastic neoplasm that can arise anywhere in the body with no potential for metastasis and a high recurrence rate after surgical resection. Mesenteric fibromatosis are locally aggressive DF of the mesentery with a high propensity for bowel involvement. The real etiology of these tumors remains unknown, occurring sporadically or in association with familial adenomatous polyposis (FAP), as Gardner's syndrome. **Case report.** A 34-year-old female patient presented with a palpable solid tumefactive mass in the left hemiabdomen. Contrast enhanced computed tomography (CT) and magnetic resonance imaging (MRI) revealed multiple massive solid tumefactions in the mesentery and in between the small bowel loops. Colonoscopy confirmed the presence of multiple sessile polyps characteristic of FAP. Tissue samples of the mesenteric mass were acquired via ultrasound guided biopsy with histopathologic confirmation of desmoid fibromatosis with immunohistochemical analysis. The risk of surgery was deemed too high at the time due to the size of the mass and proximity to mesenteric vascular structures, therefore the patient was planned for chemotherapy with a potential for further surgical reevaluation. **Conclusion.** Mesenteric fibromatosis is a rare neoplasm that presents with a wide range of histologic and imaging features. CT and MRI play a crucial role in evaluation and planning an optimal treatment model for patients with mesenteric fibromatosis.

Key words:

biopsy, needle; colonoscopy; diagnosis; fibromatosis, abdominal; fibromatosis, aggressive; immunohistochemistry; magnetic resonance imaging; mesentery; tomography, x-ray computed.

Apstrakt

Uvod. Agresivna fibromatoza, takođe poznata kao desmoidna fibromatoza (DF), je lokalno agresivna fibroblastična neoplazma koja se može javiti bilo gde u ljudskom telu, bez potencijala metastaziranja, sa visokom stopom recidiviranja nakon hirurškog uklanjanja. Mezenterijalne fibromatoze su lokalno invazivne fibromatoze mezenterijuma sa čestim zahvatanjem crevnih vijuga. Etiologija ovih tumora je nepoznata, a javljaju se sporadično ili udruženi sa familijarnom adenomatoznom polipozom (FAP) kao Gardnerov sindrom. **Prikaz bolesnika.** Bolesnica, stara 34 godine, javila se na pregled sa palpabilnom solidnom tumorskom masom u levom hemiabdomenu. Kompjuterizovanom tomografijom (KT) sa aplikacijom kontrastnog sredstva i magnetno-rezonantnim (MR) snimanjem otkrivene su višestruke solidne tumefakcije u mezenterijumu, kao i između crevnih vijuga tankog creva. Kolonoskopijom su viđeni multipli sesilni polipi karakteristični za FAP. Ultrazvučno navođenom biopsijom dobijeni su uzorci tkiva mezenterične mase sa patohistološkom verifikacijom DF, uz primenu imunohistohemijske analize. Procenjeno je da je rizik od hirurške intervencije prevelik s obzirom na veličinu promene i njen odnos prema mezenterijalnim vaskularnim strukturama, zbog čega je planirana hemioterapija, uz potencijalnu naknadnu hiruršku reevaluaciju. **Zaključak.** Mezenterijalna fibromatoza je retka neoplazma sa širokim spektrom histoloških i slikovnih karakteristika. KT i MR snimanje igraju važnu ulogu u proceni i planiranju optimalnog terapijskog modela kod bolesnika sa mezenterijalnom fibromatozom.

Ključne reči:

biopsija iglom; kolonoskopija; dijagnoza; fibromatoza, abdominalna; fibromatoza, agresivna; imunohistohemija; magnetna rezonanca, snimanje; mezenterijum; tomografija, kompjuterizovana, rendgenska.

Introduction

Aggressive fibromatosis, also known as desmoid type fibromatosis (DF) is a locally aggressive fibroblastic neoplasm that can arise anywhere in the body with no potential for metastasis and a high recurrence rate after surgical resection. The term desmoid was first used by Muller in 1838 and is derived from the Greek word *desmos* meaning band or tendon ¹. DF is a rare neoplasm with an estimated annual incidence of 2–4 cases per million people, accounting for approximately 0.03% of all neoplasms and less than 3% of all soft tissue tumors ². It is commonly seen in the reproductive years of women, often during and after pregnancy ¹. By their location, these tumors can be classified as intraabdominal, extraabdominal, or abdominal wall. Mesenteric fibromatosis is locally aggressive DF of the mesentery with a high propensity for bowel involvement ³. The real etiology of these tumors remains unknown, occurring sporadically or in association with familial adenomatous polyposis (FAP) as Gardner's syndrome ^{2, 3}. While they are non-metastasising, they can be locally aggressive, causing symptoms due to pressure effect, which can lead to complications such as small bowel obstruction, ischemia and perforation ⁴.

We presented a case of FAP-associated aggressive mesenteric fibromatosis, presenting as a palpable abdominal mass, with computed tomography (CT) and magnetic resonance imaging (MRI) findings of this rare neoplasm.

Case report

A 34-year-old female patient presented with a palpable solid tumefactive mass in the left hemiabdomen. On abdominal examination, the mass was firm, approximately 22 x 20 cm in diameter, immobile with no associated tenderness. Her general physical examination was unremarkable. All her baseline blood investigations were normal. Contrast enhanced CT revealed multiple massive solid tumefactions in the mesentery and in between the small bowel loops, inhomogeneous in structure, the largest one being approximately 131 x 101 x 190 mm in diameter (Figure 1). CT angiography of the abdomen revealed the tumor was vascularized via branches of the superior mesenteric artery, with venous drainage via the superior mesenteric vein. There was no significant reduction of lumen of the celiac trunk and superior mesenteric artery. A colonoscopy was performed

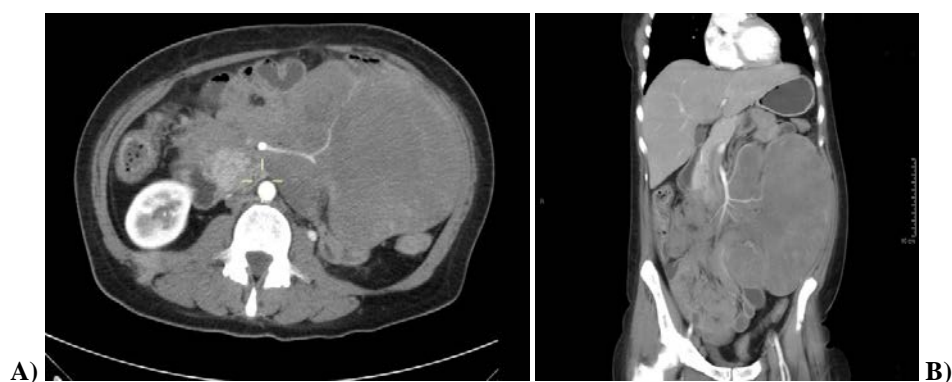


Fig. 1 – Contrast enhanced computed tomography (CT) of the abdomen: A) transversal and B) coronal images show. A large inhomogeneous solid mass in the mesentery with arterial supply via branches of the superior mesenteric artery.

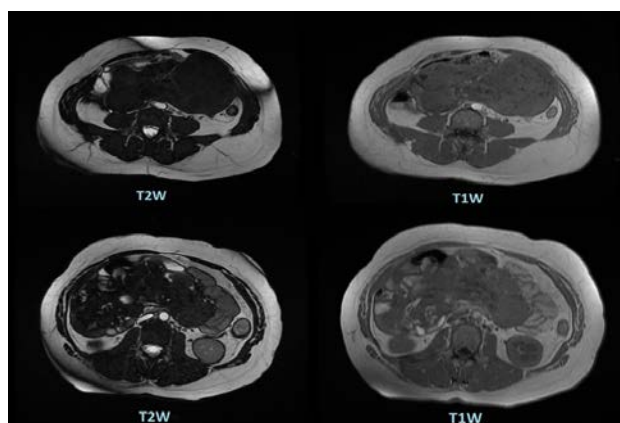


Fig. 2 – Magnetic resonance imaging scan. Transversal T2W and T1W images. Massive tumor formation stretching from the ascending colon to the anterior abdominal wall bearing a T2W hypointense signal with relative T1W isointensity.

which confirmed the presence of multiple sessile polypomatous lesions of different diameter characteristic of FAP with similar lesions visible in the stomach and duodenum on esophagogastroduodenoscopy. An MRI scan of the abdomen was performed a little bit later, showing a massive intraabdominal tumor formation, stretching from the ascending colon through the mesentery to the anterior abdominal wall, with slight compression of the left rectus abdominis muscle and contact with the descending colon. The tumor was hypointense on T2 weighted images, with a relative isointensity on T1W scans and no signs of restricted diffusion (Figure 2). There was mild dominantly peripheral inhomogeneous alteration of signal after a paramagnetic contrast was administered with prominent central hypovascularity (Figure 3). The superior mesenteric artery and celiac trunk were within close proximity of the tumor tissue with no signs of vascular compression or thrombosis.

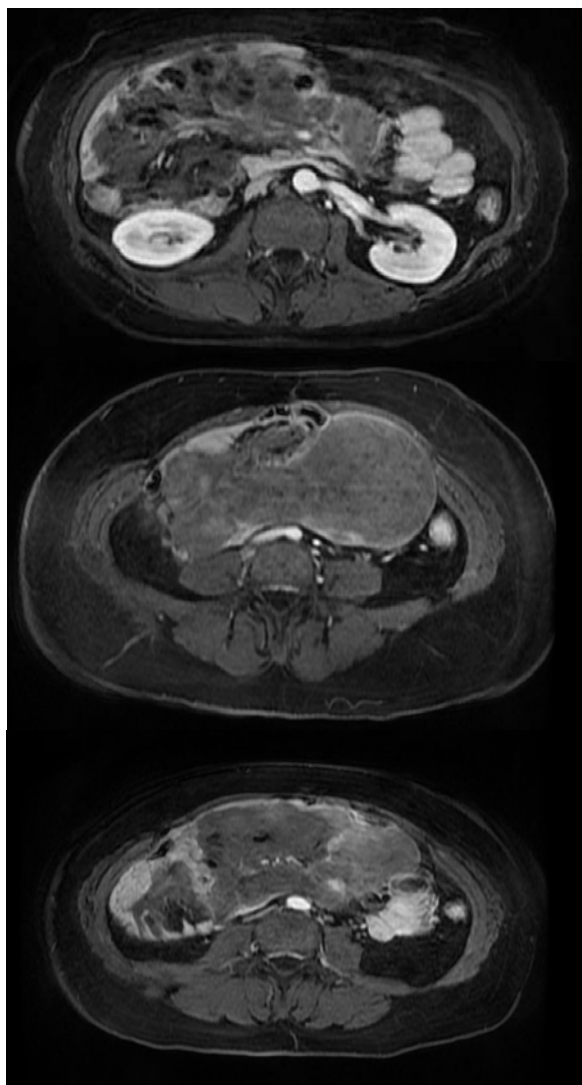


Fig. 3 – Magnetic resonance imaging scan. Transversal gadolinium enhanced liver acquisition with volume acquisition images showing mild enhancement of the lesion with prominent central hypovascularity.

Tissue samples were acquired via ultrasound guided biopsy with histopathologic confirmation of DF with imunohistochemical analysis. After an abdominal surgeon was consulted, it was concluded that there was an increased risk of surgery due to the size of the lesion and increased possibility of bleeding, therefore the patient was planned for chemotherapy with potential further reevaluation for a possible surgical procedure.

Discussion

Desmoid tumors are rare tumors arising from musculoaponeurotic elements accounting for 0.03% of all tumors and 3.5% of all fibrous tissue tumors⁵. Patients with FAP, Gardner's syndrome, are especially predisposed to the development of mesenteric fibromatosis⁶. FAP is an autosomal dominant disease, caused by a germline mutation in the adenomatous polyposis coli tumor suppressor gene leading to the development of multiple colorectal adenomatous polyps. The modern management of FAP, incorporating predictive genetic testing and prophylactic surgery, has meant that extracolonic manifestations of FAP, particularly desmoid tumors and polyposis of the upper gastrointestinal tract are now the leading cause of mortality among patients having gone prophylactic colectomy⁷⁻⁹.

Desmoid tumors develop in approximately 10% of patients with FAP and most are intraabdominal, following a more aggressive course with recurrence after resection being common. Aggressive mesenteric desmoids can lead to small bowel obstruction, ischaemia and perforation with surgical excision being difficult, due to their proximity to the superior mesenteric artery⁴.

The most common imaging modalities used for detection and evaluation of DF are CT and MRI. Imaging characteristics of DF closely reflect the distribution of histologic components: spindle cells, myxoid matrix and collagenous stroma¹⁰. These tumors appear as soft tissue masses that are either sharply margined or with ill-defined infiltrative margins¹¹. On CT images attenuation is variable, with the majority of masses demonstrating mild to moderate enhancement¹². The signal intensity of the tumor on MRI is highly dependable on the proportion of collagen fibers, spindle cells and extracellular matrix present, with decreased signal intensity on T2 weighted images most likely resulting from dense collagen and hypocellularity, while increased T2 signal intensity reflects a high content of spindle cells¹³⁻¹⁵. Gadolinium enhancement is variable, with more prominent enhancement being present in the more cellular, less fibrotic areas.

Our mass demonstrated a significant signal hypointensity on T2 weighted images and mild gadolinium enhancement, which would suggest a very dominant presence of collagenous stroma.

Wide field surgical resection is the first line of treatment for most mesenteric fibromatosis with most cases requiring resection of the attached segment of the bowel³. Neurovascular structure encasement as well as invasion of the viscera should be detectable by imaging and included in

the radiologists report. Lesion location, multiplicity, infiltrative margins and relationship with mesenteric vessels and intraabdominal organs are important surgical considerations². In our case, due to the localization of the tumor and its close proximity to the mesenteric vascular structures, the risk of surgery was deemed too high at the time, therefore chemotherapy was planned to achieve reduction in tumor size, which would make a future surgical procedure possible.

Conclusion

Mesenteric fibromatosis is a rare neoplasm that presents with a wide range of histologic and imaging features. CT and MRI are the imaging modalities of choice in the management of mesenteric fibromatosis. Defining lesion characteristics, localization, neurovascular and visceral affection are key in evaluating the potential for surgical resection, therefore playing a crucial role in planning an optimal treatment model.

REFERENCES

1. Mukut D, Ghalige HS, Santhosh R, Sharma MB, Singh TS. Mesenteric fibromatosis (Desmoid tumour) – a rare case report. *J Clin Diagn Res* 2014; 8(11): ND01–2.
2. Braschi-Amirfarzan M, Keraliya AR, Krajewski KM, Tirumani SH, Shinagari AB, Hornick JL, et al. Role of imaging in management of desmoid-type fibromatosis: A primer for radiologists. *Radiographics* 2016; 36(3): 767–82.
3. Gari MK, Guraya SY, Hussein AM, Hego MM. Giant mesenteric fibromatosis: Report of a case and review of the literature. *World J Gastrointest Surg* 2012; 4(3): 79–82.
4. Sinha A, Hansmann A, Bhandari S, Gupta A, Burling D, Rana S, et al. Imaging assessment of desmoid tumours in familial adenomatous polyposis: Is state-of-the-art 1.5 T MRI better than 64 MDCT? *Br J Radiol* 2012; 85(1015): e254–61.
5. Tseng KC, Lin CW, Tzeng JE, Feng WF, Hsieh YH, Chou AL, et al. Gardner's syndrome – emphasis on desmoid tumours. *Tzu Chi Med J* 2006; 18: 57–60.
6. Wronski M, Ziarkiewicz-Wroblewska B, Slodkowski M, Cebulski W, Gornicka B, Krasnodebski IW. Mesenteric fibromatosis with intestinal involvement mimicking a gastrointestinal stromal tumor. *Radiol Oncol* 2011; 45(1): 59–63.
7. Vasen HF, Moslein G, Alonso A, Aretz S, Bernstein I, Bertario L, et al. Guidelines for the clinical management of familial adenomatous polyposis (FAP). *Gut* 2008; 57(5): 704–13.
8. Bulow S. Results of national registration of familial adenomatous polyposis. *Gut* 2003; 52: 742–6.
9. Heiskanen I, Luostarinen T, Jarvinen HJ. Impact of screening examinations on survival in familial adenomatous polyposis. *Scand J Gastroenterol* 2000; 35: 1284–7.
10. Vandevenne JE, De Schepper AM, De Beuckeleer L, Van Marck E, Aparasi F, Bloem JL, et al. New concepts in understanding evolution of desmoid tumors: MR imaging of 30 lesions. *Eur Radiol* 1997; 7(7): 1013–9.
11. Shinagare AB, Ramaiya NH, Jagannathan JP, Krajewski KM, Giardino AA, Butrynski J, et al. A to Z of desmoid tumors. *AJR Am J Roentgenol* 2011; 197(6): W1008–14.
12. Murphey MD, Ruble CM, Tyszkowski SM, Zbojnicki AM, Potter BK, Miettinen M. From the archives of the AFIP: musculoskeletal fibromatoses: radiologic-pathologic correlation. *RadioGraphics* 2009; 29(7): 2143–73.
13. McCarville MB, Hoffer FA, Adelman CS, Khoury JD, Li C, Skapek SX. MRI and biologic behavior of desmoid tumors in children. *AJR Am J Roentgenol* 2007; 189(3): 633–40.
14. Kasper B, Baumgarten C, Bonvalot S, Haas R, Haller F, Hobenberger P, et al. Management of sporadic desmoid-type fibromatosis: a European consensus approach based on patients' and professionals' expertise—a sarcoma patients EuroNet and European Organisation for Research and Treatment of Cancer/Soft Tissue and Bone Sarcoma Group initiative. *Eur J Cancer* 2015; 51(2): 127–36.
15. Guglielmi G, Cifaratti A, Scalzo G, Magarelli N. Imaging of superficial and deep fibromatosis. *Radiol Med* 2009; 114(8): 1292–307.

Received on July 22, 2020

Revised on September 8, 2020

Accepted on September 22, 2020

Online First September, 2020



Ring chromosome 20: a further contribution to the delineation of epileptic phenotype

Ring hromozom 20: doprinos boljem sagledavanju karakteristika epileptičnog fenotipa

Milan Borković*, Goran Čuturilo^{†‡}, Nataša Cerovac*[†]

*Clinic for Neurology and Psychiatry for Children and Youth, Belgrade, Serbia;

[†]University of Belgrade, Faculty of Medicine, Belgrade, Serbia; [‡]University Children's Hospital, Belgrade, Serbia

Abstract

Introduction. Ring chromosome 20 [r(20)] syndrome is a rare genetic abnormality where two arms of the 20th chromosome fuse forming a ring chromosome, resulting in intractable epilepsy and wide range of behavioral problems and cognitive deficits. **Case report.** We presented four patients with r(20) syndrome diagnosed between the years 2000–2018. In all patients we analyzed clinical epilepsy features (seizure semiology, seizure frequency/drug response, the presence of nonconvulsive status epilepticus), cognitive status and the phenotype characteristics. The average age of epilepsy onset was 6 years. All four patients had nocturnal epileptic events and normal brain magnetic resonance (MR) imaging. Dysmorphism was present in two children, behavioral problems also in two children and intellectual disabilities were observed in three children. R(20) syndrome mosaicism ranged between 17% and 83% of blood lymphocytes. **Conclusion.** Despite the small size of our group, we think that our findings have clinical relevance. Refractory childhood onset epilepsy and especially the occurrence of nocturnal epileptic events should help physicians to recognize this chromosomopathy. Routine karyotyping can be employed to identify the patients easily.

Key words:

chromosome aberrations; clinical medicine; cognitive dysfunction; drug resistant epilepsy; ring chromosome 20 syndrome; drug therapy.

Apstrakt

Uvod. Sindrom prstenastog hromozoma 20 (r20) je veoma retka genetička abnormalnost, gde se dva kraka 20. hromozoma spajaju i formiraju prstenasti hromozom, što dovodi do farmakorezistentne epilepsije i širokog spektra poremećaja u ponašanju i kognitivnog deficita. **Prikaz bolesnika.** Prikazana su četiri bolesnika sa r(20) sindromom dijagnostikovanim između 2000. i 2018. godine. Kod svih bolesnika su analizirane kliničke karakteristike epileptičkih napada (semiologija napada, njihova učestalost/odgovor na terapiju, prisustvo nekonvulzivnog epileptičnog statusa), kognitivni status i fenotipske karakteristike. Napadi su se u proseku javljali u uzrastu od 6 godina. Sva četiri bolesnika su imala suptilne noćne napade i normalne nalaze magnetne rezonance (MR) mozga. Dismorfizmi su bili prisutni kod dva deteta, problemi u ponašanju kod dva deteta, a kognitivni deficit kod tri deteta. Hromozomski mozaicizam r(20) kretao se između 17% i 83% limfocita krvi. **Zaključak.** Uprkos malom broju ispitanika, smatramo da dobijeni rezultati imaju klinički značaj. Farmakorezistentna epilepsija sa početkom u dečjem uzrastu i posebno pojava noćnih napada je karakteristična za sindrom prstenastog hromozoma 20, a može se jednostavno dijagnostikovati analizom kariotipa.

Ključne reči:

hromozomi, aberacije; medicina, klinička; saznanje, poremećaji; epilepsija, farmakorezistentna; ring hromozom 20 sindrom; lečenje lekovima.

Introduction

Ring chromosome 20 [r(20)] syndrome is a rare genetic abnormality that occurs in about 1/30,000 to 1/60,000 living births¹. It was described for the first time in 1972 by Atkins et al.², with roughly 150 individuals

reported worldwide^{2–4}. It is hypothesized that telomere regions of the short arm 20p13, and long arm 20q13.3, fuse to form the ring chromosome^{3,4}. During this fusion, inversions, mutations, deletions and duplications can happen, which result in intractable epilepsy and a wide range of behavioral problems and cognitive deficits, while dys

morphic signs are not significant¹. The 20q13.3. locus contains at least two channel genes that have been related to epilepsy. The first one is CHRNA4 (nicotinic acetylcholine receptor) that has been related to autosomal dominant nocturnal frontal lobe epilepsy (ADNFLE). The second gene is potassium channel gene KCNQ2, which is responsible for benign familial neonatal epilepsy (BFNE)^{5, 6}. However, ADNFLE and BFNE manifest with a clearly different clinical presentation, suggesting pathogenetic mechanism whose contributions likely differ in r(20) syndrome⁷.

The main concern, considering this diagnosis in a patient with epilepsy occurring in childhood or adolescence, is associated with the changes in intellectual capacities and behavior, because early diagnosis could help with adequate treatment. The ring abnormality may be seen in as few as 10% of all cells and therefore cytogenetic analysis for chromosomal mosaicism is crucial for the diagnosis. It has been recommended to use standard metaphase chromosome analysis, examining at least 50 cells to properly detect mosaicism⁸.

We presented four patients with the genetically confirmed diagnosis of r(20) with intent to analyze clinical parameters (sex, the age at the onset of epilepsy and the age of confirmed diagnosis, family history, the presence of dysmorphism, behavioral problems, intellectual functioning, brain magnetic resonance imaging (MRI) results, genetic findings), including clinical epilepsy features [presence of nonconvulsive status epilepticus (NCSE), seizure type and frequency], antiepileptic therapy and the refractory nature of epilepsy in patients with genetically confirmed diagnosis of r(20).

Case report

Four patients (1 male, 3 females, mean age 13 years – range from 9 to 18 years) were presented with the diagnosis of r(20) syndrome at ages 7–12. All patients had refractory epilepsy and were clinically evaluated and treated at the Clinic for Neurology and Psychiatry for Children and Youth, Belgrade, between the years 2000–2018. The electroencephalography (EEG) pattern demonstrated long-lasting, bilateral, paroxysmal high-voltage slow waves, with occasional spikes over the frontal/temporal lobes lasting for several minutes in-

terictally or during the seizures in all patients. Karyotyping was done at University Children's Hospital-Tiršova in Belgrade. They were diagnosed by cytogenetic analysis, which was performed using G-banding on lymphocytes from each proband. Conventional protocols were used to set up the cultures and chromosome preparations. Because of possible chromosomal mosaicism, metaphase count was extended to at least 100 cells for all patients.

In all patients, we analyzed the following parameters: sex and age of patients (years), age at seizure onset (years) and age at confirmed diagnosis of r(20) (years). Also, we evaluated the family history, the presence of dysmorphism, behavioral problems and intellectual disability [intelligence quotient (IQ) < 71]. Structural brain MRI was done and analyzed in all patients. Genetic analysis and the degree of mosaicism ranging from 1–100% of lymphocytes were evaluated in all patients, too.

We also analyzed the presenting epileptic phenotype: the presence of NCSE, seizure features and frequency, antiepileptic therapy and the refractory nature of epilepsy.

The average age of epilepsy onset was 6 years (range from 4.5 to 7 years) and the final diagnosis was made from the age of 7 to 12 years. Family history was negative pointing to a genetic syndrome. Dysmorphisms were present in two subjects (mild facial abnormalities in both) and growth failure in one, whereas behavioral problems (attention deficit and irritability) were identified in two subjects. Intellectual disabilities were observed in three subjects and absent in one. The child with normal intellectual functioning is attending regular school, while the other three require personal supervision. Brain MRIs were performed in all subjects, and were normal. Karyotype analysis in all the patients confirmed the presence of r(20) chromosomal abnormality with different percentage of mosaicism ranging between 17% and 83% of blood lymphocytes (Table 1, Figure 1).

NCSE was present in two patients. Nocturnal epileptic events were observed in all our patients, while tonic-clonic seizures and convulsive status epilepticus occurred in two patients (Figure 2). After confirming the diagnosis of epilepsy, all the patients were on multiple antiepileptic drugs in mono- and polytherapy. Seizures were drug-resistant and all patients experienced frequent (daily and weekly) seizures, in spite of the therapy with many antiepileptic drugs: carbamazepine, clobazam, lamotrigine, levetiracetam, lacosamide,

Table 1

Clinical and genetic features of ring chromosome 20 [r(20)] patients

Patient	Sex/Age at the study (years)	Epilepsy onset age (years)	Age at diagnosis (years)	FH	Dysmorphisms	Behavioral problems	Intellectual disability	MRI	r (20) mosaicism (% of blood lymphocytes)
1	F/9	4.5	7.5	NR	+ mild facial, growth failure	-	yes	N	17
2	F/13	5	11	NR	-	-	yes	N	68
3	M/11	7	7	NR	-	+ attention deficit	no	N	48
4	F/18	6	12	NR	+ mild facial	+ irritability	yes	N	83

M – male; F – female; FH – family history; MRI – magnetic resonance imaging; NR – not reported; N – normal.

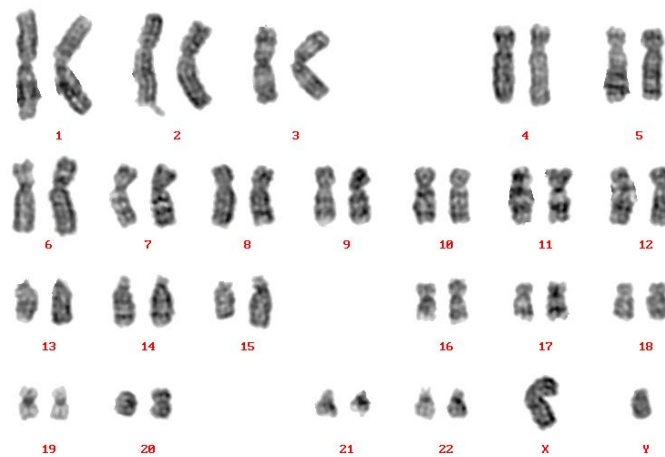


Fig. 1 – Karyotype analysis shows the presence of ring chromosome 20 [r(20)] abnormality.

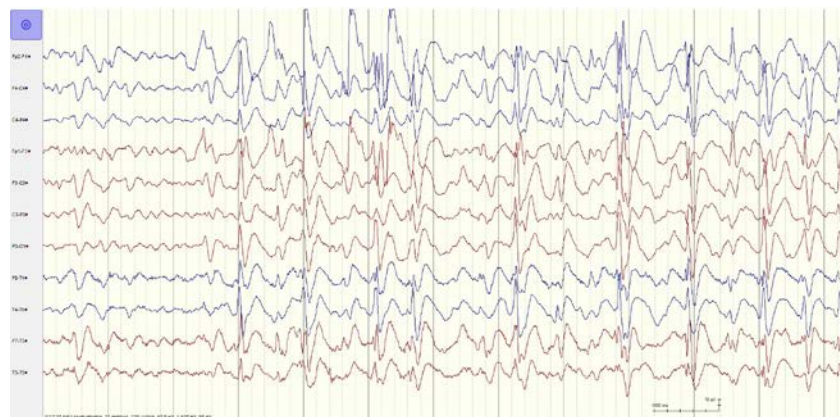


Fig. 2 – Electroencephalography (EEG) finding shows ictal EEG: atypical absence-epileptic status.

Table 2

Epilepsy features of ring chromosome 20 [r(20)] patients							Treatment	
Patient	NCSE	Subtle nocturnal seizures	Tonic-clonic seizures	CSE	Daily seizures	Nocturnal hypermotor seizures	no improvement	improvement in seizures
1	-	+	-	-	+	+	VPA monotherapy	VPA+LTG ketogenic diet
2	+	+	+	+	+	+	TPM, OXC, VPA, LEV, LCS, PRM ketogenic diet	LTG+ETS, VNS
3	-	+	-	-	+	+	CBZ, LEV, CLB	VPA+LTG ketogenic diet
4	+	+	+	+	+	+	CBZ, VPA, TPM, ketogenic diet	LTG, VNS

NCSE – nonconvulsive status epilepticus; CSE – convulsive status epilepticus; VPA – valproate; LTG – lamotrigine; TPM – topiramate; OXC – oxcarbazepine; LEV – levetiracetam; LCS – lacosamide; PRM – primidon; ETS – ethosuximide; VNS – vagal nerve stimulation; CBZ – carbamazepine; CLB – clobazam.

ethosuximide, topiramate, valproate, oxcarbazepine, primidone. Seizures were worsened by topiramate in two patients and by carbamazepine and levetiracetam also in two patients. An antiepileptic combination therapy which offered both remarkable seizure control and tolerable quality of life was valproate and lamotrigine. In two patients this combination succeeded in reducing the seizure frequency. In one patient lamotrigine monotherapy was effective, and in an-

other one the combination of lamotrigine and ethosuximide. In this way, the most common antiepileptic drug taken was lamotrigine. All patients were also tried on a ketogenic diet, with a significant decrease in seizures in two patients (other two patients showed no improvement on ketogenic diet and it was discontinued). Vagal nerve stimulation succeeded in reducing the seizure frequency in two patients (Table 2).

Discussion

We have described epileptic phenotype of r(20) syndrome in four patients aged 9 to 18 years. All patients with a confirmed cytogenetic diagnosis of r(20) syndrome had drug-resistant frontal lobe seizures, two of them had recurrent NCSE and all patients showed characteristic EEG pattern involving frontotemporal lobes. These three electroclinical characteristics easily recognizable in childhood have been found repeatedly in patients with this chromosomal disorders and are, therefore, thought to be highly suggestive of r(20) syndrome⁹⁻¹².

The recurrent NCSE features displayed a prolonged confusional state of varying intensity, staring, a frightened expression and mild gestural automatism, reduced spontaneous motor activity and speech production with slowness of response and behavior^{1,4,5}. These features were observed in two patients. Refractory frontal lobe seizures include three types of seizures and were observed in all our patients.

Nocturnal seizures (hypermotor) are manifested by waking up, staring, mild tonic stiffening evolving to clonic movements of the face and extremities, followed by agitation and confusion. Subtle nocturnal seizures are expressed as minimal motor activity, such as stretching, turning of body, or rubbing. We underline the characteristic occurrence of nocturnal subtle seizures, especially in children, which should, in our opinion, be considered highly suspicious of r(20)⁹. Focal impaired awareness seizures consists of dyscognitive symptoms, blank staring, with or without oral or motor automatisms, frightened expression, sometimes evolving to bilateral tonic-clonic seizure, and focal aware seizures with motor symptoms including head turning¹⁰. The characteristic EEG patterns consists of brief frontal epileptic discharges, long-lasting high-voltage slow waves with occasional spikes usually predominant over the frontal lobes and frequent trains of theta waves in frontotemporal areas^{13,14}.

In our study group, the age at the onset of seizures was between 4.5 and 7 years and ictal fear was noticed in all children. The most frequently reported patients' fears concerned animals as insects, spiders and snakes. Consistent with other studies, our data indicate that at epilepsy onset, especially in childhood, patients experience attacks of sudden fear during frontal lobe seizures, which is related to an earlier age at seizure onset⁴. It is a characteristic feature of the syndrome and may be helpful in establishing the diagnosis^{4,9,15}. It has been confirmed that the fear feeling connected with seizures originates from frontotemporal or frontal lobes. The analysis of intracranial ictal EEGs and observations of clinical manifestations precipitated by electrical stimulation has confirmed that the limbic structures, especially the amygdale, are closely linked to fear⁴. Interictal positron emission tomography (PET) and single photon emission computed tomography (SPECT) studies provided evidence for the participation of subcortical structures and basal ganglia in the control of epileptic seizures in r(20) syndrome¹³. They showed dopaminergic disturbances in the ni-

grostriatal system that could be related to the genesis and maintenance of prolonged seizures and NCSE in r(20). Furthermore, the involvement of the cortical-subcortical network in epileptic manifestation of patients with r(20) syndrome was revealed by means of ictal EEG-fMRI. Altogether, these data support a hypothesis that a dysfunction of the frontal lobes-basal ganglia network is a key feature of this chromosomal disorder^{4,13}.

Concerning dysmorphism, in our series two patients displayed mild facial abnormalities and one patient growth failure. Growth failure is present in all the ring chromosome syndromes and is considered to be a constitutive feature of the majority of chromosomal abbreviations¹¹. Mild to moderate cognitive impairment and behavioral problems are very frequent^{4,9}. Three of our patients, however, had cognitive impairment and two of them behavioral difficulties before the onset of epilepsy. This cognitive deficit is associated with the frontal lobe involvement, probably due to epileptiform discharges, cognitive brain network activity and dopaminergic deficits¹⁶.

Because of the wide spectrum of clinical expressions and the rarity of this chromosomal disorder, the time gap from the onset of epilepsy to the diagnosis is usually considerable¹¹. For instance, in two patients (patient 2 and 4), six years passed between the onset of epilepsy and the final diagnosis. Most of the patients have a normal brain MRI, as was seen in all our patients¹⁷.

At the chromosomal level, r(20) replaces one of the two chromosome 20 in a percentage of cells, ranging from 1% to 100% of lymphocytes. The relation between the variable mosaicism and the clinical phenotype has been and is still controversial, although the studies have shown that a high degree of mosaicism is associated with the earlier age at the seizure onset, but not with the response to the drug treatment^{1,8}. In our series we did not see a correlation between a high degree of mosaicism compared to the age of seizure onset.

All patients with r(20) in our study group had refractory epilepsy despite multiple antiepileptic drugs tried singly or in combination. According to the results of other studies, the refractory nature of epilepsy in patients with r(20) is a common finding⁴. In all of our patients, lamotrigine was very effective. In two patients, a combination of valproate and lamotrigine allowed better seizure control and this combination is supported in the literature as very effective for treating epilepsy^{4,13}. One patient improved with a combination of lamotrigine and ethosuximide and another patient with lamotrigine as monotherapy. Two patients also improved with vagus nerve stimulation, in line with the previous reports. All patients were treated with a ketogenic diet, resulting in significant improvement in seizure control only in two patients.

In general, the prognosis is showing seizure worsening over a long period of time¹¹. The histories of patients 1, 2 and 4 illustrate this unfavorable outcome. There is only one case report with favorable seizure control in patient 3 with the progressive stabilization of refractory epilepsy. He has infrequent seizures on a monthly basis, lives independently

and goes regularly to school, although refractory epilepsy prevents him from certain activities.

Conclusion

Neuroimaging-negative refractory childhood onset epilepsy, accompanied by variable cognitive delay, behavioral problems and the absence of a consistent pattern of dysmorphic features should help physicians to recognize possible genetic disorder. These patients should be referred to genetic counseling, where proper genetic testing will be of-

fered. It is important to reduce a considerable gap between the onset of epilepsy and the diagnosis in these patients, in order to give adequate treatment and avoid long term deterioration in the patients' quality of life. We described the small group of r(20) patients, delineating semiology and age-dependent course of epilepsy. Subtle nocturnal seizures showed better sensitivity than NCSE in diagnosing r(20) syndrome. The disadvantage of that case includes the lack of the possible correlation between a delayed diagnosis and a cognitive outcome, which should be interesting to evaluate in future studies.

REFERENCES

1. Conlin LK, Kramer W, Hutchinson AL, Li X, Riethman H, Hakonarson H, et al. Molecular analysis of ring chromosome 20 syndrome reveals two distinct groups of patients. *J Med Genet* 2011; 48(1): 1–9.
2. Atkins L, Miler WL, Salam M. A ring-20 chromosome. *J Med Genet* 1972; 9(3): 377–80.
3. Borgaonkar DS, Lacassie YE, Stoll C. Usefulness of chromosome catalog in delineating new syndrome. *Birth Defects Orig Artic Ser* 1976; 12(5): 87–95.
4. Vignoli A, Bisulli F, Darra F, Mastrangelo M, Barb C, Giordano L, et al. Epilepsy in ring chromosome 20 syndrome. *Epilepsy Res* 2016; 128: 83–93.
5. Inoue Y, Fujiwara T, Matsuda K, Kubota H, Tanaka M, Yagi K, et al. Ring chromosome 20 and nonconvulsive status epilepticus. A new epileptic syndrome. *Brain* 1997; 120(Pt 6): 939–50.
6. Canevini MP, Sgro V, Zuffardi O, Canger R, Carrozzio R, Rossi E, et al. Chromosome 20 ring: a chromosomal disorder associated with a particular electroclinical pattern. *Epilepsia* 1998; 39(9): 942–51.
7. Scheffer IE, Bhatia KP, Lopes-Cendes I, Fish DR, Marsden CD, Andermann E, et al. Autosomal dominant nocturnal frontal lobe epilepsy. A distinctive clinical disorder. *Brain* 1995; 118(Pt 1): 61–73.
8. Giardino D, Vignoli A, Ballarati L, Recalcati MP, Russo S, Camporeale N, et al. Genetic investigations on 8 patients affected by ring 20 chromosome syndrome. *BMC Med Genet* 2010; 11: 146.
9. Gago-Veiga AB, Toledano R, Garcia-Morales I, Perez-Jimenez MA, Bernar J, Gil-Nagel A. Specificity of electroclinical features in the diagnosis of ring chromosome 20. *Epilepsy Behav* 2018; 80: 215–20.
10. Daber RD, Conlin LK, Leonard LD, Canevini MP, Vignoli A, Hosain S, et al. Ring chromosome 20. *Eur J Med Genet* 2012; 55(5): 381–7.
11. Elens I, Vanrykel K, De Waele L, Jansen K, Segeren M, Van Paesschen W, et al. Ring chromosome 20 syndrome: Electroclinical description of six patients and review of the literature. *Epilepsy Behav* 2012; 23(4): 409–14.
12. Walleigh DJ, Ledigo A, Valencia I. Ring chromosome 20: A Pediatric Potassium Channelopathy Responsive to Treatment with Ezogabine. *Pediatr Neurol* 2013; 49(5): 368–9.
13. Aranzini P, Vaudano AE, Vignoli A, Ruggieri A, Benuzzi F, Darra F, et al. Low frequency mu-like activity characterizes cortical rhythms in epilepsy due to ring chromosome 20. *Clin Neurophysiol* 2014; 125(2): 239–49.
14. Zou YS, Van Dyke DL, Thorland EC, Chhabra HS, Michels VV, Keefe JG, et al. Mosaic ring 20 with no detectable deletion by FISH analysis: Characteristic seizure disorder and literature review. *Am J Med Genet A* 2006; 140(15): 1696–706.
15. Zambrelli E, Vignoli A, Nobili L, Didato G, Mastrangelo M, Turner K, et al. Sleep in ring chromosome 20 syndrome: a peculiar electroencephalographic pattern. *Funct Neurol* 2013; 28(1): 47–53.
16. Vaudano AE, Ruggieri A, Vignoli A, Canevini MP, Meletti S. Emerging neuroimaging contribution to the diagnosis and management of the ring chromosome 20 syndrome. *Epilepsy Behav* 2015; 45: 155–63.
17. Radhakrishnan A, Menon RN, Hariharan S, Radhakrishnan K. The evolving electroclinical syndrome of “epilepsy with ring chromosome 20”. *Seizure* 2012; 21(2): 92–7.

Received on June 1, 2020

Revised on September 3, 2020

Accepted on September 22, 2020

Online First September, 2020

LETTER TO THE EDITOR
(RESEARCH LETTER)
(CC BY-SA) 



UDC: 929:61-05(091)

DOI: <https://doi.org/10.2298/VSP200410051J>

In Memory of Dr. Elizabeth Ross

Sećanje na dr Elizabetu Ros

To the Editor:

Following the outbreak of the First World War, the first humanitarian medical missions arrived in Serbia from the allied and neutral countries' Red Cross Societies¹. These Red Cross doctors and medical staff expressed great dedication and enthusiasm².

Kragujevac was one of "the main hospitalization centres for the wounded Serbs and prisoners of war". Early in 1915, four foreign medical missions arrived: English (located in the tents in Upper Park, with a capacity of one hundred beds), Russian (located at the Military Hospital, one of the two units of the Slovenian charity, with 18 members), Scottish (located in the school endowed by Milovan Gušić; the building was turned into a civilian hospital, thanks to Dr Elsie Maud Inglis; today the building is Radoje Domanović Elementary School) and French, to vaccinate Serbian soldiers and prevent an epidemic, already present in the vicinity of Kragujevac, from spreading. Due to poor medical care, the epidemic affected the rural population, and tents with basic medical equipment were placed at various points along the Kragujevac–Topola–Mladenovac road³.

Late in 1914, another enemy, deadlier and more ruthless than the Austro-Hungarian soldiers, attacked Serbia. Within only a few months, 35,000 soldiers, between 100,000 and 200,000 civilians, and about a third of the medical staff⁴ died from typhoid in Serbia.

When the epidemic escalated, Serbia requested assistance from the Allies. Many countries, including Great Britain, France and Russia, helped Serbia by sending medical missions (200 doctors and 500 nurses), materials and equipment necessary to combat the typhoid fever epidemic. Elizabeth Ross, a young medical doctor of Scottish descent, was among them (Figure 1). She had volunteered and arrived in Kragujevac, where she cared for about 1,000 patients⁵.

Elizabeth Ross was born in Tain in 1878 into a progressive, wealthy, adventurous family. Her father was a banker, one of the directors at the Bank of Scotland in London. Her brother David worked for many years in Japan with the Hong Kong and Shanghai Bank. She had four sisters, one of whom was a professor of mathematics and science, and spent many



**Fig. 1 – Dr Elizabeth Ross
(graduation portrait)**

(<http://www.universitystory.gla.ac.uk/image/?id1=2845&id2=1129022825&p=4>)

years in India. Another sister was a secretary for an explosives company in Glasgow. Her third sister was also a qualified doctor, working in York. Her fourth sister became a farmer⁶.

Elisabeth Ross studied at the College of Queen Margaret and graduated in 1901, as one of the first women in the United Kingdom with a degree in medicine. After graduation, she briefly worked as a physician in Tain, before she became a medical officer for the Island of Colonsay. Contemporaries described her as an adventurous, open-minded, courageous woman, who did not allow anything or anyone to prevent her from carrying out her intentions. She travelled and studied the medicine of ancient Persia (now Iran), and in 1910 she accepted a post as a doctor onboard a ship, and travelled to India and Japan. She was the first female naval doctor in Great Britain⁷.

Dr Ross spent most of her career in humanitarian missions in Persia and then in Serbia. When she heard about the horrors faced by Serbia, she applied as a volunteer and came to Serbia in mid-January 1915, under the patronage of the Russian government. The French and the British did not allow women to volunteer, not even at the fronts where their own armies fought, and Elizabeth Ross asked for Russian

mediation. She was a doctor at the First Military Hospital in Kragujevac, the city heavily affected by the typhoid epidemic in 1915. Dr Ross must have known where she was going, but nothing could prepare her for the horrors of the epidemic in Serbia in those months. Serbia had 409 doctors at the beginning of the Great War, and most of them were assigned to the army (doctors in the Serbian employment, foreigners who came to Serbia in the initial months of the war, mostly contractors from Russia and Greece)⁸. Dr Elizabeth Ross arrived after a coded dispatch, sent by Dr Elizabeth Solto, reached the Scottish Women's Hospital headquarters in Britain. Serbian censorship, at the behest of the government, did not allow mentions of the epidemic, but dispatches stressed a demand for infectologists, epidemiologists, and nurses trained to care for febrile, infected patients. Dr Ross first went to Niš, and late in January of 1915 she volunteered to go to the Kragujevac hospital for typhoid patients, instead of to the Scottish Women's Hospital that was set up nearby. When she arrived at the First Reserve Military Hospital in Kragujevac, converted to typhoid patients' treatment facility, terrible scenes shocked her. There were only 200 beds in the hospital, with a large number of patients, so that two patients were lying in the same bed. There were not enough nurses. At the time of the typhoid epidemic, Kragujevac was justifiably called the "City of the Dead". The doctors and other medical staff were desperately trying to cope with typhoid, which was spreading incredibly fast. Treating the patients day and night, Dr Ross weathered the heaviest wave of the epidemic. Despite the horrible conditions and the belief that it would be very difficult to avoid contagion, she continued her work. "She knew she really hadn't much of a chance of surviving because typhus was rife and they didn't know at that time what caused it"⁸. In Kragujevac, she worked in the environment where doctors and nurses were lying sick among the patients, or had already passed away. In spite of this, she was ready to accept the risk. Unflinchingly, she worked round the clock. Clearly visible was her devoted effort to follow the course of European medicine and to implement it in the treatment of the Serbian people. Just a week after arriving in Kragujevac, Dr Ross began to feel the first signs of typhus. She continued working as long as she could stand on her feet. "All around her was collapsing, she was watching it with her own eyes, aware that the same fate was awaiting her; but in spite of the requests and admonitions to spare herself a bit, she fearlessly continued her work until the end. She was still braver in the disease, quietly lying, severely ill, in a very modest ward. The only thing she regretted was not being able to administer aid to our sick soldiers for longer", wrote her colleague and Head of the Kragujevac Hospital, Dr Dimitrije Antić⁹.

After 13 days of fighting the disease, Dr Elizabeth Ross died. It was February 14th 1915, on her 37th birthday. During the First World War, 22 British women lost their lives to typhoid in Serbia, attempting to aid wounded and sick soldiers¹⁰.

Dr Elizabeth Ross was buried with all military honors in the city cemetery in Kragujevac, in February of 1915¹¹. Two of her colleagues in the British humanitarian missions,

Lorna Ferris and Mabel Dearmer, repose next to her. There is an epitaph at the monument to the courageous British lady: "Here lies Dr Elizabeth Ross", and underneath it says in Cyrillic script "You gave your heart to the people of Serbia"¹² (Figure 2).



Fig. 2 – Gravestones of Dr Elizabeth Ross, Lorna Ferris and Mabel Dearmer in Kragujevac, Serbia (image courtesy of Aleksandra Tomić)

In memory of her heroism, the compassion she had for the Serbian people, and the ultimate sacrifice she made for them, the youth field unit of the Red Cross (established in 1986), as well as a street in the centre of Kragujevac, bear the name of Dr Elizabeth Ross. Traditionally, on 14th February each year, on the day of her death, the representatives of the city of Kragujevac, the British Embassy, the Red Cross and other organizations and associations, lay wreaths at the graves of the three British women, and commemorate these courageous humanitarians whose work and sacrifice are deeply respected in our historical and cultural tradition. On the centenary of her death, on 14th February 2015, her memorial plaque was uncovered in the courtyard of the Red Cross in Kragujevac¹³. Today, over a hundred years later, her grave is visited by the youth of the city of Kragujevac and all patriots, who cherish the memory of the brave and dedicated heroine of medicine, with love and pride (Figure 3).



Fig. 3 – The youth of the city of Kragujevac pays tribute to the heroines of the First World War in Serbia (www.srpskilegat.rs, riznicasrpska.net)

The personal and professional contribution of Dr Elisabeth Ross to the Serbian history and medicine is immense, and her life's struggle and life's work are even greater, and deeply admired ^{14, 15}.

This paper was written as a contribution to cherishing the memory of Dr Elisabeth Ross, the heroine of medicine who gave her heart and her life to the Serbian people.

Katarina Janićijević*, Maja Sazdanović†, Mirjana A. Janićijević Petrović‡, Zoran Kovačević§

**University of Kragujevac, Faculty of Medical Sciences,
*Department of Social Medicine, †Department of Histology
and Embriology, ‡Department of Ophthalmology,
Kragujevac, Serbia;
§Clinical Centre of Kragujevac, Department of
Ophthalmology, Kragujevac, Serbia**

R E F E R E N C E S

1. *Litrinjenko S.* How the epidemics of typhoid and relapsing fever were stopped in Serbia in 1915. *Srp Arh Celok Lek* 1995; 123(11–12): 328–30. (Serbian)
2. *Gavrilović V.* Women doctors in the wars of 1876–1945 in the territory of Yugoslavia. Belgrade: Scientific Society for the History of Health Culture of Yugoslavia; 1976. (Serbian)
3. *Antić D.* Typhoid fever in Kragujevac 1st Reserve Military Hospital 1914–15. In: *Stanojević V.* editor. History of Serbian military medicine: Our war medical experience. Belgrade: V. Stanojević; 1925. p. 314–28. (Serbian)
4. *Mikić D, Nedok A, Popović B, Todorović V, Kojić M.* Epidemics of infectious diseases and engagement of the Serbian military field hospitals on their prevention and treatment in the First World War. In: *Nedok A, Popović B, Todorović V*, editors. Serbian military medical service in the First World War. Belgrade: Medija centar „Odbrana“; 2014. pp. 269–309. (Serbian)
5. Huittinen VM. Finnish language in medicine on history, ideology and practice. *Duodecim* 2002; 118(9): 958–62. (Finnish)
6. *Mikić Ž, Lešić A.* Dr Elisabeth Ross: Heroine and Victim of World War I in Serbia. *Srp Arh Celok Lek* 2012; 140(7–8): 537–42. (Serbian)
7. Story: Biography of Doctor Elizabeth Ness MacBean Ross. Glasgow: University of Glasgow. Available from: universitystory.gla.ac.uk. [retrieved 2019 January 21].
8. *Nedok A.* Serbian military field hospital at the beginning of the war and in the great battles of 1914. In: *Nedok A, Popović B*, editors. Serbian military medical service 1914–1915. Belgrade: Ministry of Defence, Military Health Department and Academy of Medical Sciences of the Serbian Medical Society; 2010; pp. 25–76.
9. *Popović-Filipović S.* For Courage and Humanity: Scottish Women's Hospitals in Serbia, and with Serbs during the First World War 1914–1918: History of Humanity and Humanity in Serbian History. Belgrade: Signature; 2007. p. 186. (Serbian)
10. *Mikić Z.* Scottish Women's Hospitals – the 90th anniversary of their work in Serbia. *Med Pregl* 2005; 58(11–12): 597–608. (English, Serbian)
11. "Dr Elisabeth Ross – the Scottish saint of Serbia". Available from: www.scotsman.com [retrieved 2019 January 21].
12. Dr. Elizabeth Ness MacBean Ross. *Br Med J* 1915; 1(2828): 491.
13. Mapping Memorials to Women in Scotland. Plaque to Dr Elizabeth Ross. Available from: womenofscotland.org.uk. [retrieved 2019 January 22].
14. Serbian stamps honour WW1 heroines. Scotland, Edinburgh: BBC News; 2015.
15. Tain through time: Dr Elizabeth Macbean Ross. Available from: http://www.tainmuseum.org.uk/dr_elizabeth_ross_g.asp?page=151

Received on April 10, 2020
Revised on May 8, 2020
Accepted on May 11, 2020
Online First May, 2020

LETTER TO THE EDITOR
(RESEARCH LETTER)
(CC BY-SA) 



UDC: 616.419-07-079.4

DOI: <https://doi.org/10.2298/VSP2202204M>

Clinical alert: “non-clonal” myelodysplastic syndrome

Kliničko upozorenje: „neklonski” mijelodisplastični sindrom

To the Editor:

We report a peculiar case of a 43-year-old female with a history of chronic moderate neutropenia (WBC range: $2.7\text{--}3.4 \times 10^9/\text{L}$, neutrophil range $0.6\text{--}0.8 \times 10^9/\text{L}$) lasting for more than five years (first evaluation: November 2014; last follow-up: October 2020). Besides neutropenia, complete blood count was normal as well as detailed biochemical, immunological (rheumatoid factor, antinuclear antibodies, anti-dsDNA antibodies, anti-Sm antibodies, anti-cardiolipin antibodies, and C3/C4 complement levels) and virological testing (HIV, HBV, HCV, CMV, EBV, adenovirus). Bone marrow aspirate was done on two different occasions – in March 2015 and December 2017 and analyzed by two independent hematopathologists. Cytological findings showed normocellular marrow with 20% of megakaryocytes with hypolobulated or “pinball” nuclei. E/G ratio was 1/2.5 with normal morphological appearance of E-lineage. Dysgranulocytopoiesis was moderate (pseudo-Pelger cells, focal or complete hypogranulation in mature cell forms). Blast accounts for 3% of all nucleated cells. Bone marrow trephine biopsy showed normocellular marrow (50–60%) with normal architecture and maturation of all lines. G-lineage was presented mainly with mature forms and excess eosinophils. In addition, two centromedullary nodular

lymphoid infiltrates were found. Since such lymphoid infiltrates are common in patients with autoimmune disorders, we performed flow cytometry of lymphocytes from peripheral blood. This analysis showed only a slight reduction of the absolute number of NK-cells and a slight elevation of $\gamma\delta\text{T}$ -lymphocytes. Karyotype of the bone marrow cells was normal (46, XX) in 20 analyzed metaphases. *In vitro* growth of hematopoietic progenitors (CFU-GEMM, CFU-MK, BFU-E, CFU-GM) was normal. Next-generation sequencing testing (MLL Muncher Leukemielabor GmbH), using a gene panel with 63 genes of myeloid and lymphatic diseases, did not reveal any of the tested genes to be mutated. The patient did not have any episode of infection during more than five years of follow-up. In February 2016, a skin lesion localized on the thoracic wall was surgically removed (pathohistological examination showed superficial melanoma, Clarks II, Breslow 0.27mm, pT1b). The oncologist suggested just observation (last follow-up in September 2020).

One of the biggest challenges is separating myelodysplastic syndromes (MDS) from reactive (i.e., nonneoplastic) causes of cytopenia and dysplasia¹, or from a wide and heterogeneous spectrum of the so-called “indolent myeloid disorders” (Table 1)². Demonstration of morphological abnormalities of the bone marrow cells is

Table 1

Spectrum of indolent myeloid hematopoietic disorders (ICUS, IDUS, CHIP, CCUS) in comparison to myelodysplastic syndromes

Feature	ICUS	IDUS	CHIP	CCUS	MDS
Somatic mutation	-	-	+/-*	+/-*	+/-
Clonal karyotype abnormality	-	-	+/-*	+/-*	+/-
Marrow dysplasia	-	+	-	-	+
Cytopenia	+	-	-	+	+

Abbreviations: ICUS – Idiopathic cytopenia of unknown significance; IDUS – Idiopathic dysplasia of unknown significance; CHIP – Clonal hematopoiesis of indeterminate potential; CCUS – Clonal cytopenia of unknown significance; MDS – Myelodysplastic syndromes.

*clonal karyotype abnormality present in ≥ 2 metaphases and/or a somatic mutation present at $>2\%$ variant allele frequency (evaluation of mutations should include sequencing of panels incorporating at least 21 most frequently mutated MDS-related genes).

still the “gold standard” for diagnosis of MDS as well as cytopenia is a *sine qua non* for any MDS diagnosis¹. According to the 2016 revision of the WHO classification of myeloid neoplasms and acute leukemia¹, our patient fulfilled diagnostic criteria for MDS with multilineage dysplasia with chronic neutropenia as the most prominent hematological feature. However, the finding of normal *in vitro* growth of hematopoietic progenitors was inconsistent with the presumptive diagnosis of MDS, as we previously reported in a large cohort of MDS patients³. In addition, cytogenetic analysis and somatic mutation analysis of genes most frequently mutated in MDS⁴ failed to demonstrate the clonal origin of the disease in this patient.

Another very important issue adds to the difficulty of identifying refractory neutropenia as an MDS subtype. Namely, following the publication of the WHO 2008 classification, a study evaluating the inter-observer variability in MDS diagnosis found a discrepancy rate of 27%, mostly in the categories with unilineage dysplasia⁵.

However, significant inter-observer variability was not the case in our patient since two additional independent hematopathologists confirmed the preliminary cytological finding. Nevertheless, the diagnosis of refractory neutropenia remains difficult and does not to date reflect an international and reliable consensus on diagnostic criteria.

Taking all these facts into account, what to say to the patient with chronic neutropenia and undoubted persistent 2-lineage bone marrow dysplasia? Does she have or have not malignant disease called “MDS”? In which cases should the clinician perform molecular testing? What is the most appropriate term for the clinical condition in this patient (i.e., “non-clonal MDS”)? So many questions and so many dilemmas.

Dragomir Marisavljević, Andrija Bogdanović

**University of Belgrade, Faculty of Medicine,
Belgrade, Serbia**

R E F E R E N C E S


1. Arber DA, Orazi A, Hasserjian R, Thiele J, Borowitz MJ, Le Beau MM, et al. The 2016 revision to the World Health Organization classification of myeloid neoplasms and acute leukemia. *Blood* 2016; 127(20):2391–405.
2. NCCN Guidelines Version 1.2020-August 27, 2019. Myelodysplastic Syndromes. <http://medi-guide.meditool.cn/ympdf/A1721A1C-DA35-3F68-122A-3429A1F100BF.pdf>
3. Marisavljević D, Rolović Z, Sefer D, Basara N, Ilić D, Bosković D, Colović M. Biological and clinical significance of clonogenic assays in patients with myelodysplastic syndromes. *Med Oncol* 2002; 19(4): 249–59.
4. Kohlmann A, Bacher U, Schnittger S, Haferlach T. Perspective on how to approach molecular diagnostics in acute myeloid leukemia and myelodysplastic syndromes in the era of next-generation sequencing. *Leuk Lymphoma* 2014; 55: 1725–34.
5. Font P, Loscertales J, Benavente C, Bermejo A, Callejas M, Garcia-Alonso L, et al. Inter-observer variance with the diagnosis of myelodysplastic syndromes (MDS) following the 2008 WHO classification. *Ann Hematol* 2013; 92: 19–24.

Received on March 15, 2021

Revised on September 6, 2021

Accepted on December 30, 2021

Online First January, 2022

LETTER TO THE EDITOR
(RESEARCH LETTER)
(CC BY-SA) 



UDC: 355.11-055.2::355.357]:618-052
DOI: <https://doi.org/10.2298/VSP2202206J>

Clinical characteristics of gynecological patients treated in MINUSCA level II Military Hospital, Bangui, Central African Republic

Kliničke karakteristike ginekoloških pacijentkinja lečenih u MINUSCA vojnoj bolnici nivoa 2, Bangui, Centralnoafrička Republika

To the Editor:

Up until one century ago, armies were predominantly comprised of men. However, women are becoming more prevalent in modern armies in all countries worldwide, with about 30%, which is why appropriate gynecological care is necessary¹. Papers on this topic in professional journals are quite scarce, therefore, any experience of that matter is valuable in order to improve the health care of the female military staff.

The current division consists of five medical care levels applied by the United Nations Peacekeeping: basic level, level 1, level 2, level 3, and level 4². Nevertheless, this five-level organization of health care sometimes overlaps in the field, depending on the contingent and resource capabilities. Hence, there is no firm division^{3,4}. In practice, however, the need for gynecology and orthopedics services was recognized at level 2. On that account, we accept solutions that are beneficial and economically sustainable^{3,5}. Bearing in mind that national organizations of different medical care contingents are formed from different countries using their own terminology, there is a need to standardize the terminology for better understanding. For that reason, the English language and the 10th revision of the International

Classification of Diseases and Related Health Problems (ICD-10) are used.

Medical resources are planned according to the mandate of the peacekeeping operation, the medical infrastructure, geographical factors, and the estimated medical threats^{6,7}. Procurement of equipment, necessary instruments, apparatus, medicine, and a gynecologist trained to provide the necessary medical procedures has proven to be the most important factor in practice.

The aim of this paper was to present our experiences in providing gynecological care to female military staff engaged in a peacekeeping mission in the Central African Republic (CAR) during the period from May 29, 2019, to March 1, 2020. The survey included patients treated in the Gynecological Clinic of MINUSCA Level II Hospital, Bangui, CAR. We performed 369 examinations/treatments: 68% related to patients with gynecological problems and 32% to pregnant women. The mean age of the patients was 27.2 years. Observing the regional-geographical affiliation of patients, the most represented were patients from Africa (45.8%), followed by Europe (26.6%), Asia (10.8%), North America (8.4%), South America (7.3%), and the least represented were from Australia (1.1%). The leading diagnosis in

Table 1
Review of diagnoses, diseases, and conditions in patients with gynecological problems according to the ICD-10

Disease code	Morbidity list (ICD-10)	n	%
N91.2	Amenorrhea, unspecified	107	42.5
D 25	Leiomyoma of uterus	72	28.6
N 76	Acute vaginitis	47	18.7
Z30	Contraceptive management	8	3.2
N83.2	Other and unspecified ovarian cysts	7	2.8
N94.6	Dysmenorrhea, unspecified	7	2.8
N85.7	Haematometra	1	0.4
R10.30	Lower abdominal pain unspecified	1	0.4
O 031	Spontaneous abortion	1	0.4
O009	Ectopic pregnancy, unspecified	1	0.4
Total		252	100

ICD – International Classification of Diseases, 10th revision.

Table 2**Review of diagnoses, diseases, and conditions in pregnant women according to the ICD-10**

Disease code	Morbidity list (ICD-10)	n	%
Z35	Supervision of high-risk pregnancy	13	11.1
Z34	Supervision of normal pregnancy	17	14.5
D50	Iron deficiency anemia	30	25.6
D 25	Leiomyoma of uterus	19	16.2
N 76	Acute vaginitis	6	5.1
O02.1	Missed abortion	5	4.3
B 50	Malaria	5	4.3
O21.9	Vomiting of pregnancy, unspecified	4	3.4
R19.7	Diarrhea, unspecified	4	3.4
L30.3	Infective dermatitis	4	3.4
N39.0	Urinary tract infection, site not specified	3	2.6
R50.9	Fever, unspecified	2	1.7
O60.10	Preterm labor with preterm delivery	1	0.9
E 03.9	Hypothyroidism, unspecified	1	0.9
J 00	Acute nasopharyngitis	1	0.9
J02	Acute pharyngitis	1	0.9
Q05	Spina bifida	1	0.9
Total	Total	117	100.0

ICD – International Classification of Diseases, 10th revision.

gynecological patients was Amenorrhea, unspecified (42.5%), followed by Leiomyoma of the uterus (28.6%), and Acute vaginitis (18%) (Table 1). The leading diagnosis in pregnant women was Iron deficiency anemia (25.6%), then Leiomyoma of the uterus (16.2%), and Acute vaginitis (5.1%). With a prevalence of 4.3% were Malaria and Missed abortion (Table 2). Two cases of emergency hospitalization should be emphasized: one due to abortion and the other due to ectopic pregnancy (Table 1). Emergency surgical interventions were performed on both patients; equipment and training were crucial. Therefore, Anemia predominates in pregnant women and Amenorrhea in patients with gynecological problems. Leiomyoma of the uterus is in second place in

both groups. Acute vaginitis is highly prevalent and is in third place in both groups. On that account, the preventive use of antibiotics is justified in certain situations.

The results presented might be useful in future planning and preparation of medical resources needed to support peacekeeping operations. The importance of providing necessary equipment, instruments, medicine, and a trained gynecologist should be emphasized.

Nebojša Jovanović

**Military Medical Academy, Specialist Outpatient
Clinic, Department of Gynecology, Belgrade, Serbia**

R E F E R E N C E S

1. Smit T, Tidblad-Lundholm K. Trends in Women's Participation in UN, EU and OSCE Peace Operations. Stockholm International Peace Research Institute. SIPRI 2018; 47: 3–21.
2. Seet B. Levels of Medical Support for United Nations Peacekeeping Operations. Mil Med 1999; 164(7): 451–6.
3. Sarjoon A, Yusoff MA. The United Nations Peacekeeping Operations and Challenges. Acad J Interdisry Studies 2019; 8(3): 202–11.
4. Erendor ME. Peacekeeping Operations and The United Nations. J Sec Studies Glob Pol 2017; 2(1): 61–7.
5. Blanchfield L, Alexis A, Ploch Blanchard L. U.N. Peacekeeping Operations in Africa. Congressional Research Service 2019; [cited 2020 September 23]; Available from: <https://fas.org/sgp/crs/row/R45930>
6. Ghittoni M, Lehouck L, Watson C. Elsie Initiative for Women in Peace Operations: Baseline Study. Geneva: DCAF Geneva Centre for Security Sector Governance 2018. p. 4–10.
7. Nsengimana L. African Female Military in United Nations Peacekeeping Missions. Master of Military art and science. Brussels, Belgium: Bachelor of Social and Military Science, Royal Military Academy; 2018. p. 101.

INSTRUCTIONS TO THE AUTHORS

The Vojnosanitetski pregled (VSP) is an Open Access Journal. All articles can be downloaded free from the web-site (<http://www.vma.mod.gov.rs/sr/vojnosanitetski-pregled>) with the use of license: the Creative Commons — Attribution-ShareAlike (CC BY-SA) (<http://creativecommons.org/licenses/by-sa/4.0/>).

The VSP publishes only papers not published before, nor submitted to any other journals, in the order determined by the Editorial Board. Any attempted plagiarism or self-plagiarism will be punished. When submitting a paper to the VSP electronic editing system (<http://aseestant.ceon.rs/index.php>), the following should be enclosed: a statement on meeting any technical requirements, a statement signed by all the authors that the paper on the whole and/or partly has not been submitted nor accepted for publication elsewhere, a statement specifying the actual contribution of each author, no conflict of interest statement that make them responsible for meeting any requirements set. What follows subsequently is the acceptance of a paper for further editing procedure. The manuscripts submitted to the VSP pass in-house and external peer review. All authors pay "Article Processing Charge" for coverage all editing and publishing expenses. Domestic authors pay 5,000 RSD, and those from abroad 150 euros. The editing and publishing fee is required for substantive editing, facts and references validations, copy editing, and publishing online and in print by editorial staff of the Journal. No additional fees, other than stated above, are required even if an author who already paid the fee would have more articles accepted for publishing in the year when fee was paid. All authors who pay this fee may, if want, receive printed version of the Journal in year when fee is paid. Please note that the payment of this charge does not guarantee acceptance of the manuscript for publication and does not influence the outcome of the review procedure. The requirement about paying "Article Processing Charge" does not apply to reviewers, members of the Editorial Board and the Publisher's Council of the Journal, young researchers and students, as well as any of the subscribers of the Journal.

The VSP publishes: **editorials, original articles, short communications, reviews/meta-analyses, case reports, medical history** (general or military), personal views, invited comments, letters to the editor, reports from scientific meetings, book reviews, and other. Original articles, short communications, meta-analyses and case reports are published with abstracts in both English and Serbian.

General review papers will be accepted by the Editorial Board only if the authors prove themselves as the experts in the fields they write on by citing not less than 5 self-citations.

Papers should be written on IBM-compatible PC, using 12 pt font, and double spacing, with at least 4 cm left margin. **Bold** and *italic* letters should be avoided as reserved for subtitles. Original articles, reviews, meta-analyses and articles from medical history should not exceed 16 pages; current topics 10; case reports 6; short communications 5; letters to the editor and comments 3, and reports on scientific meetings and book reviews 2.

All measurements should be reported in the metric system of the International System of Units (SI), and the standard internationally accepted terms (except for mmHg and °C).

MS Word for Windows (97, 2000, XP, 2003) is recommended for word processing; other programs are to be used only exceptionally. Illustrations should be made using standard **Windows** programs, **Microsoft Office (Excel, Word Graph)**. The use of colors and shading in graphs should be avoided.

Papers should be prepared in accordance with the **Vancouver Convention**.

Papers are reviewed anonymously by at least two editors and/or invited reviewers. Remarks and suggestions are sent to the author for final composition. Galley proofs are sent to the corresponding author for final agreement.

Preparation of manuscript

Parts of the manuscript are: **Title page; Abstract with Key words; Text; Acknowledgements** (to the authors' desire), **References, Enclosures**.

1. Title page

- The title should be concise but informative, while subheadings should be avoided;
- Full names of the authors signed as follows: *, †, ‡, §, ||, ¶, **, ††, ...
- Exact names and places of department(s) and institution(s) of affiliation where the studies were performed, city and the state for any authors, clearly marked by standard footnote signs;
- Conclusion could be a separate chapter or the last paragraph of the discussion;
- Data on the corresponding author.

2. Abstract and key words

The second page should carry a structured abstract (250-300 words for original articles and meta-analyses) with the title of the article. In short, clear sentences the authors should write the **Background/Aim**, major procedures – **Methods** (choice of subjects or laboratory animals; methods for observation and analysis), the obtained findings – **Results** (concrete data and their statistical significance), and the **Conclusion**. It should emphasize new and important aspects of the study or observations. A structured abstract for case reports (up to 250 words) should contain subtitles **Introduction, Case report, Conclusion**. Below the

abstract **Key words** should provide 3–10 key words or short phrases that indicate the topic of the article.

3. Text

The text of the articles includes: **Introduction, Methods, Results, and Discussion**. Long articles may need subheadings within some sections to clarify their content.

Introduction. After the introductory notes, the aim of the article should be stated in brief (the reasons for the study or observation), only significant data from the literature, but not extensive, detailed consideration of the subject, nor data or conclusions from the work being reported.

Methods. The selection of study or experimental subjects (patients or experimental animals, including controls) should be clearly described. The methods, apparatus (manufacturer's name and address in parentheses), and procedures should be identified in sufficient detail to allow other workers to reproduce the results. Also, give references to established methods, including statistical methods. Identify precisely all drugs and chemicals used, with generic name(s), dose(s), and route(s) of administration. State the approval of the Ethics Committee for the tests in humans and animals.

Results should be presented in logical sequence in the text, tables and illustrations. Emphasize or summarize only important observations.

Discussion is to emphasize the new and significant aspects of the study and the conclusions that result from them. Relate the observations to other relevant studies. Link the conclusions with the goals of the study, but avoid unqualified statements and conclusions not completely supported by your data.

References

References should be superscripted and numerated consecutively in the order of their first mentioning within the text. All the authors should be listed, but if there are more than 6 authors, give the first 6 followed by *et al.* Do not use abstracts, secondary publications, oral communications, unpublished papers, official and classified documents. References to papers accepted but not yet published should be cited as "in press". Information from manuscripts not yet accepted should be cited as "unpublished data". Data from the Internet are cited with the date of citation.

Examples of references:

Jurhar-Pavlova M, Petlichkovski A, Trajkov D, Efinska-Mladenovska O, Arsov T, Strezova A, et al. Influence of the elevated ambient temperature on immunoglobulin G and immunoglobulin G subclasses in sera of Wistar rats. *Vojnosanit Pregl* 2003; 60(6): 657–612.

DiMaio VJ. *Forensic Pathology*. 2nd ed. Boca Raton: CRC Press; 2001.

Blinder MA. Anemia and Transfusion Therapy. In: Ahya NS, Flood K, Paranjothi S, editors. *The Washington Manual of Medical Therapeutics*, 30th edition. Boston: Lippincott, Williams and Wilkins; 2001. p. 413–28.

Christensen S, Oppacher F. An analysis of Koza's computational effort statistic for genetic programming. In: Foster JA, Lutton E, Miller J, Ryan C, Tettamanzi AG, editors. *Genetic programming. EuroGP 2002: Proceedings of the 5th European Conference on Genetic Programming*; 2002 Apr 3–5; Kinsdale, Ireland. Berlin: Springer; 2002. p. 182–91.

Aboud S. Quality improvement initiative in nursing homes: the ANA acts in an advisory role. *Am J Nurs* [serial on the Internet]. 2002 Jun [cited 2002 Aug 12]; 102(6): [about 3 p.]. Available from: <http://www.nursingworld.org/AJN/2002/june/Wawatch.htm>

Tables

Each table should be typed double-spaced 1.5 on a separate sheet, numbered in the order of their first citation in the text in the upper left corner and supplied with a brief title each. Explanatory notes are printed under a table. Each table should be mentioned in the text. If data from another source are used, acknowledge fully.

Illustrations

Any forms of graphic enclosures are considered to be figures and should be submitted as additional databases in the System of Assistant. Letters, numbers, and symbols should be clear and uniform, of sufficient size that when reduced for publication, each item will still be legible. Each figure should have a label on its back indicating the number of the figure, author's name, and top of the figure (**Figure 1, Figure 2** and so on). If a figure has been published, state the original source.

Legends for illustrations are typed on a separate page, with Arabic numbers corresponding to the illustrations. If used to identify parts of the illustrations, the symbols, arrows, numbers, or letters should be identified and explained clearly in the legend. Explain the method of staining in photomicrographs.

Abbreviations and acronyms

Authors are encouraged to use abbreviations and acronyms in the manuscript in the following manner: abbreviations and acronyms must be defined the first time they are used in the text consistently throughout the whole manuscript, tables, and graphics; abbreviations should be used only for terms that appear more than three times in text; abbreviations should be sparingly used.

An alphabetical list of all abbreviations used in the paper, followed by their full definitions, should be provided on submission.

Detailed Instructions are available at the web site:

www.vma.mod.gov.rs/vsp

UPUTSTVO AUTORIMA

Vojnosanitetski pregled (VSP) je dostupan u režimu otvorenog pristupa. Članci objavljeni u časopisu mogu se besplatno preuzeti sa sajta časopisa <http://www.vma.mod.gov.rs/sr/> uz primenu licence Creative Commons Autorstvo-Deliti pod istim uslovima (CC BY-SA) (<http://creativecommons.org/licenses/by-sa/4.0>).

VSP objavljuje radove koji nisu ranije nigde objavljivani, niti predati za objavljivanje redosledom koji određuje uređivački odbor. Svaki pokušaj plagijarizma ili autoplagijarizma kažnjava se. Prilikom prijave rada u sistem elektronskog uređivanja „Vojnosanitetskog pregleda“ (<http://asestant.ceon.rs/index.php>) neophodno je priložiti izjavu da su ispunjeni svi postavljene tehnički zahtevi uključujući i izjavu koju potpisuju svi autori da rad nije ranije ni u celini, niti delimično objavljen niti prihvaćen za štampanje u drugom časopisu. Izjavu o pojedinačnom doprinosu svakog od autora rada potpisanu od svih autora, treba skenirati i poslati uz rad kao dopunsku datoteku. Takođe, autori su obavezni da dostave i potpisanu izjavu o nepostojanju sukoba interesa čime postaju odgovorni za ispunjavanje svih postavljenih uslova. Ovome sledi odluka o prihvatanju za dalji uređivački postupak. Rukopisi pristigli u redakciju časopisa podležu internoj i eksternoj recenziji. Svi autori dužni su da plate „Article Processing Charge“ za pokriće troškova jezičke, stručne i tehničke obrade rukopisa, kao i njegovog objavljivanja. Domaći autori plaćaju iznos od 5 000 dinara, a inostrani 150 eura. Dodatna plaćanja nisu predviđena čak i u slučaju da autor koji je već prethodno platio tražen iznos, ima više prihvaćenih radova za objavljivanje u godini u kojoj je izvršio uplatu. Svi autori koji su platili „Article Processing Charge“ mogu, ukoliko žele, dobiti štampanu verziju časopisa tokom godine u kojoj je izvršena uplata. Plaćanje ovog iznosa ne garantuje prihvatanje rukopisa za objavljivanje i ne utiče na ishod recenzije. Od obaveze plaćanja rukopisa navedenih troškova oslobođeni su recenzenti, članovi Uređivačkog odbora i Izdavačkog saveta VSP, studenti i mladi istraživači, kao i pretplatnici časopisa.

U VSP-u se objavljuju **uvodnici, originalni članci, prethodna ili kratka saopštenja**, revijski radovi tipa **opšteg pregleda** (uz uslov da autori navođenjem najmanje 5 autocitata potvrde da su eksperti u oblasti o kojoj pišu), **aktuelne teme, metaanalize, kazuistika, seminar praktičnog lekara**, članci iz **istorije medicine**, lični stavovi, naručeni komentari, pisma uredništvu, izveštaji sa naučnih i stručnih skupova, prikazi knjiga i drugi prilozi. Radovi tipa originalnih članaka, prethodnih ili kratkih saopštenja, metaanalize i kazuistike **objavljaju se uz apstrakte na srpskom i engleskom jeziku**.

Rukopis se piše sa proredom 1,5 sa levom marginom od **4 cm**. Koristiti font veličine 12, a načelno izbegavati upotrebu **bold** i *italic* slova, koja su rezervisana za podnaslove. Originalni članci, opšti pregledi i metaanalize i članci iz istorije medicine ne smeju prelaziti 16 stranica (bez priloga); aktuelne teme – deset, seminar praktičnog lekara – osam, kazuistika – šest, prethodna saopštenja – pet, a komentari i pisma uredniku – tri, izveštaji sa skupova i prikazi knjiga – dve stranice.

U celom radu obavezno je korišćenje međunarodnog sistema mera (SI) i standardnih međunarodno prihvaćenih termina (sem mm Hg i °C).

Za obradu teksta koristiti program **Word for Windows** verzije 97, 2000, XP ili 2003. Za izradu grafičkih priloga koristiti standardne grafičke programe za **Windows**, poželjno iz programskog paketa **Microsoft Office (Excel, Word Graph)**. Kod kompjuterske izrade grafika izbegavati upotrebu boja i senčenja pozadine.

Radovi se pripremaju u skladu sa **Vankuerskim dogovorom**.

Prispeli radovi kao anonimni podležu uređivačkoj obradi i recenziji najmanje dva urednika/recenzenata. Primedbe i sugestije urednika/recenzenata dostavljaju se autoru radi konačnog oblikovanja. Pre objave, rad se upućuje autoru određenom za korespondenciju na konačnu saglasnost.

Priprema rada

Delovi rada su: **naslovna strana, apstrakt sa ključnim rečima, tekst** rada, zahvalnost (po želji), literatura, prilozi.

1. Naslovna strana

a) Poželjno je da naslov bude kratak, jasan i informativan i da odgovara sadržaju, podnaslove izbegavati.

b) Ispisuju se puna imena i prezimena autora sa oznakama redom: *, †, ‡, §, ||, ¶, **, ††, ...

c) Navode se puni nazivi ustanove i organizacijske jedinice u kojima je rad obavljen mesta i države za svakog autora, koristeći standardne znake za fusnote.

d) Zaključak može da bude posebno poglavlje ili se iznosi u poslednjem pasus diskusije.

e) Podaci o autoru za korespondenciju.

2. Apstrakt i ključne reči

Na drugoj stranici nalazi se strukturisani apstrakt (250-300 reči za originalne članke i meta-analize) sa naslovom rada. Kratkim rečenicama na srpskom i engleskom jeziku iznosi se **Uvod/Cilj** rada, osnovne procedure – **Metode** (izbor ispitanika ili laboratorijskih životinja; metode posmatranja i analize), glavni nalazi – **Rezultati** (konkretni podaci i njihova statistička značajnost) i glavni **Zaključak**. Naglasiti nove i značajne aspekte studije ili zapazanja. Strukturisani apstrakt za kazuistiku (do 250 reči), sadrži podnaslove **Uvod, Prikaz**

bolesnika i Zaključak). Ispod apstrakta, „Ključne reči“ sadrže 3–10 ključnih reči ili kratkih izraza koje ukazuju na sadržinu članka.

3. Tekst članka

Tekst sadrži sledeća poglavlja: **uvod, metode, rezultate i diskusiju**. **Uvod**. Posle uvodnih napomena, navesti cilj rada. Ukratko izneti razloge za studiju ili posmatranje. Navesti samo važne podatke iz literature a ne opširna razmatranja o predmetu rada, kao ni podatke ili zaključke iz rada o kome se izveštava.

Metode. Jasno opisati izbor metoda posmatranja ili eksperimentnih metoda (ispitanici ili eksperimentne životinje, uključujući kontrolne). Identifikovati metode, aparaturu (ime i adresa proizvođača u zagradi) i proceduru, dovoljno detaljno da se drugim autorima omogući reprodukcija rezultata. Navesti podatke iz literature za uhodane metode, uključujući i statističke. Tačno identifikovati sve primenjene lekove i hemikalije, uključujući generičko ime, doze i načine davanja. Za ispitivanja na ljudima i životinjama navesti saglasnost nadležnog etičkog komiteta.

Rezultate prikazati logičkim redosledom u tekstu, tabelama i ilustracijama. U tekstu naglasiti ili sumirati samo značajna zapazanja.

U **diskusiji** naglasiti nove i značajne aspekte studije i izvedene zaključke. Posmatranja dovesti u vezu sa drugim relevantnim studijama, u načelu iz poslednje tri godine, a samo izuzetno i starijim. Povezati zaključke sa ciljevima rada, ali izbegavati nesumnjive tvrdnje i one zaključke koje podaci iz rada ne podržavaju u potpunosti.

Literatura

U radu literatura se citira kao superskript, a popisuje rednim brojevima pod kojima se citat pojavljuje u tekstu. Navode se svi autori, ali ako broj prelazi šest, navodi se prvih šest i *et al.* Svi podaci o citiranoj literaturi moraju biti tačni. Literatura se u celini citira na engleskom jeziku, a iza naslova se navodi jezik članka u zagradi. Ne prihvata se citiranje apstrakata, sekundarnih publikacija, usmenih saopštenja, neobjavljenih radova, službenih i poverljivih dokumenata. Radovi koji su prihvaćeni za štampu, ali još nisu objavljeni, navode se uz dodatak „u štampi“. Rukopisi koji su predati, ali još nisu prihvaćeni za štampu, u tekstu se citiraju kao „neobjavljeni podaci“ (u zagradi). Podaci sa interneta citiraju se uz navođenje datuma pristupa tim podacima.

Primeri referenci:

Durović BM. Endothelial trauma in the surgery of cataract. Vojnosanit Pregl 2004; 61(5): 491–7. (Serbian)

Balint B. From the haemotherapy to the haemomodulation. Beograd: Zavod za udžbenike i nastavna sredstva; 2001. (Serbian)

Mladenović T, Kandolf L, Mijušković ŽP. Lasers in dermatology. In: *Karadaglić D*, editor. Dermatology. Beograd: Vojnoizdavački zavod & Verzal Press; 2000. p. 1437–49. (Serbian)

Christensen S, Oppacher F. An analysis of Koza's computational effort statistic for genetic programming. In: *Foster JA, Lutton E, Miller J, Ryan C, Tettamanzi AG*, editors. Genetic programming. EuroGP 2002: Proceedings of the 5th European Conference on Genetic Programming; 2002 Apr 3-5; Kinsdale, Ireland. Berlin: Springer; 2002. p. 182-91.

Abood S. Quality improvement initiative in nursing homes: the ANA acts in an advisory role. Am J Nurs [serial on the Internet]. 2002 Jun [cited 2002 Aug 12]; 102(6): [about 3 p.]. Available from: <http://www.nursingworld.org/AJN/2002/june/Wawatch.htm>

Tabele

Sve tabele pripremaju se sa proredom 1,5 na posebnom listu. Obeležavaju se arapskim brojevima, redosledom pojavljivanja, u levom uglu (**Tabela 1**), a svakoj se daje kratak naslov. Objašnjenja se daju u fus-noti, ne u zaglavlju. Svaka tabela mora da se pomene u tekstu. Ako se koriste tuđi podaci, obavezno ih navesti kao i svaki drugi podatak iz literature.

Ilustracije

Slikama se zovu svi oblici grafičkih priloga i predaju se kao dopunske datoteke u sistemu **asestant**. Slova, brojevi i simboli treba da su jasni i ujednačeni, a dovoljne veličine da prilikom umanjivanja budu čitljivi. Slike treba da budu jasne i obeležene brojevima, onim redom kojim se navode u tekstu (**Sl. 1; Sl. 2** itd.). Ukoliko je slika već negde objavljena, obavezno citirati izvor.

Legende za ilustracije pisati na posebnom listu, koristeći arapske brojeve. Ukoliko se koriste simboli, strelice, brojevi ili slova za objašnjavanje pojedinog dela ilustracije, svaki pojedinačno treba objasniti u legendi. Za fotomikrografije navesti metod bojenja i podatak o uvećanju.

Skraćenice i akronimi

Skraćenice i akronimi u rukopisu treba da budu korišćeni na sledeći način: definisati skraćenice i akronime pri njihovom prvom pojavljivanju u tekstu i koristiti ih konzistentno kroz čitav tekst, tabele i slike; koristiti ih samo za termine koji se pominju više od tri puta u tekstu; da bi se olakšalo čitaocu, skraćenice i aktinome treba štedljivo koristiti.

Abecedni popis svih skraćenica i akronima sa objašnjenjima treba dostaviti pri predaji rukopisa.

Detaljno uputstvo može se dobiti u redakciji ili na sajtu:
www.vma.mod.gov.rs/vsp

